Distribution Agreement Page

In presenting this dissertation as a partial fulfillment of the requirements for an advanced degree from Emory University, I hereby grant to Emory University and its agents the non-exclusive license to archive, make accessible, and display my dissertation in whole or in part in all forms of media, now or hereafter known, including display on the world wide web. I understand that I may select some access restrictions as part of the online submission of this dissertation. I retain all ownership rights to the copyright of the dissertation. I also retain the right to use in future works; all or part of this dissertation.

Signature:

_____   _____

George A. Rogge   Date

Regulation of cocaine- and amphetamine-regulated transcript expression by cyclic AMP response element binding protein

By

George A. Rogge

Doctor of Philosophy
Graduate Division of Biological and Biomedical Sciences
Molecular and Systems Pharmacology

_____
Michael J. Kuhar, Ph.D.
Advisor

_____
Randy A. Hall, Ph.D.
Committee Member

_____
P. Michael Iuvone, Ph.D.
Committee Member

_____
Edward T. Morgan, Ph.D.
Committee Member

Accepted:

_____
Lisa A. Tedesco, Ph.D.
Dean of the James T. Laney School of Graduate Studies

_____
Date

Regulation of cocaine- and amphetamine-regulated transcript expression by cyclic AMP response element binding protein

By

George A. Rogge

B.S., Beloit College, 1999

Advisor: Michael J. Kuhar, Ph.D.

An abstract of
a dissertation submitted to the Faculty of the Graduate School of Emory University
in partial fulfillment of the requirements for the degree of
Doctor of Philosophy
in Graduate Division of Biological and Biomedical Sciences
Molecular and Systems Pharmacology

2010

ABSTRACT

Regulation of cocaine- and amphetamine-regulated transcript expression by cyclic AMP response element binding protein
By
George A. Rogge

Drug addiction is a chronic brain disorder and recovering addicts are subject to a return to drug use (relapse) even after years of drug abstinence. A major focus of drug abuse research is to elucidate the molecular mechanisms of addiction responsible for long-term behavioral abnormalities that cause drug craving and repeated relapse. One goal of that basic research is to identify pharmacotherapy targets to develop medications. Chronic cocaine intake causes long-term genetic alterations in the brain reward pathway that contribute to addictive behaviors by up-regulating CREB transcription factor activity in the nucleus accumbens (NAc). Increases in CREB activity in the NAc were correlated with decreases in the reinforcing effects of cocaine during conditioned place-preference and drug self administration assays. The CART gene promoter was found to contain a cAMP response element (CRE) proposed to bind CREB, and CART mRNA was originally identified as a transcript in the rat NAc up-regulated after cocaine administration. Intra-NAc injection of CART peptides blunted the rewarding effects of cocaine in self administration assays. The overall hypothesis of this dissertation is that CART is a CREB-regulated gene. The data presented in this dissertation demonstrated by chromatin immunoprecipitation that CREB and P-CREB in cultured cells were capable of binding to a region of the CART promoter containing the CRE site in the nuclei of living cells. Furthermore, electrophoretic mobility shift and antibody super shift assays revealed that CREB and P-CREB from the rat NAc were able to bind to a short oligonucleotide identical in sequence to the CART promoter CRE site. In the rat NAc, over expression of CREB by virally mediated gene transfer increased CART mRNA and peptide levels. In sum, the body of data from this dissertation strongly suggested that CREB and P-CREB regulated CART mRNA and peptide expression in the rat NAc by acting directly at the CRE site in the CART proximal promoter. A mechanism by which CREB blunted the rewarding effects of cocaine may have been, in part, by increased expression of CART peptides in the NAc.

Regulation of cocaine- and amphetamine-regulated transcript expression by cyclic AMP response element binding protein

By

George A. Rogge

B.S., Beloit College, 1999

Advisor: Michael J. Kuhar, Ph.D.

A dissertation submitted to the Faculty of the Graduate School of Emory University in partial fulfillment of the requirements for the degree of
Doctor of Philosophy
in Graduate Division of Biological and Biomedical Sciences
Molecular and Systems Pharmacology

2010

<u>Acknowledgements</u>

TABLE OF CONTENTS

INDEX OF FIGURES

Page

INDEX OF TABLES

INDEX OF ABBREVIATIONS

CART   Cocaine- and amphetamine-regulated transcript mRNA

CNS   Central Nervous System

PNS   Peripheral Nervous System

CARTPT   CART gene symbol

TF   Transcription factor

STAT   Signal transducer and activator of transcription

cAMP   3',5'-cyclic adenosine monophosphate

CRE   cAMP response element

AP1   Activator protein-1

Pit1   Pituitary specific transcription factor-1

Ptx1   Pituitary homeobox-1

TCF4   Transcription factor 4

IL4-STAT   Interleukin-4-STAT

CREB   cAMP response element binding protein

P-CREB   serine 133 phospho-CREB

AC   Adenylyl Cyclase

PKA   cAMP dependent protein kinase

rsCART   Rat short form CART peptides

rlCART   Rat long form CART peptides

GABA   Gamma-aminobutyric acid

PTX   Pertussis toxin

ERK   Extracellular signal-regulated kinase

MAPK	Mitogen activated protein kinase
MEK	MAPK kinase or ERK kinase
GPCR	G-protein coupled receptor
CRH	Corticotropin releasing hormone
GFP	Green fluorescent protein
GTP	Guanosine-5'-triphosphate
ATP	Adenosine-5'- triphosphate
VTA	Ventral Tegmental Area
NAc	Nucleus accumbens
DA	Dopamine
SLEA	Sublenticular extended amygdala
MDMA	3, 4-methylenedioxymethamphetamine
aCSF	Artificial cerebrospinal fluid
SEM	Standard error of the mean
DAT	Dopamine re-uptake transporters
SA	Self-administration
CPP	Conditioned place-preference
mCREB	serine 133 mutated-to-alanine mutant CREB
ChIP	Chromatin immunoprecipitation
EMSA	Electrophoretic mobility shift assays
SS	Antibody super shift analyses
Rp-cAMPS	Rp diastereomer of cyclic 3′, 5′-hydrogen phosphorothioate adenosine triethylammonium salt

ACREB	133 mutated-to-alanine mutant CREB
PCR	Polymerase chain reaction
FBS	Fetal bovine serum
CO_2	Carbon dioxide
DMSO	Dimethylsulfoxide
PBS	Phosphate buffered saline
PMSF	Phenylmethylsulfonylfluoride
HEPES	4-(2-Hydroxyethyl) piperazine-1-ethanesulfonic acid, N-(2-Hydroxyethyl) piperazine-N′-(2-ethanesulfonic acid)
EDTA	(Ethylenedinitrilo)tetraacetic acid
cpm	Counts per minute
IP	Immunoprecipitation
GAPDH	Glyceraldehyde-3-phosphate dehydrogenase
gDNA	Genomic DNA
bp	Base pairs
Tm	Melting temperature
Kb	Kilobase
KDa	Kilodalton
Ct	Cycle threshold
ATF1	Activating transcription factor-1
CREM	cAMP response element modulator
ICER	Inducible cAMP early repressor
KID	Kinase-inducible domain

CBP	CREB binding protein
TFIID	Transcription factor-2 D
CaMK	Calcium- Calmodulin-dependant Kinase
PKC	Protein Kinase C
RSK	Ribosomal protein SG kinase
AKT	v-akt murine thymoma viral oncogene homolog
HSV	Herpes simplex virus-1
IE	Immediate early protein
HSV_{ori}	Virus origin of replication sequence
"a" site	Virus cleavage/packaging site
RIA	Radioimmunoassay
Kd	Dissociation constant

Chapter 1: Overview of cocaine- and amphetamine-regulated transcript (CART): gene structure and regulation; peptide processing; putative G-protein coupled receptor signaling and physiological effects on drug reward and reinforcement.[1]

1.1 <u>Introduction</u>

CART peptides were identified as neurotransmitters and hormones widely distributed in discreet tissues of the central and peripheral nervous systems (CNS and PNS, respectively), including the brain reward pathway, involved in regulating many aspects of physiology, including; food intake and energy homeostasis, drug reward and endocrine functions. Since the discovery of CART in 1995, studies from laboratories around the world have produced a wealth of information about the location, regulation, processing and functions of CART peptides, but additional studies aimed at elucidating the physiological effects of the peptides and at characterizing the CART receptor(s) are needed to take advantage of possible therapeutic applications.

In 1995, Douglass and his colleagues at the Oregon Health Sciences University (Douglass et al 1995) found that a number of mRNA transcripts were up-regulated by acute administration of cocaine or amphetamine, one of which they cloned and named the 'cocaine- and amphetamine-regulated transcript' (GenBank accession number U10071). The transcript was referred to as CART mRNA, and the encoded peptides were referred to as CART peptides. Interestingly, Spiess et al had sequenced a peptide in 1981 that was purified from the ovine hypothalamus, and the sequence of that peptide was found to match a portion of the amino acid sequence that was encoded by CART mRNA, which indicated that CART peptides existed, at least in the sheep hypothalamus (Thim et al 1998). Moreover, the sequence identified by Spiess et al immediately followed a pair of basic amino acids that indicated the site of cleavage of a propeptide amino acid chain, and it was therefore suggested that CART propeptides, like other known propeptides, were processed into smaller, active forms. In 1999, Thim et al extracted CART peptides

from rat tissues, sequenced them, and showed that two different CART peptides, CART 55–102 and CART 62–102 (named for their amino acid compositions), were present (Thim et al 1999). Many studies subsequently showed that both of those peptides were biologically active.

There have been over 200 publications regarding CART and its active peptides since Douglass et al's discovery, reflecting the potentially important role the peptides play in essential physiological functions such as feeding (del Giudice et al 2001; Dominguez et al 2004; Kristensen et al 1998; Lambert et al 1998; Yamada et al 2002), energy homeostasis (Asakawa et al 2001), pancreatic function in relation to diabetes (Wierup et al 2006; Wierup et al 2005), analgesia (Damaj et al 2004; Damaj et al 2003; Dun et al 2000b) endocrine regulation (Dun et al 2006; Smith et al 2006; Vrang et al 2003) and depression (Dandekar et al 2009; del Giudice 2006). The research presented in this dissertation, however, was focused on CART's potential role in mediating some of the rewarding and reinforcing effects of psychostimulants like cocaine. In this chapter, because CART was originally discovered as a psychostimulant-regulated gene, the gene structure, transcriptional regulation, propeptide processing and recent evidence indicating a role for CART peptides in drug reward and reinforcement were discussed.

1.2 CART gene conservation and transcriptional regulation

The human CART gene (GenBank accession number U20325) was found to span approximately 2.5 kilobases and mapped to chromosome 5q13–q14, a susceptibility locus for obesity (Dominguez 2006). The HUGO gene nomenclature committee approved "*CARTPT*" for the gene symbol and "CART prepropeptide" as the gene name. The gene

was found to be comprised of three primary DNA units: an approximately 340 nucelotide proximal promoter found upstream of the site for transcription initiation; 2 introns; and 3 exons (Dominguez 2006). In sequence alignment studies, the CART gene was evolutionarily conserved in sequence across a number of species, which indicated that CART may play an important physiological role. Specifically, the human and rat gene sequences shared 91% nucleotide identity within their coding regions, and the rat and mouse were 98% identical in coding region sequences (Dominguez 2006). Genbank accession numbers for the rat and mouse genes, respectively, are AF519794 and AF148071. The high sequence similarity between rat and human nucleotides resulted in 95% amino acid identity between the active neuropeptides (Dominguez 2006).

The 5' proximal promoter region of the gene was also determined to be highly conserved across rat, mouse and human species (Barrett et al 2002; Dominguez 2006; Dominguez & Kuhar 2004; Dominguez et al 2002; Yamada et al 2002). Sequence alignment studies indicated a high degree of homology between the mouse and rat CART proximal promoters from -198 base pairs to +168 base pairs, where +1 was the first nucleotide of the ATG initiation codon (Barrett et al 2002; Dominguez et al 2002). The promoter regions of the genes in each species contained a number of predicted DNA *cis-*regulatory elements that were proposed to act as transcription factor (TF) binding sites. The following were predicted by database analysis in the mouse and rat genes, respectively: TATA box, signal transducer and activator of transcription (STAT), 3', 5'-cyclic adenosine monophosphate (cAMP) response element (CRE), SP1, E-Box, activator protein-1 (AP1) and pituitary specific transcription factor-1 (Pit1) (mouse gene) (Dominguez et al 2002); TATA box, pituitary homeobox-1 (Ptx1), SP1, CRE, E-Box,

transcription factor 4 (TCF4), STAT3 and interleukin 4-STAT (IL4-STAT) (rat gene,

Figure 1.1) (Barrett et al 2002).

The gamut of predicted protein-DNA interaction sequences listed above may be

able to regulate the basal and stimulus-induced gene expression of CART via interactions

with nuclear TF proteins such as the cAMP response element binding protein (CREB),

CLOCK, IL4, STAT, SP-1, c-Fos and others (Barrett et al 2002; Barrett et al 2001;

Dominguez 2006; Dominguez & Kuhar 2004) in cell-type and species-specific manners.

The variations in *cis*-element combinations between the CART genes of mice and rats

could indicate differential mechanisms of transcriptional regulation in the different

species.

In contrast, the consensus CRE DNA *cis*-regulatory element was found to be

evolutionarily conserved across rat, mouse and human species (Dominguez 2006;

Yamada et al 2002), which indicated it could play an important role in CART gene

expression that has been conserved for ages. Even though the other gene regulatory

elements such as E-box and IL4-STAT may play their own unique roles in regulating

CART gene expression, the fact that the CRE site was conserved in sequence and

position relative to the +1 site of initiation in mice, rats and humans indicated a

potentially common mechanism of CART regulation between the three species mediated

by CREB family TFs. Thus, the CRE site has been extensively studied in CART gene

transcriptional regulation studies and a goal of this dissertation was to expand upon those

findings and discover a physiological relevance for CREB regulation of the CART gene.

In experiments with cultured cells, CREB may have regulated CART promoter-

driven luciferase expression. Dominguez et al cloned a number of luciferase constructs

Figure 1.1. Database analysis identified putative *cis*-regulatory elements in the rat CART gene promoter, including a consensus CRE site. An illustration of the rat CART gene promoter specifies the positions of database-identified, putative DNA *cis*-regulatory elements relative to each other and the +1 site of transcriptional initiation, where +1 is the A of the ATG initiation codon preceding exon 1 of the expressed sequence. After the rat CART gene was cloned, each *cis*-element was hypothesized to bind to a specific family of transcription factors in response to intracellular signaling cascades initiated by extracellular stimuli, such as ligand binding to cell surface receptors, and in that way differentially regulate CART mRNA transcription via unique protein-DNA interactions. The proximal promoter from -198 base pairs to +1 showed a high degree of homology in DNA alignment studies with the mouse CART promoter (Barrett et al 2002; Dominguez et al 2002). Although many *cis*-elements were identified in the rat CART gene promoter, the consensus CRE site was found to be evolutionarily conserved in sequence and position relative to +1 across rat, mouse and human species (Dominguez 2006; Yamada et al 2002), which indicated it could represent a common, important mechanism of transcriptional regulation in the different species. Furthermore, the majority of CART gene regulation studies focused on CRE site interactions with CREB family transcription factors, which have been known to regulate the stimulus-inducible expression of neuropeptides such as c-Fos and prodynorphin in the brain reward pathway after drug exposure (Nestler 2004a). Thus, because CART was originally identified as a psychostimulant-regulated transcript, this dissertation focused on elucidating a role for the promoter CRE site in CART gene transcriptional regulation, *in vivo*, in the reward pathway of the rat brain. Figure adapted from (Barrett et al 2002).

Figure 1.1. Database analysis identified putative *cis*-regulatory elements in the rat CART gene promoter, including a consensus CRE site.

Symbol legend:

PTX1

TCF4

IL4-STAT

STAT-3

EBOX

SP1

CRE

TATA
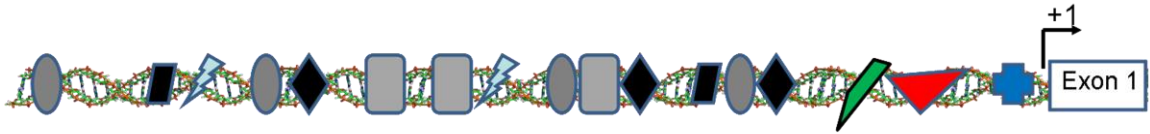
using various lengths of the mouse CART gene proximal promoter to drive luciferase expression. Those studies documented: 1) promoter competency (that is, the CART promoter was able to drive luciferase expression under basal conditions); 2) stimulated gene expression via the use of 20 μM forskolin (a direct activator of adenylyl cyclase [AC] and thus cAMP dependent protein kinase [PKA] activity) for 1 hour; and 3) that non-sense mutations in the CRE *cis*-regulatory element predicted to bind CREB and transcriptionally active P-CREB proteins resulted in the loss of both basal and forskolin-stimulated luciferase expression (Dominguez & Kuhar 2004).

1.3 RNA processing

When transcribed from DNA to mRNA, the rat CART gene was found to produce a single preRNA transcript that gave rise to two, distinct RNA species of 700 base pairs and 900 base pairs, respectively, due to differential poly A tail utilization (Douglass et al 1995). In the case of rats and mice, but not humans, alternative mRNA splicing occurred within the region translated from exon 2 and mRNA translation subsequently produced a short (116 amino acid) preproCART peptide isoform as well as a long one (129 amino acids) (Douglass et al 1995). Humans were found to express only the short preproCART isoform (116 amino acids) because there were no alternative splicing events during translation (Douglass & Daoud 1996).

Both the short and long preproCART peptides were found to have highly homologous N-terminal hydrophobic signal sequences of 27 amino acids, which allowed entry into the regulated secretory pathway for proteolytic processing of precursor peptides (Stein et al 2006b). Cleavage of the 27 amino acid signal sequences created the

short and long proCART peptides of 89 amino acids and 102 amino acids, dubbed rat

short (rs) CART and rat long (rl) CART peptides, respectively (Dominguez 2006; Stein et

al 2006b). The amino acid sequences of rlCART and rsCART after cleavage of the N-

terminal signal sequences are shown in **figure 1.2A**, where the amino acid translation

product of the 39 nucleotides inserted during mRNA alternative splicing is boxed and

highlighted in the rat long (rl) form.

The proCART peptides contained several cleavage sites that allowed for

posttranslational processing by prohormone convertases and that processing resulted in at

least two biologically active CART peptides. The names of the peptides, CART 55–102

and CART 62–102, were derived from the long form of proCART (Dey et al 2003;

Ludvigsen et al 2001; Stein et al 2006a; Stein et al 2006b; Thim et al 1998). In humans

(who produced only the short form of proCART 1-89) the equivalent peptides were

called CART 42–89 and CART 49–89. In any species that expressed both the long and

the short forms of proCART, the amino acid sequences of CART 42–89 and CART 49–

89 were found to be identical to those of CART 55–102 and CART 62–102, respectively.

One important aspect of the gene structure was a highly conserved nucleotide

sequence in exon 3 that encoded for a series of cysteine amino acid residues which

ultimately formed disulfide bonds in active CART peptides and were found to be

essential for maintaining neuropeptide functionality (Thim et al 1998; Yermolaieva et al

2001). **Figure 1.2B** shows the structure of rat CART 55–102, one of the active CART

peptides, including the three conserved disulfide bridges encoded by exon 3, as detailed

above. As an illustration of the conservation of the above cysteine residues across

unrelated species, the rat and human CART peptides exhibited 100% amino acid

Figure 1.2. Amino acid sequences of rat proCART peptides and the conserved, "ball-and-chain" structure of biologically active CART peptides. A) In the rat, CART mRNA was found to have two splice variants (not shown): one that encoded a long form of proCART and one that encoded a short form. The mRNA that encoded the long form was translated into a 102-amino-acid sequence (rlCART, top). In the other variant, the section that encoded amino acids 27–39 of the long form (shown in blue) was spliced out, and the resulting short-form CART mRNA was therefore translated into an 89 amino-acid sequence peptide (rsCART, bottom). The fragments of the long form of proCART that were reliably shown to be active were amino acids 55–102 and 62–102 (highlighted). In the short form of proCART, the numbers of the active amino acids were 42–89 and 49–89, but those amino acids were identical to those of the long form in a given species; this led to some confusion in the literature because different numbers refered to the same amino-acid sequences. Only the 89 amino acid form (the short form) of proCART has been found in humans. The amino acid sequence of that human peptide was slightly different from the amino acid sequence of the rat peptide. Amino acid 42, which is located in the active peptide fragment, was isoleucine in the rat peptide but valine in the human peptide. Pairs of basic amino acids shown in bold were determined to be sites of processing by prohormone convertases. **B)** The structure of CART 55–102, with the disulfide bridges required for biological activity, was determined by microsequencing and mass spectroscopy (Thim et al 1999). The other major active peptide was found to be CART 62–102, which had the same general structure. Part **(A)** modified from (Hubert et al 2008), with permission of Elsevier Science. Part **(B)** reproduced from (Thim et al 1998), with permission from Elsevier Science.

Figure 1.2. Amino acid sequences of rat proCART peptides and the conserved, "ball-and-chain" structure of biologically active CART peptides.

Figure reproduced with permission from Macmillan Publishers Ltd:

Nature Reviews Neuroscience, (Rogge et al 2008), copyright 2008.

similarity in alignment studies using exon 3 sequences and the human amino acid sequence aligned nearly 100% with the amino acid sequences of seven other species ranging from goldfish to cows (Dominguez 2006).

More than half a dozen biologically active CART peptide fragments have either been isolated from animal tissues, or theorized to exist in nature due to proposed dibasic sites in the peptide structure available for prohormone convertase peptide cleavage (Dylag et al 2006a; Dylag et al 2006b). Interestingly, rlCART contained a pair of basic amino acid residues within the alternatively spliced domain (not present in rsCART) that may serve as a target for prohormone convertase action, and in that way distinct, physiologically active peptide fragments may be generated from the two proCART peptides individually (Douglass et al 1995). Other fragments of proCART were found to be biologically active (Dylag et al 2006a; Dylag et al 2006b), but most animal studies involved CART 55–102 and CART 62–102, thus this dissertation focused on those peptides.

1.4 <u>CART peptides as neurotransmitters</u>

CART peptides have satisfied the general requirements for being peptide neurotransmitters. Although the descriptions of these requirements vary, they generally include demonstrations that the peptides were present in tissues, were biologically active and were released by calcium-dependent mechanisms. CART mRNA and peptides were discovered in brain tissue (Douglass et al 1995; Gautvik et al 1996; Koylu et al 1998; Spiess et al 1981) and they produced many effects when they were injected into the brain or were applied to cells in culture. CART peptides in the brain were found only in

neurons — for example, in the nucleus accumbens (Smith et al 1999; Smith et al 1997)—

and coexisted with other neurotransmitters such as γ-aminobutyric acid (GABA) (Smith

et al 1999) and substance P (Hubert & Kuhar 2005; Vrang 2006). They were found in

dense core vesicles (Smith et al 1999; Smith et al 1997) and proCART had a leader

sequence that facilitated its entry into vesicles and its subsequent processing (Douglass et

al 1995). Moreover, potassium-induced release of CART peptides from hypothalamic

explants was calcium-dependent (Murphy et al 2000).

It has been known for many years that various peptides found in the brain were

also found in the gut — they have been referred to as 'brain–gut' peptides. Indeed,

CART peptides were also found in the gut (Kuhar & Yoho 1999), and there is evidence

that they were biologically active there (Ekblad 2006; Ekblad et al 2003). Endocrine

studies also suggested that CART peptides had a hormonal role: they were found in

peripheral blood and in pituitary portal blood (Larsen et al 2003) as well as in tissues with

hormonal roles, such as the anterior and posterior pituitary and the adrenal medulla

(Koylu et al 1997). CART peptide levels in the blood and in some brain regions

exhibited a diurnal rhythm that was positively correlated with the diurnal rhythm of

corticosterone (Vicentic 2006).

1.5 <u>CART receptors</u>

Shortly after Douglass et al's landmark paper (Douglass et al 1995) describing

CART mRNA and peptides, many laboratories attempted to find a receptor for the

peptides using receptor-binding techniques. Receptor binding studies usually required

demonstrations of high affinity ligand–receptor interactions, saturability and specificity.

However, those early attempts met with failure: no specific receptor binding could be detected in brain homogenates or slices. The reasons that were proposed to explain that lack of specific binding included a supposition of a low affinity binding site that could not be detected using those approaches, and high levels of nonspecific binding. Although there was no progress in the search for a CART receptor for several years, the fact that CART peptides were biologically active in various experiments was good evidence that CART receptors existed.

For example, it was found that central administration of CART peptides increased c-fos mRNA levels in various areas of the brain (Vrang et al 1999). In addition, applying CART 55–102 to hippocampal primary cells in culture resulted in an inhibition of cocaine-induced voltage-gated calcium channel activation (Yermolaieva et al 2001). That effect was blocked by pre-treating the neurons with pertussis toxin, which suggested that the observed signaling occurred through activation of the inhibitory G proteins Gi/o. Furthermore, central administration of CART peptides resulted in phosphorylation of CREB in some hypothalamic neurons (Sarkar et al 2004). Application of the peptide to AtT20 cells, a mouse pituitary tumor cell line, activated extracellular signal-regulated kinase (ERK) signaling by increasing the levels of phosphorylated ERK, and that effect was reduced by pertussis toxin (Lakatos et al 2005), which again suggested that CART peptides activated G-protein coupled receptors (GPCRs) functionally linked to Gi/o proteins. CART signaling in cultures of bovine granulosa cells also seemed to involve a Gi/o mechanism (Sen et al 2007). The combined evidence of several laboratories thus suggested that CART peptides could activate G-protein signaling pathways (**Figure 1.3**), which strongly supported the existence of a G-protein-coupled receptor (GPCR) for

Figure 1.3. Proposed signaling mechanism of putative CART peptide G-protein coupled receptors. Several studies on CART peptide-induced cell signaling have demonstrated that CART peptides activated at least three intracellular signaling mechanisms. First, CART 55–102 inhibited cocaine activation of L-type voltage-gated calcium channels through a pertussis toxin (PTX; an inhibitor of inhibitory-G-protein (Gi/Go)-dependent signaling)-sensitive mechanism in hippocampal neurons (Yermolaieva et al 2001). Second, CART 55–102 increased the phosphorylation of cyclic AMP-response-element-binding protein (CREB) in the nuclei of corticotropin-releasing hormone (CRH) neurons in the hypothalamic paraventricular nucleus in fasted and fed rats (Sarkar et al 2004). The dashed arrow indicates that it is not yet known whether this effect of CART 55–102 was mediated by inhibitory G proteins. Third, CART 55–102 increased extracellular signal-regulated kinase (ERK) phosphorylation in AtT20 and GH3 cells, an effect that was blocked by U0126, an inhibitor of the mitogen activated protein kinase (MAPK) family member MAP kinase kinase or ERK kinase (MEK), and by PTX (Lakatos et al 2005).

Figure 1.3. Proposed signaling mechanism of putative CART peptide G-protein coupled receptors.
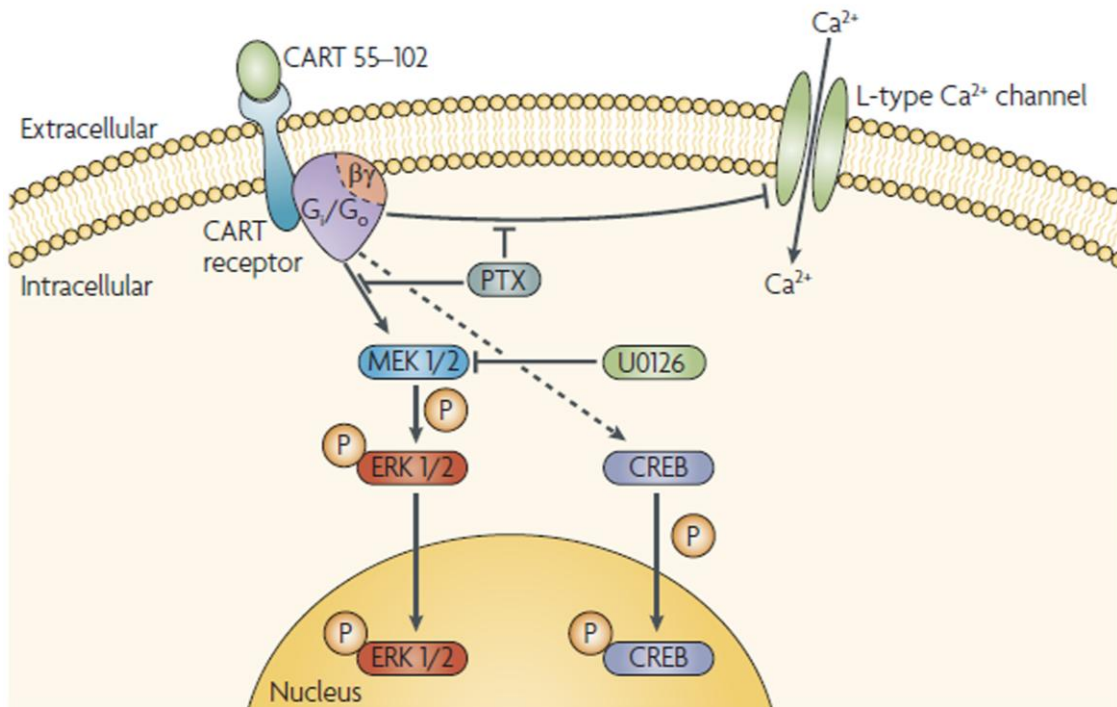
Figure reproduced with permission from Macmillan Publishers Ltd:

Nature Reviews Neuroscience, (Rogge et al 2008), copyright 2008.

CART peptides. Although some skepticism and caution has been warranted, it is difficult to explain how the peptides exerted their effects without the existence of conjugate receptors.

Binding studies were subsequently conducted in AtT20 cells because CART peptide signaling was established in that cell line (Vicentic et al 2005c). The investigation identified a high affinity, saturable binding site that was specific for the active peptides CART 55–102 and CART 62–102. Another binding study, which used a complex of CART 55–102 and green fluorescent protein (GFP), also revealed binding in HepG2 cells and in dissociated hypothalamic cells (Keller et al 2006). However, the binding was not obviously saturable at high concentrations, suggesting that the ligand might have been binding to a low affinity binding site or receptor (Keller et al 2006). A subsequent study (Maletinska et al 2007) found that CART peptide binding in differentiated and non- differentiated PC12 cells had characteristics of receptor binding.

Specific CART peptide binding was also identified in primary cultures of rat nucleus accumbens (Jones & Kuhar 2008). The binding had receptor-like characteristics, and the ligand-binding affinity was reduced in the presence of guanosine-5'-triphosphate (GTP) analogues, but not adenosine-5'-triphosphate (ATP) analogues, indicating that the binding was to a GPCR. Overall, although the binding approach has been generally successful, some results have shown the binding to be low and variable, and more consistent assays are needed. It is of note that since either of the two biologically active CART peptides were found to be active while the other was without effect in the same preparation, the possibility of multiple receptors cannot be ignored (Dylag et al 2006a).

To summarize, studies of the CART receptor indicated it may be a GPCR coupled to Gi/o. The evidence for the existence of a CART receptor supported the hypothesis that CART peptides were neurotransmitter and/or hormonal substances. Moreover, those findings set the stage for drug screening, which hopefully will result in the identification of small molecule agonists and antagonists. As discussed in a recent review (Rogge et al 2008), CART peptides have been implicated in many physiological processes, and there are many possible uses for CART system-related drugs as therapeutic agents.

1.6 <u>The CART system and addiction</u>

Drug abuse has become a significant problem, and much progress has been made in identifying the mechanisms and neuronal substrates of addiction. Data from numerous studies have suggested that the CART system is involved in drug abuse. For example, in post-mortem tissues from human victims of cocaine overdose, CART mRNA levels were increased in the nucleus accumbens (NAc) and decreased in the ventral tegmental area (VTA), two important regions of the brain reward pathway (Albertson et al 2004; Tang et al 2003). Also, in a Korean population, an association was found between a polymorphism in intron 1 of the CART gene and alcoholism, but not between that polymorphism and bipolar disorder or schizophrenia (Jung et al 2004).

1.6.1 Psychostimulants activated CART peptide-containing neurons in the nucleus accumbens

When initial studies showed an up-regulation of CART mRNA in the ventral striatum after acute injections of either cocaine or amphetamine, but not morphine

(Douglass et al 1995), the assumption was that the CART system was involved in the actions of psychostimulants. Interest bloomed in the novel mRNA transcript because it was positively regulated by psychostimulants and later neuroanatomical mapping revealed that CART expression was strategically positioned in humans and rodents to modulate reward and reinforcement behaviors in response to naturally rewarding stimuli such as food, water and sex as well as pharmacological reward caused by drugs of abuse (Hurd & Fagergren 2000; Koylu et al 1998; Koylu et al 1997; Kristensen et al 1998; Kuhar et al 2005; Larsen et al 2003). Both the mRNA transcript and translated peptides were highly enriched in discreet brain nuclei of the mesocorticolimbic dopamine (DA) system (Dall Vechia et al 2000; Dallvechia-Adams et al 2002; Douglass & Daoud 1996; Douglass et al 1995; Koylu et al 1998; Smith et al 1999; Smith et al 1997); a circuit of interconnected mid-brain regions that modulate responses to environmental cues and stimuli, regarded by experts as the "reward pathway" (Carlezon et al 1998; Hurd et al 1999; Jaworski & Jones 2006; Koob & Volkow 2009; Nestler & Malenka 2004; Wise et al 1992). The brain regions associated with the rewarding and reinforcing properties of abused substances which expressed CART included the VTA, NAc, amygdala, lateral hypothalamus, ventral pallidum, hippocampus and neocortex (Albertson et al 2004; Dallvechia-Adams et al 2002; Douglass & Daoud 1996; Douglass et al 1995; Hurd & Fagergren 2000; Philpot et al 2005; Smith et al 1997; Tang et al 2003)

Although acute injections of psychostimulants haven't always increased CART mRNA in the reward pathway (Hunter et al 2005; Jones & Kuhar 2006; Marie-Claire et al 2003; Vrang et al 2002), recent studies have shown that acute cocaine injections dose- and time-dependently increased c-Fos immunoreactivity in CART containing cells of the

NAc, (Hubert & Kuhar 2008). c-Fos expression in neurons is tightly regulated by extracellular stimuli and considered to represent neuronal activation (Herdegen & Waetzig 2001; Hubert & Kuhar 2008); thus cocaine activated CART-containing neurons in the rat NAc, even though cocaine did not reliably alter CART peptide levels. The finding also suggested that changes in CART peptide levels *per se* might not have been the best indicator of a role for the CART system in some processes. Drugs could affect many neurons without necessarily causing a change in the levels of neurotransmitters, because the neurotransmitters could have been replaced, at least in the short term, by synthesis via transcriptional or translational control mechanisms (Kuhar 2009).

Elevations in reward pathway CART mRNA were, however, consistently found when higher doses were given or repeated dosing was used (Brenz Verca et al 2001; Fagergren & Hurd 1999; Hunter et al 2005). Specifically, Faegergren and Hurd discovered increased central amygdala CART levels in male, but not female rats after a moderate dose binge cocaine administration paradigm (3 x 15 mg/kg per 1 hour) (Fagergren & Hurd 1999). The females from that study exhibited increased CART levels in the NAc shell, indicating a gender difference of cocaine regulation of the CART gene in rats (Fagergren & Hurd 1999). Higher doses of binge cocaine administration (4 x 30 mg/kg per 2 hours) increased CART in the NAc of both male and female rats (Brenz Verca et al 2001; Hunter et al 2005). Faegergren and Hurd further discovered that chronic, low-dose IV cocaine self-administration increased CART in the sublenticular extended amygdala (SLEA) of Rhesus monkeys, a region that mediates emotional responses to environmental stimuli (Fagergren & Hurd 2007).

Furthermore, it was shown that administration of methamphetamine, 3,4-

methylenedioxymethamphetamine (MDMA) or ethanol also increased CART mRNA

levels in the NAc (Jean et al 2007; Ogden et al 2004; Salinas et al 2006). It was also

shown that acute cocaine administration after intra-accumbal injection of forskolin

(which increased the levels of P-CREB by a PKA-mediated pathway and increased NAc

CART mRNA levels on its own), increased CART mRNA levels in the rat NAc above

the levels stimulated by intra-accumbal forskolin alone (Jones & Kuhar 2006). Vehicle

treatment paired with an acute cocaine injection had no effect on CART mRNA in those

studies. That result suggested that a preliminary activation of CART gene expression

made it more responsive to up-regulation by psychostimulants. From these data, it

seemed that CART gene regulation by cocaine in specific regions of the brain reward

pathway was complex; influenced by an animal's species and gender, the dose of the

drug, route of administration and administration paradigm (i.e. contingent vs. non-

contingent, acute, binge, chronic, etc.).

1.6.2 The CART system and mesolimbic dopamine

Additional data supported the idea that CART peptide-containing neurons in the

ventral striatum were activated by psychostimulants. Psychostimulants increased

dopamine levels in the synaptic cleft and in extra-neuronal spaces, and it was shown that

there were dopamine receptors on CART peptide-containing neurons (Beaudry et al

2004; Hubert & Kuhar 2006; Hunter et al 2006). Also, CART neurons in the NAc

received afferent nerve terminals that stained positive for tyrosine hydroxylase, which

implied that there was a direct dopaminergic input to CART peptide-containing cells

(Smith et al 1999; Smith et al 1997). Tyrosine hydroxylase was identified as the rate-limiting enzyme in dopamine synthesis and catalyzed the conversion of L-tyrosine to L-dihydroxyphenylalanine (L-DOPA), a precursor of dopamine.

Interestingly, neuroanatomical mapping revealed a reciprocal CART peptide input to dopamine neurons in the ventral midbrain, including the VTA, which contain dopamine-producing neurons (Dallvechia-Adams et al 2002; Hubert & Kuhar 2005; Kimmel et al 2000; Koylu et al 1998; Philpot & Smith 2006; Philpot et al 2005; Shieh 2003; Smith et al 1999). Specifically, CART-expressing neurons in the rat and monkey NAc were found to be medium spiny, striatal output neurons that co-expressed GABA and received a dopaminergic input (Hubert & Kuhar 2005; Smith et al 1999; Smith et al 1997). The majority of CART neurons which projected from the NAc to the VTA formed synapses with putative GABAergic interneurons there (Philpot & Smith 2006), while 30% of NAc to VTA projection neurons directly synapsed with DA neurons (Dallvechia-Adams et al 2002). At the present time, no studies have been able to determine the function of CART peptides released from GABA-containing NAc projection neurons onto neurons in the VTA.

The functional effects of CART peptides in the NAc were examined by a number of laboratories because CART neurons in the NAc were identified as dopaminergic and were indirectly activated by psychostimulants. Furthermore, some of those CART neurons projected back onto the VTA with the potential regulate DA synthesis and release, which could have influenced behavioral responses to psychostimulants and other drugs of abuse. The first observation was that injections of CART 55–102 alone into the NAc had no observable effect on animals' locomotor activities. Although intra-accumbal

injections of dopamine or amphetamine, or intraperitoneal injections of cocaine, increased locomotor activity as expected, pre-treatment with intra-accumbal CART peptides resulted in relative reductions in locomotor activities (Jaworski et al 2003; Kim et al 2003). Thus, CART peptides blunted the locomotor-activating effects of dopamine and psychostimulants. Another paper showed that intra-accumbal injection of CART peptides inhibited the expression of behavioral sensitization that is normally induced by repeated amphetamine administration (Kim et al 2007).

Furthermore, a recent paper indicated that CART peptides reduced the rewarding effects of cocaine in drug self-administration studies (Jaworski et al 2008). The data in **figure 1.4a** showed that the self-administration break point was dose-responsively reduced when CART peptides were injected into the NAc (Jaworski et al 2008). CART peptides in the NAc might have acted to blunt the behavioral and rewarding effects of cocaine. These findings suggested that CART peptides had a homeostatic function in the NAc. It was postulated that as dopamine levels rose after the administration of psychostimulants, CART systems were activated to reduce or control the functional effects of the rise in dopamine (although the mechanisms and specificity of the CART effect are not yet clear). That hypothesis (see **Figure 1.4b**) is interesting from a functional point of view, but also from the point of view of using the CART system as a target for developing medications for psychostimulant abuse.

Figure 1.4. CART peptides as potential regulators of dopamine activity in the nucleus accumbens. a) The effect of bilateral CART (cocaine- and amphetamine-regulated transcript) peptide infusions (0.0, 1.0 or 2.5 µg per side) into the nucleus accumbens on cocaine self-administration. Bilateral CART peptide infusions reduced the break point of cocaine self-administration in a dose-dependent manner. The break point was a reflection of how hard the animals were willing to work for a cocaine injection, and could be considered to be a measure of reward. **b)** Cocaine administration elevated dopamine levels and therefore increased behaviors, such as locomotor activity and drug reward, associated with elevated dopamine levels. According to one hypothesis, CART peptides in the nucleus accumbens acted to blunt those behavioral responses — perhaps by regulating dopamine neurotransmission in the brain reward pathway, although the precise mechanism of the blunting is not yet clear. Abbreviations: aCSF, artificial cerebrospinal fluid; SEM, standard error of the mean. Data in part **a** adapted with permission from (Jaworski et al 2008).

Figure 1.4. CART peptides as potential regulators of dopamine activity in the nucleus accumbens.
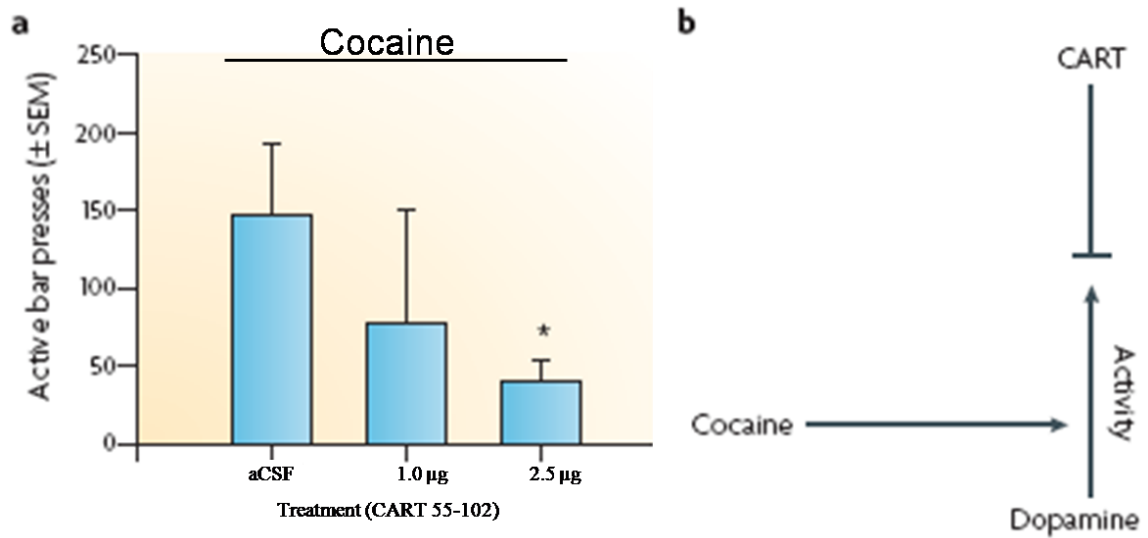
Figure reproduced with permission from Macmillan Publishers Ltd:

Nature Reviews Neuroscience, (Rogge et al 2008), copyright 2008.

1.7 <u>The goals of this dissertation</u>

Cocaine administration has been shown to have many effects on the NAc besides up-regulation of CART mRNA and peptide levels. CREB activity was also shown to be up-regulated in the NAc by cocaine (Nestler 2004a) and that over activity was associated with reductions in cocaine reward as shown by self-administration and conditioned place-preference assays (Carlezon et al 2005; Nestler 2004a; Sakai et al 2002; Self et al 1998). The overall <u>hypothesis</u> of this dissertation <u>was that CART was a CREB-regulated gene in the NAc.</u> Furthermore, CREB regulation of the CART gene may be one mechanism by which CREB reduced the rewarding properties of cocaine.

To address the hypothesis that CREB could regulate CART gene expression in the NAc, a number of different experimental paradigms were used to investigate if: 1) CREB, and its transcriptionally active form, P-CREB, made in living cells could bind to the CART promoter region containing the CRE site at the level of the chromatin, in the nucleus of neurons (**Chapter 2**); 2) CREB and P-CREB, in nuclear extracts from rat NAc and pituitary tissues, could bind to the CART promoter CRE site flanked by its neighboring promoter sequences (**Chapters 2** and **3**); and 3) CREB over expression in the rat NAc was able to positively regulate CART mRNA and peptide levels *in vivo*, in the rat NAc (**Chapter 3**). In sum, the body of research presented in this dissertation aimed to determine if CREB and P-CREB could regulate CART peptide expression in the rat NAc by directly acting at the CRE site in the proximal promoter.

Chapter 2: CREB and P-CREB in pituitary-derived GH3 cells bound to the CART promoter region containing a consensus CRE *cis*-regulatory element and CREB and P-CREB from the rat pituitary bound to the same CRE site *in vitro*.

2.1 <u>Introduction</u>

2.1.1 The role of CREB in drug addiction and pharmacodynamic tolerance

Drug addiction has been defined as a complex, chronic brain disease and recovering addicts have been subject to a return to drug use even after years of drug abstinence (Koob & Volkow 2009). In recent years, a major focus of drug abuse research was to elucidate the molecular mechanisms of addiction responsible for the long-term behavioral abnormalities that caused drug craving and repeated relapse (Carlezon et al 2005; Nestler 2004b). One goal of that basic research was to identify pharmacotherapy targets for which medications could be developed to treat addiction.

For years, many of the protein targets directly affected by most drugs of abuse were known (Nestler 2004a) and they shared a common mechanism of action in that the acute administration of nearly all abused substances increased synaptic release of dopamine (DA) along the VTA-originating mesocorticolimbic DA pathway (brain reward pathway), though each by its own unique mechanism (Nestler 2004a; Wise et al 1992). Cocaine, for instance, indirectly elevated DA in the reward pathway by binding to and blocking pre-synaptic DA re-uptake transporters (DAT) (Kuhar et al 1988; Ritz et al 1987; 1988) (**Figure 2.1**). Although cocaine had an affinity for pre-synaptic norepinephrine- and serotonin-reuptake transporters as well, DAT in the NAc region bridging NAc and VTA neurons appeared to be the drug's primary protein target (Nestler 2004a). Blockade of DAT, though, like general increases in VTA to NAc DA neurotransmission, could not fully explain the complex behavior of drug addiction.

Figure 2.1. Cocaine blocks dopamine re-uptake in the brain reward pathway. The figure shows a schematic of dopamine (DA) neurotransmission from a pre-synaptic ventral tegmental area neuron (VTA) to a post-synaptic nucleus accumbens (NAc) neuron and cocaine's mechanism of action to indirectly elevate synaptic levels of DA. Increased dopamine neurotransmission along the VTA to NAc pathway is a primary mechanism of drug reward and reinforcement. Tyrosine hydroxylase is the rate-limiting enzyme that produces DA from L-tyrosine, and DA is subsequently packaged into vesicles in VTA neurons by vesicular monoamine transporters. Upon receiving an action potential, the DA-containing vesicles fuse to the plasma membrane and emancipate the neurotransmitter via exocytosis into the synapse, where DA acts on pre-and post-synaptic DA receptors. DA G-protein coupled receptors belong to two families, D1-like and D2-like, differentially coupled to intracellular signaling pathways that either activate $G_\alpha s$ proteins and stimulate adenylyl cyclase (AC) activity which increases cAMP dependent protein kinase (PKA) activity (D1-like) or activate $G\alpha_{i/o}$ proteins that inhibit AC and PKA activities (D2-like). NAc neurons pre-dominantly express D1-like receptors, facilitating AC increases in the catalytic formation of cAMP from ATP, which can then bind to inhibitory subunits on PKA enzymes to release the active kinase, which translocates to the nucleus with the ability to phosphorylate target proteins such as CREB transcription factors. Normally, DA neurotransmission is terminated by re-uptake into pre-synaptic terminals by DA re-uptake transporters (DAT) or metabolic breakdown by monoamine oxidases. Cocaine (represented by its molecular structure shown at the bottom left of the figure) has a high affinity for DAT on VTA neurons and blocks the recycling of dopamine back up into the pre-synaptic terminal, indirectly increasing synaptic dopamine levels. Subsequent to cocaine administration, PKA has been shown to phosphorylate CREB in the nuclei of NAc neurons (Nestler 2004b). G-protein coupled receptor activation and the blockade of DAT by cocaine also have effects beyond AC regulation, but because this chapter was focused on CREB regulation of cocaine reward, the figure highlights the ability of cocaine to regulate CREB activity via PKA activation.

Figure 2.1. Cocaine blocks dopamine re-uptake in the brain reward pathway.
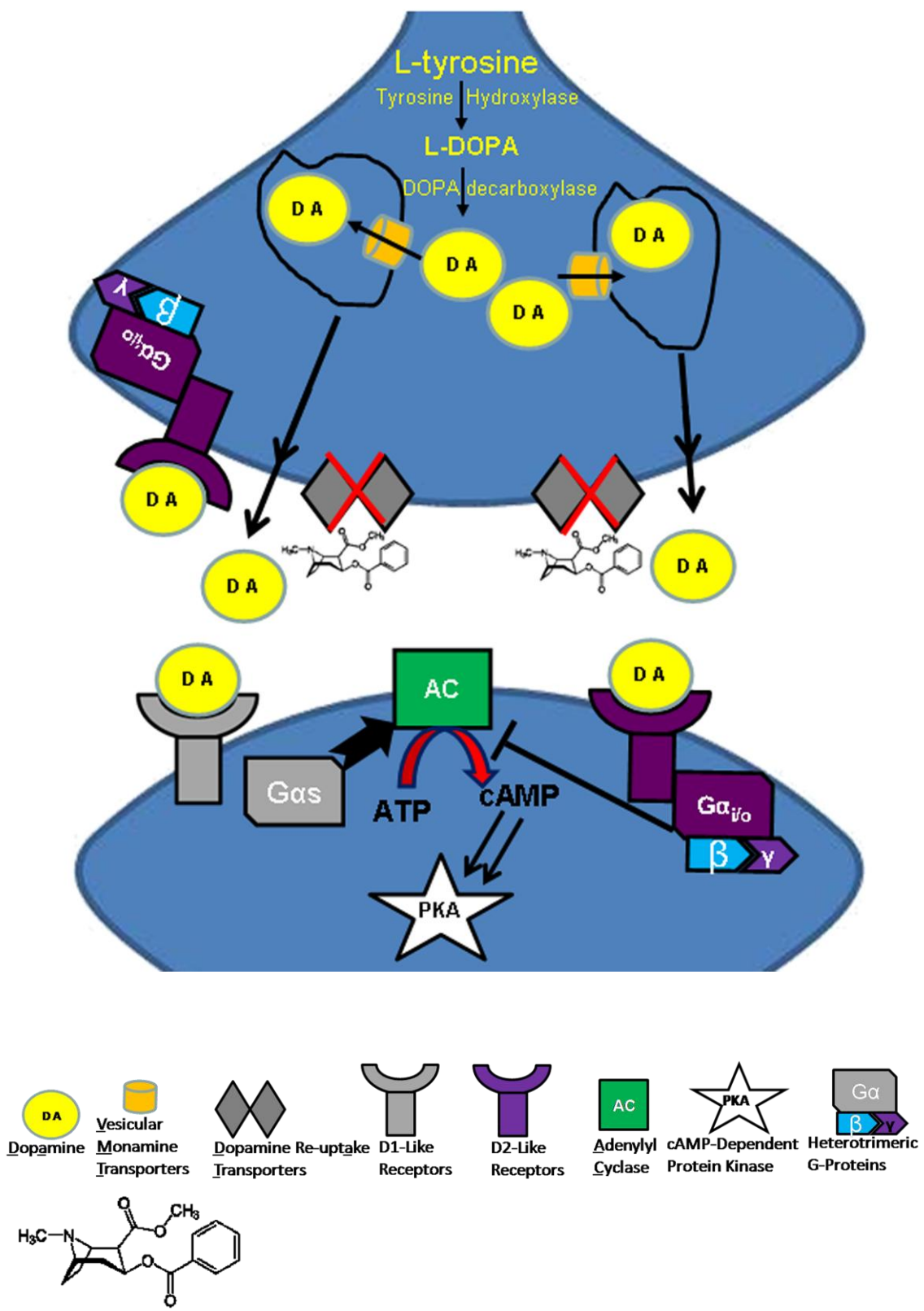
In order to treat addiction, research focused on understanding the molecular

mechanisms involved with chronic drug use. When CART was first identified in 1995,

the information being pursued was the link between cocaine- and amphetamine-

stimulated DA transmission and changes in NAc gene expression that could account for

the long-lasting molecular and behavioral changes characteristic of drug addiction. At

that time, a growing body of evidence pointed to the idea that drugs were addictive, in

part, because they caused homeostatic feedback reactions that altered the gene expression

profiles of neurons in key brain neurotransmitter systems of the reward pathway (Hope et

al 1992; Koob & Volkow 2009; Nestler & Malenka 2004). Those altered gene

expression profiles in the addicted brain caused a long-lasting disorder that required

repeated episodes of treatment because of a cycle of drug craving and seeking,

intoxication, binge use and withdrawal (Koob 2009; Koob & Volkow 2009).   That cycle,

in turn, motivated the compulsion to seek and ingest drugs, escalation of drug intake with

a loss of control in limiting drug use, and behavioral abnormalities such as continued

drug use in the face of adverse, sometimes dire consequences (Koob & Volkow 2009;

Nestler 2004b).

Researchers realized a key component of addiction was the emergence of drug

tolerance (where the same dose of a drug was no longer effective at producing the same

response) (Koob & Nestler 1997; Nestler 2004b). CREB transcriptional activity was

found to contribute to drug tolerance by up-regulating neuropeptides in the NAc such as

dynorphin (a κ opioid receptor agonist) during chronic drug intake that produced drug

tolerance by blunting drug reward (Koob & Nestler 1997; Nestler 2004b). Those same

neuropeptides up-regulated by chronic cocaine intake were then proposed to contribute to

anhedonia and dysphoria during drug withdrawal because they were up-regulated to compensate for over activation of the reward pathway by cocaine (Carlezon et al 2005). When cocaine was removed from the system during drug abstinence, substances like dynorphin became over active and created a negative mood state that was a dangerous component of psychological drug dependence (Carlezon et al 2005; Koob & Volkow 2009).

One form of drug tolerance was determined to be pharmacodynamic tolerance, where the same dose of drug was less effective because of homeostatic changes in neuronal function associated with, amongst other things: changes in pre- and post-synaptic cell surface receptor expression; altered receptor internalization dynamics or trafficking; altered intracellular protein-protein interactions; and altered 2nd messenger/effector coupling at both the pre- and post-synaptic levels (Kalinichev et al 2003). To-date, all of the mechanisms of pharmacodynamic tolerance have not been completely determined. The altered intracellular signaling patterns that manifested pharmacodynamic tolerance, though, were hypothesized to do so, in part, by coupling to the nuclear transcription machinery and altering the gene expression patterns of pre- and post-synaptic neurons via 3rd messengers such as protein kinases, like PKA, and/or phosphatases (Joyce et al 2006; Nestler 2004b). Those enzymes were found to be coupled to specific cell surface receptor-initiated intracellular signaling cascades that regulated the transcription of specific genes to possibly cause long-term adaptations (neuroplastic changes) to a changing environment such as chronic drug exposure (Koob & Volkow 2009; Nestler 2004a; b).

For example, one mechanism by which chronic cocaine intake was found to cause pharmacodynamic tolerance was up-regulation of the cAMP/PKA pathway in medium spiny, GABA-containing output neurons of the NAc (Cole et al 1995; Nestler 2004b; Terwilliger et al 1991), which were found to express both dynorphin and CART (Dallvechia-Adams et al 2002; Hubert & Kuhar 2005). The up-regulation of that whole intracellular signaling cascade occurred, in part, via up-regulation of AC I and PKA catalytic subunits, increased CREB-mediated transcription of AC subtype VIII, and down-regulation of AC-inhibitory $G\alpha_{i/o}$ proteins. Aside from increased transcription of AC VIII, the exact mechanisms of the above adaptations remained unknown (Nestler 2004b). **Figure 2.2** illustrates up-regulation of the cAMP/PKA signaling pathway in the NAc as a homeostatic, adaptive response to chronic cocaine intake. One result of increased PKA activity in the brains of cocaine exposed rats was an increase in the phosphorylation of CREB transcription factors at an activating serine 133 residue and increased P-CREB-mediated transcription of preprodynorphin (Nestler 2004b).

2.1.2 CREB transcription factors regulated cocaine reward

P-CREB was determined to be intimately involved in the neurobiological mechanisms of drug reward and reinforcement, although it was not the only TF or intracellular signaling molecule found to be affected by abused substances. Alterations in CREB activity subsequent to drug exposure represented only a small part of the complex interactions that resulted in neuroplastic changes which contributed to the long-term behavioral abnormalities characteristic of drug addiction (Nestler 2004a). That being said, manipulations of CREB and the cAMP/PKA system *in vivo*, in the NAc had

Figure 2.2. Chronic cocaine exposure caused homeostatic up-regulation of the adenylyl cyclase-protein kinase A pathway in NAc neurons. The figure illustrates one of the effects of chronic cocaine exposure in the rat ventral striatum, where DA is released from pre-synaptic VTA neurons and acts on DA G-protein coupled receptors in the membranes of post-synaptic NAc neurons. Cocaine blocks pre-synaptic DAT, indirectly increasing synaptic levels of DA and causing an excitation of NAc neurons that translates into feelings of euphoria and cocaine reward. In normal NAc neurons, D1- and D2-like receptors are functionally opposed to one another and D2-like receptors couple to $G\alpha_{i/o}$ proteins that inhibit AC activity, reducing the ability of PKA to phosphorylate target proteins such as CREB in the nucleus. In the chronically cocaine-exposed brain, however, persistent drug-induced increases in DA neurotransmission cause a down-regulation of $G\alpha_{i/o}$ proteins, which limits the ability of D2-like receptors to inhibit AC activity (represented in the figure by the dashed arrow on the right-hand side). In conjunction with that down-regulation of $G\alpha_{i/o}$, cocaine-exposed NAc neurons increase the levels of AC subtypes I and VIII (represented by the dashed arrow on the left and an arrow that originates from the nucleus pointing to an extra AC VIII molecule inserted into the cell membrane), which subsequently increases the levels of intracellular cAMP. cAMP is able to disinhibit inhibitory subunits on PKA enzymes, thus releasing the active kinase which phosphorylates CREB and other target proteins in the nucleus. PKA catalytic subunits are themselves up-regulated. Thus, a cycle of excessive cAMP formation caused by excessive $G\alpha_s$ activation, decreased $G\alpha_{i/o}$ expression and increased AC expression culminates in PKA over activity and the subsequent disregulation of P-CREB-mediated transcription in the nucleus. Increased PKA and P-CREB activities cause a shift in the gene expression patterns of NAc neurons that has not yet been completely elucidated. A major goal of drug abuse research is to identify the proteins produced as a result of the gene expression changes (such as dynorphin) that accompany chronic cocaine (and other drug) use, which could account for the gross behavioral abnormalities associated with addiction. By identifying those target genes, drugs that target them may be developed to treat addiction.

Figure 2.2. Chronic cocaine exposure causes homeostatic up-regulation of the Adenylyl Cyclase-Protein Kinase A pathway in NAc neurons.
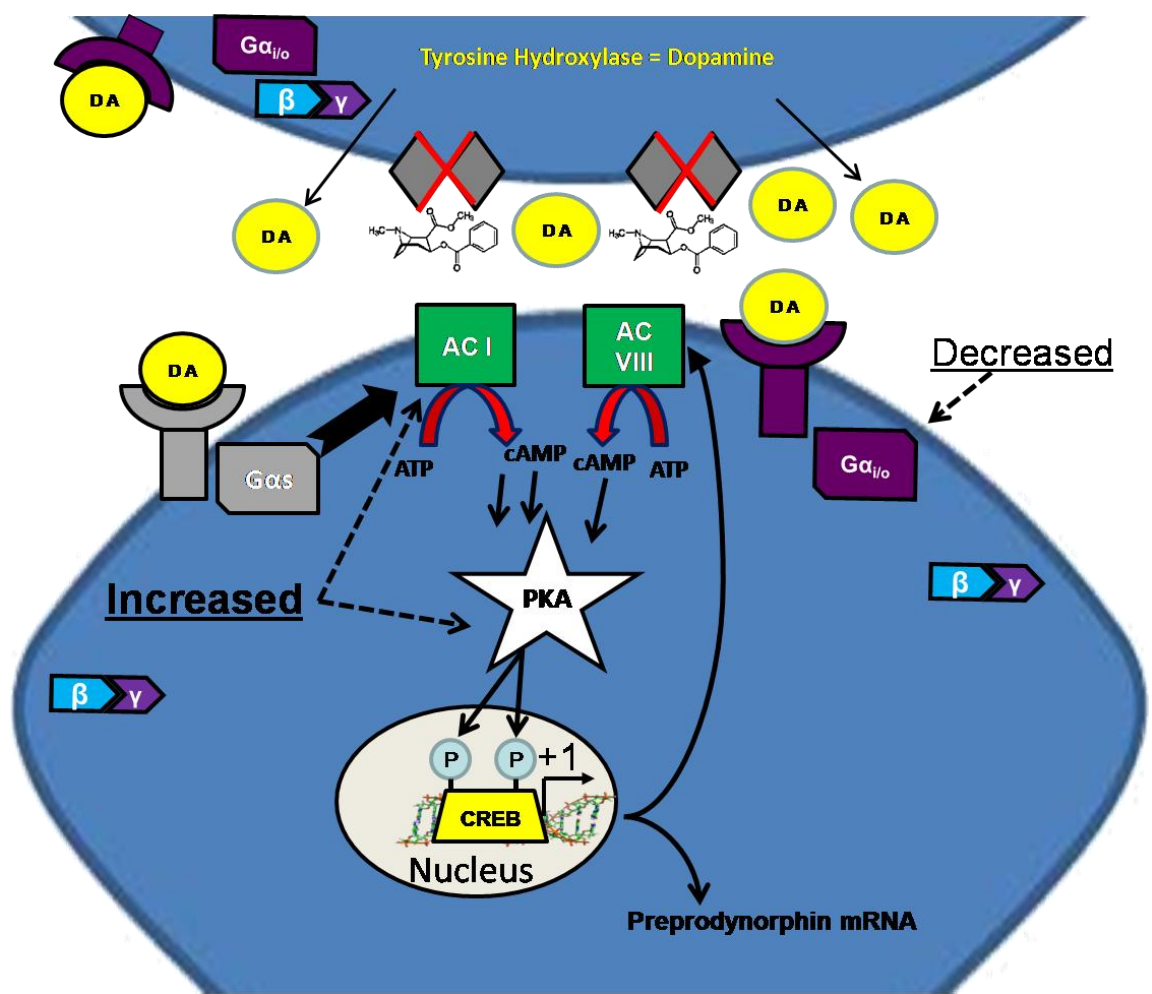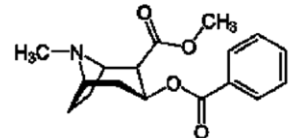
dramatic effects on such behaviors as cocaine self-administration (SA) and conditioned place-preference (CPP).

For example, the PKA activators Sp-cAMPS and dibutyryl cAMP were infused into the rat NAc and increased the levels of P-CREB while shifting the cocaine self-administration curve to the right, indicating that cocaine was less potent in animals with more PKA/CREB activity (Self et al 1998). Furthermore, intra-NAc Rp-cAMPS, an inhibitor of PKA had the opposite behavioral effect and reduced the amount of rat NAc P-CREB levels, while increasing the potency of cocaine in self-administration paradigms (Self et al 1998). These data suggested that PKA activation of CREB was a molecular mechanism of tolerance making animals less sensitive to the rewarding effects of cocaine.

Over expression of CREB itself in the rat and mouse NAc by gene transfer, using Herpes simplex virus (HSV)-1 amplicon vectors containing the CREB transgene (HSV-CREB), reduced the rewarding effects of cocaine as shown by CPP (Carlezon et al 1998; Sakai et al 2002). A dominant-negative mutant of CREB incapable of initiating transcription (HSV-mCREB) increased the sensitivity of rats and mice to cocaine (Nestler 2004a) and transgenic mice with mutations exhibited similar behaviors when CREB levels were pharmacologically tuned up or down (Sakai et al 2002). The precise mechanisms by which CREB regulated the reinforcing properties of cocaine and other drugs of abuse remained unclear. One hypothesis was that CREB was able to regulate a specific subset of genes in the brain reward pathway after drug intake that resulted in the production or down-regulation of key neuropeptides and neurotransmitters with the ability to modulate DA signaling in the brain reward pathway (McClung & Nestler 2003).

We hypothesized that CART peptides may be one of the neuropeptides regulated by CREB in the NAc. Furthermore, one mechanism by which CREB may have regulated drug reward was by increasing CART peptide levels *in vivo*.

Identifying CREB target genes in the brain reward pathway has not been an *a priori* task, though, as transcriptional regulation *in vivo,* at the level of nuclear chromatin, is a complex process requiring numerous, dynamic protein-DNA and protein-protein interactions that cannot be fully predicted based on a yet-scant understanding of the mechanisms of gene regulation. A current focus of drug abuse research has been to identify CREB target genes affected by drugs of abuse in the NAc and brain reward pathway generally (Koob & Volkow 2009; Nestler 2004b). CART peptides have been shown to decrease cocaine-reward and the CART gene may be a CREB-regulated gene in the NAc. By regulating the production of peptides such as CART subsequent to drug exposure, CREB may mediate a tolerance to repeated drug exposure that can contribute to the cycle of drug addiction in the sense that users increase the dose and quantity of drug intake and must therefore spend more time, effort and resources to acquire the drug—hallmarks of drug addiction.

2.1.3 CART gene transcriptional regulation by CREB

It was previously shown that forskolin, a direct activator of AC, regulated CART mRNA levels *in vivo*, in the rat NAc, possibly via the CRE *cis*-regulatory element. Jones and Kuhar injected forskolin into the NAc of rats and observed increased CART mRNA levels there as shown by *in situ* hybridization. That increase was blocked by both Rp-cAMPS and H89, inhibitors of PKA (Jones & Kuhar 2006). One criticism of that *in vivo*

study was that the data did not directly implicate CREB; the increases in CART mRNA may have been mediated in a non-specific fashion by forskolin or downstream by other CREB target genes activated by forskolin.

In GH3 cells, Dominguez et al observed forskolin-stimulated CART mRNA expression and H89-sensitive, forskolin-stimulated luciferase expression using the mouse CART gene promoter to drive luciferase transcription (Dominguez et al 2002). As further evidence that the CRE site in the CART gene promoter may have been involved in GH3 cell CART expression, Lakatos et al. demonstrated specific binding of CREB and P-CREB in nuclear extracts from GH3 cells to oligonucleotides identical in sequence to the mouse CART gene CRE sequence by EMSA/SS analyses using antibodies raised against CREB and P-CREB (Lakatos et al 2002). Furthermore, forskolin stimulated expression of luciferase reporter constructs driven by the CART gene promoter in Cath.a cells (derived from the locus coeruleus), and point mutations in the CRE site abolished that stimulation.

Work with cultured GH3 cells and the rat CART gene promoter also supported the notion that the CRE site mediated CART gene transcription. EMSA identified GH3 nuclear protein binding a region of the CART gene promoter containing the CRE site, forskolin stimulated rat CART promoter-driven luciferase responses in those cells, and point mutations in the CRE site itself abolished that forskolin stimulation (Barrett et al 2002). Furthermore, de Lartigue et al observed chlolecystokinin (CCK)-stimulated luciferase transcription mediated by the CART promoter in rat vagal afferent neurons. ACREB (a serine 133 mutated-to-alanine dominant-negative mutant of CREB) blocked those responses (de Lartigue et al 2007).

Although all of the above studies were convincing, the mechanisms of *in vitro* transcriptional regulation of linearized, luciferase plasmids differ from the mechanisms of transcriptional regulation of a gene in the genome *in vivo,* in a neuron, at the level of the chromatin. Due to the complexity of CREB-mediated transcription at the level of chromatin, CART promoter-driven luciferase constructs transfected into cultured cells may not have adequately represented the mechanisms of regulation of the CART gene *in vivo*, in the cell nucleus.

2.1.4 Goals of this chapter

In this chapter, because a physical interaction between CREB and the CART gene promoter has been hypothesized (Barrett et al 2001; de Lartigue et al 2007; Dominguez & Kuhar 2004; Dominguez et al 2002; Jones & Kuhar 2006; Lakatos et al 2002) but not demonstrated, and because most CART gene regulation studies were carried out with linearized luciferase plasmid constructs driven by 1 kilobase or less of the CART promoter in GH3 cells (Barrett et al 2002; de Lartigue et al 2007; Dominguez et al 2002), we tested the hypothesis that CREB and its transcriptionally active form, P-CREB, were capable of binding to a region of the rat CART promoter containing the CRE *cis-regulatory site in the native chromatin of live cells.* The goal of this portion of the thesis was to determine: 1) if CREB and P-CREB, made in rat pituitary-derived GH3 cells, could bind to the CART promoter CRE-containing region in the chromatin of live cells, *in vivo* by chromatin immunoprecipitation (ChIP) assays and; 2) if the CART gene promoter CRE site was capable of binding to CREB and P-CREB made *in vivo*, in the rat pituitary, by electrophoretic mobility shift assays (EMSA) and antibody super shift (SS)

analyses. The rationale for the latter study was that GH3 cells were pituitary-derived cells, thus it was important to show that CREB and P-CREB from the pituitary itself would bind to the CART CRE *cis*-regulatory element. CREB binding to the CART promoter CRE site was assayed in GH3 cells because the commercially available ChIP assay is a fairly new technique and not yet optimized for assaying TF-DNA interactions in dissected brain tissues (Hao et al 2008). Thus the research presented in this chapter was performed in cultured GH3 cells previously shown to express CART mRNA and CART promoter-driven luciferase after stimulation of the PKA-CREB pathway by forskolin (Barrett et al 2002; Dominguez et al 2002). By investigating a P-CREB-CART CRE interaction in the chromatin of GH3 cells, and verifying that CREB and P-CREB made *in vivo*, in the pituitary, could bind to the same CRE site, the body of evidence indicated if P-CREB could bind to the CART promoter CRE site in the nuclei of neurons. Experiments presented in the next chapter investigated CREB-CART CRE site interactions in the rat NAc.

2.2 Methods

2.2.1 Primer design and quantitative, real-time polymerase chain reaction (PCR)

Quantitative, real-time PCR reactions were performed according to the manufacturer's directions with the Applied Biosystems Step-One Plus Real-time PCR system (Applied Biosystems, Foster City, CA). Primer Express Software v3.0 (Applied Biosystems) selected the PCR primer sequences (**Table 2.1, Figure 2.3**) used in real-time PCR amplifications of the rat CART gene promoter. Primers that amplified a CRE-containing region of the c-Fos promoter were adapted from a previous publication that

Table 2.1. Primers used to amplify the CRE-containing regions of the CART and c-Fos promoters, as well as the GAPDH gene, as a normalization control in real-time PCR reactions.

Genes of interest	Genomic DNA Primer Sequences (5'-3')	Amplicon sizes (bp)	Genbank Accession Numbers
CART	Forward CCGAAGGCATTTTCCATTTC Reverse CACTGCGCTCTCCCTCTTCT	334	AF519794
GAPDH	Forward GGCACAGTCAAGGCTGAGAAT Reverse CCATTTGATGTTAGCGGGATCT	90	NM 017008
c-Fos*	Forward TTCTCTGTTCCGCTCATGACG Reverse CTTCTCAGTTGCTAGCTGCAATCG	104	AY786174

Table 2.1. Shown are the sequences of each pair of forward and reverse primers from 5' to 3', the real-time PCR predicted amplicon sizes, and each gene's Genbank accession number. The c-Fos primers were previously shown to amplify a promoter CRE site in the c-Fos gene (Hao et al 2008) and were used in positive control chromatin immunoprecipitation assays that used P-CREB antibodies. The CART primers were BLASTED and compared to genome databases for potential non-specific interactions and were found to have none.

Figure 2.3. Genomic DNA sequence of the rat CART proximal promoter region illustrates the CRE *cis*-regulatory element. Shown is the nucleotide sequence of the rat CART gene promoter (Genbank accession no. AF519794) originally identified and published by Barret et al in 2002, as well as the Genbank nucleotide numbering in the left-hand margin. The PCR primer forward and reverse sequences (corresponding to DNA sequences that are underlined, bolded and labeled as "5'-Start" and "3'-End", respectively) were recommended by Primer Express v3.0 software (Applied Biosystems, Foster City, CA). The CART gene promoter consensus CRE DNA *cis*-regulatory element is identified in bold and located between the flanking primers. That region of the promoter was amplified in PCR reactions performed after chromatin immunoprecipitations. Both the TATA box necessary to initiate promoter-driven transcription and the +1 site of CART gene transcriptional initiation are also delineated in bold to orient the reader.

Figure 2.3. Genomic DNA sequence of the rat CART proximal promoter region illustrates the CRE *cis*-regulatory element.

5'-Start (nt #807) ⟶
801 attgcc**ccga aggcattttc cattt**catgg gccctcccgc tccatatccc
851 tcaccttttg cccctcagtt tcagctctgg cccctaggga agcgtccctg
901 gctgcggggc tgacaacgtt ttgggggcag ggggtcttgt tctctgtgct
951 ccagcccatc tgtgcgcgga gcctcattcc cgggctcccg gagcccggcg

Consensus CRE site
1001 ggcat**TGACG TCA**aacggca gcggagcgct gcctacagac ggctgacccg
1051 ggctcttctc cacacccccg tccttcttct cccctccct tttcccggca

TATA box
1101 cccgatttca accggcTATA **agaagaggga gagcgcagtg** cccgagcagc

+1
⟶ Site of initiation   3'-End (nt #1140)
1151 gaggaagtcc agcacc**ATG**g agagctcccg cctgcggctg ctacccgtcc

performed ChIP with P-CREB antibodies (Hao et al 2008), and primers used to amplify

the glyceraldehyde-3-phosphate dehydrogenase (GAPDH) gene were recommended by

Applied Biosystems technical services. The CART primer sequences were BLASTED

and compared to genome databases for potential non-specific interactions and found to

have none. In each experiment, the relative quantities of DNA amplified by real-time

PCR were determined by the StepOne Plus software and the $\Delta\Delta$Ct method (Livak &

Schmittgen 2001). The specificity of DNA enriched by antibody immunoprecipitations

in ChIP assays and amplified by PCR were verified by their melting temperatures and

amplicon sizes in 2% agarose gels, that were supplemented with ethidium bromide

(Fisher Scientific, Pittsburgh, PA) electrophoresed at 100 volts at room temperature for 1

hour, and photographed using ImageOne software (Biorad, Hercules, CA).

2.2.2 Tissue culture and drug treatments

Rat pituitary-derived, GH3 cells (ATCC, Manassas, VA) were cultured on 100

cm^2 dishes in Ham's F-12 media supplemented with 10% fetal bovine serum (FBS) and

5% penicillin/streptomycin (P/S) (Life technologies, Carlsbad, California) in a

humidified incubator at 37ºC and 5% CO_2. After harvesting and lysing cells from pairs

of culture dishes without performing any drug treatment, cell lysates immunoprecipitated

with anti-CREB were treated in parallel with cell lysates immunoprecipitated with IgG

and the pairs of lysates were assayed together in real-time PCR reactions. In the case of

treatments with 7β-Acetoxy-8,13-epoxy-1α,6β,9α-trihydroxylabd-14-en-11-one

(forskolin; Sigma-Aldrich, St. Louis, MO), cells were grown to 80-85% confluency

before a 20-24 hour period of serum-starvation. After serum-starvation, the media was

replaced with 10ml of fresh Ham's F-12 media supplemented with 10% FBS and 5% P/S and either 10µl of 20mM forskolin dissolved in dimethylsulfoxide (DMSO), or 10µl of DMSO alone. Forskolin-treated cells were cross-linked in media supplemented with both 1% formaldehyde and 30nM okadaic acid (Sigma-Aldrich).

2.2.3 Nuclear protein extraction

The nuclear protein extraction protocol was adapted from Xu and Cooper (Xu & Cooper 1995). The cell pellet was resuspended in 250 µl of 1x low salt solution composed of 10mM 4-(2-Hydroxyethyl) piperazine-1-ethanesulfonic acid, N-(2-Hydroxyethyl) piperazine-N′-(2-ethanesulfonic acid) (Hepes; pH 7.6), 1.5 mM magnesium chloride, 10 mM potassium chloride, 0.5 mM dithiothreitol, 2 mM phenylmethylsulfonylfluoride (PMSF), 2.5 µM leupeptin, 1 µM pepstatin and 1.5 µM aprotinin and incubated on ice for 10 minutes. The resuspended cells were then vortexed vigorously and centrifuged at 13,000 x rpm for 10 seconds at 4ºC. The supernatant was transferred to a pre-chilled tube as the cytoplasmic fraction and stored at -80 ºC. The remaining pellet was resuspended in 50-100 µl of high salt solution composed of 20 mM Hepes, 25% glycerol, 420 mM sodium chloride, 1.5 mM magnesium chloride, 0.2 mM (ethylenedinitrilo)tetraacetic acid (EDTA), 0.5 mM dithiothreitol, 2 mM PMSF, 2.5 µM leupeptin, 1 µM pepstatin and 1.5 µM aprotinin and incubated for 20 minutes on ice. The resuspension was vigorously vortexed and centrifuged for 10 seconds at 13,000 x rpm, 4ºC. The supernatant was aliquoted and stored at -80ºC.

2.2.4 Chromatin Immunoprecipitation (ChIP) assays

ChIP assays were performed with a kit from Millipore (Billerica, MA) according to the manufacturer's instructions with the following modifications. Approximately 10^8 GH3 cells in 100 cm^2 culture dishes were cross-linked in 1% formaldehyde solution (Fisher Scientific, Pittsburgh, PA) for 20 minutes at 37ºC, washed with 1M glycine (Fisher Scientific), 1x PBS (Life Technologies) and harvested in 1-ml of 1x PBS + protease inhibitor cocktail + PMSF (Sigma-Aldrich). They were then pelleted by centrifugation at 125 x g for 8 minutes, 4ºC and the pellet was resuspended in 200µl of fresh ChIP kit SDS lysis buffer + protease inhibitor cocktail + PMSF, rotated at 4ºC for 30 minutes, and sonicated using the Sonic Dismembrator model 100 (Fisher Scientific) to shear the DNA to an average length of 300 to 500 base pairs (six, 8-s bursts at 50% maximum output power on ice). Samples were centrifuged at 14,000 x rpm for 20 minutes at 4ºC and the supernatant diluted in a fresh 2.0 ml tube with ChIP kit dilution buffer supplemented with 75µl of 1:1 salmon sperm:protein A slurry and rocked at 4ºC for 30 minutes. Afterwards, the samples were centrifuged at 1,000 x g for 1 minute, 4ºC and the supernatant was transferred to a fresh 2.0 ml tube.

As recommended by Cell Signaling Technology (Boston, MA), CREB immunoprecipitations were carried out with 6 µg of CREB antibodies and P-CREB immunoprecipitations with 0.32µg of anti-P-CREB (all antibodies were from Cell Signaling Technology). Purified anti-rabbit IgG was used as a non-specific precipitator and control. After overnight immunoprecipitation (IP) on a rotator at 4ºC, ChIP samples were then washed and eluted and DNA was un-crosslinked with NaCl and subsequently treated with proteinase K, Tris-Hcl and EDTA. DNA isolation occurred via

phenol/chloroform/isoamyl alcohol extraction (Fisher Scientific). The final DNA pellets were resuspended in ultra-pure H_2O (Life Technologies) and subjected to real-time PCR.

2.2.5 Animals and drug administration

Male, Sprague-Dawley rats weighing 250-325g, aged 6-8 weeks were housed on a 7:00 to 19:00 light-dark cycle and fed and watered *ad libitum*. All animal care and experimentation were performed with institutional animal care and use committee (IACUC) approval in accordance with the National Institutes of Health guide for the care and use of laboratory animals.

Binge cocaine administration: Cocaine HCl was received from the National Institute for Drug Abuse and dissolved in 0.9% bacteriostatic sodium chloride (saline; Hospira, inc., Lake Forest, IL) to a final concentration of 10 mg/ml. The binge administration protocol was adapted from (Brenz Verca et al 2001; Hunter et al 2005), where rats were given 4 doses of 30 mg/kg body weight of cocaine or 1 ml/kg body weight 0.9% saline every two hours intraperitoneally and sacrificed two hours after the last dose. In that study, a number of animals died or suffered seizures, thus the protocol was adapted with consideration of Fagergren and Hurd's findings that a moderate binge dosing regimen increased CART mRNA levels in the rat ventral striatum (3 x 15mg/kg every 1 hour and sacrificed 1 hour after the last injection) (Fagergren & Hurd 1999). In this study, rats were administered 4 doses of 20 mg/kg body weight or an equivalent volume of 0.9% saline by intraperitoneal injection every two hours and sacrificed 2 hours after the last injection. Rats were anesthetized with isofluorane (Abbot, Chicago, IL), decapitated by

guillotine, and their brains removed from the skull. The pituitaries were dissected from the base of the skull with pre-chilled forceps and immediately frozen at -80ºC for use in EMSA/SS assays.

2.2.6 Electrophoretic mobility shift assay (EMSA) and antibody super shifts (SS)

DNA–protein interactions were studied by EMSA/SS. Nuclear protein extracts were separated from cytoplasmic proteins in preparations detailed by Xu and Cooper (Xu & Cooper 1995). Pituitary nuclear proteins (pituitary TF) from three cocaine- or saline-treated rats were pooled together into cocaine and saline groups. Protein content was normalized by Bradford assay (Biorad) previous to pooling the animals and equal amounts of protein from each animal were used. Total nuclear protein was incubated for 45 min at room temperature with approximately 2×10^5 counts per minute (cpm) of ^{32}P-5′ end-labeled double stranded (ds) oligonucleotides which were identical in sequence to the CART promoter CRE *cis*-regulatory element (5'-CGG CGG GCA T̲T̲G̲ ̲A̲C̲G̲ ̲T̲C̲A̲ AAC GGC AGC-3'), in binding buffer composed of 10 mM Tris–HCl (pH 7.5), 50 mM NaCl, 1 mM EDTA, 5% glycerol, and 0.05 μg/μl Poly[d(I-C)] (Roche, Indianapolis, IN).

In some cases, a 50-fold molar excess of a specific competitor (non-radiolabeled CART oligonucleotide of the same sequence as the ^{32}P-labeled oligonucleotide), or 50-fold molar excess of a non-specific competitor, was added to the mixture prior to the addition of the ^{32}P-labeled CART CRE *cis*-element oligonucleotide. Non-radiolabeled, dsSP1 oligonucleotides identical in sequence to a consensus SP1 site in the mouse CART promoter (5'-TCC TTC TTC TCC C̲C̲C̲ ̲T̲C̲C̲ CTC TTC CCG GCA-3') were used as non-specific competitors in the same buffer. After a 45 minute incubation with unlabeled

oligonucleotide at room temperature, the ^{32}P-labeled CART CRE oligonucleotide was added and incubation was continued for another 45 minutes.

In the case of antibody super shift assays, 2 μg of anti-CREB (Cell Signaling Technology) or –P-CREB antibody (Santa Cruz Biotechnology, CA) were pre-incubated with the nuclear extract for 45 minutes at room temperature followed by incubation with the ^{32}P-labeled CART CRE oligonucleotide for 45 minutes at room temperature. The ^{32}P-labeled CART CRE oligonucleotide + protein complex was separated by electrophoresis on a 6% non-denaturing (80:1) polyacrylamide gel (1× TBE, 2.5% glycerin). Gels were run at 200 V in the presence of 0.5× TBE buffer for 45 minutes at 4°C. Dried gels were exposed to Kodak BioMax MR Film (Eastman Kodak Company, Rochester, NY) and images were developed in a dark room.

2.2.7 Western blot analysis

Li-Ling Chen from Dr. Kuhar's laboratory significantly contributed to these data. GH3 cells were harvested in fresh 1x PBS + protease inhibitor cocktail solution (Sigma-Aldrich), pelleted and resuspended in T-PER Tissue Protein Extraction Reagent (Thermo Scientific, Waltham, MA). Protein content between samples was normalized by Bradford assays (Biorad). Equal amounts of each sample were then combined with 4x LDS sample buffer and 10x reducing buffer (Life technologies), heated to 70ºC for 10 minutes, briefly centrifuged and loaded into 4-20% SDS-PAGE gels (Biorad). Electrophoresis occurred at 120 volts, room temperature for about two hours before overnight transfer at 25 volts, 4ºC. After transfer, the membranes were blocked with 5%

non-fat milk in 1x TBS-T (TBS + 0.1% Tween-20 [pH 7.6]) for 3 hours, and incubated with the primary antibody overnight.

The immunoreactivities of CREB and P-CREB transcription factors (approximately 45 KDa) were visualized with the same antibodies used in ChIP assays (Cell Signaling Technology). Antibodies specific to CART peptides (approximately 6.5 KDa) were supplied by the Kuhar laboratory. Immunoreactive signals were detected by using horseradish peroxidase (HRP)-conjugated anti-rabbit IgG secondary antibodies (Cell Tignaling Technology) and an enhanced chemiluminescence (ECL) kit (Amersham, Arlington Heights, IL).

Antigen pre-absorption assays: A protocol from Abcam (Cambridge, MA) was followed. 1µg primary antibody:5µg immunizing peptide were incubated at room temperature for 1 to 2 hours and diluted in 1X TBS-T before being incubated with the membrane overnight side-by-side with a separate membrane incubated with the non-preabsorbed primary antibody. Both blots were then visualized with secondary antibodies and ECL as described above.

2.2.8 Quantification of data and statistical analyses

All statistical analyses were calculated with Graphpad Prizm software (Graphpad Software, inc., La Jolla, CA). Fold-enrichment of DNA was determined by calculating the ratio of experimental values divided by control values (e.g. DNA enriched after anti-P-CREB immunoprecipitation (IP) divided by anti-rabbit IgG IP). All values were determined by the StepOne Plus Real-time PCR system (Applied Biosystems). Fold-

enrichment values were averaged together from at least 3 ChIP assays/antibody/drug

treatment and subjected to the student's one-sample t-test, which tested the hypothesis

that the mean fold-enrichment was greater than 1.0. A fold-enrichment greater than 1.0

determined by $p < 0.05$ indicated that there was more DNA enriched in a ChIP assay (e.g.

anti-P-CREB IP) compared to another ChIP assay (e.g. anti-rabbit IgG IP).

To be sure differences between samples (e.g. anti-P-CREB IP Vs anti-rabbit IgG

IP) were not simply due to different amounts of DNA being subjected to the ChIP assay,

the amount of DNA immunoprecipitated from a sample was normalized to the total

amount of DNA, defined here as the "starting material". "Starting material" was defined

as the amount of DNA in the same sample before the immunoprecipitation reaction. By

normalizing the amount of DNA immunoprecipitated to the total amount of DNA present

before immunoprecipitation (starting material), fold-enrichment values of ChIP products

from different culture dishes controlled for possible differences in the total amount of

DNA subjected to the ChIP protocol and comparisons of DNA enrichment could be made

between samples. For all experiments using anti-P-CREB, samples were normalized to

the starting material.

Although equal numbers of cells were treated in all assays, the ChIP assay had

inherent variability associated with: 1) formaldehyde cross-linking (where only about 1-

10 % of the DNA is randomly cross-linked to associated proteins); 2) washing and

harvesting; 3) DNA shearing via sonication; 4) immunoprecipitation and subsequent

wash steps; 5) elution; and 6) phenol:chloroform extraction (Hao et al 2008). The

variability associated with steps 1, 4, 5 and 6 above may not have been taken into account

when using the starting material for normalization because the total amount of DNA

saved before antibody immunoprecipitation may not have accurately reflected the amount of DNA cross-linked, washed, immunoprecipitated, eluted and extracted by phenol:chloroform.

In only the ChIP assays using CREB antibodies to enrich CART DNA, but not assays using P-CREB antibodies, we attempted to control for the variability inherent to ChIP assays by assaying the amount of GAPDH gene isolated at the end of the ChIP procedure in the exact same experimental sample, called the "input". GAPDH DNA reflected the actual amount of DNA cross-linked, washed, immunoprecipitated, eluted and isolated by phenol:chloroform extraction which was loaded into the PCR reaction and the levels of GAPDH DNA were similar between ChIP samples treated in parallel and isolated on the same days. In contrast, the CREB antibody always isolated more of the CART promoter fragment containing the CRE *cis*-element than did the IgG antibody because the CREB antibody was reacting with both a specific target (CREB proteins bound to the CART promoter) and some non-specific, background targets (which could have been bound to GAPDH DNA), while the IgG antibody just reacted with non-specific protein targets (background, which could have caused precipitation of GAPDH DNA).

Although the latter method used to normalize the quantity of CART DNA isolated by CREB antibodies compared to IgG antibodies was unconventional, the enrichment of CART promoter fragments by P-CREB-specific antibodies using the conventional method of normalization with starting material further verified that CREB could indeed bind to the CART promoter. In addition, if the fold-enrichment of CREB IP over anti-rabbit IgG IP was calculated with the equation fold-enrichment $= 2^{\Delta Ct}$ (AB technical

services) assuming equal numbers of cells were used from paired samples harvested at the same time, and subjected to ChIP in parallel, the mean fold-enrichment was 6.025 ± 1.121 ($p < 0.05$, one-sample t-test, $n = 3$ assays/antibody). Thus, the same qualitative result that CREB bound to the CRE-containing region of the CART promoter was obtained using three different methods of normalization.

The student's two-sample t-test was used to test the hypothesis that 30 minutes of forskolin treatment stimulated more P-CREB binding to the CART promoter than did 15 minutes of forskolin treatment compared to DMSO treatments. In that case, the fold-enrichment values from anti-P-CREB immunoprecipitations after 15- or 30-minutes of forskolin compared to 15- or 30-minutes of DMSO, respectively, were averaged into mean fold-enrichment values and subjected to the two-sample t-test.

A one-way ANOVA was used to determine if the ratios of forskolin- to DMSO-treated cells differed after 0, 0.5, 2.0 and 4.0 hours of treatment. Dunnette's post-hoc test was subsequently used to determine which means were different from the 0 hour untreated control. In all tests, significant differences were designated if $p < 0.05$.

Western blots were performed using pairs of forskolin or DMSO treated GH3 cells. Working with individual pairs and utilizing the ratios of each pair minimized the inter-experimental variability of raw optical density values inherent to Western blots which required varying exposure times depending on how much protein sample was present in the membrane. Protein content was variable because basal levels of P-CREB, as well as levels after 2 hours, were low and required longer exposure times. The ratios of paired samples treated for the same amount of time, however, were consistent from experiment-to-experiment and were thus used in one-way ANOVA and Dunnette's post-

hoc test to determine differences between groups. The ratios from individual time-points were determined by scanning raw Western blot data into computer files and using Scion Image software (NIH, Bethesda, MD) to quantify the optical densities of immunoreactive bands after background subtraction.

For Western blot assays that examined potential differences between binge cocaine and saline treated rats, the CART immunoreactive bands were quantified with laser scanning densitometry using Scion Image software. To compare between different autoradiographic films, the density of bands was expressed as a percentage of the average of saline treated controls. Statistical analyses were performed with the Student's two-sample t-test using Graphpad Prizm (La Jolla, CA).

2.3 <u>Results</u>

2.3.1 Chromatin immunoprecipitation (ChIP) assays identified appropriate chromatin fragments from the CART, c-Fos and GAPDH genes

Several experiments were carried out to validate the ChIP assay. **Figure 2.3** and **Table 2.1** showed the forward and reverse primers used in quantitative, real-time PCR reactions to amplify DNA enriched after ChIP assays. Specifically, **Figure 2.3** illustrated how the CART gene promoter consensus CRE DNA *cis*-regulatory element was located between the flanking primers. **Table 2.1** specified the nucleotide sequences and predicted amplicon lengths of the primers used to amplify the CRE-containing regions of the CART and c-Fos promoters. The primers used to amplify the GAPDH gene as a normalization control were shown as well. The c-Fos promoter was previously shown to bind P-CREB in ChIP assays (Hao et al 2008) and c-Fos mRNA was regulated by

forskolin treatment in GH3 cells (Herdegen & Leah 1998). It was thus used as a positive control in this study.

To verify that amplicons generated in PCR reactions were of the predicted sizes (334 base pairs [bp] for CART, 104 bp for c-Fos, and 90 bp for GAPDH), PCR products were loaded into 2% agarose gels supplemented with ethidium bromide and separated by electrophoresis (**Figure 2.4**). The data were represented as a composite figure of several gels of PCR amplicons produced in separate ChIP assays. CART promoter fragments were the predicted size of 334 bp after PCR amplification of DNA from: forskolin treatment and anti-P-CREB immunoprecipitation (IP) (lane 3); anti-CREB IP (lane 5); and GH3 genomic DNA (gDNA) isolated with a genomic DNA isolation kit from Qiagen (Valencia, CA) (lane 8). The 334 bp amplicons correlated with melting temperatures (Tm's) around 87.5ºC (**Figure 2.4B**). Slight variations in Tm values ± 1ºC were normal due to small differences in the general conditions of the final PCR products such as salt and DNA amplicon concentrations at the end of the PCR run (AB technical services personal communication). c-Fos promoter fragments were the predicted size of 104 bp (lanes 10 and 11), with melting temperatures around 80.5ºC (**Figure 2.4C**). GAPDH primers also produced a predicted 90 bp DNA fragment (lane 14), with a melting temperature around 78.5ºC (**Figure 2.4D**). Lanes 2 and 13 were negative control PCR reactions with H_2O templates and CART and GAPDH gene primers, respectively that did not produce any PCR amplicons.

2.3.2 Verification that GH3 cells contained CREB proteins and the CART gene promoter region containing the CRE site

Figure 2.4. Composite figure of gels of DNA enriched in chromatin immunoprecipitation (ChIP) assays by anti-CREB and –P-CREB antibodies and amplified in PCR reactions. A) Agarose gel electrophoresis was used to verify that PCR amplicons produced by CART, c-Fos and GAPDH primers were their predicted sizes. In the composite figure of different gels, CREB and P-CREB antibodies were used in separate ChIP assays and PCR amplicons from different assays were divided by 2 kilobase (kb) ladders (lanes 1, 4, 7, 9 and 12). CART primers produced an amplicon 334 bp long when GH3 DNA enriched by antibody immunoprecipitations (IP) (lanes 3 and 5) and GH3 genomic DNA (lane 8) were used as templates in PCR reactions. Anti-rabbit IgG IP (lane 6) was a non-specific IP control that did not significantly enrich the CART promoter. Some non-specific amplification was present below 100 bp in lanes 3, 5, 6 and 8, which were likely primer dimers that arose because of low template DNA quantities. c-Fos primers amplified a predicted 104 bp long segment of the promoter (lanes 10 and 11) and GAPDH primers likewise amplified a predicted 90 bp long DNA fragment (lane 14). **B)** Melting temperatures (Tm's) of the CART gene fragments enriched by ChIP assays using CREB antibodies (not shown) and P-CREB antibodies (a̱ and ḇ) were determined in melt curves to be approximately 87.5ºC, similar to Tm's of CART promoter fragments amplified from GH3 cell gDNA. Some non-specific amplification was observed after IgG IP (c̱), but not when H_2O was used as a PCR template (ḏ). Melt curves after 15 minutes of treatment (not shown) also revealed Tm values around 87.5ºC for CART DNA enriched by anti-P-CREB IP and IgG IP. Thus, PCR amplicons with Tm's around 87.5ºC were the predicted size of 334 bp long. **C)** The Tm's of c-Fos promoter fragments amplified from gDNA (e̱) or enriched after 15 minutes of forskolin

(<u>f</u>) or DMSO (<u>g</u>) treatment and P-CREB IP were around 80.5ºC, which confirmed the PCR amplicons were the predicted size of 104 base pairs. Some non-specific amplification of 104 bp amplicons was observed after IgG IP (<u>h</u>), but not when H_2O was used as a PCR template (<u>i</u>). **D)** The Tm's of GAPDH gene fragments amplified from gDNA or enriched after anti-CREB IP (<u>j</u>) and IgG IP (<u>k</u>) were around 78.5ºC.

The x-axis of melt curves reported the temperature in ºC at which amplicons denatured (indicated by a peak) and the y-axis reported the derivative of raw fluorescence signals. Increases in derivative raw fluorescence values occurred as dsDNA was denatured and the raw fluorescence decreased because SYBR green could no longer bind to dsDNA minor groves.

Figure 2.4. Composite figure of gels of DNA enriched in chromatin immunoprecipitation (ChIP) assays by anti-CREB and –P-CREB antibodies and amplified in PCR reactions.

A.

1) 2 Kb Ladder

2) H₂O template negative control using CART primers

3) CART DNA enriched after forskolin treatment and anti-P-CREB immunoprecipitation (334 bp)

4) New assay, 2 Kb Ladder

5) CART DNA enriched after anti-CREB immunoprecipitation (334 bp)

6) CART DNA not enriched after anti-rabbit IgG immunoprecipitation

7) New assay, 2 Kb Ladder

8) CART DNA amplified from genomic DNA as a positive control

9) New assay, 2 Kb Ladder

10) c-Fos DNA starting material after forskolin treatment (104 bp)

11) c-Fos DNA amplified from genomic DNA as a positive control

12) New assay, 2kb ladder

13) H₂O template negative control using GAPDH primers

14) GAPDH DNA enriched after anti-CREB immunoprecipitation (90 bp)

B. Melt curves of CART promoter fragments after 30m of forskolin treatment
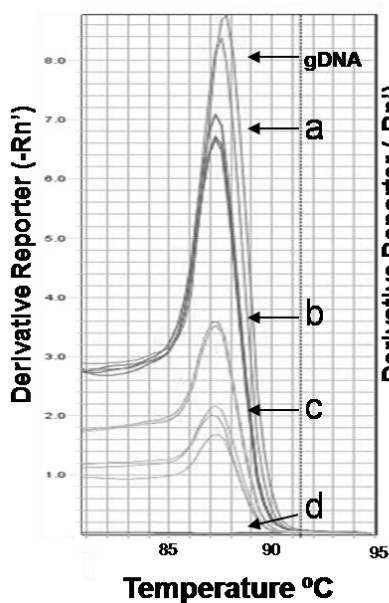
C. Melt curves of c-Fos promoter fragments after 15m of forskolin treatment
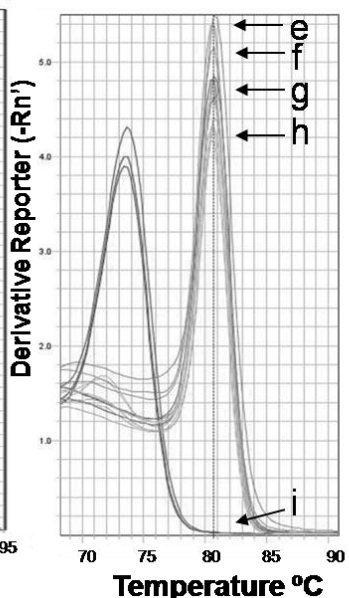
D. Melt curves of GAPDH DNA fragments
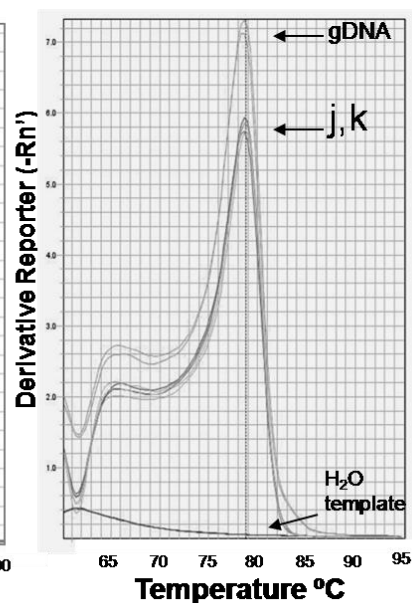
To verify that GH3 cells contained CREB transcription factors, Western blot analyses were performed and CREB was identified (**Figure 2.5A**). To also verify that GH3 cells contained the CART gene and that our assay would amplify the promoter region containing the CRE *cis*-regulatory site, GH3 cell gDNA was assayed in real-time PCR reactions using CART primers (**Figure 2.5B, a**). The amplicons were the predicted size of 334 bp (**Figure 2.4, lane 8**) and consistently amplified with Tm's around 87.5° C (**Figure 2.4B**), which confirmed that the Tm of 87.5°C correlated with an amplicon size of 334 bp and that the rat CART gene was present in GH3 cells. These results justified the use of GH3 cells in the following experiments as they expressed CREB and the rat CART gene.

2.3.3 Enrichment of the CART promoter CRE-containing region in GH3 cells by Chromatin Immunoprecipitation (ChIP) with a CREB-specific antibody

ChIP assays were carried out as described in the Methods. The use of CREB antibodies isolated more of the CART promoter region containing the CRE *cis*-regulatory element than did ChIP assays using anti-rabbit IgG antibodies (IgG) (**Figure 2.5**). The lower cycle threshold (Ct) value of sample (d) compared to sample (e) in **figure 2.5B** meant more CART DNA was enriched by anti-CREB IP compared to IgG IP.

Real-time PCR data were quantified by the StepOne Plus real-time PCR system software (Applied Biosciences) using the ΔΔCt method. In three independent experiments/each antibody, the mean enrichment of the CART promoter CRE region by anti-CREB IP was 3.383 ± 0.735 (mean ± SEM) compared to IgG control IP ($p < 0.05$, one sample t-test, n = 3 ratios; **Figure 2.5C**). Comparing just differences in Ct values

Figure 2.5. Enrichment of the CART promoter CRE-containing region in GH3 cells by ChIP assays after immunoprecipitation with a CREB-specific antibody. A) Western blot analysis identified a CREB immunoreactive band (approximately 45 KDa) from GH3 cell lysates (shown in triplicate), indicated by an arrow on the left of the gel. **B)** Representative PCR amplification plots showed: <u>a</u>) gDNA amplified by CART primers; <u>b,c</u>) DNA amplified by GAPDH gene primers as normalization controls; CART DNA enriched after <u>d</u>) anti-CREB IP and <u>e</u>) anti-rabbit IgG IP and <u>f</u>) an H$_2$O-template negative control PCR reaction amplified by CART primers. The x-axis denoted PCR cycle numbers and the y-axis indicated the ratio of dsDNA fluorescence detected by SYBR green dye (which bound the minor grove of DNA) divided by fluorescence of the passive reference ROX dye (which fluoresced irrespective of DNA) after background subtraction (where background was the amount of normalized fluorescence in cycles 1-15). The circles represented the y-axis position of the cycle threshold (Ct) setting used in relative quantitation calculations to determine fold-enrichment values. The lower Ct value of sample (<u>d</u>) compared to sample (<u>e</u>) meant more CART DNA was enriched by CREB IP compared to rabbit IgG IP. Anti-CREB IP was compared to IgG IP because IgG was expected to enrich DNA non-specifically while anti-CREB IP was expected to enrich DNA primarily bound to CREB. **C)** The ChIP assay was repeated a total of three times with CREB and IgG antibodies, and when the fold-enrichment of CART promoter DNA isolated by ChIP assays were normalized to the amount of GAPDH DNA in the same experimental sample, the mean fold-enrichment value was 3.383 ± 0.735 (mean ± SEM), statistically greater than 1.0 (*p < 0.05, one-sample t-test, n = 3 fold-enrichment ratios). **D)** In a statistical analysis that compared cycle threshold values between the

amount of CART promoter enriched after anti-CREB IP compared to anti-rabbit IgG IP

(ΔCt), assuming that an equal number of cells from paired samples subjected to ChIP in

parallel, on the same days, the mean fold-enrichment was 6.025 ± 1.121 (mean $\pm$ SEM,

*$p < 0.05$, one-sample t-test, n = 3 ratios). Fold-enrichment was calculated with the

equation fold-enrichment $= 2^{\Delta Ct}$ (AB technical services). Thus, the same result was

obtained by two different normalization methods; CART promoter fragments isolated by

anti-CREB IP were more abundant than those from IgG IP (used as a non-specific IP

control) in three separate ChIP assays, indicating that CREB was bound to the CART

promoter region containing the CRE *cis*-regulatory element.

Figure 2.5. Enrichment of the CART promoter CRE-containing region in GH3 cells by ChIP assays after immunoprecipitation with a CREB-specific antibody.
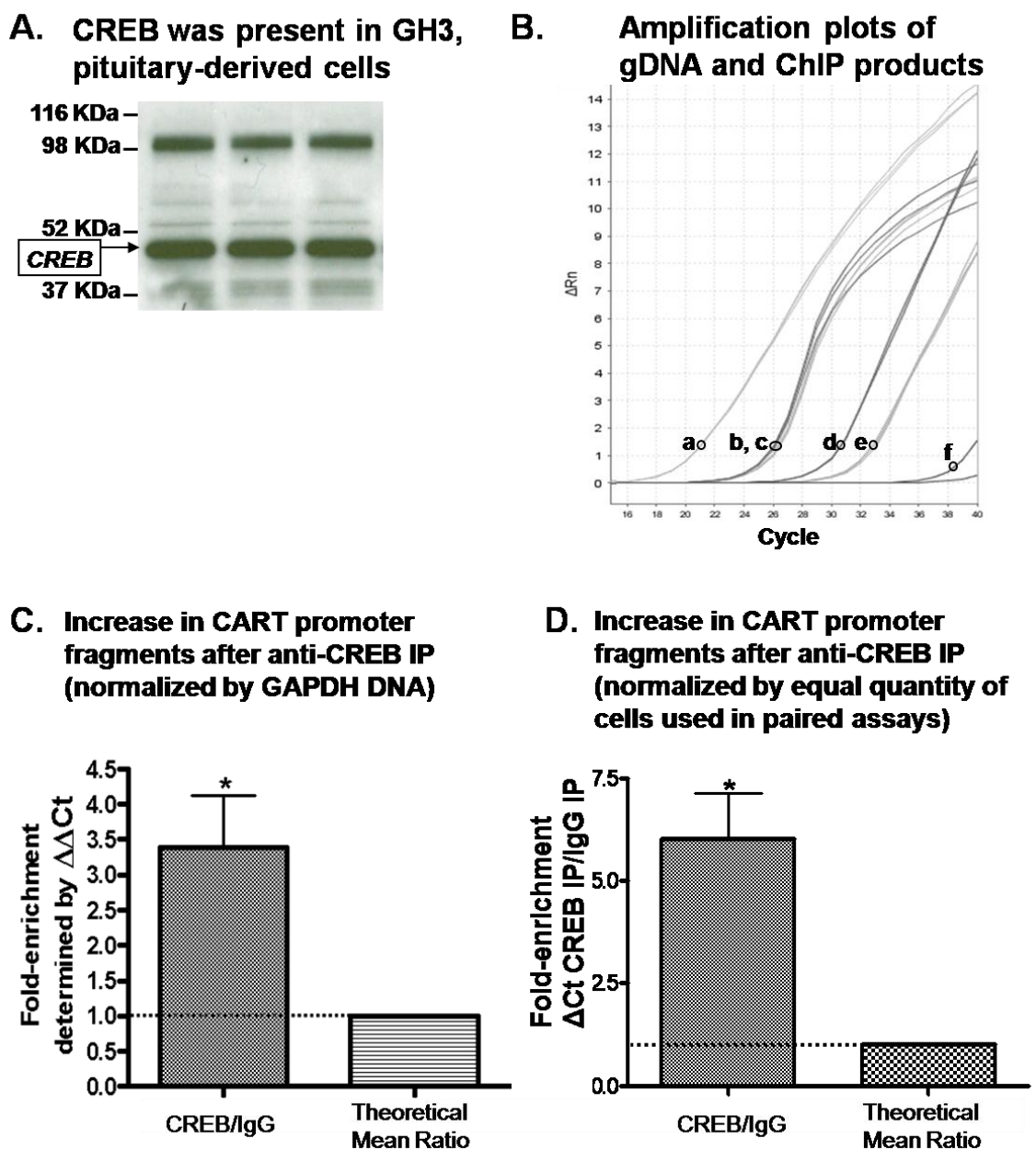
between paired samples, without normalizing to GAPDH DNA, the mean fold-enrichment of CART promoter isolated after CREB IP compared to IgG IP was 6.025 ± 1.121 (mean ± SEM, *p < 0.05, one-sample t-test, n = 3 ratios; **Figure 2.5D**). The fold-enrichment greater than 1.0 signified that a greater amount of the CART promoter was isolated by anti-CREB IP compared to IgG IP. The ChIP results indicated that CREB transcription factors were bound to the CART promoter region containing the CRE *cis-*regulatory element.

2.3.4 Western blot analyses verified that forskolin time-dependently increased P-CREB protein levels in GH3 cells

Western blot analyses were performed with antibodies specific to P-CREB (anti-P-CREB) on pairs of cultured cells that were treated with either 20μM forskolin or DMSO (vehicle) for various time periods because it was previously shown that forskolin increased CART mRNA levels in GH3 cells by a PKA-mediated pathway (Dominguez et al 2002) (**Figure 2.6A**). The data in the composite figure showed different Western blots from pairs of GH3 cell dishes treated with either forskolin or DMSO and harvested together at the different time points.

After 30 minutes of treatment, the ratio of forskolin-stimulated P-CREB levels compared to DMSO-stimulated levels was increased compared to no treatment (F [3,31] = 3.60, p < 0.05, one-way ANOVA, Dunnette's post-hoc test). The ratios of P-CREB levels in forskolin treated cells compared to DMSO treated cells at each time point were (mean ± SEM,): 0 h = 1.03 ± 0.045 (n = 3); 0.5 h = 2.07[*] ± 0.416 (p < 0.05, Dunnette's post-hoc test, n = 5); 2.0 h = 1.55 ± 0.131 (n = 4); and 4.0 h = 1.09 ± 0.140 (n = 4; **Figure**

Figure 2.6. Forskolin time-dependently stimulated P-CREB levels in GH3 cells. A)

A composite figure of representative P-CREB Western blots from the lysates of paired

plates of GH3 cells after 0.0, 0.5, 2.0 or 4.0 hours of either 20μM forskolin or DMSO

(vehicle) stimulation showed forskolin stimulation of P-CREB levels after 30 minutes of

treatment. Immunoreactive P-CREB bands (approximately 45 KDa) were indicated by

an arrow in the left-hand margin of panel. Blots from the different time points had

different raw optical densities because of differences in exposure times. Thus, the ratios

of forskolin- to DMSO-treated pairs of dishes at the individual time points were

compared to determine if forskolin stimulated P-CREB levels at that time point compared

to DMSO. The mean ratios of P-CREB levels in forskolin treated cells versus DMSO

treated cells at different time points were presented graphically in panel **(B)** (n of 3-5

groups/time point). The asterisk indicated a significantly greater ratio of P-CREB levels

in forskolin- Vs. DMSO-stimulated cells after 30 minutes of treatment compared to no

stimulation (0 hours) ($F[3,31] = 3.60$, $*p < 0.05$, one-way ANOVA and Dunnette's post-

hoc test).

Figure 2.6. Forskolin time-dependently stimulated P-CREB levels in GH3 cells.

A. **Composite serine 133 phospho-CREB Western blot from forskolin treated GH3 cell lysates**
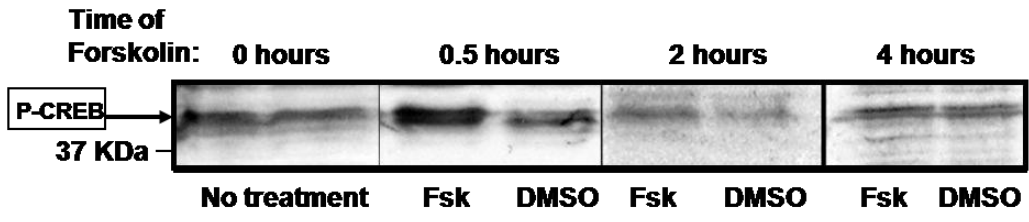
B. **The ratio of serine 133 phospho-CREB in Fsk- Vs DMSO-treated cells was significantly increased after 30 minutes of treatment**
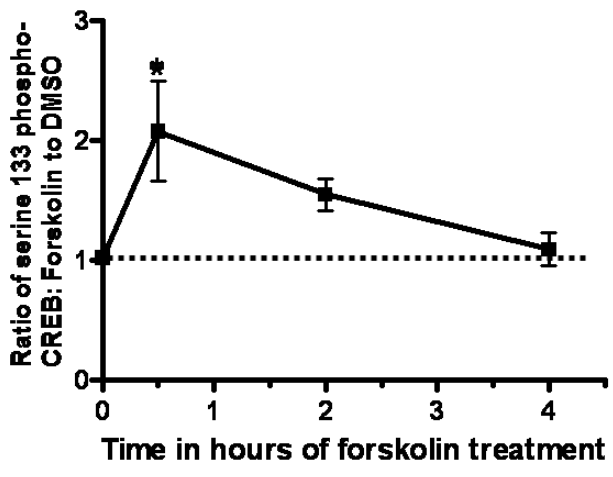
2.6B). Thus, P-CREB levels were significantly higher after 30 minutes of forskolin treatment, but not after 2 or 4 hours. These data showed that forskolin increased the amount of P-CREB protein in GH3 cells and we hypothesized that the previously demonstrated forskolin-regulation of CART mRNA in GH3 cells (Barrett et al 2001; Dominguez et al 2002) may have occurred by increased P-CREB binding directly to the CART promoter CRE site. That hypothesis was tested in the next set of experiments.

2.3.5 Enrichment of the CART promoter CRE-containing region in GH3 cells by ChIP with a P-CREB-specific antibody; effects of forskolin

 P-CREB protein values were increased most by forskolin after 30 minutes (**Figure 2.6**). Thus, to determine if forskolin likewise stimulated P-CREB binding to the CART promoter region containing the CRE *cis*-element, ChIP assays were performed with anti-P-CREB after 15 and 30 minutes of forskolin treatment. CART DNA enriched after 15 minutes of forskolin treatment and precipitated with anti-P-CREB yielded a mean fold-enrichment of 2.964 ± 0.265 (mean $\pm$ SEM) above forskolin or DMSO treatment followed by IgG IP (**p < 0.001, one-sample t-test, n $= 9$ ratios; **Figure 2.7A, 15m P-CREB/IgG**). In addition, anti-P-CREB IP of cells treated with forskolin for 15 minutes enriched more of the CART promoter than did anti-P-CREB IP of cells treated for 15 minutes with DMSO, where the mean fold-enrichment above DMSO was 2.899 ± 0.316 (mean $\pm$ SEM, **p < 0.001. one-sample t-test, n $= 9$ ratios; **Figure 2.7A, 15m Fsk/DMSO**). These data indicated that P-CREB was bound to the CART promoter after 15 minutes of forskolin treatment and that forskolin stimulated that binding compared to DMSO treatment.

Figure 2.7. Forskolin stimulation (15 min and 30 min) enhanced P-CREB binding to the CART gene promoter region containing the CRE *cis*-regulatory element as determined by ChIP assays. A) After 15 and 30 minutes of forskolin treatment, CART promoter fragments were enriched in GH3 cell lysates after anti-P-CREB immunoprecipitations (IP) compared to DNA from forskolin or DMSO treated cell lysates immunoprecipitated with IgG. The average fold-enrichment of P-CREB immunoprecipitated DNA compared to IgG immunoprecipitated DNA after 15 minutes of forskolin stimulation was 2.964 ± 0.265 (mean $\pm$ SEM) and after 30 minutes of stimulation was 5.590 ± 1.712 (mean $\pm$ SEM; **P-CREB/IgG bars)**, which indicated that P-CREB was bound to the CART promoter at those times. CART DNA was also enriched in forskolin- Vs DMSO-treated cell lysates immunoprecipitated with anti-P-CREB where the fold-enrichment of CART promoter isolated after 15 minutes of treatment was 2.899 ± 0.316 (mean $\pm$ SEM) and 5.934 ± 1.234 (mean $\pm$ SEM) after 30 minutes of treatment (**Fsk/DMSO bars**), which indicated that forskolin stimulated P-CREB binding to the CART promoter compared to DMSO treatment. The effect was time-dependent, where the mean difference between 15 minutes of treatment and 30 minutes of treatment was 3.304 ± 1.400 (mean $\pm$ SEM). In the figure, *$p < 0.05$, one-sample t-test; **$p < 0.001$, one-sample t-test; [a]$p < 0.05$, two-sample t-test. **B)** Representative PCR amplification plots of CART promoter fragments (in triplicate) showed relative DNA enrichment after: a) 30 min of forskolin and anti-P-CREB IP; b) DMSO and anti-P-CREB IP; c) DMSO and IgG IP and; d) an H_2O-template negative control PCR reaction amplified with CART primers. A slight variation in one of the triplicate samples of (a) made it appear as two separate lines. The lower cycle threshold

value for sample (<u>a</u>) compared to samples (<u>b</u>) and (<u>c</u>) indicated that more CART DNA

was enriched after forskolin treatment and anti-P-CREB IP compared to DMSO followed

by either anti-P-CREB IP or IgG IP. **C)** In determining the fold-enrichment of CART

DNA after anti-P-CREB IP compared to IgG IP, values were determined by normalizing

the amount of CART promoter enriched by anti-P-CREB IP or IgG IP to the total amount

of CART promoter present in those samples before antibody IP, defined as the "starting

material". Melt curves of starting material amplified by CART primers revealed that they

also had Tm's around 87.5ºC, which meant the DNA fragments amplified in those PCR

reactions were the predicted 334 bp long (<u>a-c</u> corresponded to the samples in panels **B**

and **C**).

Figure 2.7. Forskolin stimulation (15 min and 30 min) enhanced P-CREB binding to the CART gene promoter region containing the CRE *cis*-regulatory element as determined by ChIP assays.

A. CART promoter fragments were enriched after 15 and 30 minutes of forskolin and anti-P-CREB IP
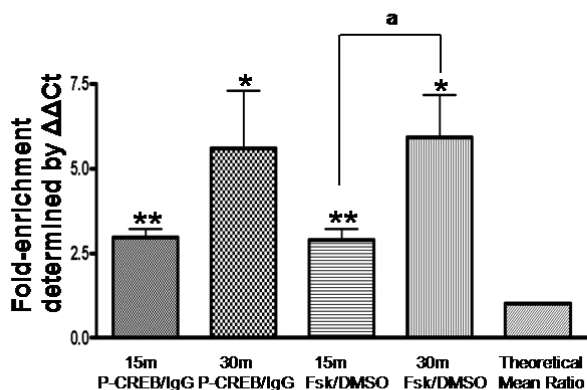
B. Amplification plots after 30m of forskolin treatment
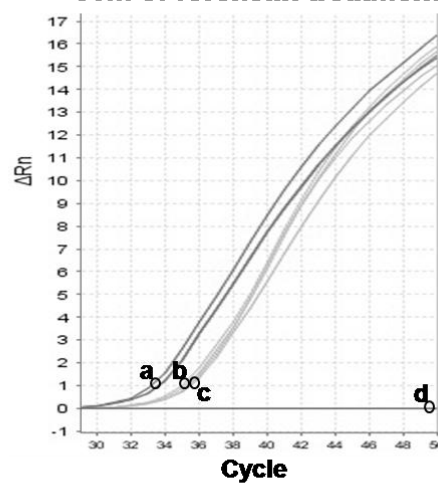
C. Melt curves of starting material after 30m of forskolin treatment
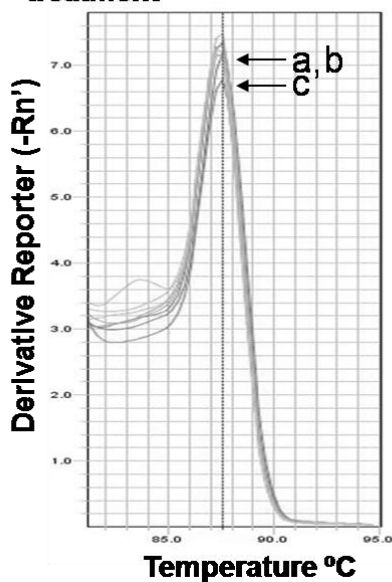
The CART promoter was also enriched by anti-P-CREB IP after 30 minutes of forskolin treatment compared to IgG IP after 30 minutes of either forskolin or DMSO treatment, where the mean fold-enrichment was 5.590 ± 1.712 (mean $\pm$ SEM, $*p < 0.05$, one-sample t-test, n = 12 ratios; **Figure 2.7A, 30m P-CREB/IgG**). When CART promoter enrichment by anti-P-CREB IP from forskolin treated cells was compared to anti-P-CREB IP enrichment from DMSO treated cells, the mean fold-enrichment above DMSO was 5.934 ± 1.234 (mean $\pm$ SEM, $*p < 0.05$, one-sample t-test, n = 11 ratios; **Figure 2.7A, 30m Fsk/DMSO**), which indicated that forskolin stimulated P-CREB binding to the CART promoter relative to DMSO treatment. After DMSO treatments for 15 or 30 minutes, anti-P-CREB IP did not enrich CART DNA compared to IgG IP (**Figure 2.7**, b compared to c), which suggested that P-CREB was not bound to the CART promoter under those conditions. There was also a time-dependence of P-CREB binding to the CART promoter, where more P-CREB was bound to the CART promoter after 30 minutes of forskolin Vs DMSO treatment compared to 15 minutes of forskolin Vs DMSO treatment, where the difference was 3.3036 ± 1.400 (mean $\pm$ SEM, [a]$p < 0.05$, two-sample t-test; **Figure 2.7A, 15m Vs 30m Fsk/DMSO**).

The data in **figure 2.7B** showed that P-CREB was bound to the CART promoter CRE-containing region and that forskolin stimulated that binding relative to DMSO as shown by the lower Ct value of (a) compared to (b) and (c). Data in **figure 2.4B** showed that the DNA isolated by anti-P-CREB and IgG IP (a, b, c) had Tm's of approximately 87.5ºC which were similar to the Tm for gDNA amplified with the same CART primers. The Tm's for some IgG immunoprecipitated DNA and H_2O amplicons were non-specific around 75ºC, which resulted in lower peaks at the 87.5ºC Tm for those samples. Melt

curves in **figure 2.7C** showed that Tm values were also 87.5ºC for CART promoter

fragments amplified from the starting material, (a-c the same as in panel **B**).

2.3.6 Enrichment of the c-Fos promoter CRE-containing region in GH3 cells by ChIP with a P-CREB-specific antibody; effects of forskolin

c-Fos, a CREB regulated gene previously found in ChIP assays to bind P-CREB

at a CRE-containing region of its promoter (Hao et al 2008), and to be regulated by

forskolin in GH3 cells (Herdegen & Leah 1998) was used as a positive control in this

study and found to bind P-CREB in GH3 cells (**Figure 2.8**). After fifteen minutes of

forskolin stimulation, the mean enrichment of the c-Fos promoter by anti-P-CREB IP was

18.01 ± 6.806 (mean $\pm$ SEM) compared to forskolin or DMSO treatment and IgG IP (*p

< 0.05, one-sample t-test, n = 8 ratios; **Figure 2.8A, P-CREB/IgG**).   When forskolin

treated cells were compared to DMSO treated cells after anti-P-CREB IP, the mean fold-

enrichment of c-Fos promoter isolated above DMSO was 2.957 ± 0.354 (mean $\pm$ SEM,

p < 0.001, one-sample t-test, n = 8 ratios; **Figure 2.8A, Fsk/DMSO).

The data in **figure 2.8B** showed that anti-P-CREB IP isolated more of the c-Fos

promoter after forskolin stimulation compared to DMSO stimulation or IgG IP after

forskolin stimulation, represented by the lower Ct value of (b) compared to (c) and (d).

Interestingly, comparing sample (c) to (d) revealed that P-CREB was bound to the c-Fos

promoter after DMSO stimulation. Thus, in contrast to the findings with the CART

promoter, these data suggested that P-CREB was bound to the CRE-containing region of

the c-Fos promoter even under DMSO-stimulated conditions and that forskolin only

slightly increased the binding to that site.

Figure 2.8. Forskolin stimulation (15 min) enhanced P-CREB binding to the c-Fos gene promoter region containing the CRE *cis*-regulatory element. A) After 15 minutes of forskolin treatment in GH3 cells and anti-P-CREB immunoprecipitations, c-Fos promoter fragments were enriched compared to DNA from forskolin or DMSO treated cells immunoprecipitated with IgG (**P-CREB/IgG**). The mean fold-enrichment was 18.01 ± 6.806 (mean $\pm$ SEM), which indicated that P-CREB was bound to the c-Fos promoter. c-Fos DNA was slightly enriched in forskolin Vs DMSO treated cell lysates immunoprecipitated with anti-P-CREB where the fold-enrichment of DNA isolated was 2.957 ± 0.354 (mean $\pm$ SEM), indicating forskolin stimulated P-CREB binding to that CRE site on the c-Fos promoter (**Fsk/DMSO**; in the figure *$p < 0.05$, **$p < 0.001$, one-sample t-test). **B)** Representative PCR amplification plots of c-Fos promoter fragments showed relative DNA enrichment after: a) forskolin treatment and anti-P-CREB IP; b) DMSO treatment and anti-P-CREB IP; c) forskolin treatment and IgG IP and; d) an H_2O-template negative control PCR reaction. The lower cycle threshold value of sample (a) compared to samples (b) and (c) indicated that the c-Fos promoter region containing a CRE *cis*-element was more enriched after forskolin treatment followed by anti-P-CREB IP compared to both DMSO treatment and anti-P-CREB IP as well as forskolin treatment and IgG IP. Furthermore, the difference in Ct values of sample (c) compared to (d) indicated that P-CREB was bound to the c-Fos promoter after DMSO stimulation. **C)** Starting material amplified by c-Fos promoters, which was used to normalize the quantity of DNA enriched by antibody IP's, also had melting temperatures around 80.5ºC, which meant the DNA fragments amplified in PCR reactions were the predicted 104 base pairs long (b-d the same as in panels **B** and **C**).

Figure 2.8. Forskolin stimulation (15 min) enhanced P-CREB binding to the c-Fos gene promoter region containing the CRE *cis*-regulatory element.

A. c-Fos promoter fragments were enriched after 15 minutes of forskolin and anti-P-CREB IP
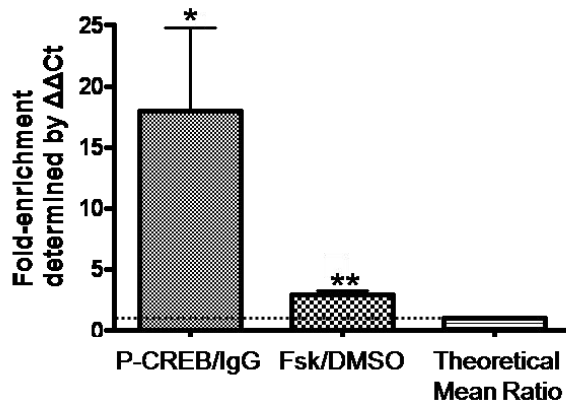
B. Amplification plots after 15m of forskolin treatment
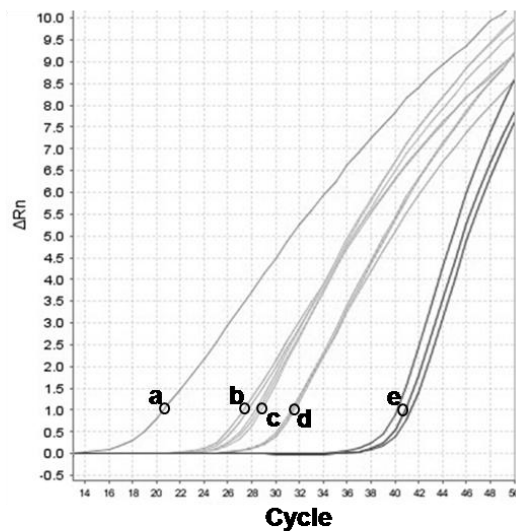
C. Melt curves of c-Fos starting material after 15m of forskolin
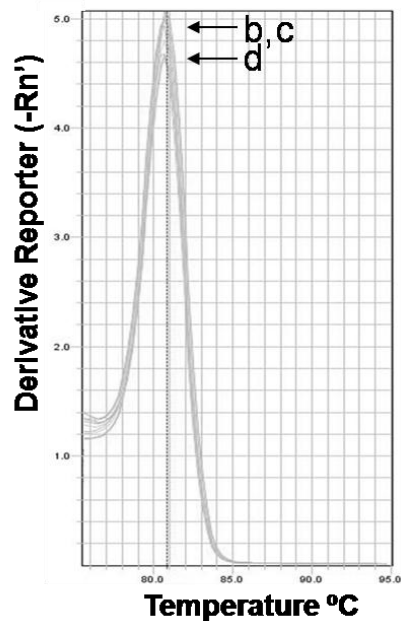
The data in **figure 2.4C** showed that the DNA isolated by anti-P-CREB IP and IgG IP (f, g, h) had Tm's corresponding to the Tm for gDNA amplified with c-Fos primers (e) of approximately 80.6°C. The data in **figure 2.4** (**lanes 10** and **11**) previously showed example c-Fos promoter amplicons with the same Tm that were the predicted size of 104 base pairs. Furthermore, starting material, which was a measure of the total amount of c-Fos promoter present in ChIP samples before antibody IP, had the same Tm around 80.6°C (**Figure 2.8C**, b-d same as in panel **B**).

2.3.7 CREB and P-CREB from the rat pituitary gland bound the rat CART promoter CRE *cis*-element in EMSA/SS assays

Having shown that CREB and P-CREB could bind to a region of the CART promoter containing a consensus CRE site in native, chromatin DNA in the nucleus of live pituitary-derived GH3 cells, we tested the hypothesis that CREB and P-CREB made in the rat pituitary itself could specifically bind to the CART CRE site. The rationale was that immortalized, cultured cell lines such as GH3 over expressed many proteins, and *in vivo*, in the pituitary, CREB may have been bound up with different TF heterodimer partners or otherwise unable to access the CRE site due to complex *in vivo* protein-protein and protein-DNA interactions that were not yet completely understood (Carlezon et al 2005; Mayr & Montminy 2001). Thus, electrophoretic mobility shift assays (EMSAs) and antibody super shifts (SS) were performed with pituitary nuclear extracts and a radioactively labeled oligonucleotide identical in sequence to the rat CART gene CRE *cis*-regulatory sequence (**Figure 2.9**).

Figure 2.9. CREB and P-CREB from the rat pituitary gland bound the rat CART CRE *cis*-regulatory element in EMSA/SS assays. Pituitary nuclear proteins (pituitary TF) from three cocaine- or saline-treated rats were pooled together into cocaine and saline groups represented as Coc and Sal in the gel, respectively. The sequence of the CART promoter containing the CRE *cis*-element from 5' to 3' (referred to as CRE) was given below the picture of the gel in the box, and the core binding sequence was underlined. The data were represented as: a negative control radioprobe alone (no protein added) reaction lane (lane 1; free ^{32}P-CRE was indicated by an arrow on the bottom left of the gel); specific protein-DNA interactions from three cocaine- or three saline-treated rats pooled together (lanes 2 and 3, respectively; the complexes were denoted by arrows at the figure's top left); competition with 50x unlabeled dsCRE oligonucleotides (lanes 4 and 5); a non-specific competition reaction with 50x unlabeled dsSP1 oligonucleotides unrelated in sequence to the CRE oligonucleotide (lanes 6 and 7); CREB antibody super shifts (lanes 8 and 9); and P-CREB antibody super shifts (lanes 10 and 11; see box at top right denoting ^{32}P-CRE + pituitary TF + antibody complex). These data showed that CREB and P-CREB in nuclear extracts from the rat pituitary had the potential to bind to the CART promoter CRE site *in vivo*.

Figure 2.9. CREB and P-CREB from the rat pituitary gland bound the rat CART CRE *cis*-regulatory element in electrophoretic EMSA/SS.

Rat, CART CRE *cis*-element sequence (5' to 3')

CGG CGG GCA TTGACG TCA AAC GGC AGC

1. ³²P-CRE rat oligonucleotide alone
2.   + Cocaine pituitary nuclear proteins (Coc)
3.   + Saline pituitary nuclear proteins (Sal)
4.   + Coc + dsCRE
5.   + Sal + dsCRE
6.   + Coc + dsSP1
7.   + Sal + dsSP1
8.   + Coc + CREB antibody
9.   + Sal + CREB antibody
10. + Coc + ser-133 phospho-CREB antibody
11. + Sal + ser-133 phospho-CREB antibody
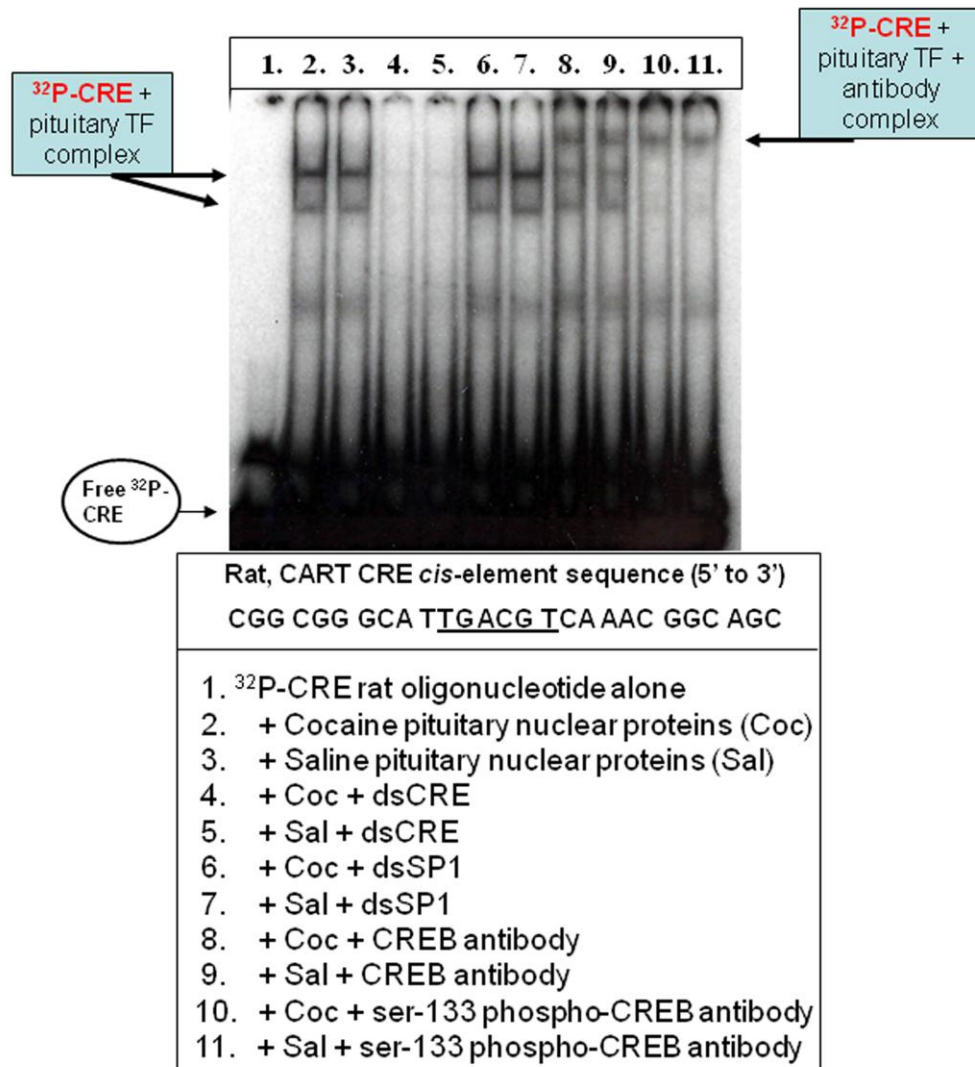
In this case, nuclear proteins were used from the pituitaries of rats treated with a binge cocaine regimen similar to one previously shown to up-regulate CART mRNA in the NAc of rats by a potentially stress-regulated mechanism (Hunter et al 2005). To date, no group had shown regulation of the CART gene in the pituitary, an important gland of the hypothalamus-pituitary-adrenal gland (HPA) axis, by cocaine and this was an attempt to do so. CART peptides were, however, not increased in Western blot assays by cocaine treatment ($p > 0.05$, $n = 8$/group, two-sample t-test; **Figure 2.10**). The specificity of the CART antibody was previously determined using antigen pre-absorption and Western blot analysis (Koylu et al 1997) and further verified in assays represented by **figure 2.11.** In the EMSA/SS assays, similar levels of CREB and P-CREB binding to the CART promoter CRE site were observed in both cocaine- and saline-treated groups as indicated by specific mobility shifts (lanes 2 and 3), specific competition with 50x non-radiolabeled CRE oligonucleotides (lanes 4 and 5) and no competition with 50x non-radiolabeled, SP1 oligonucleotides with a sequence unrelated to the CRE oligonucleotide, and antibody super shifts with CREB and P-CREB antibodies (lanes 8-11). Separate EMSA/SS analyses with untreated rats confirmed that CREB and P-CREB in nuclear extracts from their pituitaries could also bind to the rat CART promoter CRE site (not shown).

The data presented in **figure 2.9** confirmed that the CRE site in the CART promoter was able to bind to CREB and P- CREB in nuclear extracts from rat tissue, and the ChIP data presented in **figures 2.5** and **2.7** bolstered the hypothesis that CREB and P-CREB could bind to the CART promoter in its histone-bound, chromatin state in the nucleus of pituitary cells, *in vivo*.

Figure 2.10. Binge cocaine treatment did not significantly increase CART peptide levels in the rat pituitary gland. **(A)** Western blot analyses were performed with pituitary cytoplasmic proteins from rats administered a binge regimen of cocaine using antibodies specific for the C-tail portion of CART peptide (approximately 6.5 KDa). A representative Western blot showed CART peptide levels normalized to whole protein content by Bradford assay from the pituitaries of three cocaine treated (lanes marked "Coc") and three saline treated rats (lanes marked "Sal") rats. **(B)** Densitometry of the immunoreactive bands below 7KDa from a total of 8 animals/treatment group (represented graphically below the gel) revealed that there was not a statistically different quantity of CART peptides between the two groups. The mean difference between groups was 2.276 ± 6.756 (mean $\pm$ SEM, $p = 0.7389$, two-sample t-test, n = 8 cocaine, 8 saline). In some experiments CART peptide levels were normalized to Actin levels and the same result was obtained in individual experiments; the mean difference between groups was not significant.

Figure 2.10. Binge cocaine treatment did not significantly increase CART peptide levels in the rat pituitary gland.
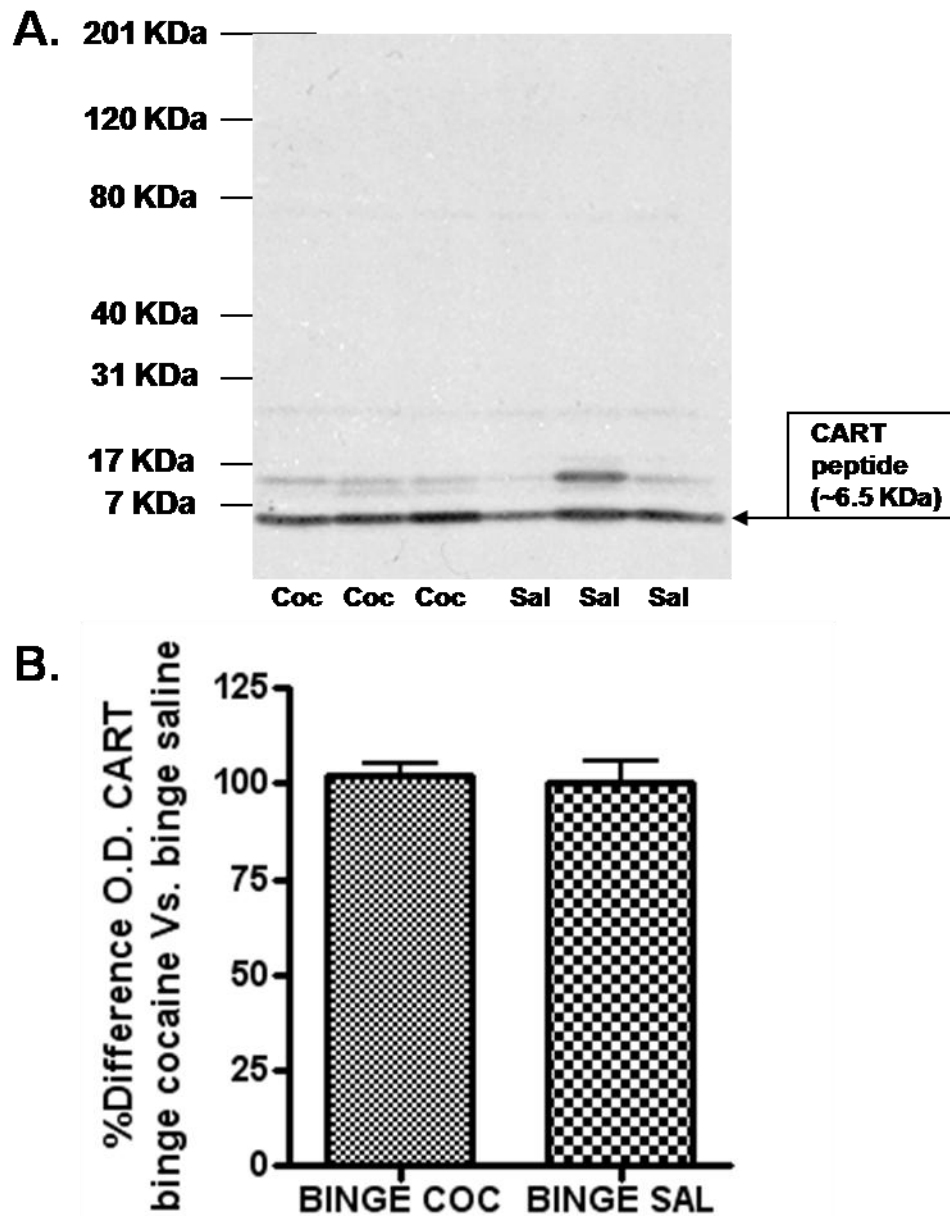
Figure 2.11. CART 55-102 peptide pre-absorption with CART antibody competed for antibody binding to proteins visualized below 7 kilodaltons in Western blots. On the left quadruplicate repeats of rat nucleus accumbens (NAc) lysates were assayed by Western blot with an antibody raised against the C-terminus of CART 55-102. The C-terminus of CART 55-102 was identical in sequence between CART 55-102 and CART 62-102 and in that way the antibody was able to recognize both peptides. CART peptides were visualized below 7 KDa as a large band, and the antibody was specific as shown by the data on the right, where the same NAc lysates were assayed by Western blot with the same antibody that had been pre-incubated with CART 55-102 peptide in an antigen pre-absorption reaction. The presence of other bands above 7 KDa, but not the large band around 6.5 KDa (identified as CART 55-102 and/or CART 62-102 based on their predicted molecular weights) indicated that although the antibody recognized some non-specific proteins from NAc lysates, it was specific in recognizing CART peptides as the primary antigen.

Figure 2.11. CART 55-102 peptide pre-absorption with CART antibody competed for antibody binding to proteins visualized below 7 Kilodaltons in Western blots.
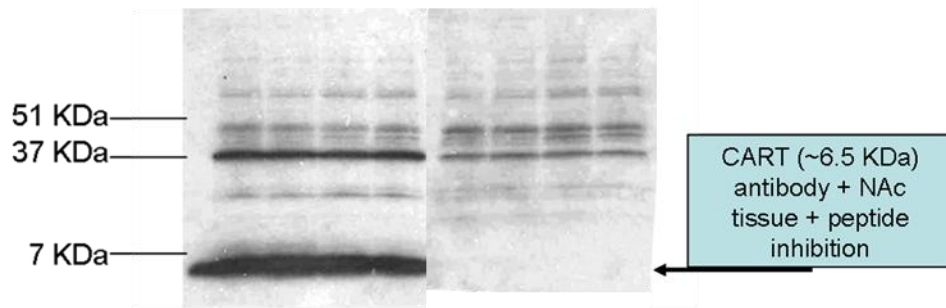
2.4 <u>Discussion</u>

There has been great interest in understanding how CART expression is regulated because, as the name suggests, expression of the cocaine- and amphetamine-regulated transcript was regulated in specific neuronal populations of key CNS and PNS regions associated with fundamental physiological processes such as feeding, drug reward, endocrine and pancreatic function, depression, anxiety and HPA axis function (del Giudice 2006; Dun et al 2000a; Hunter et al 2005; Jaworski et al 2008; Jaworski & Jones 2006; Kristensen et al 1998; Wierup et al 2004). Since the identification of a CART receptor to mediate its physiological actions has remained elusive, some of the research emphasis has been shifted to understanding CART's regulation as a means to understanding its physiological functions. For example, the work presented in this chapter linking CART gene expression to a well-characterized signaling cascade such as the PKA-CREB pathway supports a rationale to study CART's physiological importance as a CREB-regulated gene *in vivo* in relation to drug addiction.

The CART gene was described as a candidate CREB target after the promoter was cloned in 2002, but because no one gene promoter CRE *cis*-regulatory element is the same with regard to flanking sequence and global DNA topology, CREB regulation of the CART gene in the nucleus, at the level of the chromatin, was not a given. Studies have determined that flanking sequences, especially GC-rich regions directly adjacent to core CRE regulatory sequences, global DNA topology, the presence or absence of enhancer elements and other nearby *cis*-elements, variations in core CRE site sequences themselves, the position of the CRE site relative to the TATA box and accessibility of the CRE site to TFs such as CREB in the midst of the nuclear chromatin all affected the

affinity of CRE *cis*-regulatory elements for CREB family TFs in the chromatin (Carlezon et al 2005; Lonze & Ginty 2002; Mayr & Montminy 2001). As one example, the CRE element is less active in locations more than 100 base pairs upstream of the TATA box and when flanked by GC-rich sequences (Mayr & Montminy 2001).

In the rat CART gene, the consensus CRE *cis*-regulatory elementwas near a GC-rich SP1 *cis*-regulatory element at nucleotide position -146 from the site of transcriptional initiation (Barrett et al 2002). Due to the complexity of CREB-mediated transcription at the level of chromatin, the observations presented in this chapter that CREB and P-CREB physically interacted with the CART promoter CRE-containing region bolstered the hypothesis that CREB could regulate CART *in vivo*, in the nucleus of a neuron.

In vivo CREB was found to have the ability to regulate numerous, but not all, genes which contained CRE DNA *cis*-regulatory elements in their promoters (Carlezon et al 2005). Moreover, genes containing CRE elements were differentially regulated by different stimuli linked to unique intracellular signaling pathways in different tissues (Lonze & Ginty 2002; Mayr & Montminy 2001). The basic mechanism(s) of how genes containing identical core CRE regulatory elements were differentially regulated by CREB remains a prominent issue in gene regulation studies. The data presented in this chapter examining P-CREB-DNA promoter interactions in two different CRE-containing genes, c-Fos and CART, via ChIP analysis revealed a differential P-CREB binding profile between the two genes. P-CREB binding to the CART gene CRE site was stimulated by forskolin, but in the absence of forskolin P-CREB was not significantly bound to the CART promoter CRE site (**Figure 2.7B**, b compared to c). In contrast, the c-Fos gene was previously shown by ChIP to bind to P-CREB at the CRE site examined under non-

stimulated conditions (Hao et al 2008), although the effects of forskolin or DMSO on c-Fos promoter-P-CREB interactions were not previously investigated by ChIP. In our study, P-CREB was bound to the c-Fos promoter CRE site in the absence of forskolin (**Figure 2.8B**, c compared to d). Responses to forskolin after longer treatments were not tested because c-Fos mRNA was previously shown to be up-regulated within 30 minutes of stimulation by forskolin in GH3 cells (Herdegen & Leah 1998).

These data were of interest from a basic gene regulation study point-of-view because it was previously shown that c-Fos mRNA was expressed within 30 minutes after forskolin stimulation in GH3 cells (Herdegen & Leah 1998) and after the same dose of forskolin, the CART gene took 3 hours to be expressed (Dominguez et al 2002). There has been great interest in understanding the transcriptional mechanisms by which specific CRE-containing promoters were regulated by P-CREB in temporal-, cell- and stimulus-specific manners compared to other genes in the same nucleus, containing the same consensus CRE element.

Further ChIP studies regarding the temporal recruitment of P-CREB associated co-factors like CREB-Binding Protein (CBP) and transcription factor II D (TFIID) to the CART and c-Fos promoters may help to elucidate why the CART gene was less responsive to forskolin stimulation of the PKA-P-CREB pathway than the c-Fos gene. Those studies would significantly contribute to understanding basic mechanisms of differential gene regulation by P-CREB, and may elucidate why different brain regions and tissues express different patterns of CREB-regulated genes even though the genomic DNA of those tissues contain the same assortment of genes containing CRE *cis*-regulatory elements in their promoters.

The work presented in this chapter also showed for the first time that CREB and P-CREB extracted from the nuclei of rat pituitary neurons were able to specifically bind to the CRE site in the CART promoter in EMSA/SS analyses (**Figure 2.9**). That result indicated that in the pituitary, CREB and P-CREB existed in conformations and dimerization combinations with the ability to bind to the CART promoter CRE site. In conjunction with the ChIP data showing that CREB and P-CREB were able to bind to the histone-bound CRE site in the cell nucleus, the fact that pituitary proteins also bound to that site make it highly likely that CREB could regulate the CART gene in the nucleus of genes while coiled around histones in the nuclear chromatin.

Chapter 3: Regulation of CART mRNA and peptide expression by CREB in the rat nucleus accumbens *in vivo*.[1]

3.1 <u>Introduction</u>

The goal of this portion of the dissertation was to determine if CREB and P-CREB could regulate expression of the rat CART gene *in vivo*, in the rat NAc. A hypothesis about one physiological function of CART was that CART peptides in the NAc opposed the rewarding actions of cocaine by opposing the effects of dopaminergic neurotransmission (Jaworski et al 2008). Since over expression of CREB in the NAc was likewise shown to decrease cocaine-mediated reward (Carlezon et al 1998), the CART promoter contained a consensus CRE *cis*-regulatory element (Barrett et al 2002), and production of mRNA from the CART gene was regulated by cocaine and other drugs of abuse in the NAc (Douglass et al 1995; Hunter et al 2005), the <u>hypothesis</u> tested in this portion of the dissertation <u>was that CART may be a target gene for CREB in the NAc and that over expression of CREB would increase CART mRNA and peptide levels there.</u>

3.1.1 CART gene transcriptional regulation by CREB

Data presented in chapter 2 indicated that a region of the CART promoter containing a consensus CRE site could bind to CREB and P-CREB in native chromatin in the nuclei of neurons. Furthermore, an abundance of *in vitro* findings indicated that the CART gene could be regulated by CREB in cultured cells (Barrett et al 2002; de Lartigue et al 2007; Dominguez & Kuhar 2004). Studies performed *in vivo*, however, examining rat CART gene regulation in the rat NAc have not been extensively carried out. A single publication revealed that intra-NAc infusion of forskolin, a direct activator of adenylyl cyclase and thus PKA, increased rat NAc CART mRNA levels. That publication did not examine the role of CREB specifically nor forskolin-induced changes in CART peptide

levels. Thus, this portion of the dissertation directly addressed the question of whether transcription factors in nuclear extracts from the rat NAc could bind to the previously identified CART promoter CRE *cis*-regulatory element, and whether or not over expression of CREB in the rat NAc affected the levels of CART mRNA and peptides.

3.1.2 Psychostimulant regulation of CREB and its "transcriptome"

As early as 1994, amphetamine-induced activation of D1 DA receptors in the rat striatum was shown to increase rat brain P-CREB levels in the reward pathway (Konradi, 1994). CREB phosphorylation at serine 133 in the NAc was later confirmed in numerous species after cocaine administration as well as after other drugs of abuse such as methamphetamine and opiates (Nestler 2004a). At that time, it was known that P-CREB could transcriptionally regulate the immediate early gene c-Fos, an activator protein-1 (AP1) TF family member, as well as a plethora of neuropeptide genes such as proenkephalin and somatostatin in cultured cells (Konradi et al 1994; Lonze & Ginty 2002). *In vivo*, though, the consequences of CREB phosphorylation at serine 133 in the NAc after drug administration remained a mystery. It was hypothesized that active CREB would bind to CRE *cis*-regulatory elements nestled within the chromatin of certain gene promoters such as the c-Fos gene and in that way regulate the expression of those gene products.

Research thus focused on identifying a CREB "transcriptome" (the set of genes regulated by CREB in specific neuronal populations) stimulated in the brain reward pathway by cocaine and other drugs of abuse (Carlezon et al 2005; Nestler 2004b). A thorough analysis of gene promoters in the genomes of various animals revealed that

CRE DNA *cis*-regulatory elements were present upstream of the transcriptional start sites of a few thousand genes (Carlezon et al 2005; Nestler 2004b). It remained unclear how many of those genes could actually bind to CREB in the nucleus of a cell and under what conditions. It was clear, though, that not all genes containing CRE sites for transcriptional regulation were CREB target genes *in vivo* (Carlezon et al 2005).

3.1.3 The CREB superfamily of transcription factors

The factors involved in CREB's ability to regulate distinct subsets of genes within each brain region and neuron-type were discovered to be diverse and complex (Carlezon et al 2005; Lonze & Ginty 2002; Mayr & Montminy 2001; Nestler 2004a). One factor was that CREB belonged to the bZIP superfamily of transcription factors composed of both transcriptional activators and repressors that could all bind to gene promoter CRE *cis*-regulatory elements (Lonze & Ginty 2002). The superfamily members CREB and activating transcription factor-1 (ATF1) were expressed ubiquitously throughout the nervous system, while cAMP response element modulator (CREM) was abundant in neuroendocrine tissues (Lonze & Ginty 2002). Inducible cAMP early repressor (ICER) was a variant transcribed from the CREM gene induced by a cAMP-dependent mechanism involving an alternative CRE-driven intronic promoter (Mayr & Montminy 2001).

In addition to the above primary genes in the CREB superfamily, several alternative splice variants of each family member gave rise to TFs with characteristic repressor or activation potentials (Lonze & Ginty 2002; Mayr & Montminy 2001). As the bZIP superfamily name suggested, each member of the CREB superfamily could

homo- and/or heterodimerize via a zipper-like, leucine-rich alpha helical motif in the proteins encoded by highly conserved C-tail portions of each gene (Lonze & Ginty 2002; Mayr & Montminy 2001). Within that C-tail region was embedded the pH basic DNA binding domain, which allowed for all the various permutations of CREB family dimers to bind to gene promoter CRE sites (Lonze & Ginty 2002; Mayr & Montminy 2001).   In addition, the closely related AP1 superfamily of TFs could heterodimerize with CREB family members and bind to CRE as well as AP1 *cis*-elements in gene promoters (Hai & Curran 1991). The individual TFs in a homo- or heterodimer were found to affect the affinity of that dimer for CRE sites in gene promoters (Hai & Curran 1991; Lonze & Ginty 2002; Mayr & Montminy 2001).

Because all of the bZIP family members had both dimerization and DNA binding capabilities, repressors such as ICER and S-CREM (a splice variant of CREM) could heterodimerize with transcriptional activators like CREB or ATF-1 to act as dominant-negative inhibitors of transcription (Lonze & Ginty 2002; Mayr & Montminy 2001). The reason the former TFs repressed transcription was because S-CREM and ICER lacked a centrally-located 60-amino acid kinase-inducible domain (KID) which contained amino acid serine 133 in the midst of a PKA phosphorylation recognition sequence RRPSY (Lonze & Ginty 2002; Mayr & Montminy 2001).

Phosphorylated serine 133 was found to be indispensible for recruitment of the transcriptional coactivator CREB binding protein (CBP) (Carlezon et al 2005; Lonze & Ginty 2002; Mayr & Montminy 2001). When bound to phospho-serine 133 via its KIX domain, CBP had the ability to acetylate histones and subsequently recruit a larger transcriptional complex of cofactors that enabled DNA transcription by RNA polymerase

II (Carlezon et al 2005). In experiments where serine 133 was mutated to a non-phosphorylated amino acid such as alanine, CREB family members lost trans-activation potential, or the ability to recruit the transcriptional complex and initiate gene expression (Carlezon et al 2005; McClung & Nestler 2003).

3.1.4 Mechanisms of CREB-regulated transcription

The complexity of CREB-mediated transcription was compounded by the fact that CRE sequences in gene promoters varied in core sequences, flanking sequences and spatial distance from the TATA box, widely considered as the "start" site for loading of the eukaryotic transcriptional machinery (Mayr & Montminy 2001; Yanagisawa & Schmidt 1999). As a result, interactions with CREB dimers and promoter CRE sites varied in strength based on characteristics of the CRE site itself and the TF dimers that bound to it. In addition, chromatin structure in native, genomic DNA affected CREB dimer accessibility to promoter CRE sites (Lonze & Ginty 2002; Mayr & Montminy 2001).

Once CREB dimers bound to DNA, though, they were unable to initiate transcription on their own (Carlezon et al 2005; Mayr & Montminy 2001). For the initiation of transcription, CREB dimers required phosphorylation by an intracellular kinase as well as interactions with numerous co-factors and other transcription factors to initiate transcription (Mayr & Montminy 2001). Upon binding to CRE sites in the promoters of genes and subsequent phosphorylation by kinases activated by cell-surface receptor intracellular signaling cascades, such as PKA, a complex, not completely understood, series of interactions with co-factors such as CBP and (TFIID occurred.

CBP was recruited to gene promoters by serine 133 phosphorylated CREB family members and had intrinsic histone acetyltransferase activity that acetylated histone tails and opened the chromatin to allow for further TF-DNA interactions by other co-factors that modulated CREB-mediated transcription (Carlezon et al 2005; Mayr & Montminy 2001; Ogryzko et al 1996). Recruitment of CBP to gene promoters also initiated a cascade of further recruitment of the basal transcription machinery (including RNA polymerase II) which began transcribing DNA to RNA (Mayr & Montminy 2001).

3.1.5 Intracellular signaling cascades regulated CREB activity

Although amino acid serine 133 in CREB was one of the primary targets for PKA phosphorylation in neurons (Carlezon et al 2005; Lonze & Ginty 2002), an array of kinases including ERK (Mattson et al 2005), Calcium- Calmodulin-dependent Kinase (CaMK) IV (Matthews et al 1994), Protein kinase C (PKC) (Lonze & Ginty 2002), ribosomal protein SG kinases (RSKs) and v-akt murine thymoma viral oncogene homolog (AKT) (Carlezon et al 2005) all exhibited competency in phosphorylating CREB at serine 133 and initiating transcriptional responses under various conditions. It was noted that serine 133 was not the only phosphorylation site on the CREB protein. There were other sites, some of which acted as transcriptional repressor motifs such as serine 142, which upon phosphorylation by CaMK II caused dissociation of CREB family dimers and in effect reduced CREB target gene expression (Carlezon et al 2005; Matthews et al 1994). Neurons also differentially expressed proteins like phosphodiesterases and AC subtypes which could directly affect CREB superfamily

phosphorylation status and cAMP levels, respectively and cause differential regulation of CREB in distinct cell types (Mayr & Montminy 2001).

Because CREB-mediated transcription was regulated by a diverse array of kinases as well as variations in CRE *cis*-regulatory site characteristics and the expression levels of individual CREB and AP1 TF family members, putative CREB target genes were expected to encode for proteins in a cell-specific manner that modulated diverse stimulus-induced functions such as signal transduction, transcription, neurotransmission and metabolism (Lonze & Ginty 2002).

3.1.6 The goals of this chapter

The current chapter was an investigation into the transcriptional role CREB may play in mediating CART mRNA and peptide abundances *in vivo*, in the rat NAc. Since intra-NAc CART peptide injections appeared to oppose cocaine's behavioral actions, and since CREB over expression reduced cocaine reward, we hypothesized that the CART gene was a physiologic target of CREB, such that CREB over expression would increase CART mRNA and peptide levels *in vivo*, in the NAc. CREB and P-CREB were first extracted from the rat NAc and binding to an oligonucleotide identical in sequence to the CART gene consensus CRE *cis*-regulatory element and adjacent flanking sequences was assayed. To determine if NAc CREB and P-CREB binding to the CART CRE site had physiological significance, we further examined if over expression of CREB in the rat NAc was able to increase the levels of CART mRNA and peptides there.

3.2 Methods

3.2.1 Cell culture and Transfections

GH3 cells were cultured as described in **section 2.2.2**, while nuclear and

cytoplasmic proteins were separated by the method described in **section 2.2.3**. GH3 cells

were transfected with FuGENE 6 Transfection Reagent (Roche Diagnostics, Indianapolis,

IN). The dominant-negative mutant ACREB was previously packaged in the PCMV500

plasmid vector and 2 µg of either PCMV500-ACREB (ACREB) or PCMV500 alone

(PCMV) were mixed with FuGENE 6 in serum-free media and incubated at room

temperature for 45 minutes as proscribed by the manufacturer. 100 µl of the complexed

DNA/FuGENE 6 mixture were added to 1 x 10^6 cells. 24 hours later, cells were washed

and harvested in 1x phosphate buffered saline (PBS) + protease inhibitors and subjected

to the nuclear protein extraction protocol.

3.2.2 Animals and intra-accumbal injections

Male, Sprague-Dawley rats weighing 250-325g, aged 6-8 weeks were housed on a

7:00 to 19:00 light-dark cycle and fed and watered *ad libitum*. All animal care and

experimentation were performed with IACUC approval in accordance with the National

Institutes of Health guide for the care and use of laboratory animals.

Intra-accumbal injections: CREB over expression was achieved by microinjecting HSV-

1 viral vectors containing the CREB transgene (HSV-CREB) directly into the rat NAc.

In complementary assays, HSV-mCREB was microinjected into the NAc to investigate

the effects of depleting P-CREB on CART mRNA and peptide expression. Rats were

anesthetized with a mixture of medetomidine (0.5 mg/kg, IP) and ketamine (75 mg/kg,

IP). The target stereotaxic coordinates for bilateral infusions of HSV-1 amplicon vectors over expressing CREB, mCREB or LacZ as a control (relative to Bregma) were; A/P +1.6, M/L ± 1.5 and D/V -7.6 (Paxinos & Watson 2002). Injections were performed using 10 µl Hamilton microsyringes (Hamilton Co., Reno, NV) secured onto an UltraMicroPump II microsyringe injector and Micro4 Controller (World Precision Instruments, Inc., Sarasota, FL) mounted directly onto the stereotaxic frame. The bilateral NAc's were infused separately with 2 µl over 10 minutes of HSV-CREB, HSV-LacZ, or HSV-mCREB. Unilateral injections were performed on animals used in the *in situ* hybridization studies.

The above dosing regimen was optimized to reduce neurotoxicity (Carlezon et al 2000; Neve et al 2005). Dose-response analyses were not performed using graded doses of the viral vectors because our study aimed to look at the neurochemical changes associated with CREB over expression under the same conditions as those used in conditioned-place preference studies showing blunted effects of cocaine after intra-accumbal HSV-CREB injections (Carlezon et al 1998; Sakai et al 2002).

Non-replicative, HSV viral vectors were a kind gift from Dr. Nestler (Mt. Sinai, NY) generated according to published protocols. A brief description of the HSV-1 virus and how it was packaged is provided. Naturally occurring HSV-1 was a double-stranded, enveloped DNA virus with the ability to express its genome in a host cell (Carlezon et al 2000). It was a neurotropic (neuron-preferring), episomal entity that specifically infected terminally differentiated neurons (as opposed to astrocytes or glial cells) with high efficiency and used the host machinery to produce gene products from its genome

without integration into the host genome, which could cause disastrous effects such as DNA insertion that could disrupt a host gene's normal functioning (Carlezon et al 2000).

Replication-incompetent viruses had two genes that encoded for the immediate-early (IE) proteins ICP4 and ICP27 deleted. Those IE proteins were required for viral replication and replication-incompetent HSV-1 could only propagate in permissive host cells that substituted the deleted IE proteins in trans (from a DNA strand separate from the viral DNA) (Carlezon et al 2000). The HSV-1 used in this dissertation to infect NAc neurons and over express CREB, mCREB or LacZ as a control were amplicon vectors carrying the transgene DNA sequence in a plasmid incorporated with an HSV_{ori} sequence (a virus origin of DNA replication sequence) and the "a" site (a virus cleavage/packaging site) (Carlezon et al 2000). The viruses were packaged in a way that eliminated almost all wild-type virus from the final preparation and banded on a sucrose step gradient which was subjected to high-speed centrifugation to separate the virus from cytotoxic factors present in the crude cell lysates of helper cells used to package the amplicon vectors. The resulting pellet of HSV-1 transgene constructs concentrated to titers that exceeded 10^8/ml, allowing for robust expression in host neurons (Carlezon et al 2000). For comprehensive reviews and further details of how the vectors were constructed, how CREB and mCREB were incorporated and how treatment times/doses were optimized, please see references 1) (Neve et al 2005); and 2) (Carlezon et al 2000). The dominant-negative mutant, mCREB, contained a serine-133-to-alanine point mutation which prevented an activating phosphorylation at that serine 133 site. In effect, mCREB was not able to bind to CBP, a transcription factor co-regulator essential for the initiation of transcription at gene promoter CRE *cis*-regulatory elements. As a dominant-negative

mutant, though, the serine-133-to-alanine mutation in the mCREB gene did not affect hetero- and homo-dimerization with other, wild-type CREB TF family members or DNA binding to gene promoter CRE elements. The point mutation in mCREB did, however, prevent the initiation of transcription when it bound to gene promoter CRE *cis*-regulatory sites as a dimer because it could not interact with CBP (Lonze & Ginty 2002).

Experiments, except for *in situ* hybridization, were done with pairs of animals, each treated within hours of one another; for example, one member of the pair was treated with HSV-CREB and the other member of the pair with HSV-LacZ on the same day, within 1-2 hours as a control. The order of injections was reversed in alternate pairs (see below also in the statistical analysis section). The pairs were handled together in all assays and housed individually after the surgeries until approximately 36 hours post-injection when they were euthanized (see below).

NAc dissections: Rats were anesthetized with isofluorane (Abbot, Chicago, IL) and decapitated by guillotine. Brains were removed from the skull and soaked in ice-cold 0.9% bacteriostatic saline solution (Hospira, inc., Lake Forest, IL) for 10 to 15 minutes. The NAc shell and core were microdissected according to coordinates delineated in the Rat Atlas (Paxinos & Watson 2002). Dissected NAc were immediately frozen at -80ºC.

3.2.3 Nissl staining

The sites of stereotaxic injections were visualized in two control animals by Nissl stain with the generous help of Dr. Walton Hubert in Dr. Kuhar's laboratory, as well as Susan Maxson and Jeff Pare in the laboratory of Dr. Yoland Smith (adapted from

(Carlezon et al 1998). Whole brains were dissected from the rat skulls after control intra-

accumbal injections and soaked in 4% paraformaldehyde and 0.1% glutaraldehyde

(Fisher Scientific) for two nights. A freezing vibratome was then used to cut the brain

into 45μm sections that were slide mounted and dried over a formaldehyde bath in an

oven at 37ºC for 26 hours. Slides were then soaked in 95% alcohol containing 20%

formaldehyde for 5 minutes, 95% alcohol for 5 minutes, 100% alcohol for 5 minutes,

Toluene (Fisher Scientific) for 30 minutes, 100% alcohol for 5 minutes, 95% alcohol for

5 minutes, 70% alcohol for 5 minutes, 50% alcohol for 5 minutes, distilled water for 2

minutes, 0.1% thionin for 1-2 minutes (1 g thionin [Fisher Scientific]/1 liter distilled

H_2O), 1% acetic acid (Fisher Scientific) in distilled water, 1% acetic acid in 70% alcohol,

95% alcohol for 5 minutes, 100% alcohol for 5 minutes and Toluene for 5 minutes.

Slides were then covered and photographed at 1.6 x 1.0 magnification using a DC500

Leica (Allendale, NJ) camera attached to a Leica DMRB fluorescence microscope and

IM50 Leica software. One millimeter of the scale bar corresponding to 1.6 x 1.0

magnification was measured in Adobe Photoshop to determine the scale of the image.

3.2.4 *In situ* **hybridization and autoradiogram image analysis**

In situ hybridization was preformed as previously described (Jones & Kuhar

2006) with the generous assistance of Dr. Doug Jones in the Kuhar laboratory. Rats were

sacrificed 36 hours following viral infection and 14μm brain slices around the injection

site were cut on a cryostat and slide mounted. Sections were fixed in 4%

paraformaldehyde followed by consecutive washes in 2X SSC, triethanolamine/0.5%

acetic anhydride (0.1M), H_2O, 70%, 95%, and 100% ethanol, 5% chloroform, 95% and

70% ethanol, and then air dried. Slides were incubated at 37°C in pre-hybridization

buffer (50% deionized formamide, 4X SSC, 1X Denhardt's solution, 0.02M NaPO4 [pH 7.0], 1% N-lauroylsarcosine, 10% dextran sulfate) in a humidifying chamber for 2 hrs.

An oligodeoxynucleotide probe complementary to rat CART mRNA (nucleotides 223-270 (Douglass et al 1995) synthesized by Emory Microchemical Facility (Emory University, Atlanta, GA) was labeled on the 3' end with ^{35}S-dATP (NEN, Boston, MA) to a specific activity of 5 X 10^9 cpm/µl using terminal deoxynucleotide transferase (Amersham Biotech, Piscataway, NJ) and then purified with a QIAquick nucleotide removal kit (Qiagen Inc, Valencia, CA). Hybridization solution (pre-hybridization buffer plus 500 mg/l denatured salmon testis DNA and 200mM dithiothreitol) containing the CART probe (~5 X 10^5 cpm/slide) was applied to each section. Slides were hybridized overnight in a humidifying chamber at 42°C. Slides were then washed in 2X SSC, 50% ethanol/0.3M ammonium acetate, 85% ethanol/0.3M ammonium acetate, 100% ethanol, and $H_2$0. Sections were air dried and exposed to Kodak BioMax MR autoradiography film (Rochester, NY) for 10 days.

CART mRNA levels were quantified by capturing the autoradiograms with a Photometrics CoolSNAP camera (Photometrics, Roper Scientific Inc, Tucson, AZ) and analyzing with MCID Basic imaging software (Imaging Research Inc, Ontario, Canada). Relative OD was measured using an outline with a consistent area (60 x 80 pixels) centered over the NAc shell/core junction. Magnification and illumination were held constant throughout the analysis so that optical densities were within the linear portion of a standard curve. Measurements were taken through the injection site and without knowledge of treatment in brain slices at 2.2, 1.7, 1.6, and 1.2mM from bregma, which represents a major portion of the NAc.

3.2.5 EMSA and antibody super shift analyses

See **Chapter 2, section 2.2.6** for detailed methodologies. In this chapter, the dsAP2 oligonucleotide used as a non-specific competitor was identical to a putative AP2 *cis*-regulatory identified in the mouse CART promoter and the sequence from 5' to 3' used was 5'-TTC CCG GGC TCC CGG AGC CCG GCG GGC ATT-3', where the core binding sequence has been underlined.

3.2.6 Western blot analysis

The nuclear proteins from dissected NAc were separated from their cytoplasmic counterparts and each fraction was separately frozen at -80ºC as detailed by Xu and Cooper (Xu & Cooper 1995). See **chapter 2, section 2.2.3** for the nuclear extraction protocol. 25 µg of total protein determined by Bradford assay (either nuclear or cytoplasmic), were boiled for five minutes in 1:3 diluted 3x SDS sample buffer (187.5 mM Tris [pH 6.8 at 25°C], 6% [w/v] SDS, 30% glycerol and 0.03% [w/v] bromophenol blue supplemented with 125 mM DTT; Cell Signaling Technology). The mixture was quickly centrifuged and run at 120-V for two-hours on a 4-20% Biorad, pre-cast SDS-Tris-Glycine gel (Biorad). After overnight transfer at 30-V and 4°C, the membranes were blocked with 5% non-fat milk in 1× TBS-T (Tris-Buffered Saline, 0.1% Tween-20 [pH 7.6]) for 2 hours, and then incubated with the primary antibody overnight. The primary antibodies used were: CREB anti-rabbit mAb (Cell Signaling Technology); ser133 phospho-CREB anti-mouse mAb (Cell Signaling Technology); actin anti-mouse mAb (Sigma-Aldritch); histone 2B anti-rabbit mAb (Cell Signaling Technology); and CART anti-rabbit polyclonal Ab (produced by the Kuhar laboratory, Emory University,

Atlanta, GA). The signal was detected by using horseradish peroxidase (HRP)-conjugated

anti-rabbit antibodies (Cell Signaling Technology), or HRP-conjugated anti-mouse

antibodies (Cell Signaling Technology) and an enhanced chemilluminescence kit

(Amersham, Arlington Heights, IL).

CART peptide immunoreactive bands were normalized to the signals from actin

immunoreactive bands because actin was a cytoskeletal protein extracted along with

CART peptides in the cytoplasmic fraction during sample preparation from NAc tissues.

CREB and P-CREB immunoreactive bands were normalized to signals from the nuclear

localized histone 2B proteins identified in nuclear fractions of samples prepared from

NAc tissues. Antigen pre-absorption assays were performed as described in **Chapter 2**,

section 2.2.6.

3.2.7 Quantification of data and statistical analyses

Western and EMSA raw data were digitally scanned into computer files. Scion

Image software (NIH, Bethesda, MD) was subsequently used to quantify the optical

densities of individual Western bands. Briefly, the optical densities were obtained by

first outlining the Western band of interest and measuring its optical density. Three

geometrically identical areas above or below the band of interest, but separate from other

bands in the same lane as well as the band of interest, were measured as background.

The average of those background optical densities was subtracted from the band of

interest's optical density to calculate the Western band of interest optical density.

As noted in the text, experiments were carried out with pairs of animals. A "pair"

was defined as two sequentially treated animals, one with the LacZ vector (HSV-LacZ)

as a control, and the other with a CREB expressing vector (HSV-CREB) or with a

dominant negative mutant vector of CREB (HSV-mCREB) within hours. The

experimental values from HSV-CREB or HSV-mCREB animals in each pair were

divided by the value from the HSV-LacZ vector controls to produce a ratio. The ratios of

results from paired animals (4-8 pairs and ratios/group depending on the protein

examined) were subjected to a one-sample student's t-test to determine if the ratio

significantly differed from 1.00 (Motulsky 2003). Ratios were considered significantly

different from 1.00 if $p < 0.05$. A ratio greater than 1.0 indicated a significant increase

over control, and a ratio less than 1.0 indicated the opposite. Working with individual

pairs and utilizing the ratio of each pair minimized inter-experiment variability such as

that due to diurnal variations in CART levels with time of day (Vicentic et al 2005b),

small variations in the time of sacrifice, possible decay of viral vectors over time, and the

use of different batches of viral vectors. The statistical tests were performed using

Graphpad Prizm software (Graphpad Software, inc., La Jolla, CA).

3.3 Results

3.3.1 EMSA/SS analyses of the CART promoter CRE and NAc nuclear proteins

An oligonucleotide 27 base pairs in length, containing the CRE *cis*-regulatory

element and adjacent sequences identical to those found in the rat CART gene promoter

(Barrett et al 2002), was examined in EMSA/SS assays with nuclear extract proteins from

the rat NAc. Nuclear extract proteins from the rat NAc added to radiolabeled

oligonucleotides containing the CART gene consensus CRE core binding site and

flanking sequences (^{32}P-CRE) resulted in a shift in the mobility's of the ^{32}P-CRE

oligonucleotides in polyacrylamide gel electrophoresis separations (**Figure 3.1**). The binding of ^{32}P-CRE oligonucleotides to nuclear extract proteins was blocked by excess double-stranded CRE oligonucleotides but not by unrelated, double-stranded AP2 oligonucleotides, which indicated specificity of the binding. Addition of anti-CREB or -P-CREB antibodies to the ^{32}P-CRE + TF complex resulted in super shifted bands. The interpretation of these data was that CREB and P-CREB, as they existed in the rat NAc, were able to bind to the CART promoter CRE site and potentially regulate gene expression in that brain reward pathway region.

In the following set of experiments, we tested the hypothesis that CREB over expression could increase CART mRNA and peptide levels, potentially by increasing the quantity of TFs bound to the CART promoter CRE site. To bolster the rationale for using Western blots and EMSA/SS assays to examine that hypothesis, a set of experiments using GH3 cell nuclear extracts and ACREB, a dominant-negative mutant of P-CREB where serine 133 was mutated to a non-phosphorylatable alanine, were done to show that: 1) changing P-CREB levels in the cells could affect TF binding to the CART promoter CRE oligonucleotide; 2) the EMSA was a semi-quantitative assay that could detect differences in levels of TF binding to the CRE site; and 3) the Western analysis was also semi-quantitative and could detect changes in protein levels. Antigen pre-absorption assays were also executed with the P-CREB specific antibody to ensure its specificity.

CREB and P-CREB were super shifted in EMSA/SS assays that examined GH3 cell TF binding to the CART promoter CRE site ((Lakatos et al 2002) and **Figure 3.2**).

Figure 3.1. Oligonucleotides containing the CART promoter CRE *cis*-regulatory element bound to CREB and P-CREB in nuclear extracts from the rat NAc. EMSA and super shift analyses were performed using nuclear proteins from the NAc (the gel is representative of at least five other animals assayed separately in independent experiments). The sequence of the region of the CART promoter containing the CRE *cis*-element (the 27mer is referred to as the "CRE") is given below the picture of the gel in the box, and the core binding sequence is underlined. The data in lane 1 showed a negative control where only the ^{32}P-CRE probe was loaded but no protein (some non-specific protein binding is seen at the bottom of the gel along with free ^{32}P-CRE). In lane 2, nuclear proteins from the NAc bound to the radioprobe which reduced the mobility of the radioactive protein-DNA complex (denoted by a boxed arrow at the figure's top left). Lane 3 was a competition reaction with 50x non-radiolabeled CRE and lane 4 was a non-specific competition reaction with 50x non-radiolabeled AP2 oligonucleotides unrelated in sequence to the CRE. The identities of the proteins in the ^{32}P-CRE + NAc TF complex were determined by antibody super shift analyses using either CREB- or P-CREB-specific antibodies (see box at top right denoting the ^{32}P-CRE + NAc TF + antibody complex, lanes 5 and 6). Figure reproduced from (Rogge et al 2009), with permission from Elsevier Science.

Figure 3.1. Oligonucleotides containing the CART promoter CRE *cis*-regulatory element bound to CREB and P-CREB in nuclear extracts from the rat NAc.
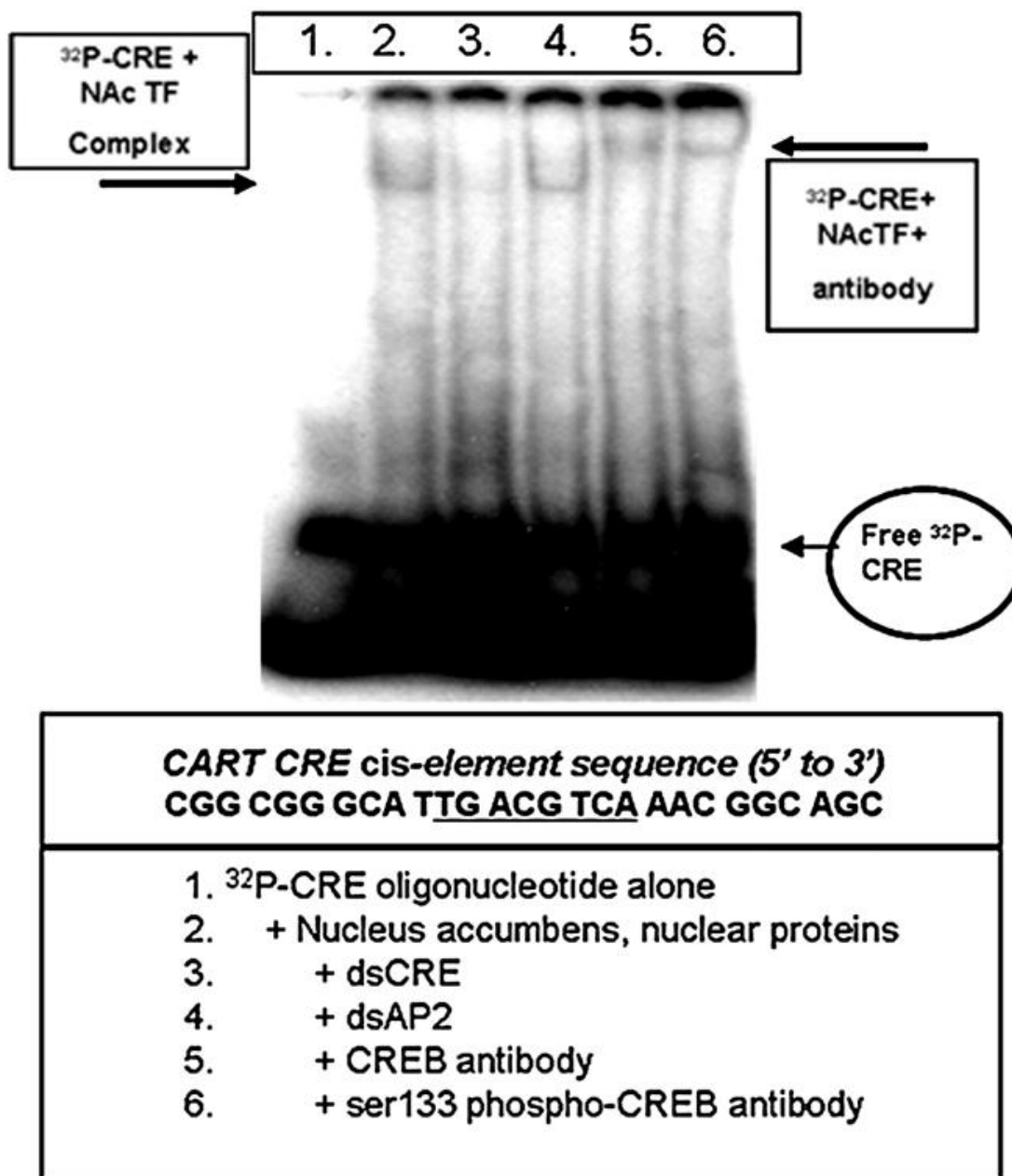
Figure 3.2. PCMV-ACREB (s133a) treated GH3 cells showed reduced CREB and P-CREB binding to the CART promoter CRE *cis*-regulatory element compared to PCMV (vector alone) treated cells. The EMSA/SS assay shown used nuclear proteins from GH3 cells transfected with either PCMV-ACREB (ACREB) or PCMV-alone as a vector control (n = 2/group). The sequence of the region of the CART promoter containing the CRE *cis*-element is given below the picture of the gel in the box, and the core binding sequence is underlined. Lane 1 was a negative control where only the ^{32}P-CRE probe was loaded but no protein (free ^{32}P-CRE is denoted at the bottom right of the gel) ; lanes 2 through 7 showed binding of proteins to the radioprobe, which reduced the mobility of the radioactive protein-DNA complex (indicated by the boxed arrow at the top left of the gel). The identities of the proteins in the ^{32}P-CRE + GH3 TF complexes were determined by antibody super shift analyses using either CREB- or P-CREB-specific antibodies (see box at top right denoting the ^{32}P-CRE + GH3 TF + antibody complex, lanes 8-12). In this experiment, over expression of the dominant-negative mutant of P-CREB, ACREB, resulted in reduced binding of nuclear proteins to the CART promoter CRE sequence (lanes 2, 4 and 6) compared to vector-alone treated controls (lanes 3, 5 and 7). In addition, CREB and P-CREB antibody super shifts of ACREB transfected GH3 TF + ^{32}P-CRE complexes had reduced optical densities compared to vector alone-treated control cells, indicating that there was less CREB and/or P-CREB bound.

Figure 3.2. PCMV-ACREB (s133a) treated GH3 cells showed reduced CREB and P-CREB binding to the CART promoter CRE *cis*-regulatory element compared to PCMV (vector alone) treated cells in EMSA/SS assays.

Rat, CART CRE *cis-element* sequence (5' to 3')
CGG CGG GCA TTG ACG TCA AAC GGC AGC

1. ^{32}P-CRE rat oligonucleotide alone	7. + GH3 PCMV nuclear proteins
2. + GH3 ACREB nuclear proteins	8. + GH3 ACREB + CREB antibody
3. + GH3 PCMV nuclear proteins	9. Empty
4. + GH3 ACREB nuclear proteins	10. + GH3 PCMV + CREB antibody
5. + GH3 PCMV nuclear proteins	11. + GH3 ACREB + P-CREB antibody
6. + GH3 ACREB nuclear proteins	12. + GH3 PCMV + P-CREB antibody

In the assay presented in **figure 3.2**, GH3 cells were transfected with plasmids that over expressed PCMV-ACREB (ACREB) or the empty vector PCMV. ACREB reduced the amount of TF binding to the CART CRE site. The over expression of ACREB also reduced the amount of P-CREB protein, but not CREB, in the same cells (**Figure 3.3**).

In separate experiments with NAc lysates, the specificity of the P-CREB antibody was determined by antigen pre-absorption using the peptide epitope for anti-P-CREB (**Figure 3.4**). Moreover, the data in **figures 3.5** and **3.6** indicated that proteins visualized by Western blot and protein-DNA interactions visualized by EMSA could be measured semi-quantitatively because increasing concentrations of protein correlated with increasing optical densities of P-CREB proteins in Western assays and ^{32}P-CRE + TF complexes in EMSAs.

3.3.2 Effects of CREB over expression by viral vectors on CART mRNA and peptide levels in the rat NAc

In order to manipulate CREB levels, animals were injected intra-NAc with non-replicative Herpes-simplex (HSV) viral vectors (**Figure 3.7**) as described in the Methods. In the NAc of animals treated with HSV-CREB viral vectors, there was an over expression of CREB protein as measured by Western blot analysis (**Figure 3.8, Table 3.1**). The mean ratios of CREB levels in treated animals compared to control animals was greater than one (ratio of 1.42 ± 052; mean $\pm$ SEM) and significant (*p = 0.0013, n = 5 pairs). P-CREB levels were not significantly changed (ratio of 0.81 ± 0.171; mean $\pm$ SEM, p = 0.355, n = 4 pairs, **Figure 3.9**, **Table 3.1**). CART peptide levels, though, were significantly increased in animals treated with HSV-CREB compared to HSV-LacZ

Figure 3.3. Western blot analysis of ACREB (s133a) treated GH3 cells showed reduced P-CREB, but not CREB, protein levels compared to PCMV (vector alone) treated cells. Equal amounts of lysates from GH3 cells transfected with either PCMV-ACREB (ACREB) or PCMV-alone as a vector-alone control (n = 2/group) were assayed by Western blot analysis for CREB and P-CREB (approximately 45 KDa) protein content using specific antibodies. Each lane was normalized to whole protein content by Bradford assay. The arrow on the right indicates CREB and P-CREB immunoreactive bands below 52 KDa. The data in the blot on the left showed proteins from two separately transfected plates/group (PCMV-alone lanes 1 and 3, ACREB lanes 2 and 4) visualized with CREB-specific antibodies. The data showed no differences between groups. On the right, proteins from the same transfected plates/group (PCMV-alone lanes 5 and 7, ACREB lanes 6 and 8) were visualized with P-CREB antibodies. As expected, ACREB transfected cells had significantly reduced amounts of P-CREB compared to PCMV-alone transfected cells because the mutation of serine 133 to alanine inhibited phosphorylation at that site, and the antibody was unable to interact with as many P-CREB molecules in the cells lysates.

Figure 3.3. Western blot analysis of PCMV-ACREB (s133a) treated GH3 cells showed reduced P-CREB, but not CREB, protein levels compared to PCMV (vector alone) treated cells.

CREB and P-CREB (~45 KDa) + GH3 lysates

98 KDa

52 KDa
37 KDa
29 KDa

CREB	P-CREB
1. PCMV	5. PCMV
2. ACREB	6. ACREB
3. PCMV	7. PCMV
4. ACREB	8. ACREB
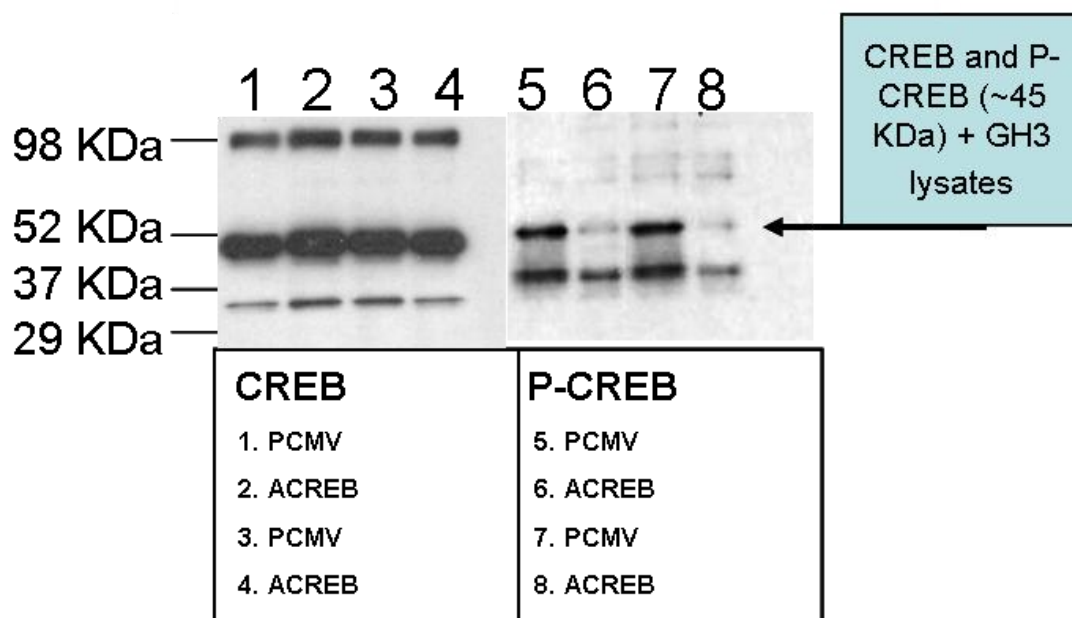
Figure 3.4. Antigen pre-absorption assays with anti-P-CREB and the peptide epitope it was raised against verified that the immunoreactive band below 52 KDa was specific in identifying P-CREB in Western blot assays. NAc lysates were assayed in a Western blot with an antibody raised against the phosphorylated serine 133 region of P-CREB (approximately 45 KDa). P-CREB was visualized below 52 KDa as a large band and some bands were also observed just above 39 KDa. Lane 1 showed P-CREB immunoreactivity in the NAc lysate. Lane 2 showed that immunoreactivity was reduced by pre-treating the NAc lysate with Antarctic phosphatase, a dephosphorylating enzyme. Although the band below 52 KDa was not completely ablated, it, along with a band around 90 KDa (possibly P-CREB dimers) and the 39 KDa band were reduced in intensity. In lane 3, untreated NAc lysate was probed with the anti-P-CREB antibody that had been pre-incubated with the peptide antigen it was raised against. The data showed that the possible dimers around 90 KDa were significantly reduced and the immunoreactive band below 52 KDa was completely competed away, indicating that the peptide antigen competed for antibody binding to that protein in the Western and it was most likely the P-CREB protein. Again, the bands above 39 KDa were present, but lessened in intensity. Pre-treating the NAc lysate with Antarctic phosphatase and probing with antigen pre-absorbed anti-P-CREB (lane 4) did not further reduce the intensity of the P-CREB immunoreactive band below 52 KDa.

Figure 3.4. Antigen pre-absorption assays with anti-P-CREB and the peptide epitope it was raised against verified that the immunoreactive band below 52 KDa was specific in identifying P-CREB in Western blot assays.
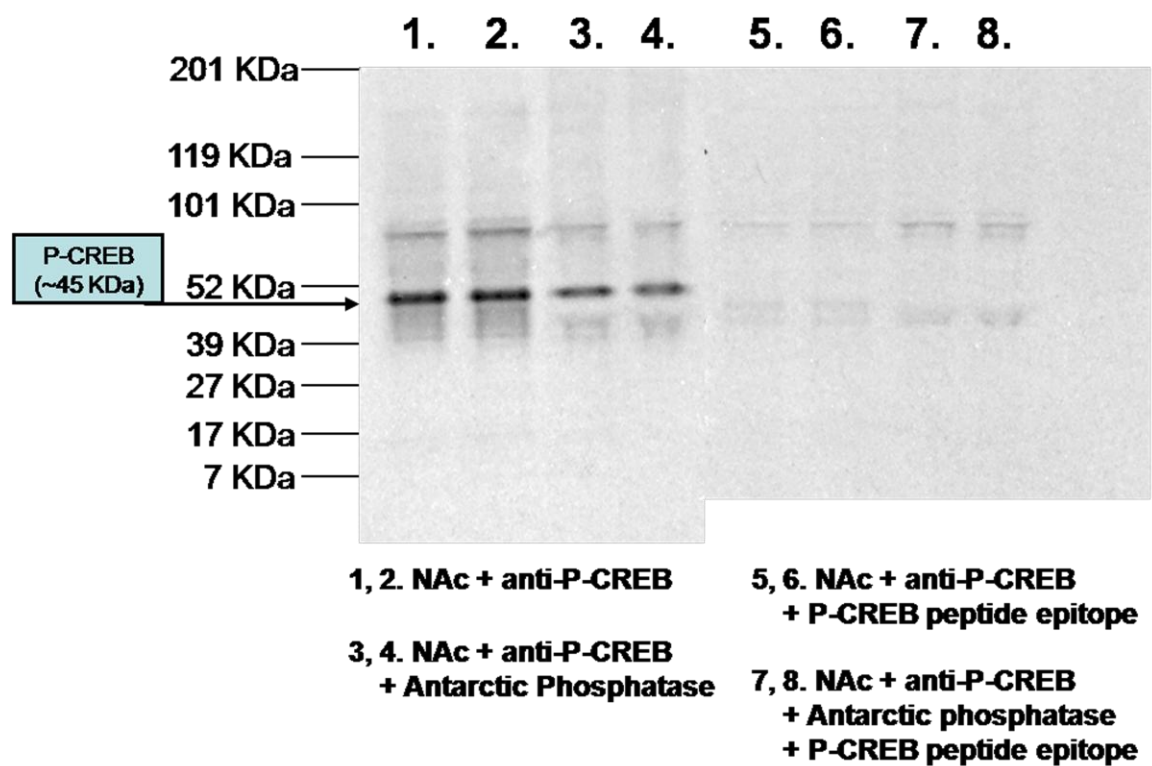
Figure 3.5. Increasing amounts of NAc lysates correlated with increasing optical densities of P-CREB proteins visualized by Western blot analysis, indicating the assay could measure protein content from lysates semi-quantitatively. A) Western blots using antibodies specific to P-CREB (approximately 45 KDa) were performed as described in the Methods with increasing amounts of NAc lysates. Commercially available SK-N-MC cell lysates (far left lane) were used as a positive control to identify P-CREB immunoreactive bands. Rat pituitary cell lysates were also loaded into the assay to verify that the immunoreactive band above 40.1 KDa was, in fact, the P-CREB protein. NAc proteins were loaded into the five right lanes in increasing concentrations and the P-CREB antibody recognized a triplet of bands around 40 KDa, possibly due to some protein degradation during dissection of the NAc from the rat brain and subsequent processing for Western analysis and the presence of phospho-ATF-1 recognized by the antibody. The uppermost band was measured for optical density values used in panel **B** because it migrated at a molecular weight closest to the immunoreactive band from SK-N-MC cells and the pituitary. **B)** Densitometric analysis revealed that as the amount of NAc lysate increased, the optical density of P-CREB visualized in the Western analysis increased, too, indicating that proteins could be measured in a semi-quantitative fashion when assayed in the linear portion of the curve with the assay.

Figure 3.5. Increasing amounts of NAc lysates correlated with increasing optical densities of P-CREB proteins visualized by Western blot analysis, which indicated the assay could measure protein content from lysates semi-quantitatively.
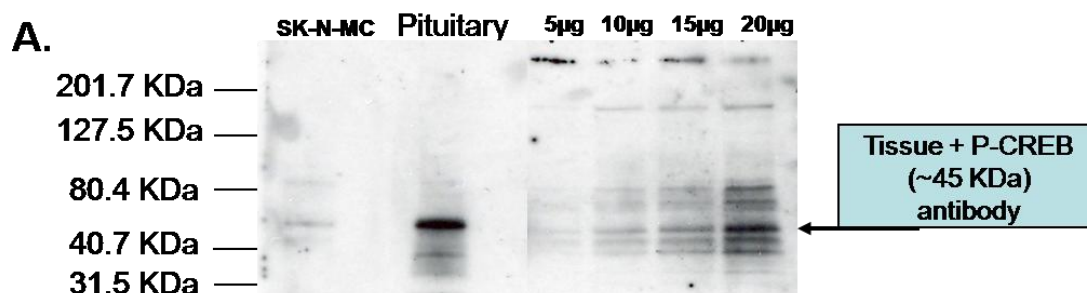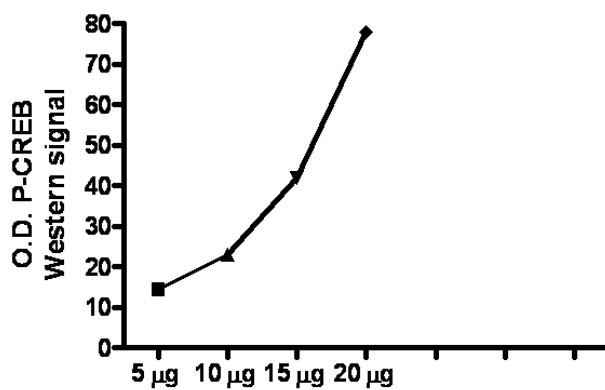
**Figure 3.6. Increasing concentrations of GH3 nuclear proteins (TF) caused
increasing optical densities of band shifts in ^{32}P-CRE EMSA assays.** EMSA assays
were performed using nuclear proteins from rat pituitary-derived GH3 cells. **A)** The CRE
cis-element sequence is given below the picture of the gel in the box, and the core
binding sequence is underlined. Lanes 1-6 showed that as the concentration of GH3
nuclear proteins (TF) added to the reaction mix increased, so too did the EMSA bands
corresponding to the ^{32}P-CRE + GH3 TF complex (denoted by the boxed arrow at the top
right of the gel). **B)** Transcription factor binding to the CART CRE site by nuclear
extracts from GH3 cells was detected in a semi-quantitative fashion as indicated by
increases in optical density as protein levels added to the EMSA reaction mix were
increased and a small linear portion of the curve between 75 and 100 optical density
units. Optical densities were measured with Scion image software (NIH, Bethesda, MD)
and plotted using Graphpad Prizm statistical software (La Jolla, CA).

Figure 3.6. Increasing concentrations of GH3 nuclear proteins (NE) caused increasing optical densities of band shifts in ^{32}P-CRE EMSA assays.
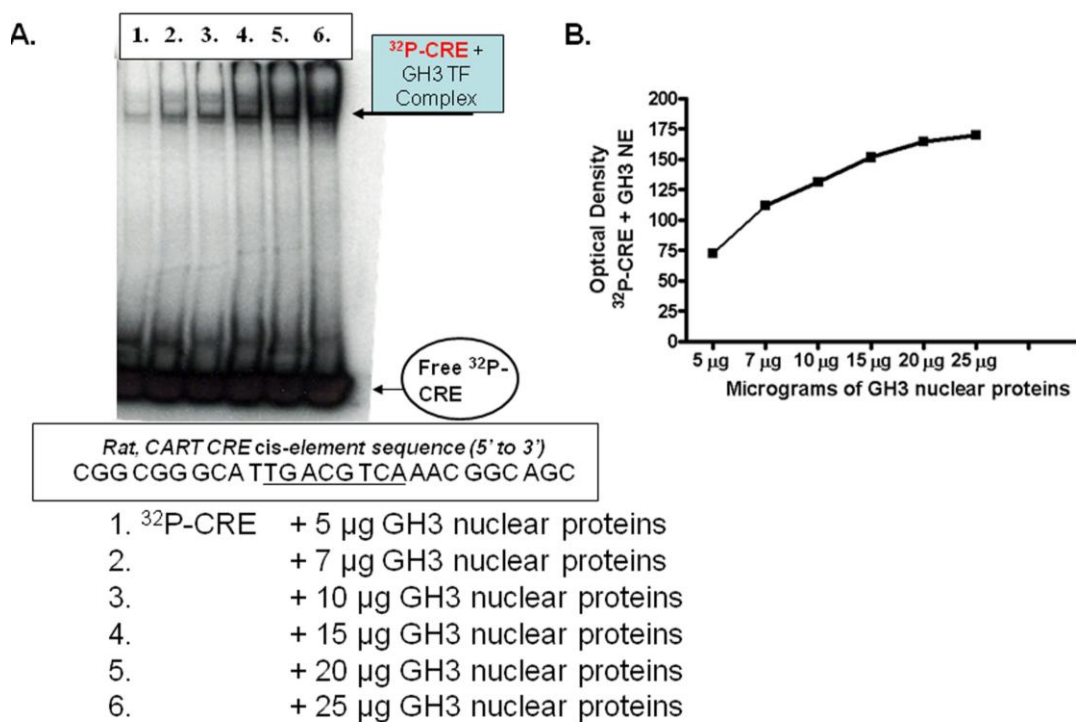
1. ^{32}P-CRE   + 5 µg GH3 nuclear proteins
2.   + 7 µg GH3 nuclear proteins
3.   + 10 µg GH3 nuclear proteins
4.   + 15 µg GH3 nuclear proteins
5.   + 20 µg GH3 nuclear proteins
6.   + 25 µg GH3 nuclear proteins

Figure 3.7. Nissl-stained hemisection in the coronal plane shows the site of injection of HSV viral vectors over expressing CREB, mCREB or LacZ into the rat NAc. HSV vectors over expressing CREB, serine 133 mutated-to-alanine dominant-negative mutant CREB (mCREB), or LacZ proteins were microinjected into the rat NAc as described in the Methods. Stereotaxic coordinates were determined from the Rat Atlas (Paxinos & Watson 2002). The section shown is from one of two control animals that were not injected with virus, but surgerized and injected with a small amount of dye at A/V +1.5, M/L ±1.6 and D/V -7.6. The image is shown at 1.6 x 1.0 magnification and the scale bar represents 1mm in the picture. The anterior commissure, ventricles and injection site are delineated and the accumbens region has been circled to orient the reader. The assay recognized Nissl substance in the cytoplasm of neurons and glial cells by a process called chromatolysis where thionin interacted with RNA-associated proteins in the endoplasmic reticulum. In neuronal injury, such as occured with intra-accumbal injection, Nissl substance disappeared as cells became damaged. In the image, the site of injection is identified by the loss of Nissl substance in the nucleus accumbens region. Figure reproduced from (Rogge et al 2009), with permission from Elsevier Science.

Figure 3.7. Nissl-stained hemisection in the coronal plane shows the site of injection of HSV viral vectors over expressing CREB, mCREB or LacZ into the rat NAc.

Scale: 1 inch = 1mm in the picture
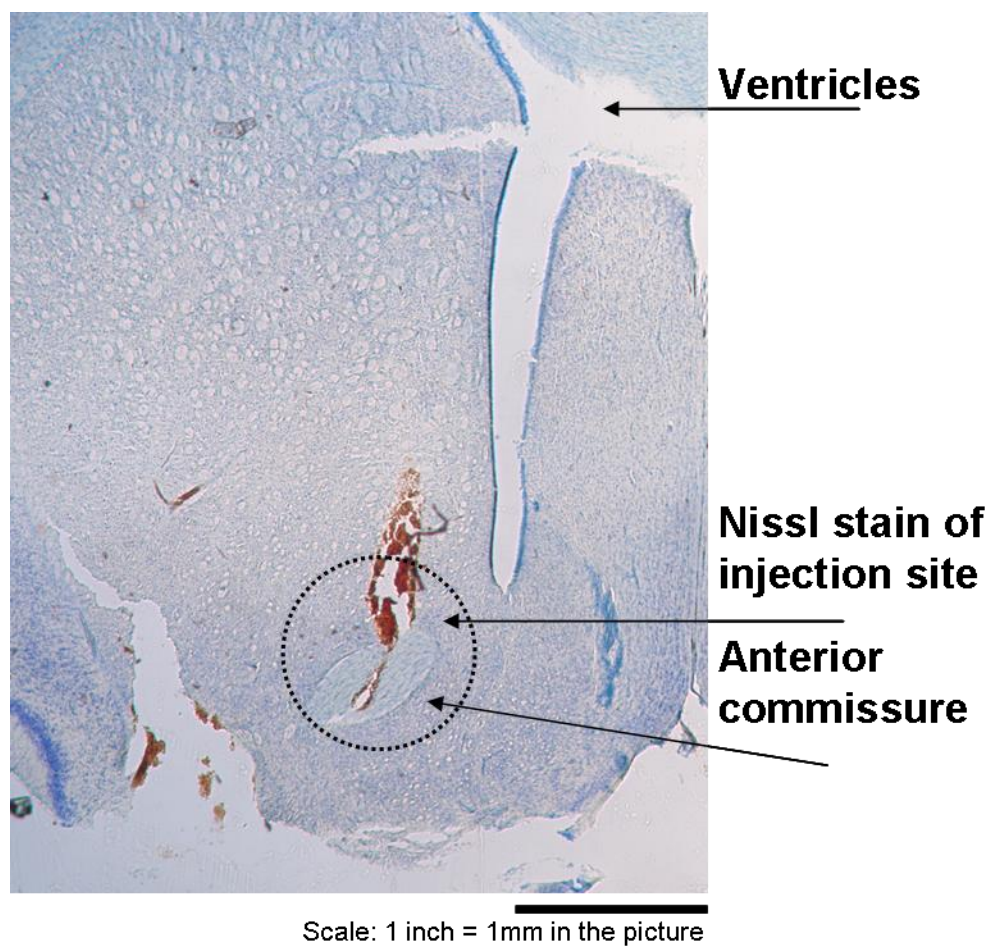
Table 3.1. Summary of CREB, P-CREB and CART protein level changes in rat NAc injected with either HSV-CREB or HSV-mCREB Vs. HSV-LacZ, paired controls.

Protein ID	Treatment	
	HSV-CREB	**HSV-mCREB**
CREB	1.422 ± 0.053 *p = 0.0013, n = 5 pairs	0.7297 ± 0.148 p = 0.143, n = 5 pairs
Serine 133 phospho-CREB	0.8128 ± 0.171 p = 0.355, n = 4 pairs	0.6438 ± 0.145 *p = 0.0440, n = 8 pairs
CART	1.318 ± 0.073 *p = 0.0074, n = 6 pairs	1.015 ± 0.071 p = 0.842, n = 7 pairs

Table 3.1. To test for changes in rat NAc protein levels subsequent to treatment with either the HSV-CREB over expressing virus or its dominant-negative mutant, HSV-mCREB, animals were paired during treatment procedures (one received either HSV-CREB or HSV-mCREB and the other received HSV-LacZ) as described in the Methods. Western blot assays were performed and optical densities of CREB, P-CREB and CART were normalized by Bradford assay or whole lysate actin (for CART) and histone 2B (for CREB and P-CREB) content and compared between paired subjects. Data are reported as the mean ± SEM of the ratio of the protein under examination for HSV-CREB/HSV-LacZ or HSV-mCREB/HSV-LacZ treatments. Asterisks indicate $p < 0.05$, student's one-sample t-test, n = pairs of animals assayed. Table adapted from (Rogge et al 2009), with permission from Elsevier Science.

Figure 3.8. HSV-CREB injections into the rat NAc increased CREB protein levels comped to HSV-LacZ control injections. **(A)** The levels of NAc CREB protein (approximately 45 KDa) from an HSV-CREB treated animal was determined by Western blot and compared to CREB levels in a control animal treated with HSV-LacZ at the same time. The two lanes on the left show duplicate repeats using tissue from one of a pair of animals, and the two lanes on the right are duplicate repeats from the other, control animal of the pair. All lanes were loaded with the same amount of tissue protein as measured by Bradford assay previous to loading the gel. Similar results were obtained when the amount of CREB was normalized to histone 2B content. This result was representative for a total of five pairs of animals prepared and assayed separately in independent experiments. **(B)** Quantification and statistical analysis of immunoreactive bands from a total of 5 pairs of animals were performed as described in the Methods. The mean ratio of CREB protein in HSV-CREB/HSV-LacZ treated subjects was statistically greater than 1.0 (*$p < 0.05$), indicating that CREB levels were increased after HSV-CREB intra-NAc injections compared to HSV-LacZ treatments. Figure reproduced from (Rogge et al 2009), with permission from Elsevier Science.

Figure 3.8. HSV-CREB injections into the rat NAc increased CREB protein levels compared to HSV-LacZ control injections.
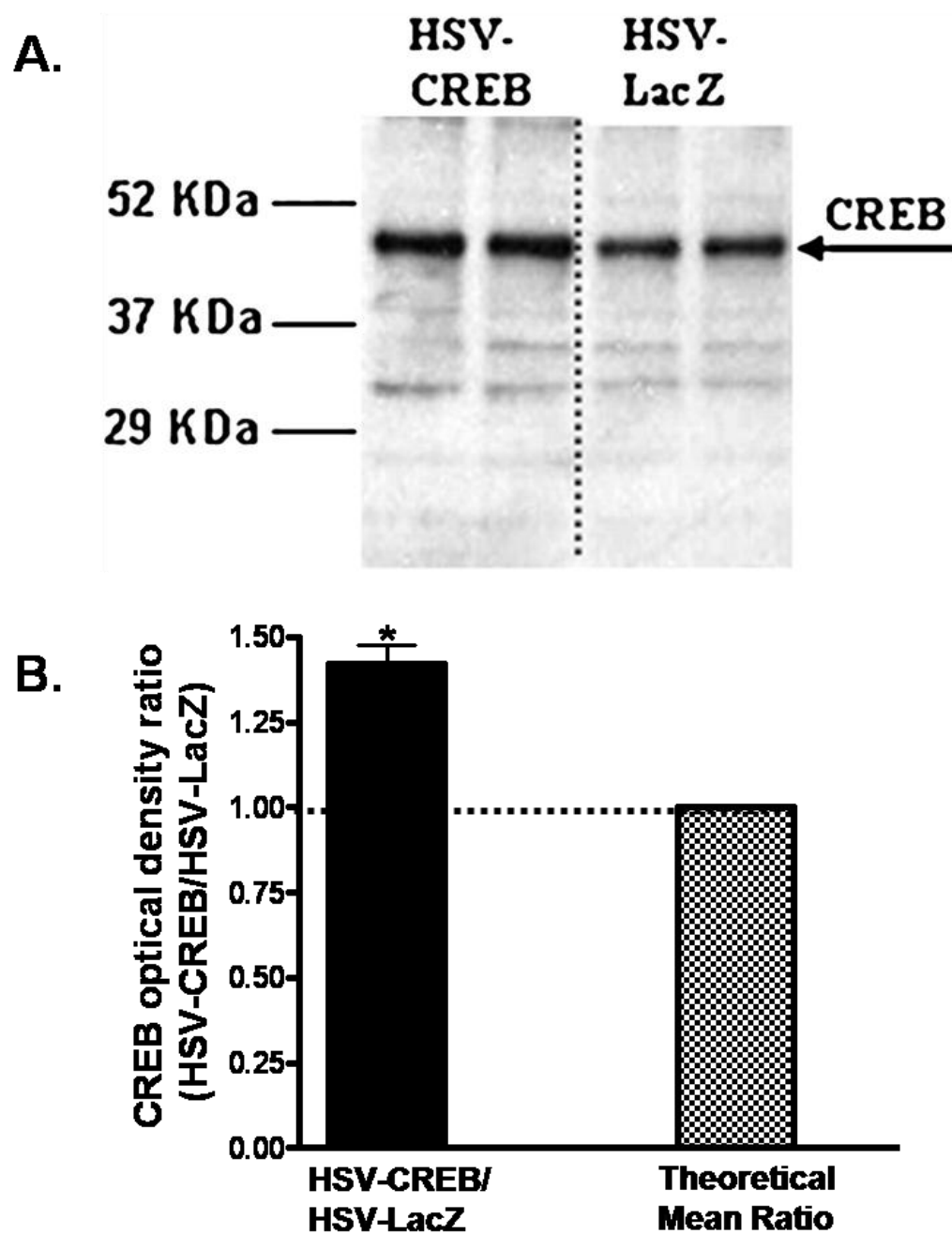
Figure 3.9. HSV-CREB injections into the rat NAc did not affect P-CREB protein levels compared to HSV-LacZ control injections. The levels of P-CREB protein (approximately 45 KDa) in the rat NAc were determined by Western blot analysis in two separate pairs of HSV-CREB or HSV-LacZ treated animal (HSV-CREB treated animals are shown in the five leftmost lanes, while HSV-LacZ animals are shown in the last four lanes on the right). Shown are the results from two separately treated pairs of animals and are representative for a total of 4 animals/treatment group, or 4 pairs assayed separately in independent experiments. The two lanes on the left show duplicate repeats using tissue from one of a pair of animal's injected intra-NAc with HSV-CREB, followed by triplicate repeats of another animal from a separate pair treated with HSV-CREB, as well. The next two lanes to the right are duplicate repeats from a control animal injected inta-NAc with HSV-LacZ and the last two lanes on the right are proteins from the other control animal injected with HSV-LacZ, as well. All lanes were normalized to histone 2B content (visualized around 14 KDa and indicated by an arrow on the right of the gel) in the same sample. **(B)** The mean ratio of P-CREB protein in HSV-CREB/HSV-LacZ treated subjects after 4 independent experiments was not statistically different from 1.0 (p > 0.05), indicating that P-CREB levels were not changed after HSV-CREB intra-NAc injections.

Figure 3.9. HSV-CREB injections into the rat NAc did not affect P-CREB protein levels compared to HSV-LacZ control injections.
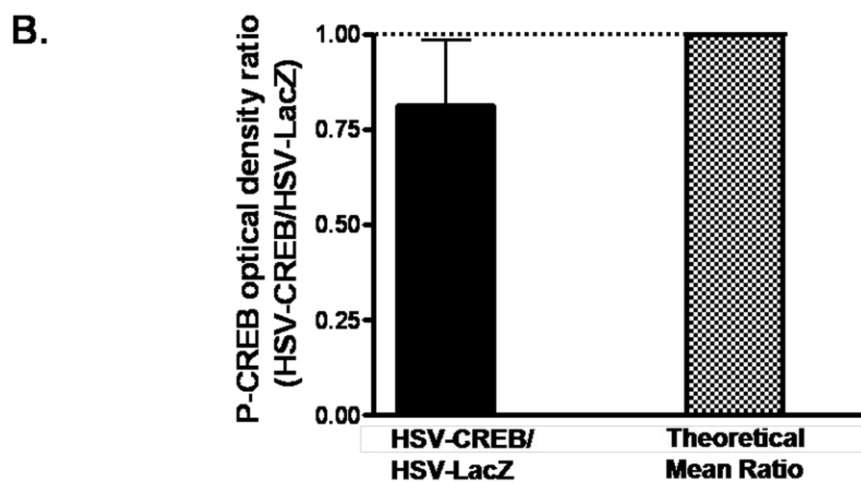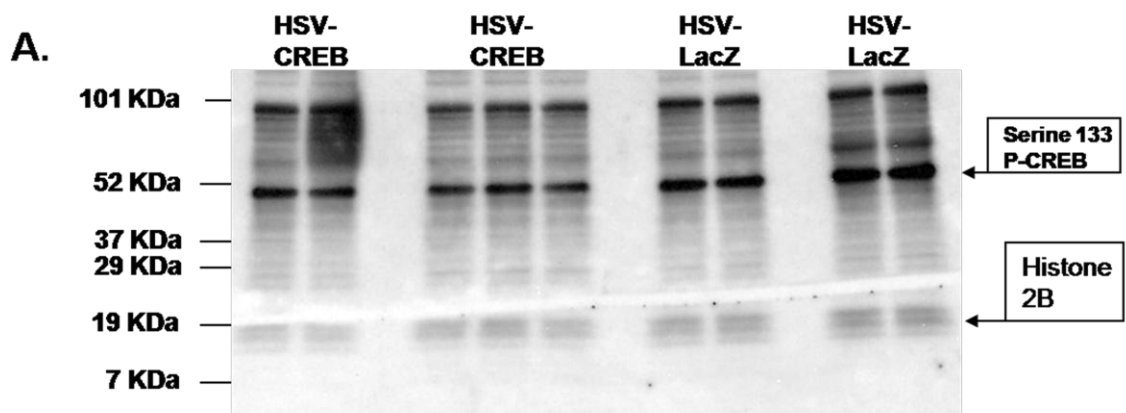
controls as determined by Western blot analysis (ratio of 1.32 ± 0.073; mean $\pm$ SEM, *p $= 0.0074$, n = 6 pairs, **Figure 3.10**, **Table 3.1**).

In order to explore if a transcriptional mechanism of HSV-CREB induced increases in CART peptide abundance was involved, *in situ* hybridization using a molecular probe complementary to the CART gene mRNA transcript (see Methods for details) was performed with a separate group of animals (**Figure 3.11**). Those experiments demonstrated that HSV-CREB intra-NAc injections increased CART mRNA levels in the rat NAc compared to sham, vehicle and HSV-LacZ injected control animals.

To investigate whether or not over expression of CREB in the NAc caused an increase in CREB and/or P-CREB binding to the CART promoter CRE site, EMSA/SS assays were performed with sham, HSV-LacZ and HSV-CREB intra-NAc injected animals (**Figure 3.12**). The data revealed that there were no observable increases in binding to the promoter CRE *cis*-element when equal amounts of protein were incubated with ^{32}P-CRE oligonucleotides identical in sequence to the rat CART promoter CRE.

3.3.3 Effects of mCREB over expression by viral vectors on CART mRNA and peptide levels in the rat NAc

To further test the hypothesis that CREB levels could affect CART mRNA and peptide levels, a viral vector over expressing a dominant-negative mutant of CREB, HSV-mCREB, was injected into the NAc of rats. As above, the animals were treated in pairs, one with HSV-mCREB and the other with a control HSV-LacZ expressing vector. HSV-mCREB injections significantly reduced the amount of P-CREB in treated animals compared to their paired, HSV-LacZ treated controls (ratio of 0.64 ± 0.145; mean $\pm$ SEM

Figure 3.10. HSV-CREB injections into the rat NAc increased CART peptide levels.

(A) The levels of rat NAc CART peptides (approximately 6.5 KDa) from an HSV-CREB

treated animal were determined by Western blot and compared to CART peptide levels in

a control animal treated with HSV-LacZ 36 hours post-intra-NAc injection. The three

lanes on the left showed triplicate repeats using tissue from one of a pair of animals, and

the three lanes on the right were triplicate repeats from the other, control animal of the

pair. Each lane was normalized to whole tissue actin (approximately 45 KDa) as

measured by Western blot. This result was representative for a total of six pairs of

animals prepared and assayed separately in independent experiments. **(B)** The mean ratio

of CART peptides in HSV-CREB/HSV-LacZ treated subjects after 6 independent

experiments was statistically greater than 1.0 (*$p < 0.05$), indicating that CART peptide

levels were increased after HSV-CREB intra-NAc injections compared to the levels in

paired, HSV-LacZ injected animals. Figure reproduced from (Rogge et al 2009), with

permission from Elsevier Science.

Figure 3.10. HSV-CREB injections into the rat NAc increased CART peptide levels.
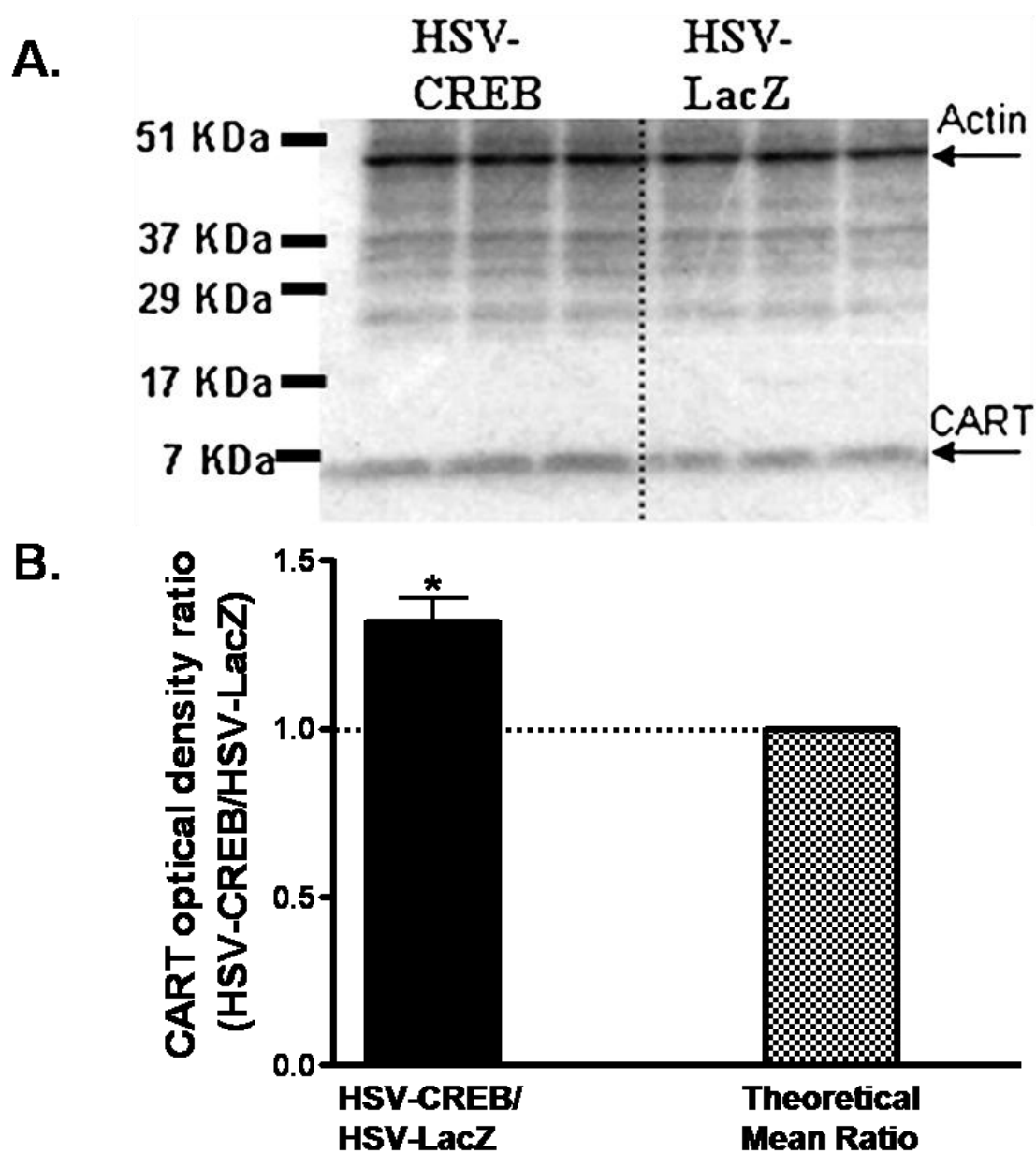
Figure 3.11. Over-expression of CREB increased CART mRNA in the rat NAc.
CART mRNA levels were measured in the rat NAc by *in situ* hybridization 36 hours
following viral infection with either HSV-CREB or -mCREB. Animals received HSV-
CREB or HSV-mCREB in one hemisphere and a control (sham injection, HSV-LacZ or
vehicle) in the contralatteral hemisphere, thus allowing each animal to serve as its own
control. **A)** Representative autoradiogram showing increased radioactive CART mRNA
signal in the NAc of the HSV-CREB treated hemisphere. **B)** Quantitative analysis was
conducted by measuring the relative optical density (OD) of the radioactive signal in the
NAc. Data was expressed as the mean ± SEM and significance was tested with a one-
way ANOVA and Newman-Keuls post hoc test. HSV-infected animals had significantly
higher CART mRNA levels compared to all controls and HSV-mCREB-infected animals
(*$p < 0.01$). CART mRNA levels in the NAc of HSV-mCREB treated rats did not differ
from those in rats treated with sham injections or HSV-LacZ alone. Figure reproduced
from (Rogge et al 2009), with permission from Elsevier Science.

Figure 3.11. Over-expression of CREB increased CART mRNA in the rat NAc.
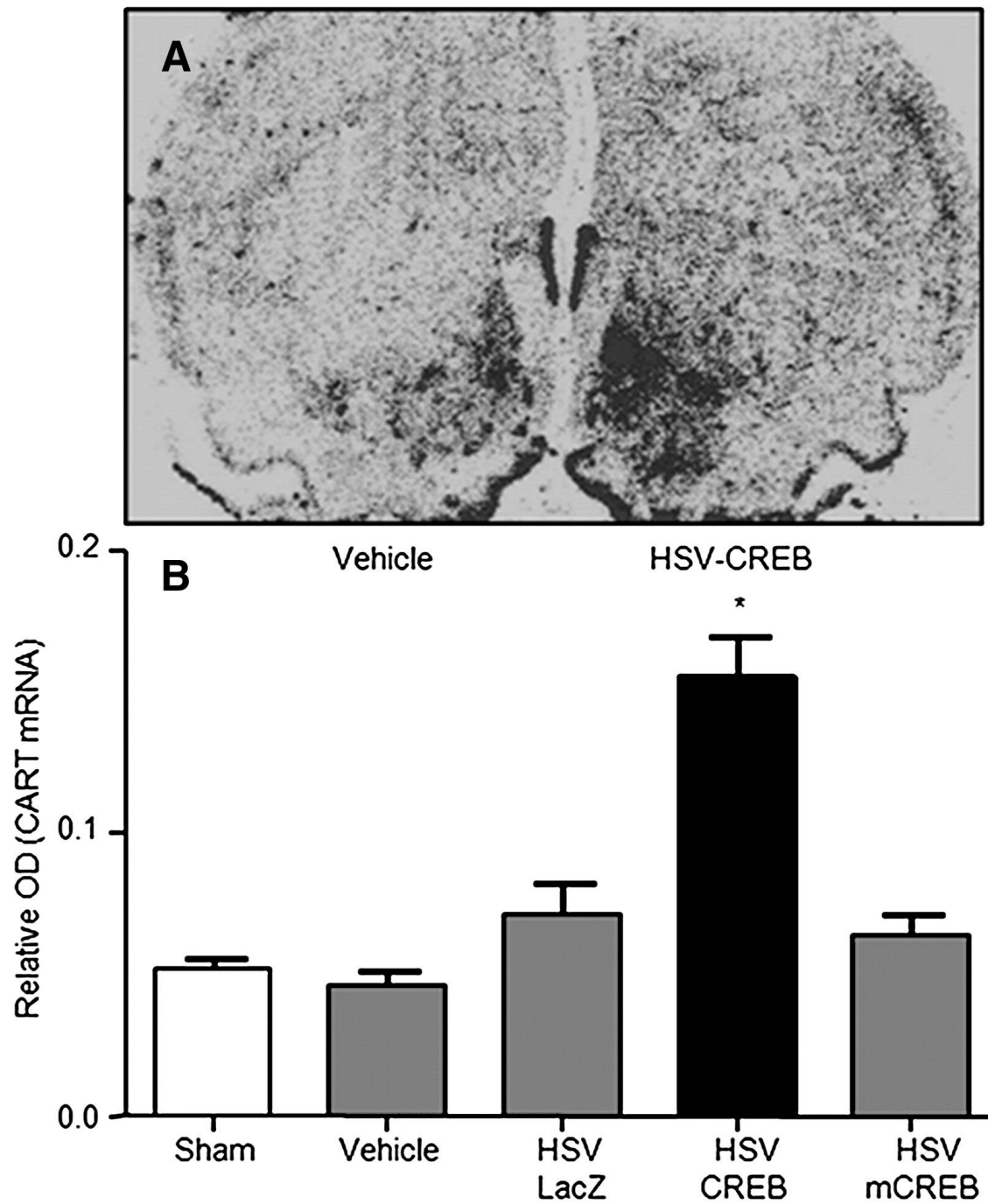
Figure 3.12. EMSA/SS analysis of NAc nuclear proteins after sham, HSV-LacZ and HSV-CREB intra-NAc injections revealed no changes in TF binding to an oligonucleotide identical in sequence to the CART promoter CRE element. The EMSA/SS assay shown used the same ^{32}P-CRE oligonucleotide (CRE) as in **figures 3.1, 3.2** and **3.6** and nuclear proteins extracted from sham (lanes 1-6), HSV-LacZ (lanes 7-11) and HSV-CREB (lanes 12-17) injected rat NAcs. Protein content was normalized by Bradford assay previous to running the assay and equal amounts of protein from each group were used. There were no differences in optical densities of TF + ^{32}P-CRE complexes between the groups. There was, however, specific binding, as shown by lanes 2, 7 and 13, where the addition of NAc proteins reduced the mobilities of the ^{32}P-CRE oligonucleotides compared to no probe alone in lanes 1 and 12. Although some non-specific protein-DNA interactions were seen in the probe alone lanes, they did not migrate to the same position as NAc TF + ^{32}P-CRE complexes and did not confound the results. 50x non-radiolabeled CRE competed for the binding of NAc TFs to CRE (lanes 3, 8 and 14) while 50x non-radiolabeled AP2, an unrelated sequence, did not (lanes 4, 9 and 15). CREB and P-CREB were identified as components of the NAc TF + ^{32}P-CRE complexes by antibody super shift assays shown in lanes 5, 6, 10, 11, 16 and 17. Free ^{32}P-CRE was indicated at the figure's bottom left and ^{32}P-CRE + NAc TF complexes were denoted by a boxed arrow at the figure's top left. The gel was representative of similar results obtained with 6 pairs of animals total treated with HSV-CREB and HSV-LacZ.

Figure 3.12. EMSA/SS analysis of NAc nuclear proteins after sham, HSV-LacZ and HSV-CREB intra-NAc injections revealed no changes in TF binding to an oligonucleotide identical in sequence to the CART promoter CRE element.

1. ^{32}P-CRE alone
2. + NAc (sham injected)
3. + dsCRE
4. + dsAP2
5. + CREB antibody
6. + P-CREB antibody

7. ^{32}P-CRE + NAc (HSV-LacZ injected)
8. + dsCRE
9. + dsAP2
10. + CREB antibody
11. + P-CREB antibody

12. ^{32}P-CRE alone
13. + NAc (HSV-CREB)
14. + dsCRE
15. + dsAP2
16. + CREB antibody
17. + P-CREB antibody
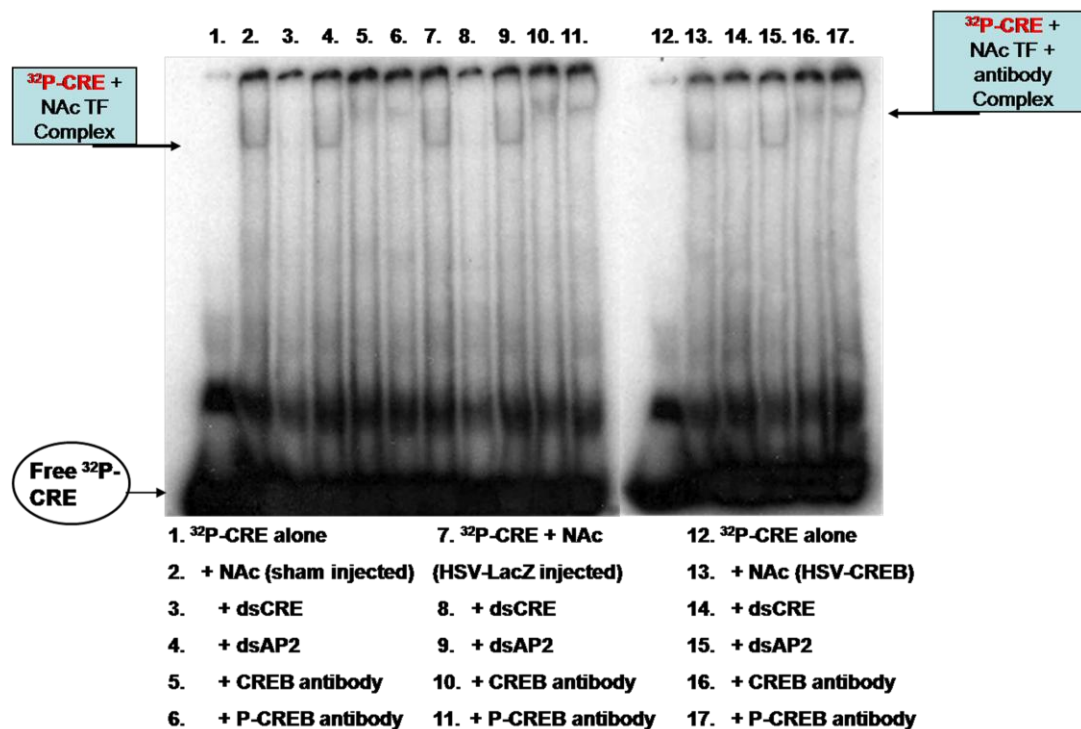
*p = 0.0440, n = 7 pairs, **Figure 3.13, Table 3.1**), but the amount of CREB was not

significantly reduced although there was a trend for reduction (ratio of 0.73 ± 0.148;

mean ± SEM, p = 0.143, n = 4 pairs, **Table 3.1**). Reductions in P-CREB levels were

expected since mCREB was mutated at serine 133 to a non-phosphorylatable alanine and

the P-CREB antibody specifically recognized phosphorylated amino acid 133 in the

CREB protein. A surprising find in HSV-mCREB experiments was that CART peptide

levels were not changed significantly after injections of HSV-mCREB compared to HSV-

LacZ injections (ratio of 1.02 ± 0.071; mean ± SEM, p = 0.842, n = 7 pairs, **Figure 3.14**,

Table 3.1). Consistent with the lack of change in CART peptide levels, CART mRNA

levels in the rat NAc also remained unchanged after HSV-mCREB administration when

examined in a separate group of animals by *in situ* hybridization (previously shown in

Figure 3.11).

3.4 <u>Discussion</u>

The behavioral similarities between animals which over expressed CREB in the

NAc, and animals injected intra-NAc with active CART peptides (i.e. reduced cocaine

reward), led us to hypothesize that because the CART gene promoter had a consensus

CRE *cis*-element, and because CREB could regulate the expression of CART mRNA in

cultured cells (Barrett et al 2002; de Lartigue et al 2007; Dominguez et al 2002), then

CART may have been a physiologic target gene for CREB-mediated transcription in the

NAc, such that over expression of CREB in that region could increase CART peptides *in*

vivo. That is, we hypothesized that CREB *in vivo* could regulate CART peptide levels *in*

vivo, which in turn could influence cocaine's rewarding effects.

Figure 3.13. HSV-mCREB injections into the rat NAc decreased P-CREB levels.

(A) The levels of P-CREB (approximately 45 KDa, indicated by an arrow on the right of the gel) in NAc from HSV-mCREB treated animals were determined by Western blot and compared to phospho-CREB levels in HSV-LacZ treated control animals. In this representative blot showing P-CREB levels in a pair of animals, all lanes were normalized by whole tissue protein content as determined by overall histone 2B content using an antibody specific to histone 2B (approximately 14 KDa, indicated by an arrow on the right of the gel). The two lanes on the left show duplicate repeats using tissue from one of a pair of animals, and the two lanes on the right are duplicate repeats from the other, control animal of the pair. **(B)** The gel was representative of a total of 8 pairs of animals prepared and assayed separately in independent experiments. The mean ratio of P-CREB in HSV-mCREB/HSV-LacZ treated subjects after 8 independent experiments was statistically less than 1.0 (*$p < 0.05$), indicating that P-CREB levels were decreased after HSV-mCREB intra-NAc injections compared to the levels in paired, HSV-LacZ injected animals. Figure adapted from (Rogge et al 2009), with permission from Elsevier Science.

**Figure 3.13. HSV-mCREB injections into the rat NAc decreased P-CREB levels.**
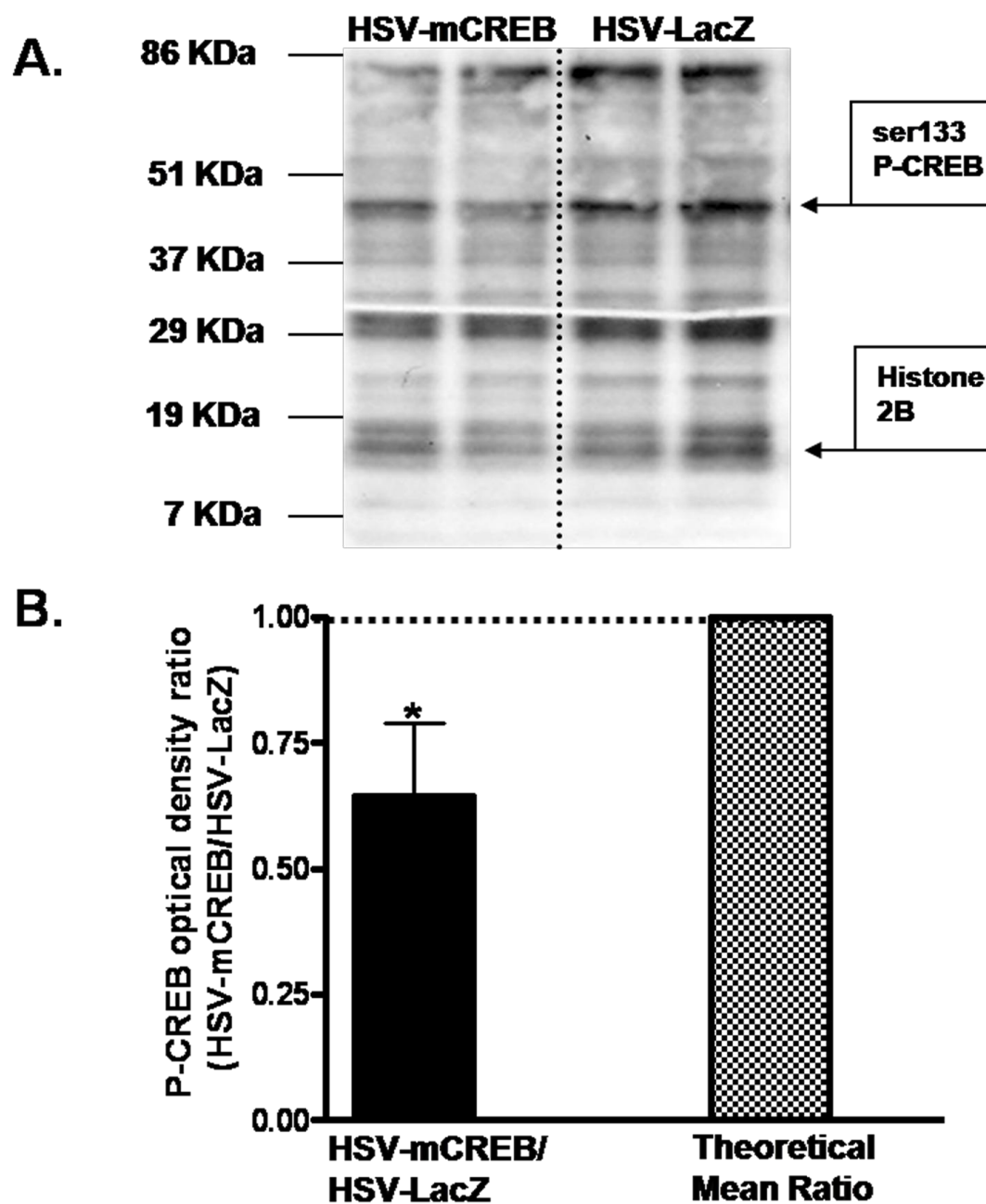
Figure 3.14. HSV-mCREB injections into the rat NAc did not change CART

peptide levels. **(A)** The levels of rat NAc CART peptides (approximately 6.5 KDa) in

tissue from HSV-mCREB treated animals were determined by Western blot and

compared to CART peptide levels in HSV-LacZ treated, control animals. In this

representative blot showing CART levels in a pair of animals, each lane was normalized

to whole tissue actin (approximately 45 KDa). The result was representative for a total of

seven pairs of animals prepared and assayed separately in independent experiments. **(B)**

The mean ratio of CART peptides in HSV-mCREB/HSV-LacZ treated subjects after 7

independent experiments was not statistically different than 1.0 ($p > 0.05$), indicating

that CART peptide levels were not changed after HSV-mCREB intra-NAc injections

compared to the levels in paired, HSV-LacZ injected animals. Figure reproduced from

(Rogge et al 2009), with permission from Elsevier Science.

Figure 3.14. HSV-mCREB injections into the rat NAc did not change CART peptide levels.
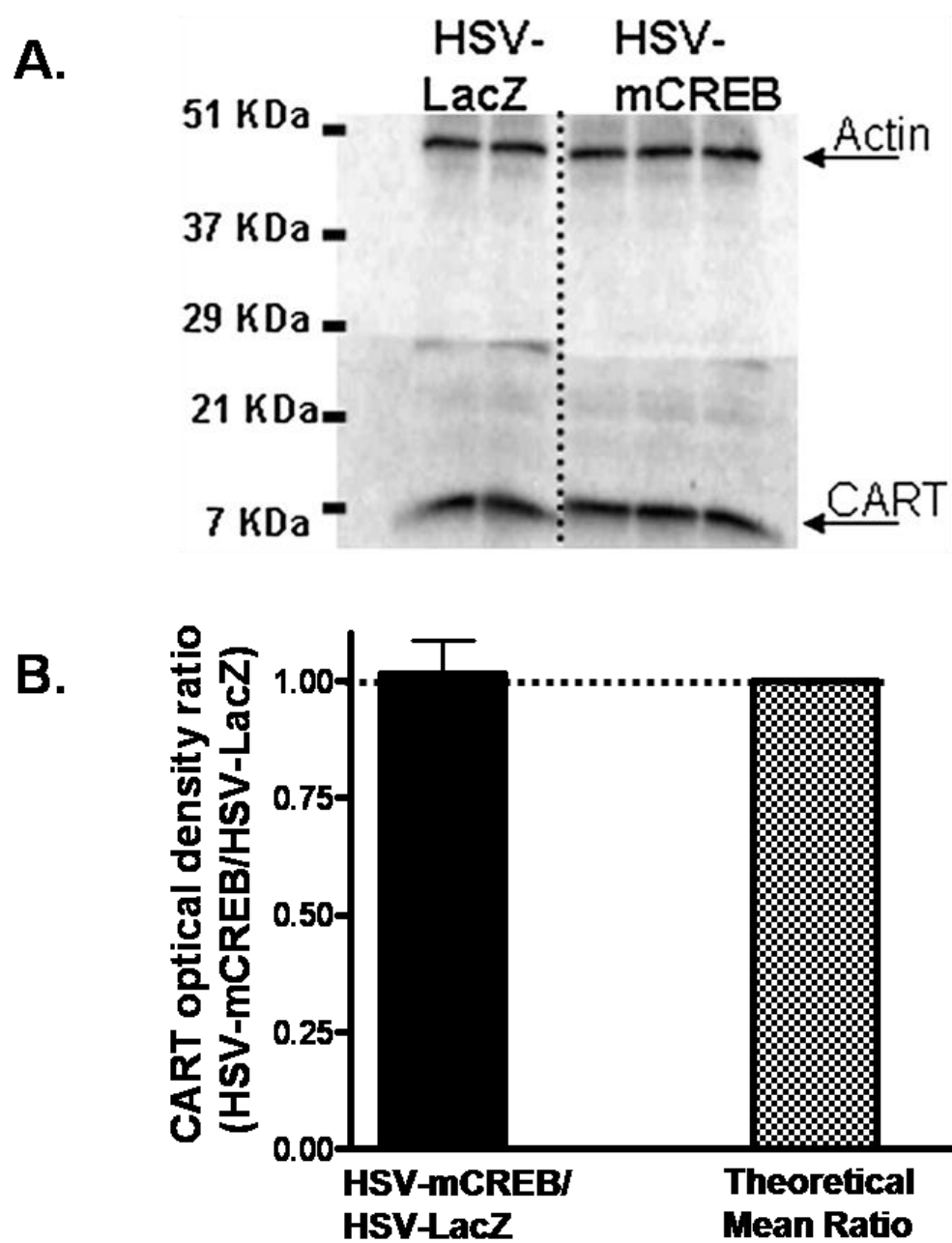
To address the hypothesis, it was first shown that the consensus CRE *cis*-element in the CART gene promoter was able to bind CREB and P-CREB in nuclear extracts from the NAc of rats. The rationale for the experiments was that CRE *cis*-element core and flanking sequences were shown to vary from species-to-species and gene-to-gene and that variability affected the binding affinity for CREB (Faiger et al 2006; Faiger et al 2007; Holmberg et al 1995; Mayr & Montminy 2001; Yanagisawa & Schmidt 1999). The CART gene CRE site had its own unique flanking sequences that could have affected CREB binding, thus it was important to show that the CART gene CRE site itself, with its unique flanking sequences, was able to bind to CREB and P-CREB in nuclear extracts from the rat NAc.

In addition, CREB could have existed in any number of homo- or heterodimer combinations in the rat NAc that may or may not have been able to bind the CART gene consensus CRE site, which was unique compared to other promoter CRE sites. Also, CREB binding to a promoter on its own could not initiate transcription; it required phosphorylation at amino acid serine 133 to recruit CBP and the basal transcription machinery (Mayr & Montminy 2001). Moreover, phosphorylation at other residues like serine 142 would have caused CREB to act as a transcriptional repressor (Matthews et al 1994). It was important, therefore, to show that both CREB and P-CREB, as they existed in NAc neurons, could bind to the CART promoter CRE site flanked by its unique neighboring sequences. We thus used a synthetic oligonucleotide to test if the CRE *cis*-regulatory element present within the rat CART gene promoter, flanked by sequences from the CART gene promoter, permitted specific binding of CREB and P-CREB in nuclear extracts from the rat NAc.

The data in **figures 3.1** and **3.12** showed that the CART gene promoter consensus CRE *cis*-element was able to bind CREB and P-CREB TFs from the rat NAc. That result suggested that in the rat NAc, CREB and P-CREB had the potential to bind to the CART gene CRE site and regulate CART mRNA expression. The data also suggested that over expression of CREB in the NAc could result in regulation of CART expression at the CART promoter consensus CRE *cis*-regulatory site *in vivo*.

In **figures 3.2** and **3.3**, the findings demonstrated that CREB and P-CREB were at least part of the protein complex that could bind to the CART promoter CRE sequence in EMSA/SS assays using GH3 cells. Since CART gene transcriptional regulation studies were previously done in GH3 cells using ACREB, the effects of ACREB on GH3 TF binding to the CART promoter CRE site were also examined. Transfections with ACREB significantly reduced the binding of GH3 TFs to the CART CRE oligonucleotide (**Figure 3.2**) and that change was concomitant with reductions in P-CREB levels (**Figure 3.3**). The results suggested that manipulating P-CREB levels in GH3 cells with ACREB transfections could affect the levels of P-CREB bound to the CART gene promoter CRE site. In sum, the experiments showing that reductions in P-CREB levels by ACREB over expression could lead to reductions in TF binding to the CART promoter CRE site and that the Westerns and EMSAs were semi-quantitative assays (**figures 3.5** and **3.6**), bolstered the rationale for using those methods to test the hypothesis that CREB over expression in the rat NAc would increase CART mRNA and peptide levels, potentially by increasing the quantity of TFs bound to the CART promoter CRE site.

The data in **figures 3.8** and **3.10** determined that, as hypothesized, over expression of CREB in the NAc via injection of the HSV-CREB viral construct

significantly increased the levels of NAc CART peptides. Western blots were performed as opposed to other techniques such as the radioimmunoassay (RIA) because CART peptides were found to be processed into various different peptide fragments from a pro-peptide precursor molecule in neurons (Dylag et al 2006a; Stein et al 2006b; Thim et al 1999). RIA did not discriminate between the differently processed CART peptide fragments, some of which showed physiological activity when exogenously administered to animals (Dylag et al 2006b). Western blots allowed both semi-quantification of the amount of active CART peptides (i.e. CART 55-102 and 62-102) present in animal tissues and also identification of the specific CART peptide fragments present by their molecular weights.

In those studies, the lack of change in P-CREB levels was probably a reflection of how tightly regulated that active transcription factor was in the animal brain. It was possible that because brains were harvested 36 hours after HSV-CREB injections (a time when the virus was found to be most active in over expression (Neve et al 2005)), the brain had already enacted homeostatic mechanisms such as activating protein phosphatases to dephosphorylate P-CREB, or down-regulating PKA and/or AC to prevent CREB phosphorylation, which resulted in the maintenance of homeostatic levels of P-CREB that were not different from HSV-LacZ treated animals. Such a feedback mechanism to ensure that P-CREB levels remained within a certain, homeostatic range was in line with the theory that when the regulation of P-CREB levels became dysfunctional, such as was the case in the NAc of chronic drug users, then the neurons underwent a change in plasticity and function related to out-of-control P-CREB-mediated transcription.

The idea that CREB may have bound to the CRE *cis*-element of the CART gene promoter in the NAc and regulated gene transcription *in vivo* was further bolstered with *in situ* hybridization observations that CART mRNA increased in the NAc after HSV-CREB injections (**Figure 3.11**). The parallel increases in NAc CART mRNA and peptide levels after HSV-CREB intra-NAc injections, in addition to the ChIP data presented in **chapter 2**, strongly supported a transcriptional role for CREB in the regulation of CART mRNA and peptide production in the rat NAc.

A possible explanation for the lack of increased binding to the CRE oligonucleotide after HSV-CREB treatments may have been that by the time the NAc had been dissected (36 hours post-injection), the brain may have enacted homeostatic mechanisms to prevent increases in P-CREB levels (data in **figure 3.9** support that idea), which could have lead to similar levels of TF binding to the CART CRE site by from HSV-CREB treated and control animals. Alternatively, other CREB family member proteins could have been up-regulated to hetero-dimerize with CREB in an effort to control its increased expression caused by viral over expression, and in that way block CREB mediated transcription by blocking CREB binding to CRE sites as a similar homeostatic mechanism to control P-CREB-mediated gene expression, which was tightly controlled by overlapping feedback mechanisms *in vivo*, in the NAc which are just now beginning to be appreciated.

Of interest was the finding that HSV-mCREB injections significantly decreased P-CREB levels (**Figure 3.13**) but not those of CART mRNA or peptide (**Figures 3.11** and **3.14**). Findings from other investigators, however, supported our observations and made it seem unlikely that methodological errors accounted for HSV-mCREB's null

effects on CART mRNA and peptide levels. First, not all genes up-regulated by CREB over expression were found to be down-regulated by mCREB over expression in the NAc (McClung & Nestler 2003). In a microarray study, 23% of the mRNAs that were up-regulated by HSV-CREB injections into the NAc were not down-regulated by HSV-mCREB intra-NAc injections (McClung & Nestler 2003), which indicated that there were many genes in the NAc whose expression could only be up-regulated upon manipulation of CREB activity.

Second, *in vitro* studies indicated that basal CART promoter-driven luciferase expression occurred in the presence of a dominant negative mutant of CREB similar to mCREB, ACREB (de Lartigue et al 2007; Dominguez & Kuhar 2004). In experiments with luciferase plasmids driven by the mouse CART gene proximal promoter in cultured CATH.a cells, ACREB did not reduce basal levels of gene transcription (Dominguez & Kuhar 2004). ACREB did, however, block increases in CART gene promoter-driven luciferase expression after stimulation with the AC activator forskolin. Stimulus-induced elevations of CART promoter-driven luciferase were also ablated by ACREB in cholecystokinin-stimulated, cultured rat vagal afferent neurons (de Lartigue et al 2007). It would seem from that data that pharmacologically-stimulated expression of CART in cultured cells required CREB, but basal expression did not.

A third series of studies found that non-sense mutations in the mouse CRE DNA *cis*-element itself abolished basal as well as forskolin-stimulated CART promoter-driven luciferase expression in CATH.a cells, although ACREB had no effect on basal activity in those same cells (Dominguez & Kuhar 2004). Similar experiments yielded identical results in GH3, AtT20 and SH-SY5Y cultured cells using rat CART promoter-driven

luciferase plasmids with non-sense mutations in the rat CART gene promoter CRE *cis*-element (Barrett et al 2002). The mutated rat CART gene promoter, like the mutated mouse promoter, was unable to initiate either basal or forskolin-stimulated luciferase gene expression in all three cell lines.

Since ACREB, a dominant-negative mutant of CREB, did not reduce basal expression of CART promoter-driven luciferase plasmids in cultured cells, yet point mutations in either the mouse or rat CART proximal promoter CRE elements did reduce that basal expression, it was possible that TFs closely related to CREB may have bound to the CRE site under basal conditions. As mentioned at the beginning of this chapter, the mammalian family of CRE activators was found to comprise a substantial number of closely related proteins arising from genes encoding CREB, CREM and ATF-1, 2 and 3 (Green et al 2008; Mayr & Montminy 2001; Nestler 2004b). The CREB superfamily also included numerous alternative splice variants of CREB, CREM and the ATFs which could all bind gene promoter CRE *cis*-elements and/or homo- and heterodimerize with CREB itself (Mayr & Montminy 2001).

Interestingly, several CREB family TFs besides CREB were regulated in the NAc by exposure to psychostimulants and influenced behavioral responses to the drugs when over expressed in that brain region (Green et al 2006; Green et al 2008). It was possible that under conditions where mCREBwas present, CREB homodimers could no longer initiate transcription at gene promoter CREs and the brain compensated for decreased CREB TF activity by increasing the activity of other CRE *cis*-element binding proteins such as one of the various CREB family members or splice variants.

One piece of evidence which indicated that other CREB family members may have been responsible for un-stimulated CART gene expression was the finding that *in vivo*, in the rat NAc, basal as well as forskolin-stimulated CART mRNA expression was blocked with Rp-cAMPS as well as H89, inhibitors of PKA signaling (Jones and Kuhar 2006). That pharmacological treatment would have affected the phospho-serine 133 levels of CREB superfamily members generally, lending credence to the idea that other CREB family members could bind to the CART promoter CRE site since ACREB had no effect on basal CART expression in cultured cells. The dominant-negative mutant mCREB was not used in the above *in vivo* study.

Another phenomenon that may have occurred in conjunction with binding of non-CREB protein CRE activators (such as CREM) to the CART gene promoter CRE sequence may have involved cooperativity amongst one or more other *cis*-regulatory elements present in the rat CART gene promoter (illustrated in **Figure 2.1**). *Cis*-elements most likely functioned in concert with one another *in vivo* (Hai & Curran 1991) and numerous other *cis*-elements, such as SP1, STAT3 and E-Box co-existed within the CART gene proximal promoter (Barrett et al 2002; Dominguez et al 2002) and probably influenced one another consequent to the effects of multiple signaling pathways convergent on the nucleus. Complex TF-TF, TF-DNA and TF-co-factor interactions which required the CART gene promoter CRE *cis*-element, but not necessarily CREB TFs themselves, may have been necessary for basal transcriptional activity of the CART gene in some tissues.

In this study, the fact that intra-NAc infusions of HSV-mCREB did not drive down basal expression of rat NAc CART mRNA or peptides seemed to indicate that P-

CREB TFs did not regulate basal levels of CART expression in the NAc. P-CREB may have regulated only the stimulated expression of the gene. Such an observation aligned with the idea that CREB was widely accepted as a stimulus-regulated transcription factor responsible for the expression of stimulus-inducible genes such as neurotransmitters (Lonze & Ginty 2002; Mayr & Montminy 2001).

The results presented in this chapter, which showed that over expression of CREB increased the quantity of CART mRNA and peptides in the rat NAc, supported an overall hypothesis that CART peptides in the NAc appeared to be homeostatic regulators with functional effects opposing the locomotor, sensitizing and rewarding effects of psychostimulants and elevated dopaminergic neurotransmission (Jaworski et al 2008). One mechanism by which CART may have attenuated the behavioral effects of cocaine, amphetamine and dopaminergic signaling was via modulation of dopamine neurotransmission. Although it was not clear if CART peptides over expressed in the rat NAc directly affected dopamine release from the VTA, neuroanatomical data showed that some of the CART neurons which projected from the NAc to the VTA were GABA-containing striatal output neurons that synapsed on GABAergic interneurons as well as DA-producing neurons in the VTA (Philpot & Smith 2006). Nothing was known about the functions of CART released from those NAc projections to the VTA. As a result, the precise mechanism(s) by which intra-NAc CART peptide administration functionally antagonized the behavioral effects of dopamine and psychostimulants in previous studies remained obscure due to a limited scope of knowledge regarding CART receptor identity(s), function(s), associated signaling cascades in discreet CNS tissues and the

complex neurocircuitry of CART neurons interconnected throughout the various regions of the rat brain associated with reward and reinforcement.

It was noted that increased CREB in the NAc may not have acted solely and directly on the consensus CRE *cis*-regulatory element in the CART gene promoter to increase CART mRNA and peptide levels; an indirect effect was possible as well. However, data presented in **chapter 2** of this dissertation and the body of scientific knowledge regarding CART gene regulation in cultured cells (Barrett et al. 2002; Dominguez et al. 2002; Lakatos et al. 2002; Dominguez and Kuhar 2004; de Lartigue et al. 2007) and *in vivo* in the rat NAc (Jones and Kuhar 2006), strongly suggested that the CART gene consensus CRE *cis*-regulatory element was able to bind P-CREB in the NAc and that that binding had an effect on the regulation of CART mRNA and peptide levels *in vivo* in that tissue.

In conclusion, CREB regulation of the CART gene in the rat NAc was an important finding because, although psychostimulants regulated CREB activity in the brain reward pathway and those TFs have been found to play an essential role in drug reward and reinforcement, the complete gamut of genes regulated by CREB in the NAc by psychostimulants which may mediate their behavioral actions have not yet been fully elucidated. Identifying candidate CREB-regulated genes in the NAc, such as CART, will further our understanding of the molecular mechanisms of the reinforcing effects of psychostimulants such as cocaine and amphetamine. That, in turn, may lead to medications developed to treat addiction.

Chapter 4: Effects of binge cocaine administration on CART gene expression and transcription factor binding to the CART promoter CRE *cis*-regulatory element.

4.1 <u>Introduction</u>

It was previously demonstrated that one-day, high dose binge cocaine administration (4 doses of 30 mg/kg body weight every 2 hours) increased CART mRNA levels in the rat NAc two hours after the last injection of drug (Brenz Verca et al 2001; Hunter et al 2005). CART peptide levels subsequent to binge cocaine administration were not examined. The binge regimen was stressful for the animals and some died while others suffered seizures. Moreover, the effect on CART mRNA levels may have been mediated, in part, by corticosterone, which is involved with CART regulation and the body's responses to stress and psychostimulants (Hunter et al 2005). Specifically corticosterone administration was previously shown to increase CART peptide levels in the blood, NAc and hypothalamus (Hunter et al 2007; Hunter et al 2005; Stanley et al 2004; Vicentic et al 2005a; Vrang et al 2003) as well as CART mRNA levels in the NAc (Hunter et al 2005). In separate studies, binge cocaine treatment was able to activate the HPA axis causing increases in circulating corticosterone (Zhou et al 2003; Zhou et al 2002) and corticosterone increases mediated by cocaine were dose-dependent (Levy et al 1991; Mello & Mendelson 1997).

The goal of the work presented in this chapter was to determine if CART peptides were increased by one-day binge cocaine treatment and if the CART promoter CRE *cis*-regulatory element was involved in cocaine regulation of the CART gene at the transcriptional level after that treatment. In an attempt to avoid the confounding variable of stress associated with the high doses previously administered, a relatively moderate one-day binge administration paradigm of 4 doses of 20 mg/kg body weight cocaine given every two hours was employed.

To verify that the novel treatment paradigm had an effect on CREB, P-CREB and CART protein levels, Western blot assays were performed with nuclear and cytoplasmic proteins from cocaine and saline treated animals. EMSA/SS assays with the CART promoter CRE site were performed with nuclear proteins from the same animals to investigate whether or not the drug treatment affected the potential for CREB to bind to the CRE site.

In addition, a commercially available consensus activator protein-1 (AP1) *cis*-regulatory element was used in EMSA/SS assays with drug treated animals. Members of the AP1 family of transcription factors were previously shown to be up-regulated in the reward pathway of rodents by acute and chronic administration of psychostimulants (Hope et al 1992; Hope et al 1994; McClung & Nestler 2003), though the effects of a one-day binge cocaine administration paradigm on AP1 activity in the rat NAc have not been studied. In this chapter, the effect of binge cocaine administration on AP1 family binding to a consensus AP1 *cis*-element was examined because acute administration of psychostimulants was found to activate the immediate early gene c-Fos in the NAc, an AP1 family member that mediated psychostimulant reward by facilitating the transcription of CREB and other target genes that appeared to increase sensitivity to the rewarding effects of cocaine (Hope et al 1992; Konradi et al 1994; McClung & Nestler 2003).

The exact panoply of genes regulated in the NAc by c-Fos subsequent to psychostimulant administration were not known, but it was able to bind to AP1 *cis*-elements in the promoters of other Fos and Jun family members, which in turn homo- and heterodimerized to regulate the transcriptional expression of even more Jun and Fos

family members. In that way AP1 family members accumulated in the NAc in response to drug administration and regulated the expression of each other and AP1-target genes. Thus, it was expected that proteins from the NAc of animals treated with binge cocaine would exhibit more binding to a consensus AP1 *cis*-element and in that way act as a positive control for the assay.

4.2 <u>Methods</u>

4.2.1 Animals and drug administration

See **Chapter 2, section 2.2.5** for detailed methodologies. In the data presented for this chapter, the same animals used in analyses of CART peptide levels in the rat pituitary subsequent to cocaine administration (**Chapter 2, section 2.3.7**) were utilized. NAc dissections were performed as described in **chapter 3, section 3.2.1**. No animals from this study had seizures or died.

4.2.2 Western blot analysis

See **Chapter 3, section 3.2.5** for detailed methodologies. Western blot analyses were performed with NAC cytoplasmic proteins (for CART assays) or nuclear proteins (for CREB and P-CREB assays) from rats administered a binge regimen of cocaine (Coc) or saline (Sal) using antibodies specific for the target protein.

4.2.3 EMSA and antibody super shift analyses

See **Chapter 2, section 2.2.6** for detailed methodologies. In this chapter, nucleus accumbens transcription factors (TF) were extracted from three cocaine- or saline-treated

rats and pooled together into cocaine and saline groups, respectively (represented as Coc and Sal in the gel shown). Protein content was normalized by Bradford assay previous to pooling the animals and equal amounts of protein from each group were used. The gelwas representative for a total of 9 animals/group assayed independently. Binding to the CART CRE DNA *cis*-regulatory site was observed by EMSA/SS using a double stranded (ds) oligonucleotide identical in sequence to the rat CART promoter CRE site (EMSA) and CREB and P-CREB antibodies (SS). The sequence of the CART promoter containing the CRE *cis*-element from 5' to 3' (referred to as CRE) was given below the picture of the gel in the box, and the core binding sequence was underlined. The dsPit1 oligonucleotide used as a non-specific competitor was identical to a putative Pit1 *cis*-regulatory element identified in the mouse CART promoter and the sequence (from 5' to 3') was ACT TTA GTT TTA ATT ATC CAT ATA TGT G.

The AP-1 consensus *cis*-regulatory element was purchased from Active Motif (Carlsbad, CA) and contained the core binding sequence (from 5' to 3') TGAGTCA. P-CREB, JunD and c-Fos antibodies as well as the immunizing peptides for P-CREB and JunD were purchased from Santa Cruz Biotechnology (Santa Cruz, CA).

4.2.4 Quantification of data and statistical analyses

Western and EMSA data were captured and quantified as detailed in **chapter 3, section 3.2.6**. To compare potential differences between different autoradiographic films, the density of bands was expressed as a percentage of the average of saline treated controls. Statistical analyses were performed with the student's two-sample t-test.

4.3. <u>Results</u>

4.3.1 Effects of binge cocaine on rat NAc CREB, P-CREB and CART peptide levels as well as TF binding to the CART promoter CRE site *in vitro*.

Western blots to examine potential changes in CREB and P-CREB protein levels between cocaine and saline treated animals revealed that cocaine-treated rats exhibited increased levels of CREB, but not P-CREB in the NAc (**Figures 4.1** and **4.2**). CART peptide levels in the NAc were also increased after binge cocaine, but not binge saline, treatment (**Figure 4.3**), where the mean percent difference between drug-treated groups was 30.35 ± 12.62 (mean % $\pm$ SEM, *p = 0.023, two-sample t-test, n = 9/group). Binding of NAc proteins to the CART promoter CRE *cis*-regulatory element as determined by EMSA, however, was not changed between cocaine and saline treated rats (**Figure 4.4**). A statistical analysis of percent differences in EMSA band shift intensities between NAc proteins bound to the CART promoter CRE after cocaine versus saline treatment revealed no difference (**Figure 4.5A**). Quantification of CREB and P-CREB antibody super shifted bands also revealed no percent differences between the groups (**Figure 4.5B** and **C**).

4.3.2 Effects of binge cocaine on rat NAc AP1 protein binding to a consensus AP1 *cis*-regulatory element

AP1 proteins were previously shown to be increased after acute and repeated cocaine administration and binding to AP1 *cis*-elements was enhanced compared to saline treated animals after chronic cocaine treatments (Hope et al 1992; McClung & Nestler 2003). In this study, binding of rat NAc nuclear proteins to the consensus AP1

4.1. CREB protein levels were increased in the rat NAc after binge cocaine administration. **(A)** A representative Western blot of rat NAc CREB protein levels from three cocaine treated rats pooled together (lanes marked "Coc") and three saline treated rats pooled together (lanes marked "Sal") revealed that CREB levels were significantly increased in the NAc of cocaine treated rats. Bradford assay was used to add equal amounts of total protein from each individual animal previous to pooling nuclear proteins. **(B)** Densitometry of the immunoreactive bands around 45 KDa (the predicted molecular weight of CREB) from a total of 9 animals/treatment group (represented graphically below the gel) revealed that there was a statistically greater quantity of protein between the two groups. The mean percent difference in CREB protein levels between the groups was 18.89 ± 7.293 (mean % $\pm$ SEM, $*p < 0.05$, two-sample t-test).

Figure 4.1. CREB protein levels were increased in the rat NAc after binge cocaine administration.
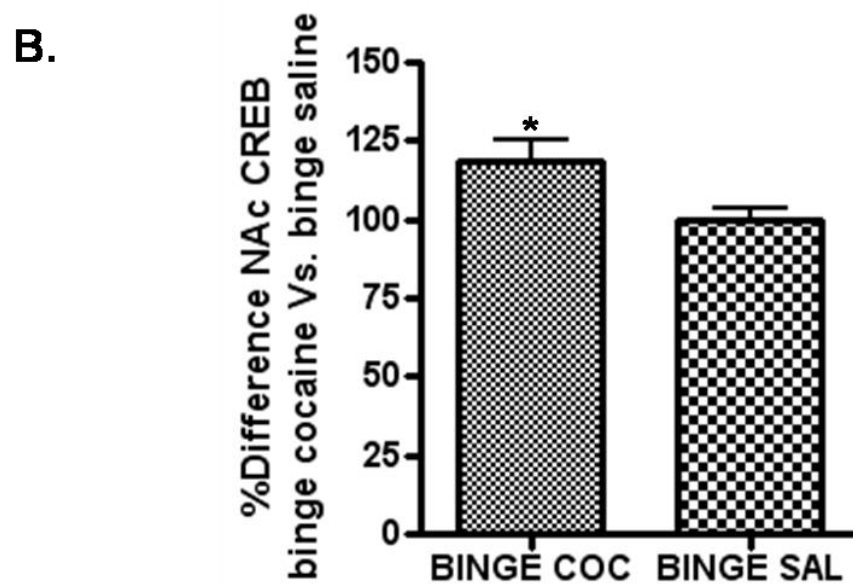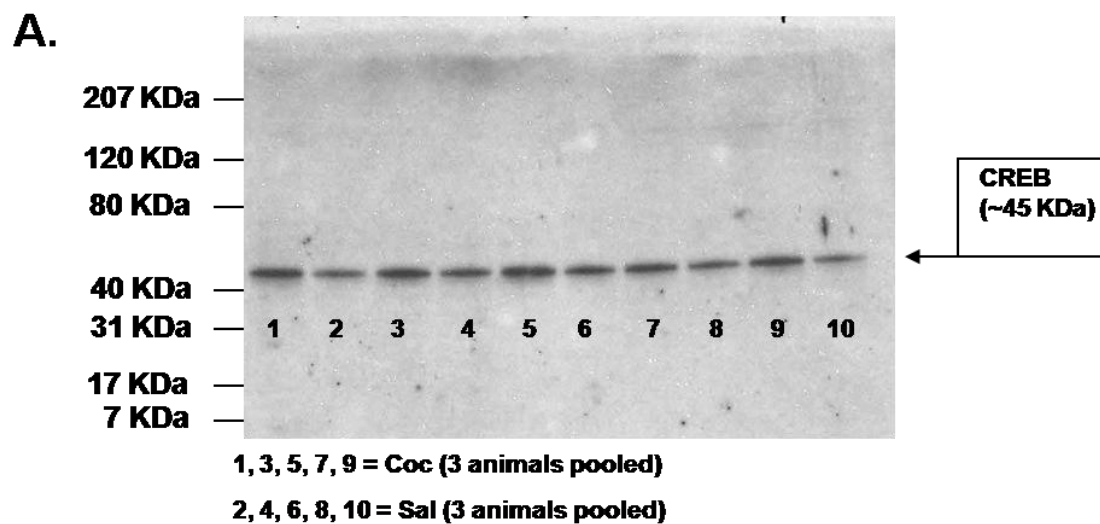
A.

207 KDa —
120 KDa —
80 KDa —

40 KDa —
31 KDa —

17 KDa —
7 KDa —

CREB
(~45 KDa)

1 2 3 4 5 6 7 8 9 10

1, 3, 5, 7, 9 = Coc (3 animals pooled)
2, 4, 6, 8, 10 = Sal (3 animals pooled)

B.

Figure 4.2. P-CREB levels were not changed in the rat NAc after binge cocaine administration. (A) A representative Western blot of P-CREB protein levels from the NAc of three cocaine treated rats pooled together (lanes marked "Coc") and three saline treated rats pooled together (lanes marked "Sal") revealed that P-CREB levels were not significantly increased in the NAc of cocaine treated rats. Bradford assay was used to add equal amounts of total protein from each individual animal previous to pooling nuclear proteins. **(B)** Densitometry of the immunoreactive bands around 45 KDa (the predicted molecular weight of P-CREB) from a total of 9 animals/treatment group (represented graphically below the gel) revealed that there was not a statistically greater quantity of protein between the two groups. The mean percent difference in P-CREB protein levels between the groups was 1.895 ± 6.093 (mean % $\pm$ SEM, $p < 0.05$, two-sample t-test).

Figure 4.2. P-CREB levels were not changed in the rat NAc after binge cocaine administration.
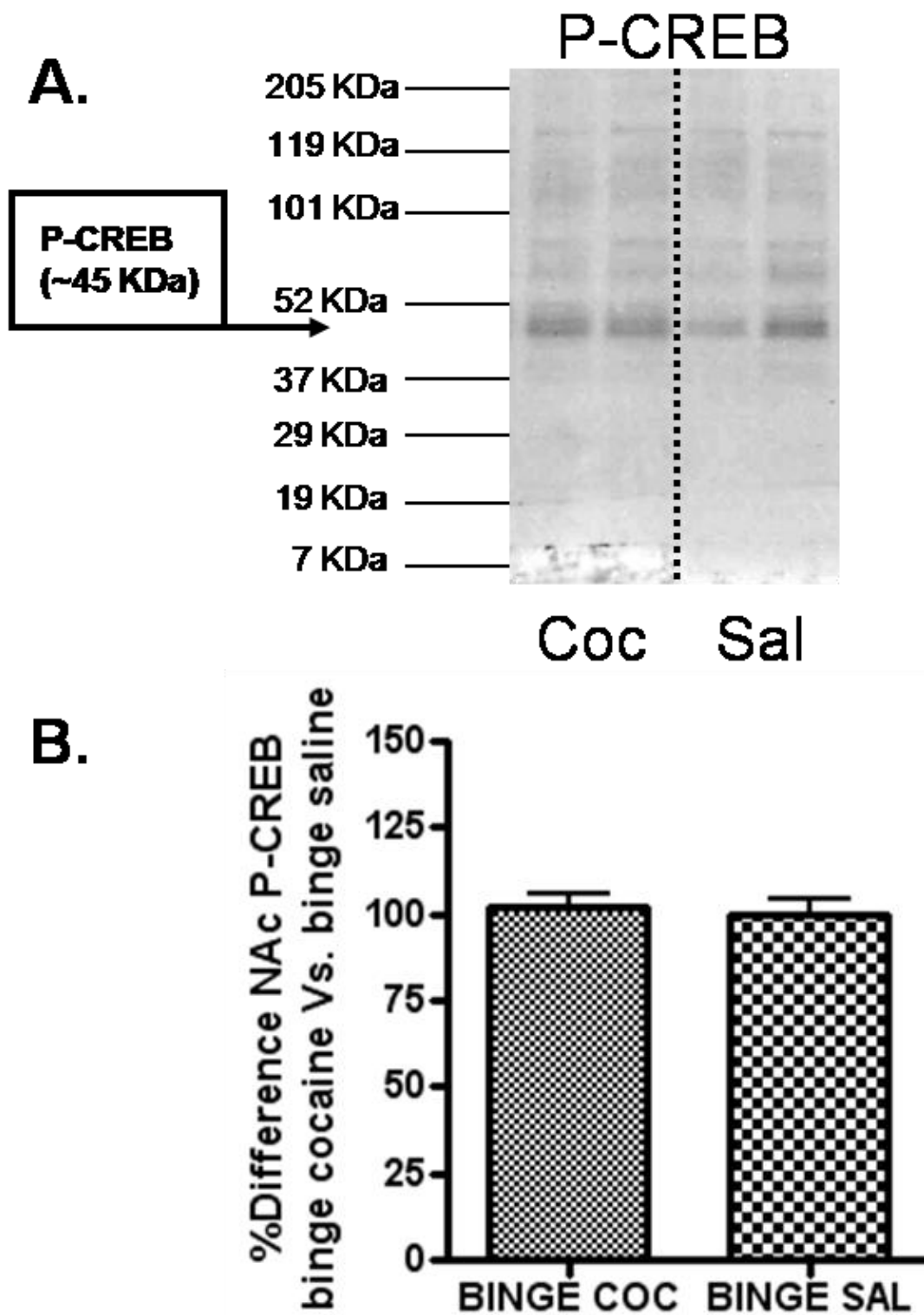
Figure 4.3. CART peptide levels were enhanced in the rat NAc after binge cocaine administration. (A) A representative Western of CART peptide levels (approximately 6.5 KDa) normalized to whole protein content by Bradford assay from the NAc of a cocaine treated (lanes marked "Coc") and saline treated rat (lanes marked "Sal") showed that CART peptide levels were significantly increased after binge cocaine, but not binge saline, treatment. **(B)** Densitometry of the immunoreactive bands below 7 KDa from a total of 9 animals/treatment group (represented graphically below the gel) revealed that the mean difference between groups was 30.35 ± 12.62 (mean % $\pm$ SEM, *p = 0.023, two-sample t-test, n = 9/group).

Figure 4.3. CART peptide levels were enhanced in the rat NAc after binge cocaine administration.
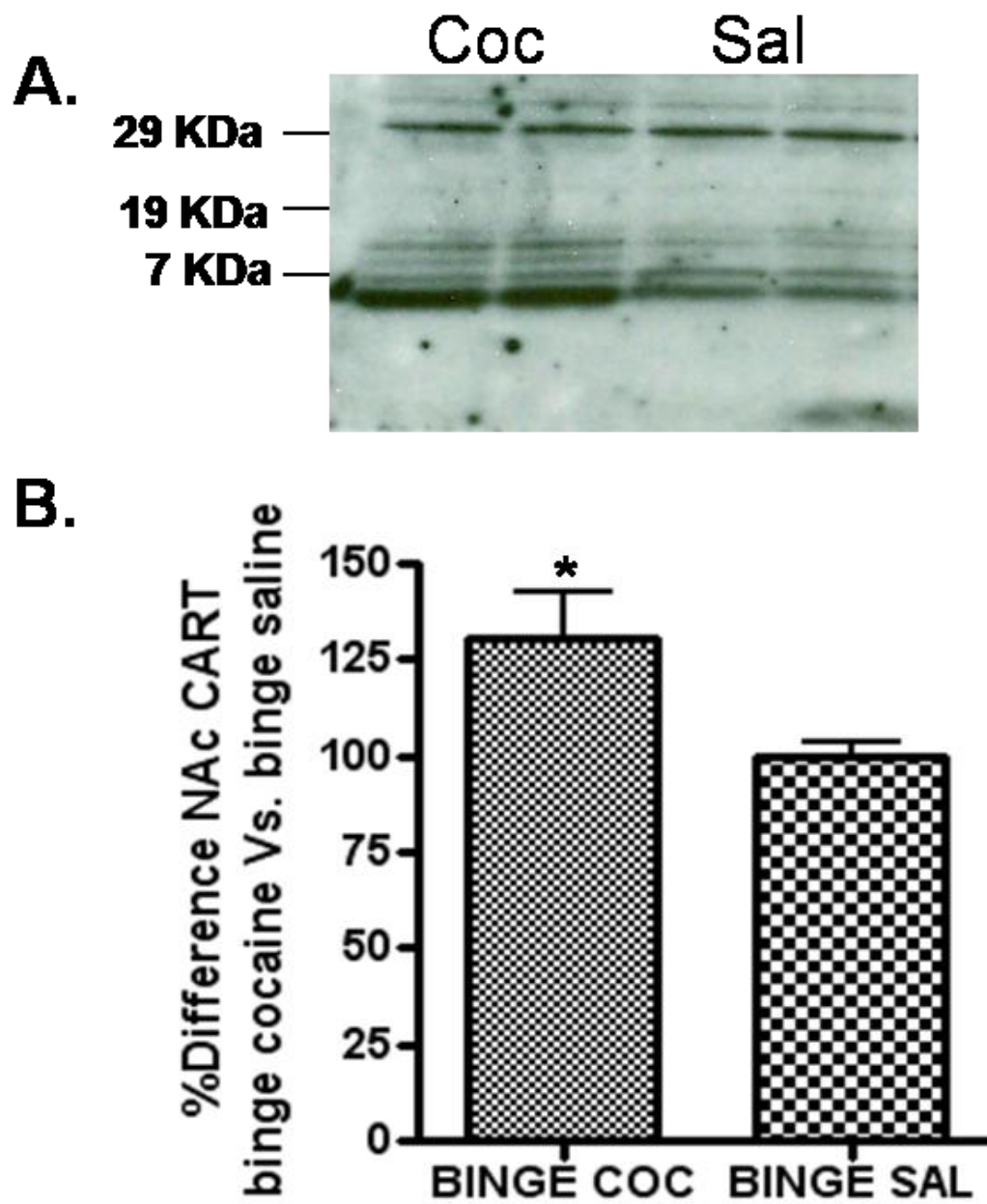
Figure 4.4. The levels of rat NAc nuclear protein binding to CART promoter CRE oligonucleotides were not changed after binge cocaine administration. In EMSA/SS assays, no differences in TF binding to the CART CRE oligonucleotide were observed. The data in the figure showed: a negative control radioprobe alone (no protein added) reaction lane (lane 1; free ^{32}P-CRE was indicated by an arrow on the bottom right of the gel); specific TF-DNA interactions from three cocaine- or three saline-treated rats pooled together (lanes 2 and 3, respectively; the complexes were denoted by arrows at the figure's top right); P-CREB antibody super shifts (lanes 4 and 5; see box at top left denoting ^{32}P-CRE + NAc TF + antibody complex); and specific TF-DNA interactions from three cocaine- or three saline-treated rats pooled together (lanes 6, 8, 10 and 7, 9, 11 respectively). Some non-specific binding was observed near the bottom of the gel, but because that complex didn't migrate near the pituitary TF + ^{32}P-CRE complexes it did not confound the results. The ^{32}P-CRE + NAc TF complexes were identified as specific TF-DNA binding events because 50x non-radiolabeled dsCRE oligonucleotides competed for binding to those proteins and 50x non-radiolabeled dsSP1 did not in separate assays (not shown). Furthermore, CREB and P-CREB antibodies specifically shifted ^{32}P-CRE + NAc TF complexes (CREB SS not shown).

Figure 4.4. The levels of rat NAc nuclear protein binding to CART promoter CRE oligonucleotides were not changed after binge cocaine administration.

^{32}P-CRE + NAc TF + antibody complex

1. 2. 3. 4. 5. 6. 7. 8. 9. 10. 11.

^{32}P-CRE + NAc TF complex

Free ^{32}P-CRE

Rat, CART CRE cis-*element sequence (5' to 3')*
CGG CGG GCA TTG ACG TCA AAC GGC AGC

1. ^{32}P-CRE rat oligonucleotide	6. + Coc TF
2. + Cocaine NAc transcription factors (TF)	7. + Sal TF
3. + Saline NAc transcription factors (TF)	8. + Coc TF
	9. + Sal TF
4. + Coc + P-CREB antibody	10. + Coc TF
5. + Sal + P-CREB antibody	11. + Sal TF
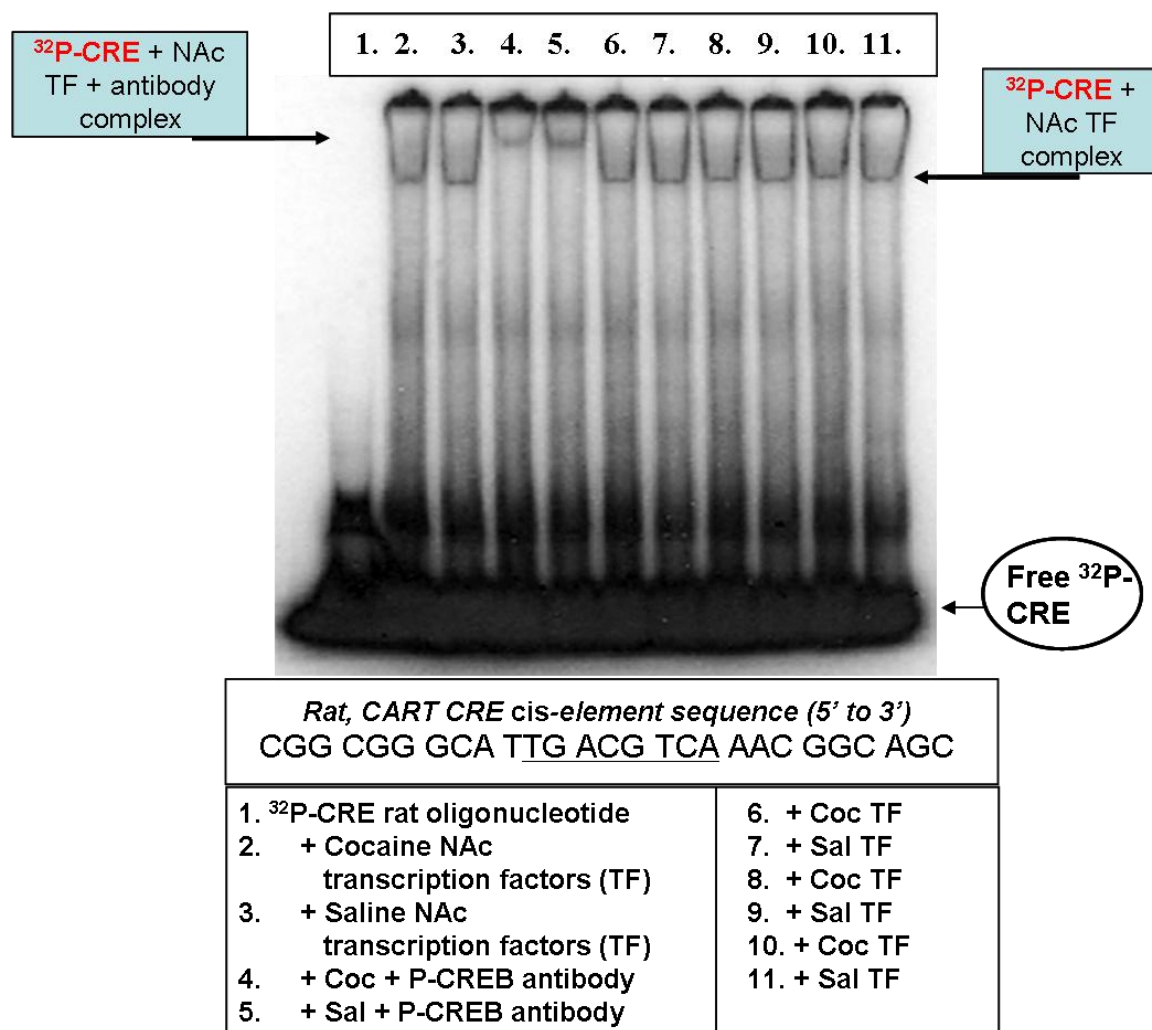
Figure 4.5. Band shift intensities of rat NAc nuclear proteins bound to the CART

CRE oligonucleotide did not significantly differ between cocaine or saline treated

animals. EMSA/SS analyses were performed with NAc nuclear proteins from rats

administered a binge regimen of cocaine (Coc) or saline (Sal) using an oligonucleotide

identical in sequence to the CART promoter CRE and its flanking regions. The data in

the figure showed a comparison of mean percent differences in optical densities of

EMSA (**A**) and CREB and P-CREB SS (**B** and **C**) band shifts from a total of 9

animals/treatment group. There was not a statistically different quantity of TFs bound to

the CRE oligonucleotide between the two groups. The mean percent difference between

groups in EMSA was 23.95 ± 19.03 (mean % $\pm$ SEM, $p > 0.05$, two-sample t-test). There

were also no differences in CREB or P-CREB SS band intensities between groups; 22.42

± 17.08 (mean % $\pm$ SEM, $p > 0.05$, two-sample t-test) for CREB and 13.31 ± 17.13

(mean % $\pm$ SEM, $p > 0.05$, two-sample t-test) for P-CREB.

Figure 4.5. Band shift intensities of rat NAc nuclear proteins bound to the CART CRE oligonucleotide did not significantly differ between cocaine or saline treated animals.

A. ^{32}P-CRE EMSA: binge cocaine- Vs saline-treated rat NAc proteins
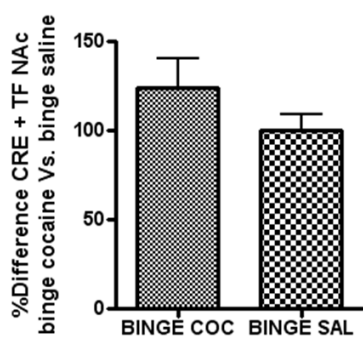
B. ^{32}P-CRE + binge cocaine- Vs saline-treated rat NAc proteins: CREB SS
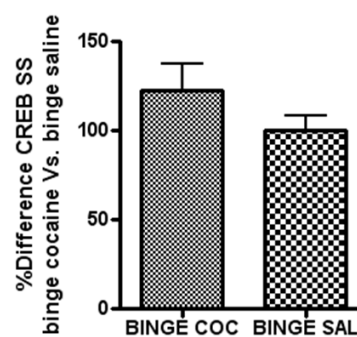
C. ^{32}P-CRE + binge cocaine- Vs saline-treated rat NAc proteins: P-CREB SS
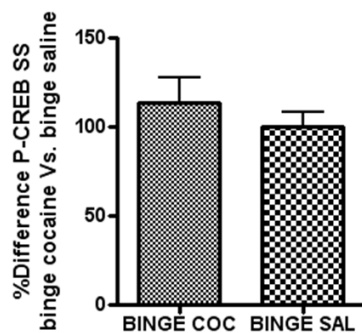
cis-regulatory element was significantly increased after one-day binge cocaine treatments (**Figure 4.6**). Antibody super shift assays with JunD and c-Fos antibodies indicated that more JunD may have been bound to that oligonucleotide after cocaine treatment compared to saline treatment. The data in **figure 4.7** showed that there was a statistically greater intensity of EMSA band shifts between cocaine and saline treated rat NAc (n = 6/group).

4.4. <u>Discussion</u>

The one-day binge cocaine administration paradigm used in this study had not been tested before in terms of examining the effects on CART peptide, CREB or P-CREB levels. The treatment increased both CREB (**Figure 4.1**) and CART peptide levels (**Figure 4.3**) in the rat NAc, but had no effect on the levels of P-CREB (**Figure 4.2**). The binding of NAc nuclear proteins to the CART promoter CRE site in EMSA/SS assays did not show differences between groups (**Figure 4.4** and **4.5**), nor did antibody super shift assays reveal more CREB or P-CREB bound to the CRE site after cocaine treatment compared to saline treatment (**Figure 4.5**).

NAc nuclear protein binding to a consensus AP1 site was increased by binge cocaine administration in these assays (**Figures 4.6** and **4.7**), which indicated that it was possible to observe differences between groups using EMSA/SS assays. The data also suggested that binge cocaine administration increased the expression of AP1-regulated genes in the brain, which could have important implications for understanding the molecular mechanisms of drug addiction since the AP1 family mediates cocaine reward and addiction behaviors by yet unknown mechanisms.

Figure 4.6. Band shift intensities of rat NAc nuclear proteins bound to a consensus AP1 sequence oliognucleotide were significantly greater after binge cocaine treatment compared to saline treatment. The data from EMSA/SS assays using a consensus AP1 *cis*-element showed: a negative control radioprobe alone (no protein added) reaction lane (lane 1; free ^{32}P-AP1 is indicated by an arrow on the bottom left of the gel); specific protein-DNA interactions from three cocaine- or three saline-treated rats pooled together (lanes 2 and 3, respectively; the complexes were denoted by arrows at the figure's top left); competition with 50x unlabeled dsAP1 oligonucleotides (lanes 4 and 5); a non-specific competition reaction with 50x unlabeled dsPit1 oligonucleotides unrelated in sequence to the AP1 oligonucleotide (lanes 6 and 7); JunD antibody super shifts (lanes 8 and 9); and c-Fos antibody super shifts (lanes 10 and 11; see box at top right denoting ^{32}P-AP1 + NAc TF + antibody complex). Some weak protein binding was seen near the middle of the gel in the competition lanes indicated it could have been non-specific. The results are representative of 6 animals/treatment group assayed in three separate EMSA/SS assays.

Figure 4.6. Band shift intensities of rat NAc nuclear proteins bound to a consensus AP1 sequence oliognucleotide were signficantly greater after cocaine treatment compared to saline treatment.
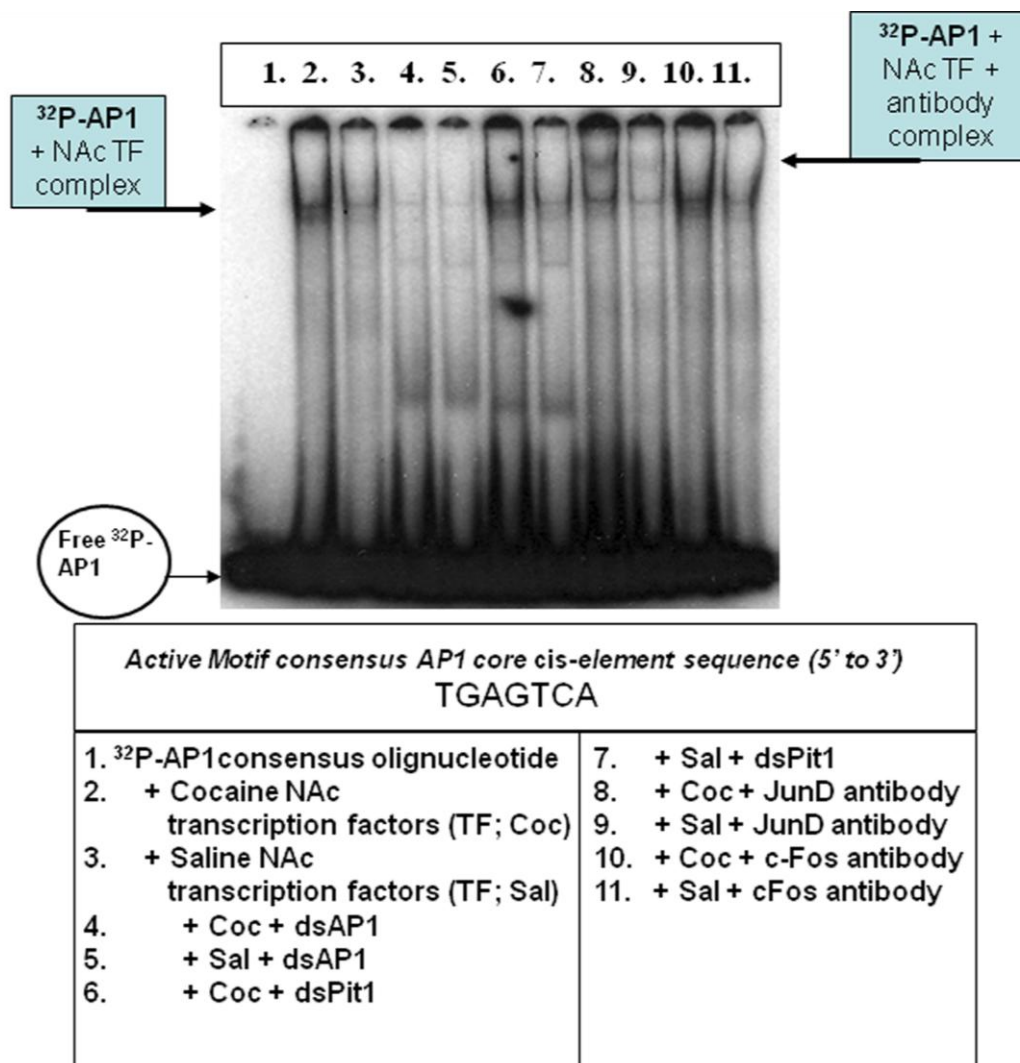
Active Motif consensus AP1 core cis-element sequence (5' to 3')
TGAGTCA

1. ^{32}P-AP1consensus olignucleotide	7. + Sal + dsPit1
2. + Cocaine NAc transcription factors (TF; Coc)	8. + Coc + JunD antibody
	9. + Sal + JunD antibody
3. + Saline NAc transcription factors (TF; Sal)	10. + Coc + c-Fos antibody
	11. + Sal + cFos antibody
4. + Coc + dsAP1	
5. + Sal + dsAP1	
6. + Coc + dsPit1	

Figure 4.7. Quantitation of the percent difference in band shift intensities of rat NAc nuclear proteins bound to the consensus AP1 oliognucleotide were significantly greater from cocaine treated animals compared to saline treated animals. EMSA/SS analyses were performed with NAc nuclear proteins from rats administered a binge regimen of cocaine (Coc) or saline (Sal) using a consensus sequence AP1 oligonucleotide. The figure showed the results from a quantitative analysis of the percent difference in band shift intensities of EMSA bands from a total of 6 animals/treatment group assayed in three separate EMSA/SS experiments. There was a statistically greater quantity of TFs bound to the AP1oligonucleotide between the two groups. The mean percent difference between groups was 30.15 ± 14.08 (mean % $\pm$ SEM, *$p < 0.05$, two-sample t-test).

Figure 4.7. Quantitation of the percent difference in band shift intensities of rat NAc nuclear proteins bound to the consensus AP1 oliognucleotide were significantly greater from cocaine treated animals compared to saline treated animals.
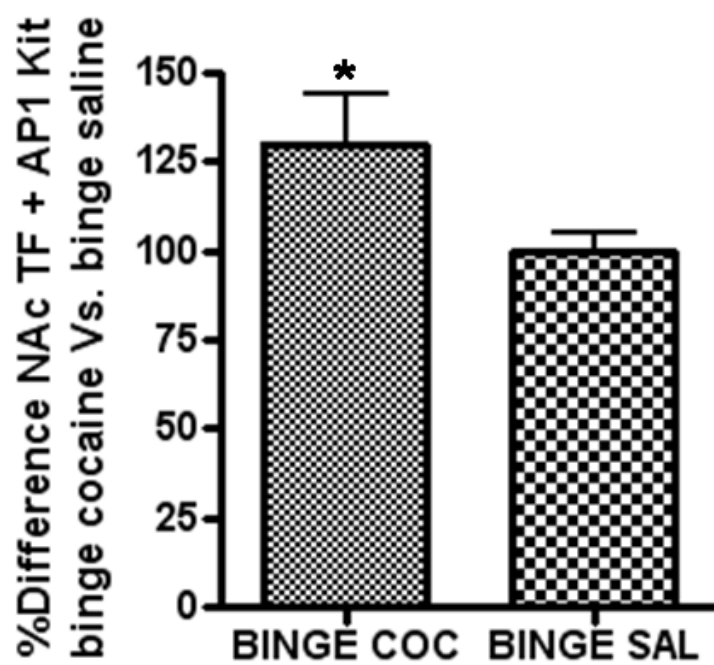
From a review of the literature, up-regulation of CART mRNA after cocaine administration appeared to be dependent upon a number of variables like gender, dose, administration paradigm and stress (see **section 4.1** above and **chapter 1, section 1.6.1**). Cocaine itself could not have directly regulated CART expression; the pharmacological action of cocaine was to directly bind to and inhibit DAT, thus indirectly increase synaptic dopamine levels in the NAc. The current focus of drug abuse research has been to determine how, from a systems pharmacology point-of-view, the body reacted to that blockade of DAT and what neurotransmitter systems were involved in homeostatic feedback mechanisms that attempted to counteract cocaine's effects.

CART mRNA expression may have been regulated by cocaine *in vivo*, as a result of simultaneously activated signaling pathways such as stress pathways like HPA axis activation, calcium-channel activation and dopamine receptor activation that all converged on P-CREB via glucocorticoids (Liu et al 1994), CaMK IV (Matthews et al 1994) and PKA (Carlezon et al 1998). In cultured cells, cocaine activated voltage-gated calcium channels (Yermolaieva et al 2001) and in separate studies intracellular calcium signaling was shown to increase CART mRNA levels (Jones et al 2009). In further support of the idea that multiple variables contributed to the regulation of CART mRNA in the rat NAc after cocaine exposure, pre-treatment of rats with intra-accumbal forskolin synergized with cocaine to increase CART mRNA levels above and beyond what forskolin or cocaine could do alone (Jones & Kuhar 2006). That is, acute cocaine had no effect on CART mRNA levels in the rat NAc in those studies, but after forskolin infusions into the NAc and an intraperitoneal injection of cocaine, CART mRNA levels were increased beyond forskolin's effects alone.

Furthermore, a separate study showed no changes in male rat NAc CART mRNA levels after a binge cocaine dosing regimen of 3 doses of 15 mg/kg body weight administered every hour and euthanization one hour after the last injection (Fagergren & Hurd 1999). That study did, however, find that in the female rat NAc, CART mRNA was up-regulated by binge cocaine, again supporting the idea that indirect elevation of dopamine by cocaine was, in itself, not the only variable involved in rat NAc CART gene regulation.

The molecular effects of one-day binge cocaine administration have not been extensively studied and drug abuse researchers have begun to realize that the acute injection paradigm may not best reflect the use patterns of human abusers. The data presented in this chapter were the first examination of CREB and P-CREB levels in the rat NAc after one-day binge cocaine treatment. Data from chronically cocaine injected mice and rats indicated that repeated dosing caused an increase in P-CREB TF levels 20-30 minutes after the last cocaine injection, but not at later time points (Kreibich & Blendy 2004; Lee et al 2008; Mattson et al 2005; Tropea et al 2008). That tight regulation of P-CREB levels was probably because of homeostatic mechanisms such as phosphatase activation or PKA desensitization which prevented further phosphorylation of CREB molecules. The fact that increases in P-CREB levels or P-CREB binding to the CART promoter CRE site were not observed during the binge regimen could have indicated that similar homeostatic feedback mechanisms were enacted in the rat NAc to counteract the cocaine-induced increases in CREB levels.

The CREB pathway has been implicated in behavioral tolerance to the reinforcing effects of drugs after long-term, chronic use by regulating genes in the limbic system that

mediated emotional responses to external stimuli (Carlezon et al 2005). Increased P-CREB activity, along with over expression of corticotropin releasing hormone (CRH) and over stimulation of the HPA axis during cocaine abstinence were found to be associated with dysphoria, anhedonia and emotional numbing; prominent factors in drug withdrawal, psychological dependence and a cycle of behaviors where such negative affective symptoms have been shown to drive drug craving and seeking because the user was unable to feel pleasure from things that were naturally pleasurable (Carlezon et al 2005; Koob 2009; Koob & Nestler 1997; Nestler 2004b). In that case, the user instead had to rely on pharmacological over stimulation of the brain reward pathway by cocaine to overcome the subjective effects of P-CREB over activity and other molecular mechanisms of psychological dependence and withdrawal such as over activation of the HPA axis. There was great interest in understanding how disregulation of P-CREB was associated with negative affective symptoms of drug withdrawal, and the identification of candidate CREB-regulated genes in the NAc, such as CART, may help to elucidate some of the molecular events that translated into those mood states.

As a CREB regulated gene that was also regulated by cocaine and stress hormones, CART may have had the ability to modulate drug dependence and withdrawal after long-term chronic use (Fagergren & Hurd 2007). Specifically, the regulation of CART by CREB and glucocorticoids such as corticosterone may have been a component of the hypothesized "anti-reward" system that was shown to be activated to counteract the effects of over activation of the reward pathway by drugs of abuse (Koob 2009; Koob & Nestler 1997).

To-date, no research has examined the role of CART in drug withdrawal and the anti-reward system. The data from this chapter which showed that moderate binge cocaine administration increased CART peptide expression, and data from a previous study showing that a more stressful binge cocaine paradigm as well as acute injections of corticosterone increased CART mRNA in the rat NAc, and the data presented in this dissertation generally showing that CREB could bind to the CRE site in the chromatin of the rat gene and that over expression of CREB could regulate CART mRNA and peptide levels in the rat NAc, provide a firm rationale for beginning to study CART in the anti-reward pathway in terms of the effects of stress and drug withdrawal on CART mRNA and peptide levels and vice versa.

The fact that AP1 proteins from the rat NAc bound more abundantly to a consensus AP1 *cis*-regulatory element after binge cocaine treatment compared to saline treatment and that the JunD antibody shifted the ^{32}P-AP1-TF complex, but c-Fos antibodies did not (**Figure 4.6**) , was probably because AP1 protein levels were still up-regulated at the time of euthanization. c-Fos was previously shown to be an immediate early gene transcribed within 30 minutes of cocaine exposure, but degraded rapidly and desensitized in response to subsequent drug administration (Hai & Curran 1991; Hope et al 1992). During its short half-life, however, c-Fos was able to bind to AP1 *cis*-regulatory elements in the promoters of other AP1 proteins like JunD, and those transcription factors remained expressed for longer periods of time to regulate distinct subsets of AP1-regulated genes (Hai & Curran 1991). The binge cocaine regimen used in these experiments appeared to stimulate NAc JunD binding to the consensus *cis*-element more so than did binge saline treatment (**Figure 4.6**, comparison of **lanes 8** and **9**).

Chapter 5: EMSA and antibody super shift analyses of other putative CART promoter *cis*-regulatory elements identified by database analysis in the rat and mouse genes.

5.1 <u>Introduction</u>

In order to further explore mechanisms of CART gene transcriptional regulation, three other putative CART promoter *cis*-regulatory elements previously identified by database analysis (the mouse AP1-like, mouse Pit1 and rat Ptx1 sites) were analyzed in EMSA/SS assays for their abilities to bind transcription factors from cultured cells, the rat NAc and the rat pituitary. Although an AP1-like sequence was not identified by Barret et al in the rat promoter (Barrett et al 2002), a highly homologous sequence aligned with the mouse promoter AP1-like sequence and was thus tested in the following experiments for its ability to bind to AP1 family TFs (Dominguez et al 2002). The rationale for examining the role of the CART promoter AP1-like *cis*-regulatory elements with nuclear protein extracts from the rat NAc was that AP1 family TF activities in the NAc both affected the rewarding properties of cocaine and were dynamically regulated throughout the course of the addiction cycle by various abused substances, including psychostimulants (McClung & Nestler 2003; Nestler 2004a; b).

The rationale for examining the pituitary-specific promoter elements was because they may have contributed to mouse CART promoter-driven luciferase activities in pituitary-derived GH3 cells (de Lartigue et al 2007; Dominguez & Kuhar 2004; Dominguez et al 2002). Specifically, sequential deletion of a region of the mouse promoter containing the Pit1 *cis*-element significantly reduced basal luciferase activity in those cells (Dominguez et al 2002). In the mouse gene, the Pit1 *cis*-regulatory element was found to be two nucleotides different from the Ptx1 *cis*-regulatory element identified in the rat gene and the two sites aligned at the same nucleotides positions relative to +1, thus the Ptx1 element may also have been able to contribute to CART gene

transcriptional regulation, although it has never been studied in relation to CART gene regulation. Importantly, the pituitary was found to be rich with CART expression and the regulatory mechanisms of that expression were not known. A portion of the experiments performed in this chapter of the dissertation explored the hypothesis that Pit1 and Ptx1 may have played some role in CART gene regulation in the pituitary.

5.2 <u>Methods</u>

5.2.1 Animals

See **chapter 2, section 2.2.5** for detailed methodologies concerning animal welfare and pituitary dissections and **chapter 3, section 3.2.1** regarding NAc dissections.

5.2.2 Cell culture

See **chapter 2, section 2.2.2** for detailed methodologies.

5.2.3 EMSA/SS assays

See **chapter 2, section 2.2.6** for detailed methodologies. Binding to the ^{32}P-labelled oligonucleotides was observed by EMSA/SS using a double stranded (ds) oligonucleotide identical in sequence to the CART promoter *cis*-element under investigation. The sequence of the site (from 5' to 3') was given below the picture of the gel in the box and the core binding site was underlined. The two nucleotides that differ between the mouse Pit1 and Ptx1 *cis*-regulatory elements in the rat CART promoter were italicized. In this chapter, the oligonucleotides used as non-specific competitors were: dsAP2 (identical in sequence to an AP2 *cis*-regulatory element identified in the mouse CART promoter with a sequence (from 5' to 3') of TTC CCG GGC TCC CGG AGC CCG GCG GGC ATT; and dsNFκB from an unrelated gene

with a sequence (from 5' to 3') of GCT ATA AGA AGC CGG AGA GCG CAG TG.

Nuclear extracts of Jurkat cells, derived from acute T cell leukemia human T

lymphoblasts and 3T3 cells, derived from the mouse embryo, were used as positive

control proteins to investigate TF-DNA interactions between AP1 and Ptx1 *cis*-regulatory

elements, respectively. Both types of nuclear extracts were purchased from Active Motif.

5.2.4 Western blot analysis

See **chapter 3, section 3.2.5** for detailed methodologies. Antibodies specific for

Pit1, Oct2 and Oct4 were obtained from Abcam (Cambridge, MA). Some assays also

used an antibody specific for Pit1 from Active Motif (Carlsbad, CA). Immunizing

peptides used in antigen pre-absorption assays were obtained from Active Motif.

5.3 <u>Results</u>

5.3.1 EMSA/SS analysis of the CART gene promoter Pit1 and Ptx1 *cis*-regulatory
elements

The sequences in **table 5.1** illustrated a comparison of oligonucleotide sequences

between the mouse CART promoter Pit-1 *cis*-regulatory element, the closely related rat

CART promoter Ptx-1 sequence and a consensus Pit-1 *cis*-regulatory sequence that was

commercially sold by Active Motif (Carlsbad, CA). Core binding sequences were

underlined in the table. The mouse and rat sequences were identical to those found in

their respective CART genes and differed by two nucleotides in their core binding sites

(italicized and bolded). In **figure 5.1**, the mouse ^{32}P-Pit1 oligonucleotide was able to

Table 5.1. Oligonucleotide sequences of the CART gene Pit1, Ptx1 and consensus Pit1 *cis*-regulatory elements assayed by EMSA/SS analyses.

Mouse CART Pit1 cis-*element sequence (5' to 3')*
ACT TTA GTT TTA **A**TT ATC CA**T** ATA TGT G
Rat, CART Ptx1 cis-*element sequence (5' to 3')*
ACT TTA GTT TTA **GT**T ATC CA**A** ATA TGT G
Active Motif Pit1 consensus sequence
AT TAT ATA TAT ATT CAT GAA

Table 5.1. The pituitary homeobox 1 (Ptx1) *cis*-regulatory element was identified by database analysis in the rat CART gene promoter and was proposed to bind to pituitary-specific transcription factors to regulate neuronal differentiation during pituitary development (Tremblay et al 1998). In relation to CART gene regulation, the site was of interest because CART mRNA expression was regulated by development in a number of tissues (Brischoux et al 2001; Brischoux et al 2002; Dun et al 2001; Wierup et al 2004) by unknown mechanisms that could have involved the Ptx1 site. In addition, CART was found to be enriched in the pituitary and the expression was highly regulated by factors such corticosterone releasing hormone and prolactin (Koylu et al 1997; Kuriyama et al 2004; Larsen et al 2003; Smith et al 2006; Smith et al 2004; Stanley et al 2004; Vicentic et al 2004). A closely related sequence, Pit1, was identified in the mouse gene in the same location as Ptx1 relative to the +1 site of transcriptional initiation and deletion of that site from luciferase constructs driven by the mouse CART promoter resulted in a significant loss of luciferase enzymatic activity in GH3 cells (Dominguez et al 2002). EMSA/SS assays were performed with the tabled oligonucleotides in order to determine if nuclear transcription factors in nuclear extracts from rat pituitary-derived GH3 cells, the rat pituitary and rat NAc could bind to them and potentially regulate the CART gene in those tissues.

Figure 5.1. Rat pituitary-derived GH3 cell transcription factors bound to the mouse CART gene promoter Pit1 *cis*-regulatory element and Pit1 antibodies super shifted the TF-DNA complex. EMSA/SS analyses were presented as: a negative control radioprobe alone (no protein added) reaction lane (lane 1; free ^{32}P-Pit1 was indicated by an arrow on the bottom left of the gel); specific protein-DNA interactions with GH3 TFs (lane 2; the complexes were denoted by arrows at the figure's top left); competition with 50x non-radiolabeled dsPit1 oligonucleotide (lane 3); a non-specific competition reaction with 50x non-radiolabeled dsSP1 oligonucleotide, unrelated in sequence to the Pit1 oligonucleotide (lane 4); Pit1 antibody super shifts (lanes 5, 6, 7; see box at top right denoting ^{32}P-Pit1 + GH3 TF + antibody complex); and an antigen pre-absorbed Pit1 antibody super shift (lane 9). No super shift was seen in lane 9, which indicated that the peptide antigen competed for antibody binding to the protein in the TF-DNA complex, which was most likely the Pit1 TF. Lane 7 used an antibody from a different company, which could account for its different migration pattern because it was raised against a different peptide epitope and may have been of itself a different molecular weight, causing the TF + antibody + DNA complex to migrate at a different rate than the other super shifted bands. At least three TF + DNA complexes were observed, but the antibody super shifts mostly shifted the top two bands, possibly indicating that Pit1 proteins were more abundant in those complexes.

Figure 5.1. Rat pituitary-derived GH3 cell transcription factors bound to the mouse CART gene promoter Pit1 *cis*-regulatory element and Pit1 antibodies super shifted the TF-DNA complex.
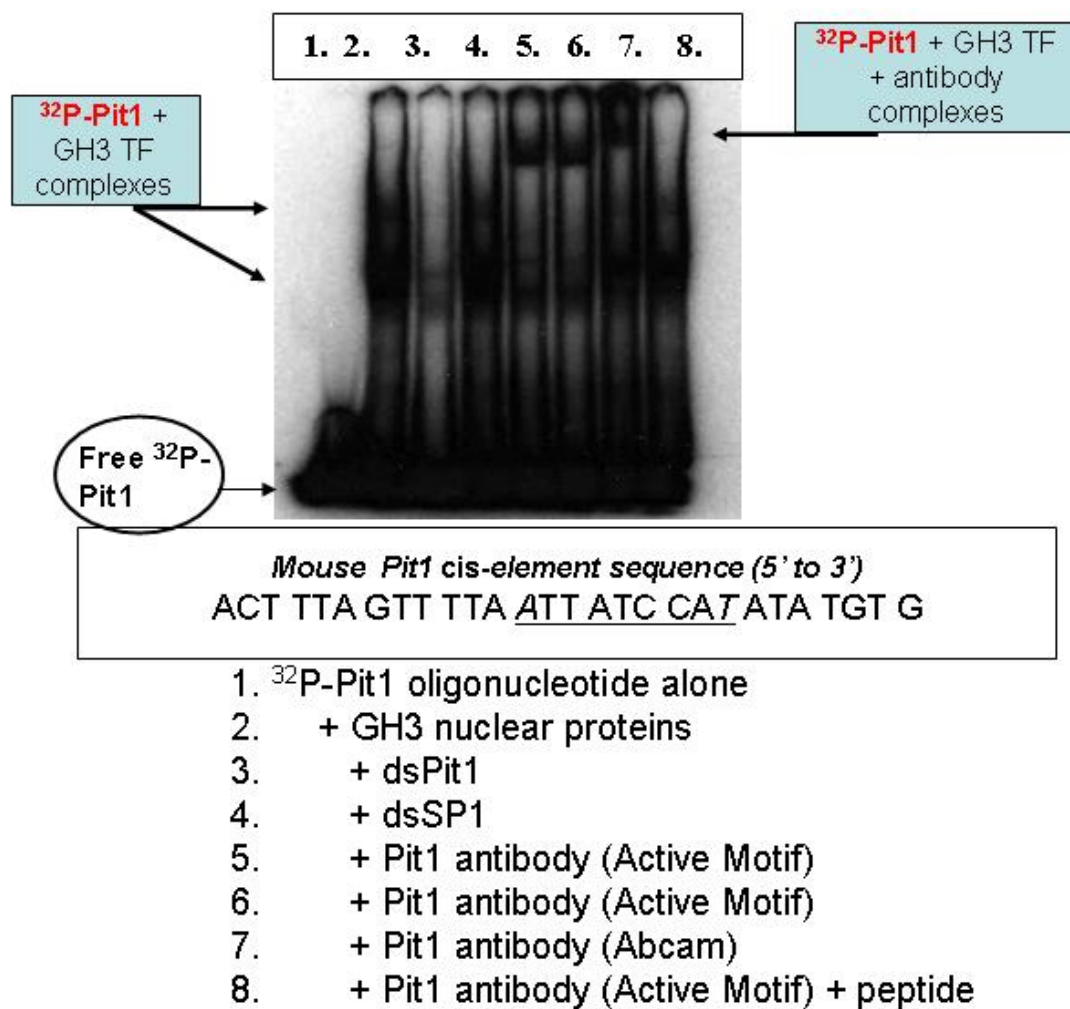
bind to Pit1 proteins extracted from the nuclei of GH3 cells as determined by EMSA/SS

assays with ^{32}P labeled Pit1 oligonucleotides and two different antibodies against Pit1

proteins (n = 5 plates). Antigen pre-absorption with an immunizing peptide one of the

Pit1 antibodies was raised against inhibited the super shift activity, which indicated that

the antibody was specific in recognizing Pit1 in the super shift assay. Western blot

analysis also verified the presence of Pit1 proteins in GH3 cells and the pituitary (**Figure

5.2**, n = 3 plates, 3 animals).

The mouse Pit1 *cis*-element was also able to bind Pit1 in nuclear extracts from the

rat pituitary (**Figure 5.3**; n = 5 animals). In contrast, nuclear proteins in nuclear extracts

from the rat NAc only weakly bound to the Pit1 *cis*-element and the Pit1 antibody did not

produce a super shift of the TF + DNA complex (**Figure 5.4**; n = 3 animals). In the

figure, GH3 cell transcription factors (far right lanes) were assayed as a positive control

to show that in that preparation, Pit1 proteins were present. CREB and P-CREB proteins

were not found to bind to the Pit1 *cis*-regulatory element in antibody super shift assays

(**Figure 5.5**), indicating that ^{32}P-Pit1 did not bind to those proteins non-specifically.

In contrast to assays with the mouse Pit1 promoter element, the <u>rat</u> Ptx1 *cis*-

regulatory element was able to bind to nuclear proteins in nuclear extracts from GH3

cells, but Pit1 was not present in the TF + DNA complex as shown by super shift analysis

using the Pit1 antibody (**Figure 5.6**; n = 3 plates). As a positive control in those assays, a

commercially available consensus Pit1 *cis*-element was radiolabeled and assayed with the

same protein preparation (see far left lanes). In agreement with the GH3 TF data, Pit1

antibodies also had no effect on pituitary TF + ^{32}P-Ptx1 complexes in separate EMSA/SS

assays (**Figure 5.7**; n = 3 animals). In the figure, antibodies specific for a closely related

Figure 5.2. Western blot analysis verified the presence of Pit1 proteins in GH3 cells and the rat pituitary. Western blot analyses were performed with GH3 and rat pituitary cytoplasmic proteins using an antibody specific for the Pit1 protein (approximately 33 KDa; indicated by the arrow on the right side of the gel). The data in the figure showed a representative Western of protein levels normalized to whole protein content by Bradford assay from two different concentrations of GH3 cells and the rat pituitary. The upper band in the gel may have been Pit1 homo- or heterodimers since they migrated at a molecular weight near 70 KDa.

Figure 5.2. Western blot analysis verified the presence of Pit1 proteins in GH3 cells and the rat pituitary.
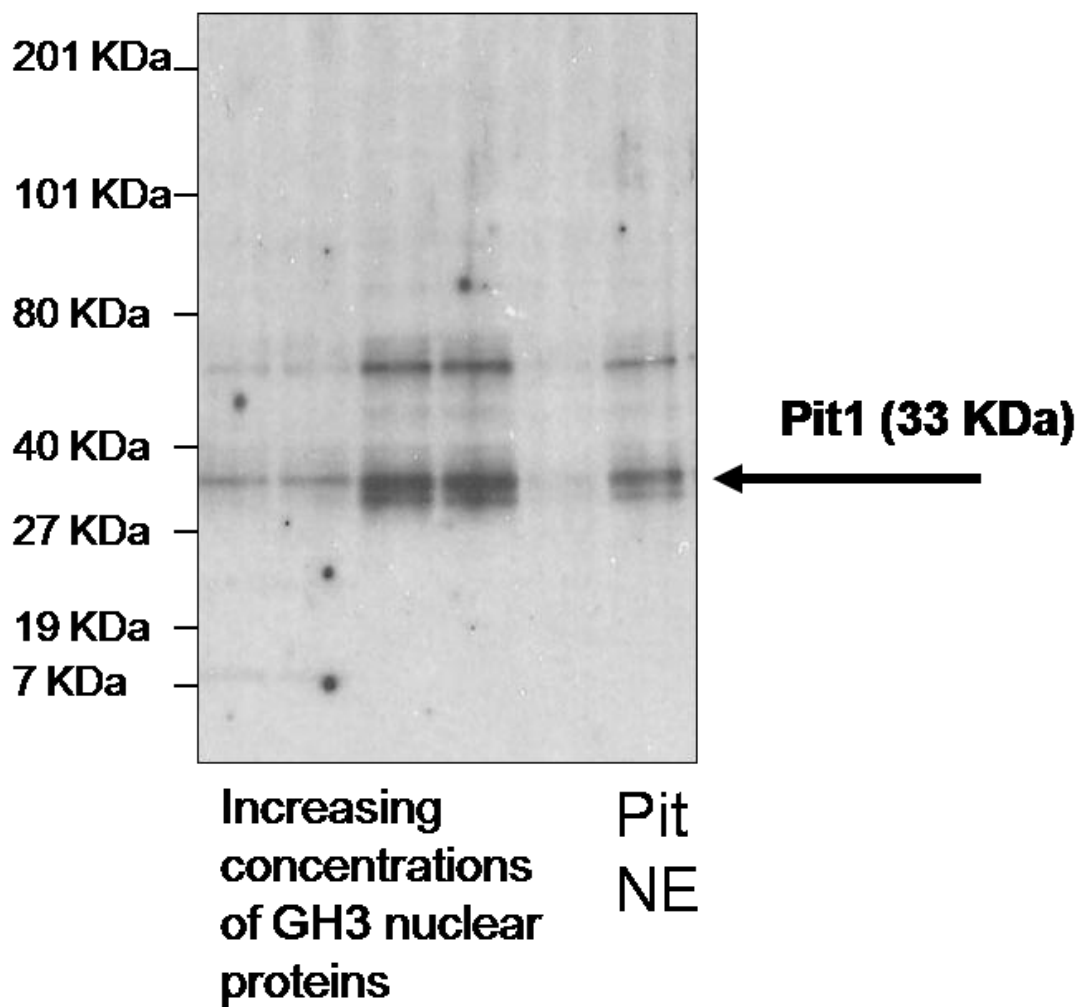
Figure 5.3. Pit1 made in the rat pituitary bound to the mouse CART promoter Pit1
*cis***-regulatory element in EMSA/SS assays.** Pituitary nuclear proteins (TF) bound to

the ^{32}P-Pit1 oligonucleotide in EMSA/SS assays using the same ds oligonucleotide as in

figure 5.2. The sequence of the site (from 5' to 3'; referred to as Pit1) was given below

the picture of the gel in the box. The data were presented as: a negative control

radioprobe alone (no protein added) reaction lane (lane 1; free ^{32}P-Pit1 was indicated by

an arrow on the bottom right of the gel); specific protein-DNA interactions with pituitary

TFs (lane 2; the complexes were denoted by arrows at the figure's top left); competition

with 50x non-radiolabeled dsPit1 oligonucleotide (lane 3); a non-specific competition

reaction with 50x non-radiolabeled dsAP2 oligonucleotide, unrelated in sequence to the

Pit1 oligonucleotide (lane 4); another non-specific competition reaction with 50x non-

radiolabeled mutant Pit1 (a nonsense sequence obtained from Active Motif; lane 5); and a

Pit1 antibody super shift (lane 6; see box at top right denoting ^{32}P-Pit1 + pituitary TF +

antibody complex). In lane 5, the TF + DNA complex was significantly reduced in

intensity, which suggested there were non-specific proteins bound to the oligonucleotide.

The use of an antibody raised against Pit1, however, almost completely shifted that band

to a higher molecular weight migration pattern, indicating Pit1 proteins were bound to the

mouse CART promoter site. In contrast to the data with GH3 cells, only one band was

consistently observed when pituitary proteins were used in EMSA/SS assays with the

Pit1 oligonucleotide.

Figure 5.3. Pit1 proteins made in the rat pituitary bound to the mouse CART

promoter Pit1 *cis*-regulatory element in EMSA/SS assays.
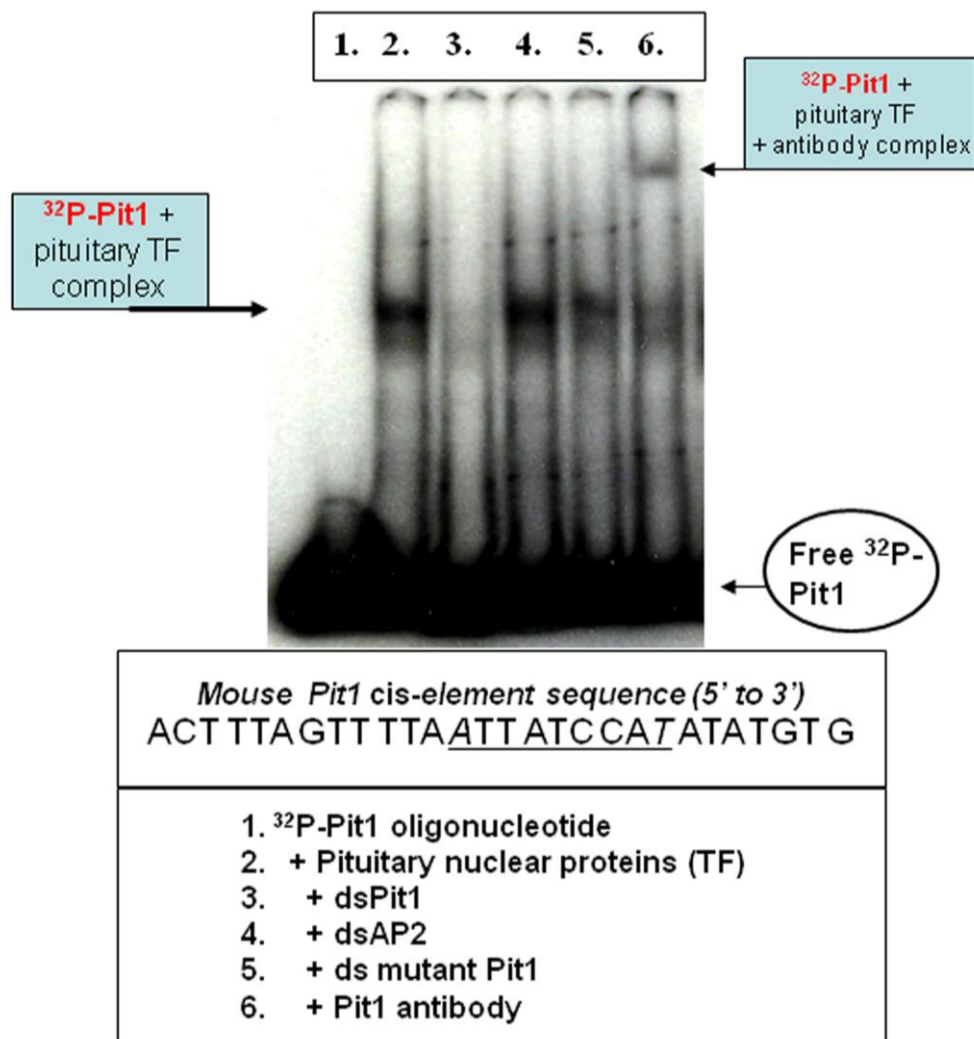
Figure 5.4. The CART promoter Pit1 *cis*-element weakly bound nuclear proteins from the rat NAc and the TF-DNA complex was not super shifted with the Pit1 antibody. NAc nuclear proteins (TF; lanes 2-8) bound weakly to the same ^{32}P-Pit1 oligonucleotide used in **figure 5.2**. As a positive control, GH3 nuclear proteins were simultaneously assayed with the same radiolabeled probe and found to bind robustly, again producing two distinct migration patterns of TF + DNA complexes in the gel (lanes 9-12). The data were presented as: a negative control radioprobe alone (no protein added) reaction lane (lane 1; free ^{32}P-Pit1 was indicated by an arrow on the bottom left of the gel); possibly non-specific protein-DNA interactions with NAc TFs (lanes 2 and 5); competition with 50x non-radiolabeled dsPit1 oligonucleotide (lanes 3 and 6); non-specific competition with 50x non-radiolabeled mouse CART promoter dsAP1-like oligonucleotide, unrelated in sequence to the Pit1 oligonucleotide (lanes 4 and 7); and an attempted Pit1 antibody super shift (lane 8; no super shift was apparent). Although some NAc protein binding was apparent that was competed away by 50x non-radiolabeled Pit1, the Pit1 antibody did not super shift any of the bands, suggesting the binding was non-specific. In contrast, GH3 cell TF binding to the Pit1 oligonucleotide was robust (lanes 9-12), where protein binding to DNA was observed (lane 9; the complexes were denoted by arrows at the figure's center right), 50x non-radiolabeled Pit1 competed for that binding (lane 10), 50x non-radiolabeled CART promoter AP1-like oligonucleotide did not (lane 11) and the Pit1 antibody fully super shifted both TF + DNA complexes (see box at top right denoting ^{32}P-Pit1 + pituitary TF + antibody complex).

.

Figure 5.4. The CART promoter Pit1 *cis*-element weakly bound nuclear proteins from the rat NAc and the TF-DNA complex was not super shifted with the Pit1 antibody.
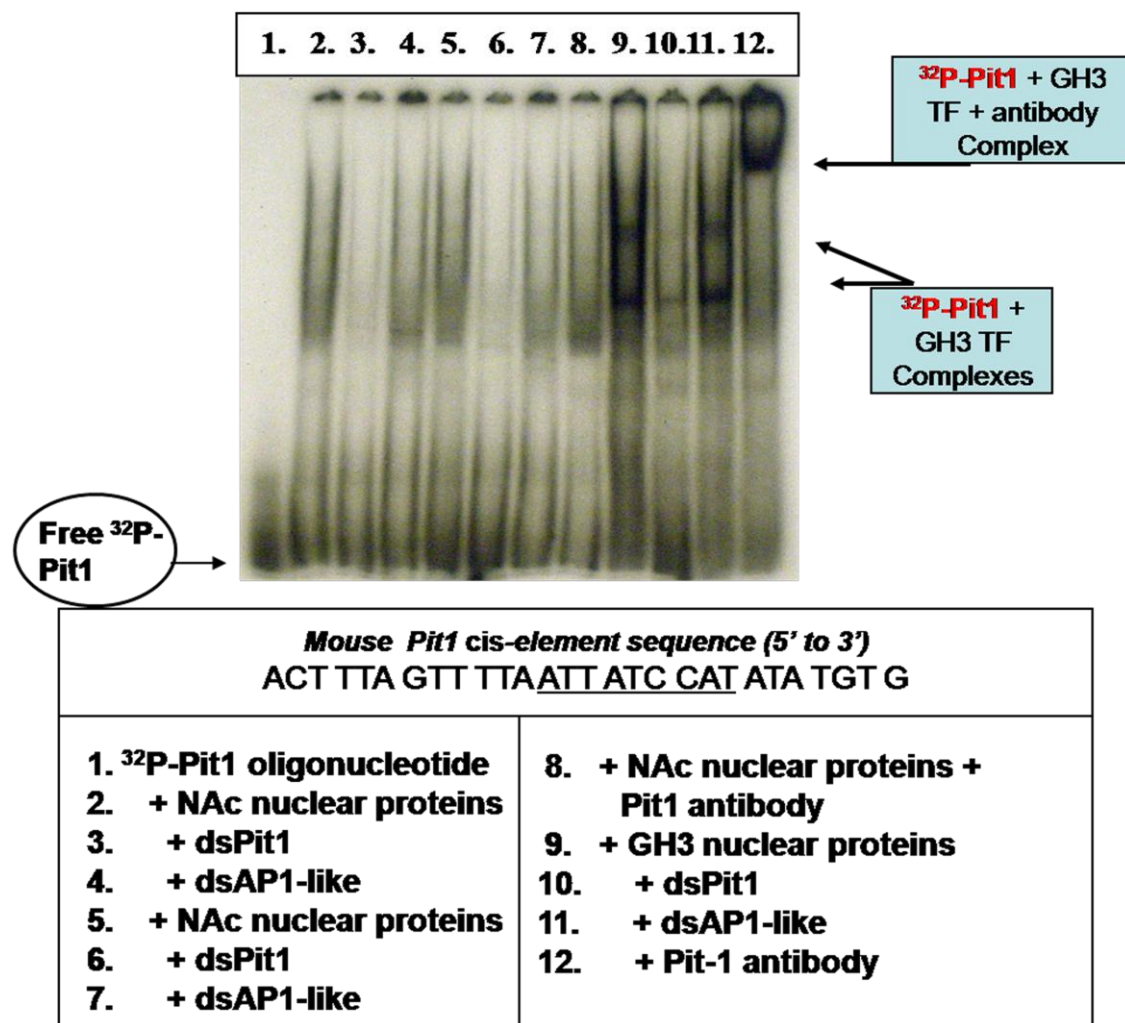
Figure 5.5. CREB and P-CREB proteins from the rat pituitary did not bind to the Pit1 *cis*-regulatory element as shown by antibody super shift analyses; an expected result. Pituitary nuclear proteins (TF) bound to the ^{32}P-Pit1 oligonucleotide in EMSA/SS assays using the same ds oligonucleotide as in **figure 5.2** (referred to in the figure as Pit1). The data showed: a negative control radioprobe alone (no protein added) reaction lane (lane 1; free ^{32}P-Pit1 was indicated by an arrow on the bottom left of the gel); specific protein-DNA interactions with pituitary TFs (lane 2; the complex was denoted by an arrow at the figure's center left); competition with 50x non-radiolabeled dsPit1 oligonucleotide (lane 3); a non-specific competition reaction with 50x non-radiolabeled dsNFκB oligonucleotide, unrelated in sequence to the Pit1 oligonucleotide (lane 4); another non-specific competition reaction with 50x non-radiolabeled CART CRE (lane 5); Pit1 antibody super shifts (lanes 6, 7, 8; see box at top right denoting ^{32}P-Pit1 + pituitary TF + antibody complex); and attempted antibody super shifts with CREB (lane 9) and P-CREB (lane 10). In contrast to the super shift assays using Pit1 antibodies, the CREB and P-CREB antibodies did not produce a super shift.

Figure 5.5. CREB and P-CREB proteins from the rat pituitary did not bind to the Pit1 *cis*-regulatory element as shown by antibody super shift analyses; an expected result.
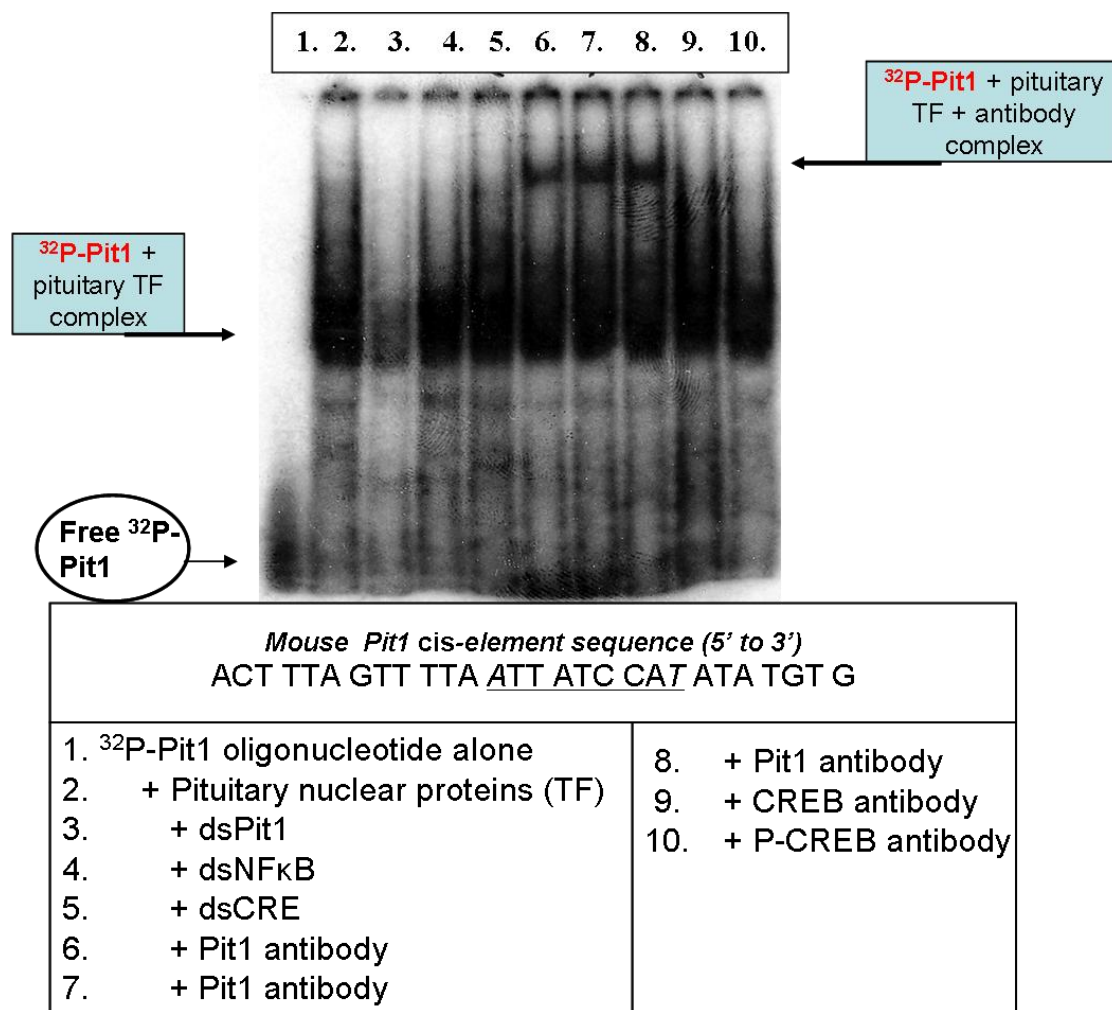
Figure 5.6. Rat pituitary-derived GH3 cell transcription factors interacted with the rat CART gene promoter Ptx1 *cis*-regulatory element, but Pit1 was not bound. GH3 nuclear proteins were incubated with a consensus Pit1 sequence ^{32}P-labeled oligonucleotide (lanes 2-7), or a ^{32}P-labeled oligonucleotide identical in sequence to the rat CART promoter Ptx1 *cis*-element. The data were presented as: a negative control radioprobe alone (no protein added) reaction lane (lane 1; free ^{32}P-Pit1 was indicated by an arrow on the bottom left of the gel); specific protein-DNA interactions with GH3 TFs (lane 2; the complexes were denoted by arrows at the figure's top left); competition with 50x non-radiolabeled dsPit1 oligonucleotide (lane 3); a non-specific competition reaction with 50x non-radiolabeled dsAP2 oligonucleotide, unrelated in sequence to the consensus Pit1 oligonucleotide (lane 4); a Pit1 antibody super shift (lane 5); and an antigen pre-absorbed Pit1 antibody super shift (lane 6). Starting at lane 7, GH3 protein interactions with the rat CART promoter Ptx1 oligonucleotide were examined. Shown were: a negative control radioprobe alone (no protein added) reaction lane (lane 7; free ^{32}P-Ptx1 was indicated by an arrow on the bottom right of the gel); protein-DNA interactions with GH3 TFs (lane 8; the complexes were denoted by arrows at the figure's top right); competition with 50x non-radiolabeled dsPtx1 oligonucleotide (lane 9); non-specific competition with 50x non-radiolabeled dsAP2 oligonucleotide, unrelated in sequence to the consensus Pit1 oligonucleotide (lane 10); an attempted Pit1 antibody super shift (lane 11; no super shift was apparent); and an antigen pre-absorbed Pit1 antibody super shift (lane 12). The three bands competed away by 50x dsPtx1 were considered to be specific binding events, but the lack of a super shift with Pit1 antibody seemed to indicate that Pit1 was not part of the TF-DNA complexes.

Figure 5.6. Rat pituitary-derived GH3 cell transcription factors interacted with the rat CART gene promoter Ptx1 *cis*-regulatory element, but Pit1 was not bound.
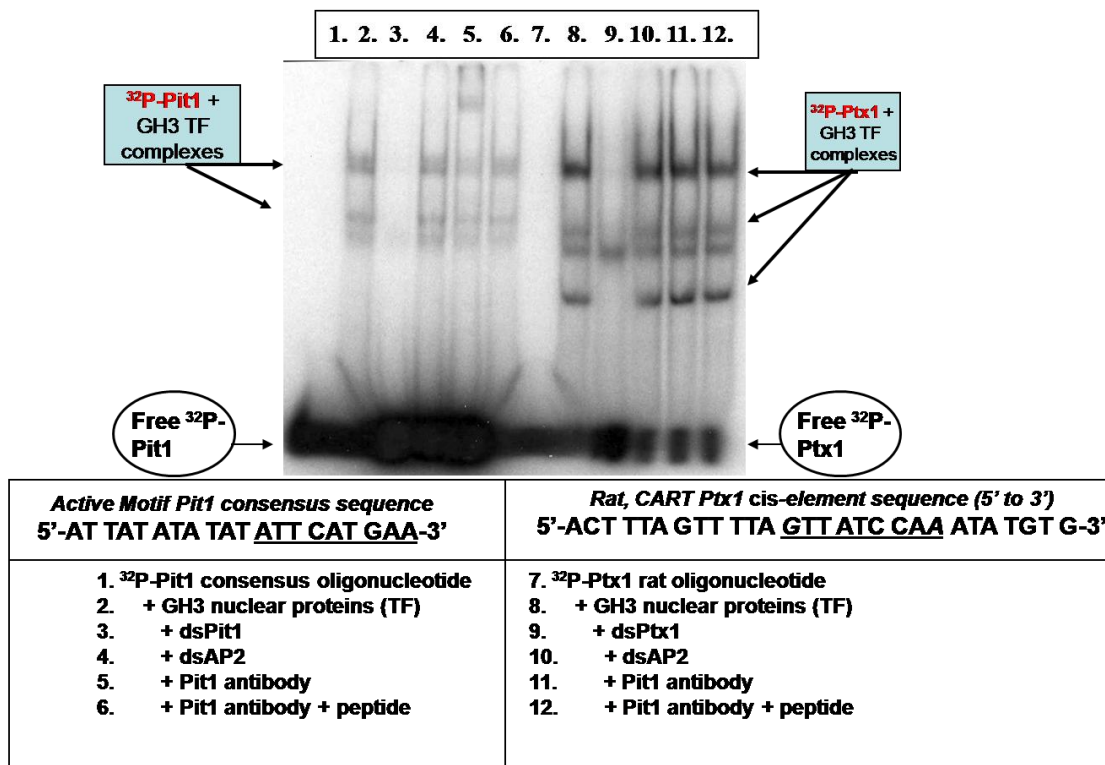
Figure 5.7. Pit1 and Oct-family antibodies had no effect on rat pituitary TF binding to ^{32}P-Ptx1 oligonucleotides in EMSA/SS assays. Rat pituitary nuclear proteins (TF) bound to the same ^{32}P-Ptx1 oligonucleotide used in **figure 5.6, lanes 7-12**. The data were presented as: a negative control radioprobe alone (no protein added) reaction lane (lane 1; free ^{32}P-Ptx1 was indicated by an arrow on the bottom right of the gel); specific protein-DNA interactions with pituitary TFs (lane 2; the complexes were denoted by an arrow at the figure's center left); competition with 50x non-radiolabeled dsPtx1 oligonucleotide (lane 3); and attempted antibody super shifts with Pit1 (lane 5), Oct-2 (lane 6), Oct-4 (lane 7), CREB (lane 8) and P-CREB (lane 10) antibodies. No super shifts were apparent for any of the antibodies tried. NAc TFs were also incubated with the ^{32}P-Ptx1 oligonucleotide in lane 10 and the binding was not super shifted with antibodies specific for Pit1 or Oct-2.

Figure 5.7. Pit1 and Oct-family antibodies had no effect on rat pituitary TF binding to ^{32}P-Ptx1 oligonucleotides in EMSA/SS assays.

Rat, CART Ptx1 cis-element sequence (5' to 3')
ACT TTA GTT TTA GTT ATC CAA ATA TGT G

1. ^{32}P-Ptx1 rat oligonucleotide
2.   + Pituitary nuclear proteins (TF)
3.   + dsPtx1 rat
4.   + dsAP2
5.   + Pit1 antibody
6.   + Oct-2 antibody
7.   + Oct-4 antibody

8.   +CREB antibody
9.   + P-CREB antibody
10. + NAc TF
11.   + Pit1 antibody
12.   + Oct-2 antibody
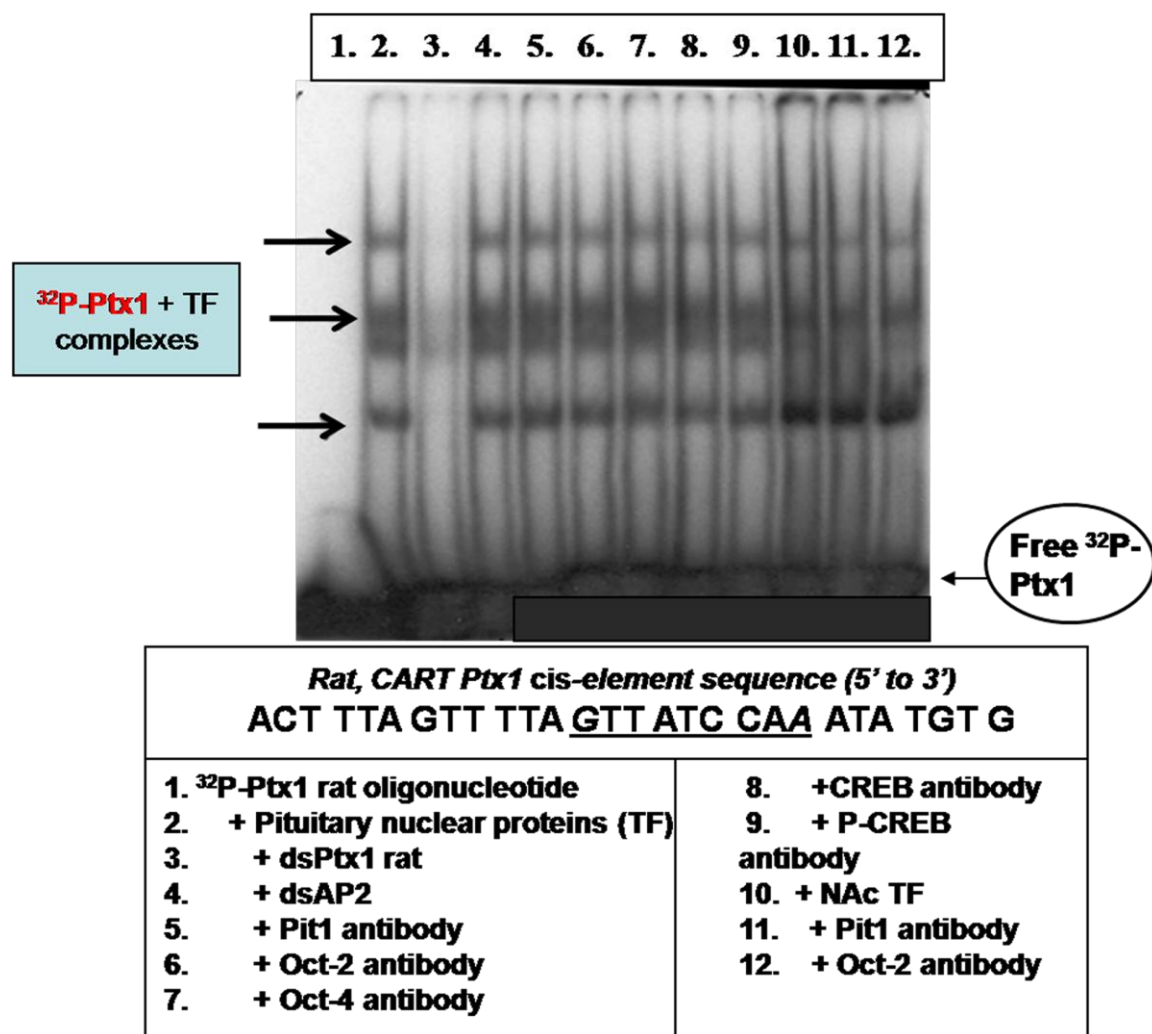
family of transcription factors (Oct-2 and -4) were used in an attempt to identify the

protein(s) bound to the Ptx1 oligonucleotide. Oct family TFs, like Ptx1 proteins, were

found to be responsible for neuronal differentiation of pituitary cells during development.

NAc TFs were also assayed for their ability to bind to the Ptx1 oligonucleotide and were

not found to be super shifted with any of the antibodies tried (**Figures 5.7** and **5.8**, n = 3

animals). In **figure 5.8**, commercially available 3T3 cell nuclear extracts were used

because those cells were derived from the mouse embryo and expressed Oct family

transcription factors, which were expressed during the early stages of development. The

data revealed that Oct-2 and -4 could not bind to the Ptx1 regulatory element.

5.3.2 EMSA/SS analysis of the mouse and rat CART promoter AP1-like *cis*-regulatory elements

The sequences in **table 5.2** illustrated a comparison of oligonucleotide sequences

between the mouse and rat CART promoter AP1-like CART promoter *cis*-regulatory

elements with a consensus AP1 *cis*-regulatory element commercially available from

Active Motif (Carlsbad, CA). Core binding sequences were underlined in the table. The

mouse and rat sequences were identical to those found in their respective CART genes

and differed by one nucleotide in their flanking sequences (italicized and bolded). The

CART gene sequences were half-palindromes, which would have reduced their affinity

for AP1 proteins, while the consensus AP1 sequence was a full palindrome.

Overall, the AP1-like *cis*-elements did not show competency in binding to nuclear

proteins from rat tissues, but could bind to proteins from cultured cells. The data in

figure 5.9 was a representative EMSA/SS analysis of the mouse CART promoter AP1-

Figure 5.8. Rat NAc nuclear proteins were able to bind to the Ptx1 oligonucleotide, but TF + DNA complexes were not super shifted with any of the antibodies tried.
NAc nuclear proteins (TF; lanes 2-9) bound to the same ^{32}P-Ptx1 oligonucleotide used in **figure 5.6**. Mouse 3T3 nuclear proteins were simultaneously assayed with the same radiolabeled probe (the 3 far right lanes) and found to bind as well, though no bands were super shifted from any of the tissues with any of the Oct-2, or -4 antibodies. The data were presented as: a negative control radioprobe alone (no protein added) reaction lane (lane 1; free ^{32}P-Ptx1 was indicated by an arrow on the bottom right of the gel); possibly non-specific protein-DNA interactions with NAc TFs (lanes 2 and 7); competition with 50x non-radiolabeled dsPtx1 oligonucleotide (lane 3); a non-specific competition reaction with 50x non-radiolabeled dsAP2, unrelated in sequence to the Ptx1 oligonucleotide (lane 4); attempted Oct-4 antibody super shifts (lanes 5 and 8); and attempted antigen pre-absorbed Oct-4 antibody super shifts (lanes 6 and 9). NAc protein binding to the Ptx1 site was apparent that was competed away by 50x non-radiolabeled Ptx1. In lanes 10-12, 3T3 nuclear proteins, which expressed Oct-2 and -4, were incubated with the ^{32}P-Ptx1 oligonucleotide. The Oct-4 antibody did not produce a super shift, but dsPtx1 did compete for binding to the proteins. That result suggested that Oct-4 could not bind to the CART promoter Ptx1 site.

Figure 5.8. Rat NAc nuclear proteins were able to bind to the Ptx1 oligonucleotide, but TF + DNA complexes were not super shifted with any of the antibodies tried.

Rat, CART Ptx1 cis-element sequence (5' to 3')
ACT TTA GTT TTA GTT ATC CAA ATA TGT G

1. ^{32}P-Ptx1 rat oligonucleotide
2. + NAc nuclear proteins (TF)
3. + dsPtx1
4. + dsAP2
5. + Oct-4 antibody
6. + Oct-4 antibody + peptide
7. + NAc TF
8. + Oct-4 antibody
9. + Oct-4 antibody + peptide
10. + 3T3 cell TF
11. + Oct-4 antibody
12. + dsPtx1
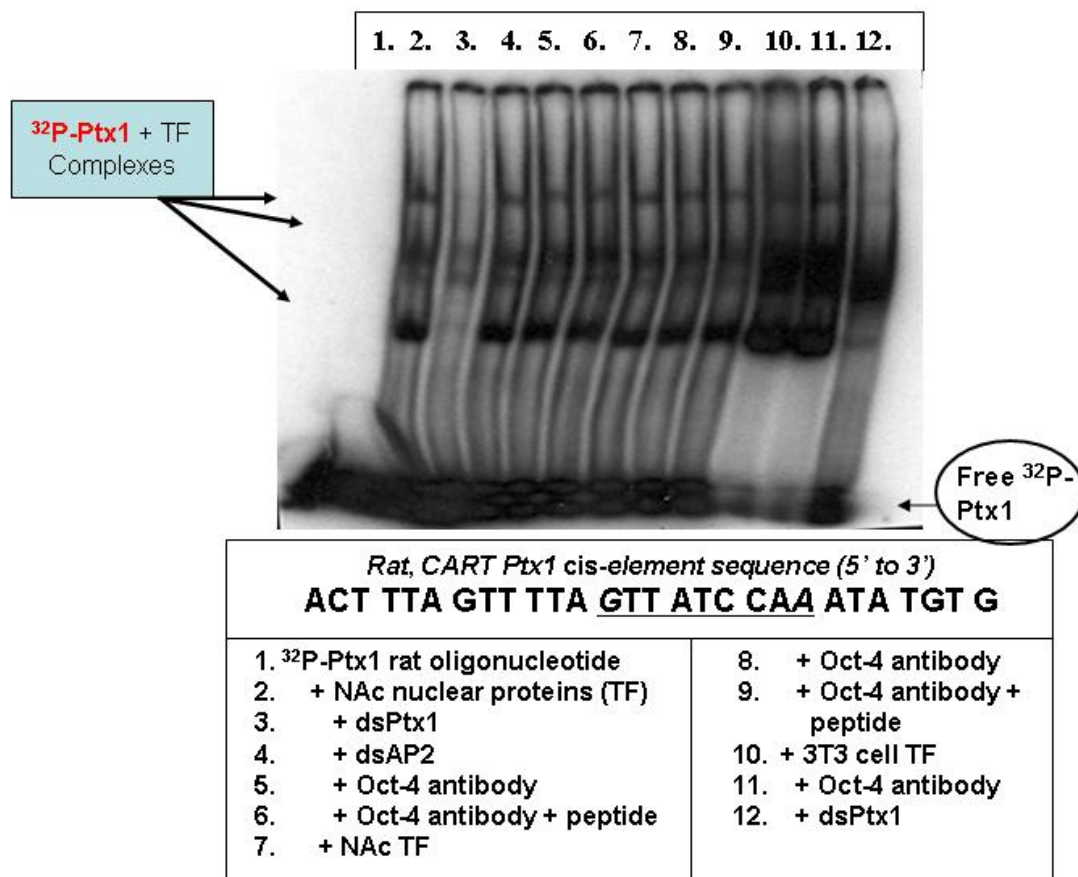
Table 5.2. Oligonucleotide sequences of the CART gene promoter AP1-like *cis-*

regulatory elements and a consensus AP1 sequence assayed by EMSA/SS analyses.

Mouse, CART AP1-like cis-*element sequence (5' to 3')*   GCC TAC AGA CGG CTG ACC CGG GCT CT**C** CTC CA
Rat, CART AP1-like cis-*element sequence (5' to 3')*   GCC TAC AGA CGG CTG ACC CGG GCT CT**T** CTC CA
Active Motif consensus AP1 core cis-*element sequence (5' to 3')*   TGAGTCA

Table 5.2. AP1 family TFs were immediate early gene products that were found to regulate drug reward and reinforcement (Konradi et al 1993). Specifically, over expression of a mutant form of the AP1 TF ΔFosB, which accumulated in the rat NAc in response to chronic, repeated drug administration, increased animals' sensitivities to cocaine as shown by conditioned place preference assays (Nestler 2004b). EMSA/SS assays were performed with the tabled oligonucleotides in order to determine if nuclear transcription factors in nuclear extracts from rat pituitary-derived GH3 cells, the rat pituitary and the rat NAc could bind to them and potentially regulate the CART gene in those tissues.

Figure 5.9. The mouse AP1-like *cis*-element did not show competency in binding to nuclear proteins from rat tissues, but could bind to proteins from Jurkat cells.

Rat NAc (lanes 2-4), cultured Jurkat (lanes 5-8) and rat pituitary (lanes 9-12) nuclear proteins (TF) were incubated with a ^{32}P-labeled oligonucleotide identical in sequence to the mouse CART promoter AP1-like *cis*-regulatory element. The sequence (from 5' to 3'; referred to as AP1-like) was given below the picture of the gel and the core binding site was underlined. The single nucleotide that differs from the rat AP1-like *cis*-regulatory element identified in the rat CART promoter was italicized. The data were presented as: a negative control radioprobe alone (no protein added) reaction lane (lane 1; free ^{32}P-AP1-like was indicated by an arrow on the bottom left of the gel); non-specific protein-DNA interactions with NAc TFs (lanes 2-4); specific TF-DNA interactions with Jurkat TFs (lane 5; the complexes were denoted by the boxed arrows at the top left of the gel); competition with 50x non-radiolabeled dsAP1-like oligonucleotide (lane 6); a non-specific competition reaction with 50x non-radiolabeled dsSP1 oligonucleotide, unrelated in sequence to the AP1-like oligonucleotide (lane 7); a JunD antibody super shift (lane 8; TF + DNA complex was disrupted, but not shifted); and non-specific protein-DNA interactions with pituitary TFs (lanes 9-12). These data indicated that the half-palindrome AP1-like sequence identified in the mouse CART promoter may not have been able to bind to JunD TFs in the rat NAc or pituitary under non-stimulated conditions. JunD present in Jurkat nuclear proteins, however, were able to bind to the sequence, which raised the possibility that under certain conditions the AP1-like site may have been functional. The fact that the antibody disrupted the TF + DNA complex, but did not super shift the band, likely indicated that the antibody was able to bind to JunD in the complex and as a result the JunD + antibody complex lost the ability to bind to the AP1-like site.

Figure 5.9. **The mouse AP1-like *cis*-element did not show competency in binding to nuclear proteins from rat tissues, but could bind to proteins from Jurkat cells.**

Mouse, CART AP1-like cis-*element sequence (5′ to 3′)*
GCC TAC AGA CGG CTG ACC CGG GCT CTC CTC CA

1. Mouse ^{32}P-AP1-like
    oligonucleotide
2. + NAc nuclear proteins (TF)
3.   + dsAP1-like
4.   + dsSP1
5. + Jurkat TF
6.   + dsAP1-like
7.   + dsSP1
8.   + Jun D antibody

9.   + Pituitary TF
10.   + dsAP1-like
11.   + dsSP1
12.   +JunD antibody
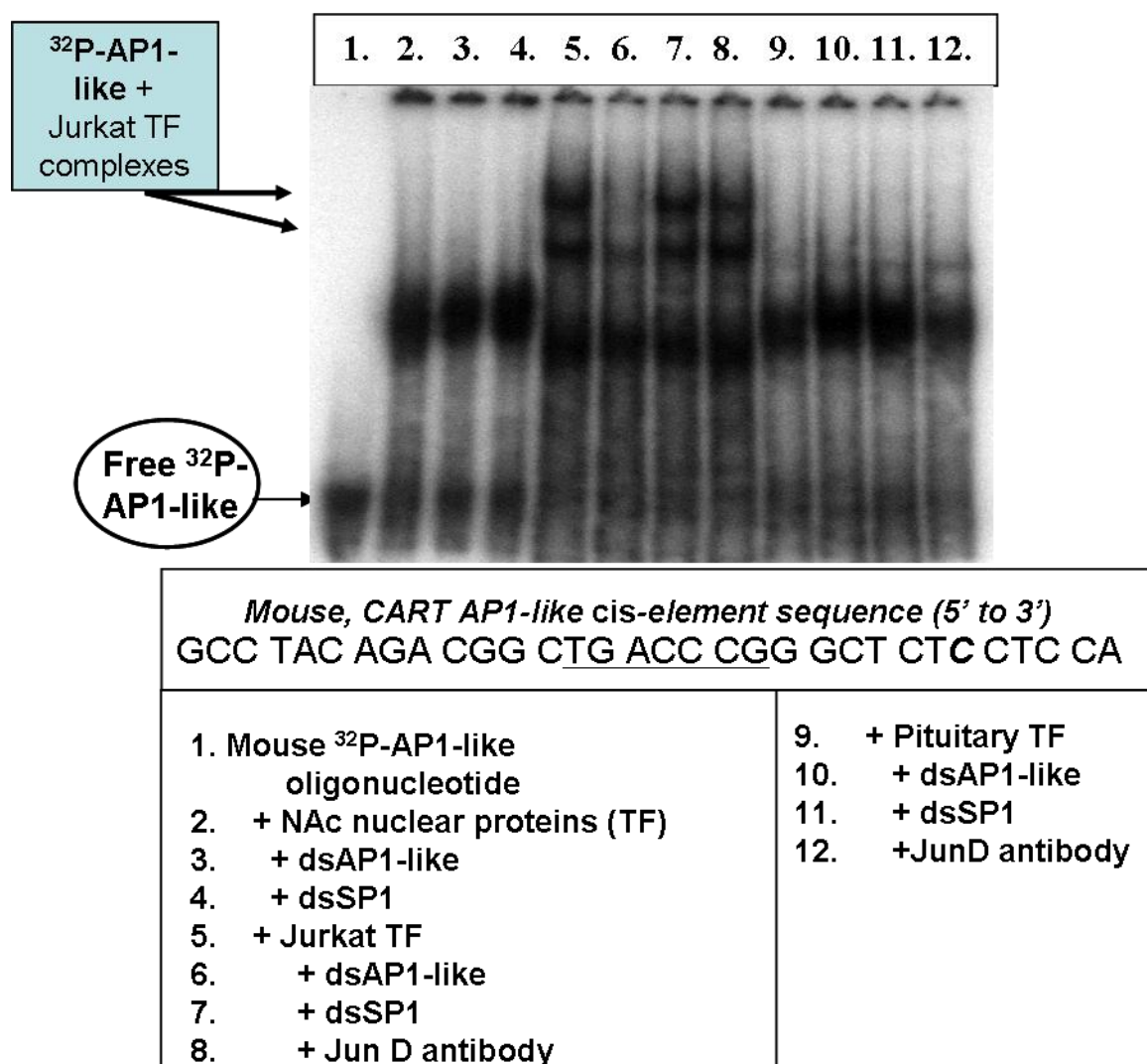
like *cis*-regulatory element. TFs in nuclear extracts from the rat NAc (far left lanes) did not bind specifically to the oligonucleotides, but Jurkat nuclear proteins were able to specifically bind (center lanes), while rat pituitary-derived TFs could not (far right lanes) (n = 3/group). The JunD antibody did not completely shift the Jurkat + DNA complex, but did reduce it in intensity which suggested that JunD was bound in the TF + DNA complex. The presence of JunD and c-Fos AP1 proteins in the rat NAc and pituitary was verified by Western blot analysis and antigen pre-absorption with the immunizing peptide JunD was raised against (**Figure 5.10**; n = 3/group). CREB and P-CREB were also identified in the rat pituitary, as shown in the far right lanes of **figure 5.10**, **panel A**.

The JunD antibody super shifted TF + DNA complexes when a radiolabeled consensus AP1 sequence was used in EMSA/SS assays with Jurkat and rat pituitary nuclear proteins (**Figure 5.11**; n = 3/group), but had no effect, as expected, on rat NAc TF + ^{32}P-CART CRE interactions in separate EMSA/SS assays (**Figure 5.12**). That result indicated that the CART promoter CRE site was specific in interacting with CRE-binding proteins, not AP1 proteins in that assay. These data indicated that AP1 proteins in nuclear extracts were able to bind to a consensus AP1 *cis*-regulatory sequence, and that the JunD antibody could specifically recognize some of the proteins in those TF-DNA complexes.

The rat CART promoter AP1-like *cis*-element was, like the mouse AP1-like site, unable to bind to proteins from the rat NAc or pituitary in a specific manner (**Figures 5.13** and **5.14**; n = 3/group). Nuclear proteins in nuclear extracts from GH3 cells, though,

Figure 5.10. Western blot analysis identified JunD and c-Fos AP1 proteins in the rat NAc as well as JunD, c-Fos, CREB and P-CREB proteins in the rat pituitary.
Western blot analyses were performed with: **A)** rat pituitary, and **B**, **C**) NAc cytoplasmic proteins using antibodies specific for JunD (31 KDa), c-Fos (40 KDa), CREB or P-CREB proteins (approximately 45 KDa). JunD was much more abundant in the NAc compared to the pituitary and migrated just below 32 KDa in the gel. c-Fos migrated around 40 KDa and CREB and P-CREB in the pituitary were visualized above 41 KDa in the gel (**A**). The blot in panel **C** showed data from NAc and pituitary proteins assayed with antigen pre-absorbed JunD antibody. Although the band around 32 KDa was not completely competed away, it was significantly reduced in intensity.

Figure 5.10. Western blot analysis identified JunD and c-Fos AP1 proteins in the rat NAc as well as JunD, c-Fos, CREB and P-CREB proteins in the rat pituitary.

A. Pituitary
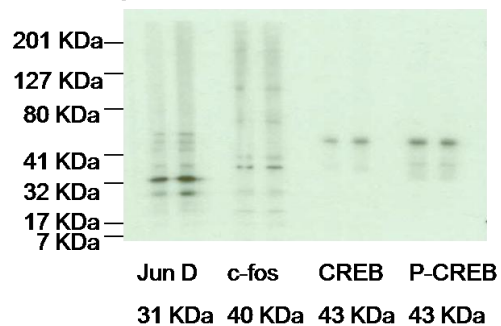
B. NAc
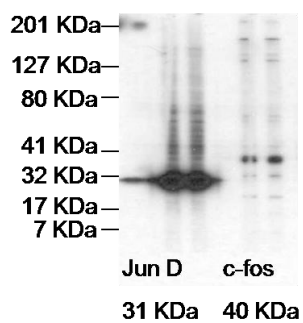
C.
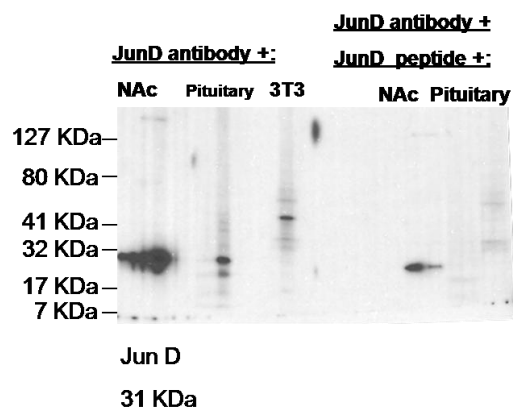
Figure 5.11. The consensus AP1 sequence bound to Jurkat and rat pituitary nuclear proteins and the JunD antibody super shifted TF + DNA complexes in EMSA/SS. Cultured Jurkat (lanes 2-5) and rat pituitary (lanes 6-12) nuclear proteins (TF) were able to bind to a consensus ^{32}P-labeled AP1 sequence. The sequence (from 5' to 3'; referred to as AP1) was given below the picture of the gel and the core binding site was underlined. Previous data from **chapter 4, figure 4.5** verified that NAc TFs could also bind to the same consensus AP1 sequence in EMSA/SS assays. The data were presented as: a negative control radioprobe alone (no protein added) reaction lane (lane 1); specific Jurkat TF-DNA interactions (lane 2; the complexes were denoted by the boxed arrows at the top left of the gel); competition with 50x non-radiolabeled dsAP1 oligonucleotide (lane 3); JunD antibody super shifts (lanes 4 and 5); specific protein-DNA interactions with pituitary TFs (lane 6; the complex was denoted by the boxed arrows at the center right of the gel); competition with 50x non-radiolabeled dsAP1 oligonucleotide (lane 7); non-specific competition with 50x non-radiolabeled dsSP1 oligonucleotide (lane 8); JunD antibody super shifts (lanes 9-11); and a c-Fos antibody super shift, which did not shift the pituitary + DNA complex. These data indicated that AP1 proteins in nuclear extracts were able to bind to a consensus AP1 *cis*-regulatory sequence, and that the JunD antibody could recognize some of the proteins in those TF-DNA complexes.

Figure 5.11. The consensus AP1 sequence bound to Jurkat and rat pituitary nuclear proteins and the JunD antibody super shifted TF + DNA complexes in EMSA/SS.

^{32}P-AP1 + Jurkat TF complexes

1. 2. 3. 4. 5. 6. 7. 8. 9.10.11.12.

^{32}P-AP1 + pituitary TF + antibody complex

^{32}P-AP1 + pituitary TF complex

Active Motif consensus AP1 core cis-element sequence (5' to 3')
TGAGTCA

1. ^{32}P-AP1 consensus oligonucleotide	7. + dsAP1
2. + Jurkat nuclear proteins (TF)	8. + dsSP1
3. + dsAP1	9. + Jun D antibody
4. + Jun D antibody	10. + 2x Jun D antibody
5. + 2x Jun D antibody	11. + 3X Jun D antibody
6. + Pituitary nuclear proteins (TF)	12. + c-fos antibody
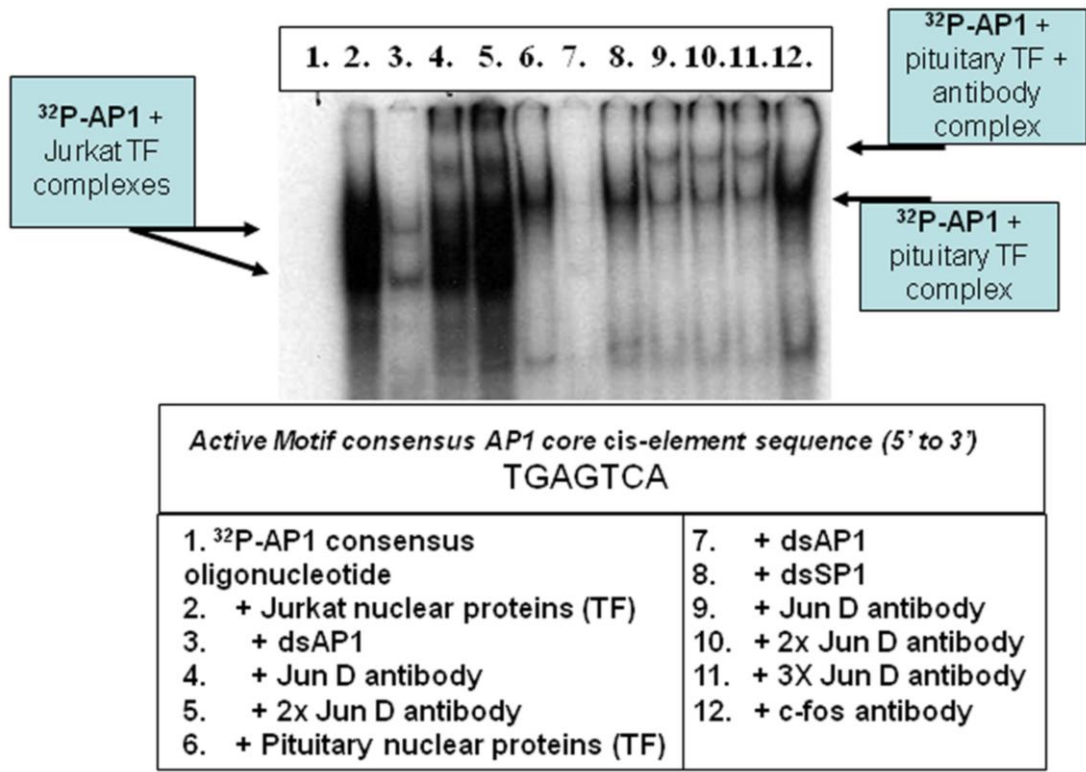
Figure 5.12. The JunD antibody was specific and did not affect rat NAc TF + ^{32}P-CRE oligonucleotide complexes in EMSA/SS assays using GH3 cell nuclear proteins.
EMSA and super shift analyses were performed using nuclear proteins from GH3 cells.
The CRE *cis*-element sequence was given below the picture of the gel in the box, and the
core binding sequence was underlined. Lane 1 was a negative control where only the ^{32}P-CRE probe was loaded but no protein, lane 2 showed binding of proteins to the probe
which reduced the mobility of the radioactive protein-DNA complex and lane 3 was a
competition reaction with 50x non-radiolabeled CRE. Some non-specific binding that
migrated below the CRE + TF complex was observed, but it was not ablated with the
addition of 50x non-radiolabeled CRE (lane 3), which indicated that the binding was not
specific to the CRE sequence. A separate band below the CRE + TF complex was
diminished by 50x non-radiolabeled mutant AP1 (a nonsense sequence), which indicated
it was not specific as well. Lane 5 showed that antibody super shift analyses using an
antibody specific for JunD AP1 proteins did not result in a super shift of the CRE + TF
band.   JunD was not expected to bind to the CRE element and the antibody did not
recognize any non-specific proteins causing a super shift. Thus, the CRE site bound
CRE-binding proteins in the EMSA/SS assays and JunD antibodies did not recognize
them.

Figure 5.12. The JunD antibody was specific and did not affect rat NAc TF + ^{32}P-CART CRE oligonucleotide complexes in EMSA/SS assays using GH3 cell nuclear proteins.
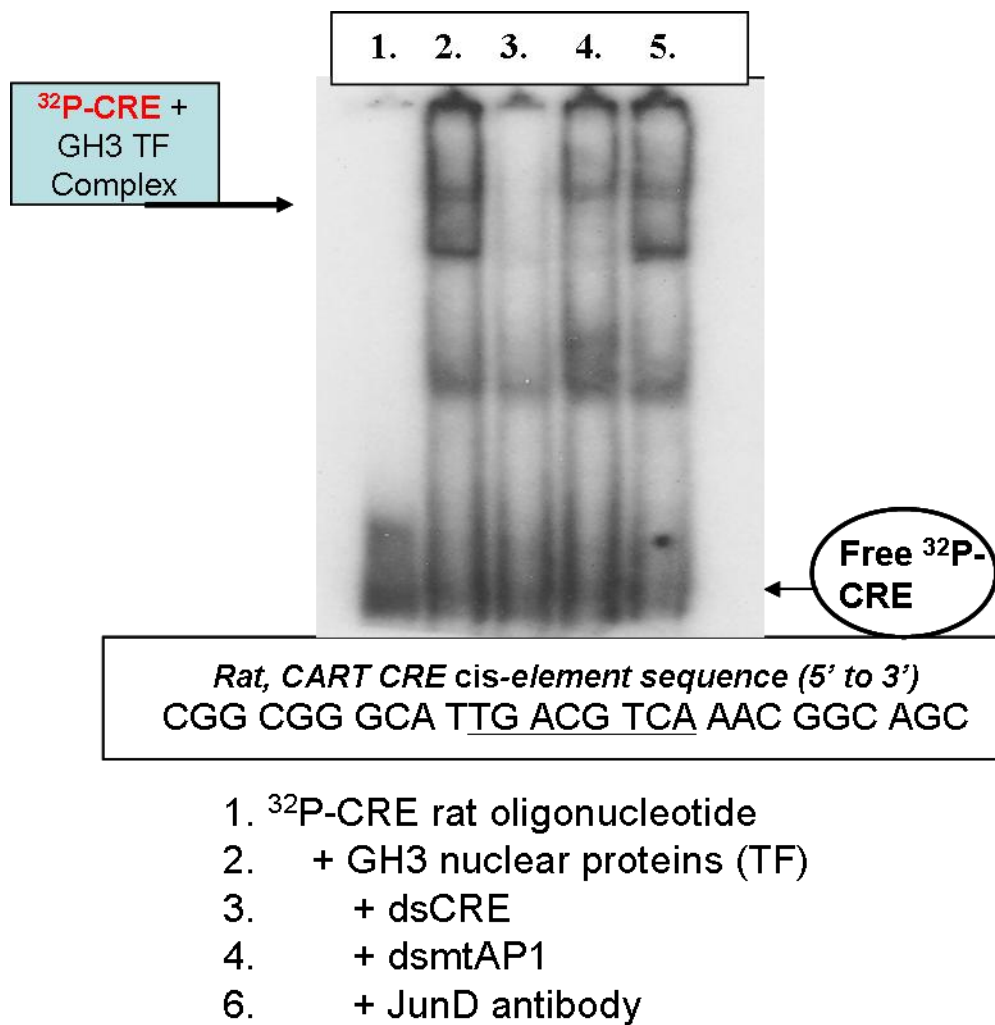
1. ^{32}P-CRE rat oligonucleotide
2.   + GH3 nuclear proteins (TF)
3.   + dsCRE
4.   + dsmtAP1
6.   + JunD antibody

Figure 5.13. The rat CART promoter AP1 *cis*-element was unable to bind to nuclear proteins from the rat NAc in a specific manner. Rat NAc nuclear proteins (TF) were incubated with a ^{32}P-labeled oligonucleotide identical in sequence to the rat CART promoter AP1-like *cis*-regulatory element. The sequence (from 5' to 3'; referred to as AP1-like) was given below the picture of the gel and the core binding site was underlined. The data were presented as: a negative control radioprobe alone (no protein added) reaction lane (lane 1; free ^{32}P-AP1-like was indicated by an arrow on the bottom left of the gel); non-specific protein-DNA interactions with NAc TFs (lanes 2-8); a competition reaction with 50x non-radiolabeled dsAP1-like oligonucleotide (lane 3); a non-specific competition reaction with 50x non-radiolabeled dsAP2 oligonucleotide (lane 7); attempted c-Jun antibody super shifts (lane 5 and 6); and attempted JunD antibody super shifts (lanes 7 and 8). These data indicated that the half-palindrome AP1-like sequence identified in the rat CART promoter may not have been able to bind to c-Jun or JunD TFs in the rat NAc under non-stimulated conditions.

Figure 5.13. The rat CART promoter AP1 *cis*-element was unable to bind to nuclear proteins from the rat NAc in a specific manner.

Non-specific ^{32}P-AP1-like complexes

Free ^{32}P-AP1-like

1. 2. 3. 4. 5. 6. 7. 8.

Rat, CART AP1-like cis-*element sequence (5' to 3')*
GCC TAC AGA CGG CTG ACC CGG GCT CTT CTC CA

1. Rat ^{32}P-AP1-like oligonucleotide
2. + NAc nuclear proteins (TF)
3.   + dsAP1-like
4.   + dsAP2
5.   + c-Jun antibody
6.   + 2x c-Jun antibody
7.   + JunD antibody
8.   + 2x JunD antibody
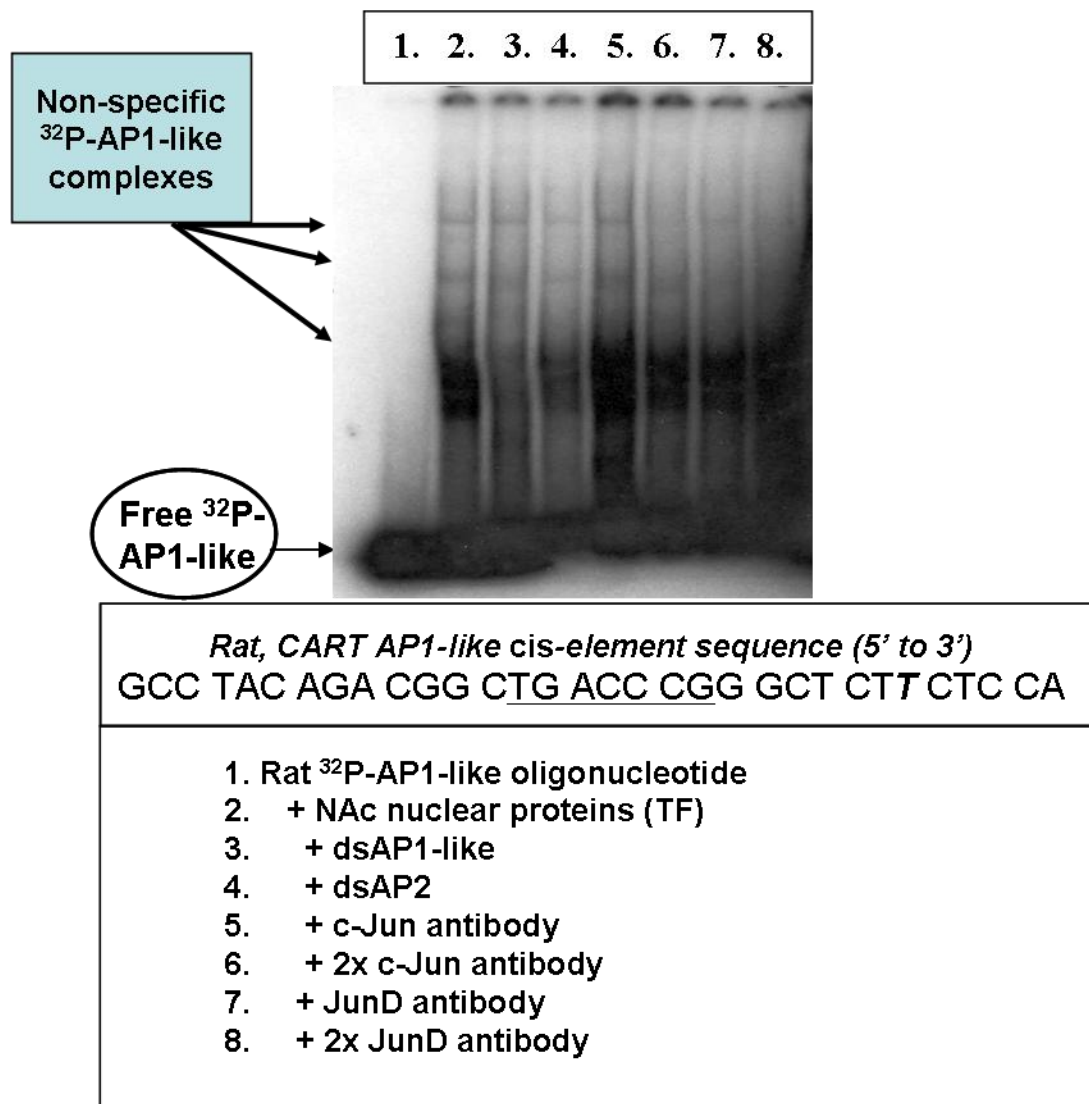
Figure 5.14. Nuclear proteins in nuclear extracts from GH3 cells, but not the pituitary, were able to bind to the rat CART promoter AP1-like sequence and JunD reduced the intensity of the GH3 TF + ^{32}P-AP1-like element band shift. Rat pituitary (lanes 2-7), and cultured GH3 (lanes 8-12) nuclear proteins (TF) were able to bind to the rat CART promoter AP1-like *cis*-regulatory element. The data shown were: a negative control radioprobe alone (no protein added) reaction lane (lane 1; free ^{32}P-AP1-like was indicated by an arrow on the bottom left of the gel); possibly non-specific protein-DNA interactions with pituitary TFs (lanes 2-7); specific TF-DNA interactions with GH3 TFs (lane 8; the complex was denoted by the boxed arrows at the center right of the gel); competition with 50x non-radiolabeled dsAP1-like oligonucleotide (lane 9); a non-specific competition reaction with 50x non-radiolabeled consensus dsAP1 oligonucleotide, closely related in sequence to the AP1-like oligonucleotide (lane 10); a JunD antibody super shift (lane 11); and an antigen pre-absorbed JunD antibody super shift (lane 12). These data indicated that the half-palindrome AP1-like sequence identified in the rat CART promoter may not have been able to bind to JunD TFs in the rat pituitary under non-stimulated conditions. There was, however, a slight reduction in protein binding to the DNA in JunD antibody super shift assays using GH3 nuclear extracts, and pre-absorption with the JunD peptide antigen inhibited that reduction. In addition, the consensus AP1 sequence may have competed for GH3 protein binding to the rat CART *cis*-element as well, suggesting that the site may have had some functionality in GH3 cells.

Figure 5.14. Nuclear proteins in nuclear extracts from GH3 cells, but not the pituitary, were able to bind to the rat CART promoter AP1-like sequence and JunD reduced the intensity of the GH3 TF + ^{32}P-AP1-like element band shift.

Rat CART AP1-like cis-element sequence (5' to 3')
GCC TAC AGA CGG CTG ACC CGG GCT CTT CTC CA

1. Rat ^{32}P-AP1-like oligonucleotide	7. + JunD + peptide
2. + Pituitary nuclear proteins (TF)	8. + GH3 nuclear proteins (TF)
3. + dsAP1-like	9. + dsAP1-like
4. + dsAP1 consensus	10. + dsAP1 consensus
5. + JunD antibody	11. + JunD antibody
6. + JunD antibody	12. + JunD antibody + peptide
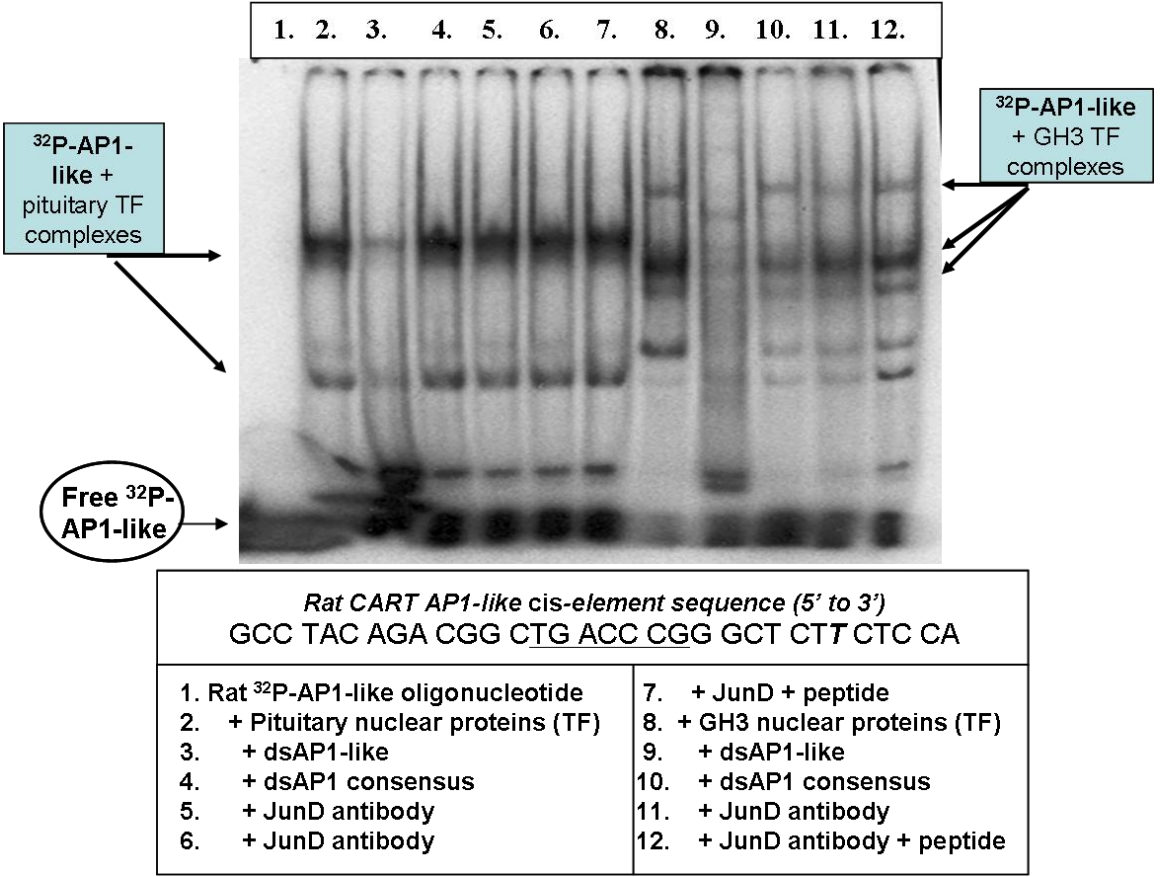
were able to bind to the rat CART promoter AP1-like sequence and JunD reduced the intensity of the TF + DNA band shift, while the pre-absorption of the JunD antibody with its immunizing peptide inhibited that reduction (**Figure 5.14, far right lanes**).

5.4 <u>Conclusions and brief discussion</u>

Although there were many unexpected findings, the data presented in this chapter were a testament to the complexity of *in vivo* TF-DNA interactions and how variations in just one or two nucleotides either in the core binding sites or flanking sequences of *cis*-regulatory elements could have dramatic effects on their interactions with brain-, pituitary- and cultured cell-derived TFs. For example, the mouse Pit1 and rat Ptx1 *cis*-elements were two nucleotides different in their core binding sites (**Table 5.1**), and identical in their flanking sequences and positions relative to +1 in the CART genes, yet they exhibited grossly different TF binding profiles. The mouse Pit1 site bound to GH3 (**Figure 5.1**) and rat pituitary (**Figure 5.3**) TFs robustly and those TF-DNA complexes were readily super shifted by Pit1 antibodies. As predicted, the mouse Pit1 site did not bind to rat NAc proteins with a high degree of specificity and Pit1 was not found to be bound in those TF-DNA complexes (**Figure 5.4**).

In contrast to the mouse CART promoter Pit1 site, the rat Ptx1 site bound to proteins from GH3 cells (**Figure 5.6b)** the rat pituitary (**Figure 5.7**) and the rat NAc (**Figure 5.8**) and Pit1 antibodies did not super shift any of the TF-DNA complexes. Binding of NAc TFs to the Ptx1 site was surprising since it should have only bound to pituitary-specific TFs. That result may have indicated that the TF + DNA complexes observed were non-specific. A thorough investigation into which proteins were able to

bind to the Ptx1 site was not undertaken because this dissertation was primarily focused on investigating the CART CRE *cis*-regulatory element in relation to drug addiction, and because so much non-specific binding was seen in NAc TF + ^{32}P-Ptx1 assays. The real possibility that Ptx1 itself may have bound to the site and regulated CART-related aspects of neuronal differentiation in the pituitary during development existed, but we did not gather any evidence for or against that hypothesis with these studies.

The AP-1-like *cis*-elements varied by only one nucleotide in their flanking sequences (**Table 5.2**) and had similar TF binding profiles in that they did not specifically interact with AP1 proteins from the rat NAc or pituitary (**Figures 5.9 [mouse], 5.13** and **5.14 [rat]**), but did bind with some specificity to TFs in nuclear extracts from immortalized, cultured cells (**Figures 5.9 [mouse]** and **5.14 [rat]**), which have been known to over express TFs and have disregulated gene expression patterns that have turned them cancerous/immortal. For example, Jurkat cells were derived from leukemic lymphoblasts and GH3 cells from a pituitary adenoma. Furthermore, JunD antibody disruptions of the ^{32}P-AP1-like + TF complexes strongly suggested that JunD proteins from those transformed cell lines were able to bind to the CART promoter AP1-like sites (**Figure 5.9 [mouse]** and **Figure 5.14 [rat]**), whereas brain- and pituitary-derived JunD could not. The fact that some protein binding remained even in the face of increasing concentrations of JunD antibody suggested that other proteins derived from the Jurkat and pituitary nuclear extractions besides JunD were bound to the consensus AP1 sequence.

The data suggested the possibility that under pathological conditions where AP1 protein levels are over expressed, such as in cancer, they may have the ability to bind to

the CART promoter half-palindrome AP1-like site and play a unique role in CART gene transcriptional regulation. In support of that hypothesis, a recent study found that CART peptide levels were elevated in the blood of patients with neuroendocrine tumors (Bech et al 2008) and that alterations in CART mRNA levels were associated with pituitary microadenomas and age-associated changes in energy homeostasis (Kappeler et al 2003). Thus the data from this chapter showing that in the mouse and rat genes, the AP1 *cis*-regulatory element was able to bind to AP1 proteins in nuclear extracts from cancer cell lines, but not healthy rat pituitary or NAc tissues, supports the rationale to pursue future studies regarding the CART gene AP1-like site in terms of pathological conditions where AP1 proteins have been found to be disregulated, such as neuroendocrine malignancy.

Chapter 6: General Discussion

6.1 CART gene regulation

During the preparation of this dissertation, the field of CART gene transcriptional regulation was in its infancy, begun in late 2002 when the rat and mouse gene promoters were first cloned (Barrett et al 2002; Dominguez et al 2002). There was still a lot of work left in terms of understanding how the mRNA was specifically regulated by specific extracellular stimuli in specific regions of the body. For example, the satiety factor leptin, released from adipose tissue in response to food intake, specifically up-regulated CART mRNA in the rat hypothalamus (Kristensen et al 1998), while cocaine and amphetamine up-regulated CART mRNA in the reward pathway (ventral striatum) of rats, but not the dorsal striatum or other brain regions expressing the gene (Douglass et al 1995). In that same study, morphine was found to have no effect on CART mRNA levels anywhere in the brain. Thus, specific neuronal populations that contained the CART gene were responsive to specific types of stimuli. Transcriptional regulation by TF interactions with unique *cis*-regulatory elements in the CART promoter may have been one mechanism of that specificity.

Although a plethora of putative TF binding sites were identified by database analysis in the rat CART gene promoter (**Figure 1.1** and (Barrett et al 2002)), the only one that has been extensively studied was the consensus CRE *cis*-regulatory element proposed to bind to CREB family TFs. In cultured GH3, CATH.a, Att20 and SH-SY5Y cells, a fragment of the CART gene promoter was able to drive luciferase expression after stimulation of the cAMP/PKA pathway, which increased the intracellular levels of P-CREB (Barrett et al 2002; de Lartigue et al 2007; Dominguez et al 2002). The results presented in this dissertation united those previous *in vitro* findings with *in vivo* evidence

to strongly suggest that in the nuclei neurons, in the rat NAc, a region of the brain reward pathway that mediated the rewarding properties of cocaine and other drugs of abuse, as well as dysphoria and anhedonia during drug withdrawal (Hope et al 1992; Pandey et al 2005; Shirayama & Chaki 2006), CREB had the ability to regulate CART mRNA and peptide levels by interacting directly with the CART promoter CRE *cis*-regulatory element.

6.2 Chromatin immunoprecipitation identified CREB and P-CREB interactions with the CART promoter CRE *cis*-regulatory element in the gDNA of GH3 cells.

In **figure 2.5**, chromatin immunoprecipitation (ChIP) was used to determine that CREB could bind to a 334 base pair fragment of the CART gene promoter containing a consensus CRE site in the chromatin of live GH3 cells. In that series of experiments, CREB was found to bind to the CRE-containing region of the promoter in the absence of pharmacological stimulation, but transcriptionally active P-CREB was not. The application of 20μM forskolin, however, stimulated P-CREB binding to the CART promoter in a time-dependent fashion (**Figure 2.8**). Those findings validated the hypothesis of previous *in vitro* studies that forskolin stimulation of CART gene expression in GH3 cells was regulated by P-CREB interactions with the CART promoter CRE site.

Although convincing, the ChIP assay did have its limitations, including a lack of resolution. The commercially available ChIP kit was not yet optimized for assaying protein-DNA interactions in the brains of live animals for a number of reasons. First of all, a large number of DNA cross-linked cells were needed for the assay (1×10^8). In the

case of assaying CREB-CART promoter interactions in the rat NAc, a heterogeneous population of neurons existed together in that brain nucleus (including non-neuronal cells) and only a fraction of those, the medium spiny output neurons, expressed the CART gene. In formaldehyde cross-linking of NAc tissue, anywhere between 1-10 % of the cells were randomly joined in protein bound to DNA complexes (Hao et al 2008), thus making it difficult to consistently cross-link CREB bound to the CART gene, much less the same amount each assay. The task of isolating TF-DNA complexes became more difficult if the TF under examination had a high dissociation constant (Kd) for the promoter *cis*-element; binding and dissociating rapidly from the gene and making it difficult to "catch" at the promoter. The Kd of CREB for consensus CRE sites was found to be about 1nM, but that value was highly variable from gene-to-gene and dependent on numerous variables like position of the CRE relative to the +1 site, neighboring sequences, neighboring *cis*-elements, genomic DNA topology, and composition of the CREB family dimers binding (Mayr & Montminy 2001). The Kd of CREB for the CART promoter CRE site was unknown, but probably more than 1nM because the site was more than 100 base pairs from +1 and flanked by GC-rich neighboring sequences.

ChIP assays with brain tissue were also difficult because during the wash steps to remove formaldehyde from the cells and subsequent harvesting, some cells were lost and the final lysate may or may not have contained the actual cross-linked samples, adding variability to the assay and reducing the total number of cells being loaded into the ChIP assay. Furthermore, DNA shearing was the major hurdle we could not overcome in attempting to perform ChIP with NAc tissue. The brain itself was rife with connective tissues that had to be broken apart in order to completely free up protein-DNA complexes

for immunoprecipitations. Normally, homogenizing the brain takes care of the problem of connective tissue, but it was not possible to homogenize brain samples because it disrupted formaldehyde cross-links by releasing hydronium ions from mitochondria and other subcellular organelles that reduced the pH of the lysate to a point where formaldehyde dissociated from the DNA (personal communication, Dr. Wei Chen, Emory University, Atlanta, GA).

Because of those factors, ChIP using P-CREB antibodies was rarely performed with brain tissue and the decision was made to study CREB-CART promoter CRE interactions in GH3 cells. The results obtained were still novel and significant in that it was determined for the first time that CREB was able to bind to a region of the CART promoter containing the CRE site in the histone-bound, genomic DNA of living GH3 cells, which were previously shown to express CART mRNA after stimulation of the cAMP/PKA pathway by forskolin (Dominguez et al 2002).

Findings with the c-Fos promoter and its interactions with P-CREB were also novel and significant. c-Fos regulation by P-CREB activating pathways has been common lore for more than a decade, but until Hao et al used a unique, modified ChIP method to identify P-CREB binding to the c-Fos promoter in rat cortical tissue, no group had actually demonstrated a physical interaction between a c-Fos promoter CRE site and P-CREB. In this dissertation, P-CREB binding to a region of the c-Fos promoter containing a CRE site in GH3 cells was demonstrated for the first time, which further validated that c-Fos was a P-CREB regulated gene and the hypotheses of previous studies that psychostimulants elevated c-Fos mRNA levels in the striatum through a CREB-mediated pathway (Hyman et al 1995).

Hao et al observed the interesting phenomenon that P-CREB was bound to the c-Fos promoter CRE site under non-stimulated conditions, where P-CREB IP enriched the c-Fos promoter 2.5-fold over IgG IP (Hao et al 2008). When that group induced hypertension with systemic phenylephrine, they observed a slight, but significant, increase in P-CREB binding to the c-Fos promoter in the rat brain (approximately 2-fold over saline conditions). The fold-increase over saline was probably low because P-CREB was bound to the CRE site in the absence of phenylephrine and after saline alone treatment. In this dissertation, P-CREB binding to the c-Fos promoter in GH3 cells was likewise observed during vehicle treatment (**Figure 2.9B**, **c** compared to **d**). Forskolin treatment was shown for the first time to slightly, though significantly, increase P-CREB binding to the c-Fos promoter in GH3 cells by 2.957 ± 0.354 fold (mean $\pm$ SEM; **Figure 2.9A P-CREB/DMSO**). A fold-increase very similar to that seen by Hao et al, possibly indicating a saturation of P-CREB binding at the CRE site, although further ChIP studies performed as skatchard-type assays would be needed to confirm that.

Previously, it was shown that c-Fos mRNA was expressed within 30 minutes after forskolin stimulation in GH3 cells (Herdegen & Leah 1998) and in a separate study, the CART gene was expressed within 3 hours after the same dose of forskolin (Dominguez et al 2002). The discovery that P-CREB was bound to the c-Fos promoter CRE site under non-stimulated conditions could explain why c-Fos so quickly responded to P-CREB activating stimuli such as forskolin whereas CART and other genes, which contained the same consensus CRE sequence, took longer to be transcribed by the same stimulation. If some P-CREB was always bound to some of the multiple CRE sites in the c-Fos promoter, then it could have potentially recruited a threshold amount of transcription co-

factors like CREB-Binding Protein (CBP) and TFIID to rapidly initiate transcription. Other genes that did not bind to P-CREB without stimulation would have taken a longer time to recruit the basal transcription machinery and thus take a longer time to become expressed.

Knowledge of the mechanisms of how CRE-containing genes were temporally regulated could allow for medications to be developed that target specific CREB-regulated genes in an effort to treat addiction. For example, the reinforcing and addicting effects of cocaine were mediated by c-Fos expression, which was regulated by CREB activation subsequent to dopamine receptor activation in the striatum (Hyman et al 1995). Targeting and degrading P-CREB molecules present in the striatum with therapeutic compounds that only have effects when P-CREB levels are low, during non-stimulated conditions, could prevent rapid c-Fos activation by cocaine without necessarily affecting other CRE containing genes that don't bind to P-CREB under non-stimulated conditions. That, in effect, could potentially inhibit the rewarding effects of cocaine and reduce its abuse liability.

Obviously, since P-CREB chromatin immunoprecipitation assays have only been done on a handful of genes in 9 separate publications, and experiments from this dissertation were amongst the few to observe differential P-CREB binding to CRE sites in two different CREB-regulated genes, much more needs to be known about the status of all the other P-CREB binding genes in the striatum before such a drug could be developed. The findings from **chapter 2** of this dissertation, though, raised the interesting possibility that such a drug could, in theory, be someday developed.

Figure 2.10 further demonstrated that CREB and P-CREB made *in vivo*, in the pituitary could bind to a short oligonucleotide identical in sequence to the rat CART promoter CRE site surrounded by its flanking sequences. That data indicated that CREB and P-CREB made in the pituitary were in conformations and associated with dimerization partners which allowed them to bind to the CART promoter CRE. In conjunction with the data in **figures 2.5** and **2.8**, the data presented in **chapter 2** strongly suggested that in the nucleus of pituitary neurons, and possibly in other tissues like the NAc, CREB and P-CREB could bind to the CART promoter CRE *cis*-regulatory element. The next issue was whether or not that binding had a functional effect, and work presented in **chapter 3** of this dissertation directly addressed that matter.

6.3 CREB regulation of the CART gene *in vivo*, in the rat NAc

The general hypothesis for this dissertation was that CART may be a CREB target gene in the NAc and in that way, CART peptides could be partly responsible for the behavioral effects associated with CREB over expression in the NAc and drug addiction (see **sections 2.1.1** and **2.1.2**). Although chronic cocaine exposure caused up-regulation of the cAMP/PKA pathway in the NAc (Terwilliger et al 1991; Unterwald et al 1996), the regulation of an individual gene *in vivo*, in the NAc by cocaine depended on dose, administration paradigm (i.e. binge versus acute versus chronic) and other factors not completely understood (Hyman et al 1995; McClung & Nestler 2003; Zhou et al 2002). For example, the AP1 family TF c-Fos was rapidly up-regulated by acute cocaine exposure, but desensitized during chronic treatments and no longer expressed after a challenge cocaine injection (Hope et al 1992). The mechanisms of that desensitization

were not known. Another member of the same AP1 gene family, however, ΔFosB which

was a stable c-truncated mutant of FosB, was *not* rapidly expressed in response to an

acute injection of cocaine, but accumulated in the NAc with repeated, chronic

administration and persisted for long periods of time in the brain after cocaine exposure

(Hope et al 1994).

CART gene regulation by cocaine, in turn, was not a foregone conclusion and

remained a complex, not completely understood phenomenon that depended on multiple

variables such as gender (Fagergren & Hurd 1999), dose of cocaine (Fagergren & Hurd

2007), route of administration, administration paradigm (Brenz Verca et al 2001; Hunter

et al 2005) and stress hormones (Hunter et al 2005). The data from **chapter 4** of this

dissertation provided a good example of how cocaine regulation of the CART gene in the

rat NAc was dependent on multiple, interacting physiological systems all trying to

compensate for cocaine's over stimulating effects. The finding from that work that

moderate binge cocaine increased AP1 TF activity at a consensus AP1 *cis*-regulatory

element (**Figure 4.6**), provided some insight into what genes were potentially regulated

by binge cocaine treatment and consequently, what physiological repercussions could

arise from that up or down-regulation.

The work from this dissertation and drug abuse research generally has attempted

to reduce the variables associated with cocaine-mediated gene regulation in the NAc and

to fully comprehend the mechanisms of differential gene expression that exist *in vivo*, in

the brain during different conditions of cocaine exposure. One technique that has been

used for over a decade to examine the role of CREB specifically in molecular

mechanisms of drug addiction and neuropsychiatric disorders is non-replicative Herpes

Simplex Virus (HSV)-1-mediated gene transfer (Carlezon et al 2000; Carlezon et al 1998). As opposed to the use of transgenic animals, which may have enacted compensatory mechanisms to counteract the effects of genetic manipulation, gene transfer allows insertion of a single gene into a specific brain region by microinjection, at a specific time-point in normally developed animals (Carlezon et al 2000). That strategy for manipulating gene expression thus allowed for the examination of a single gene's effects in a particular brain region at a particular time ontological time-point.

The data presented in **figures 3.10** and **3.11** illustrated how the over expression of CREB in the rat NAc was able to positively regulate both CART mRNA and peptide levels *in vivo*, in the rat brain. In conjunction with data in **figures 3.1** and **3.2** showing that CREB and P-CREB made *in vivo*, in the rat NAc were able to bind to the CART promoter CRE element in EMSA/SS assays, as well as the findings in **chapter 2** showing that CREB and P-CREB were able to bind to the CART promoter CRE site nestled in the chromatin of genomic DNA in the nuclei of GH3 cells, the up-regulation of CART mRNA and peptides concomitant with over expression of CREB proteins (**Figure 3.7**) strongly suggested that CREB acted directly at the CART promoter CRE site to transcriptionally stimulate expression of the gene in the NAc. Furthermore, as a CREB-regulated gene in the NAc, CART may have been a component of CREB-mediated behavioral tolerance and psychological dependence. These data from **chapters 2** and **3** provided a solid rationale for future studies beginning to study CART peptide in relation to those two aspects of addiction.

The finding that P-CREB levels were not changed by intra-NAc injections of HSV-CREB were surprising, but could have represented an important aspect of CREB

transcriptional mechanisms—the tight regulation of CREB phosphorylation within homeostatic levels. In the viral over expression assays, animals were euthanized 36 hours post-infection and itwas possible that by that time the rats had already enacted mechanisms such as protein phosphatase up-regulation or PKA down-regulation to compensate for over expression of CREB proteins. Another possible explanation could have been that the rats were not pharmacologically challenged with any substances to activate the cAMP/PKA pathway and thus P-CREB levels were not increased in HSV-CREB treated animals compared to HSV-LacZ treated controls above the level that could be detected by Western blot analysis. It was possible that with a more sensitive method like radioimmunoassay or immunohistochemistry, changes in P-CREB levels could have been detected.

Another surprising result from the HSV studies was that over expression of mCREB had no effect on CART mRNA (**Figure 3.11**) or peptide levels (**Figure 3.14**), although it did reduce the levels of P-CREB in the NAc (**Figure 3.13**). That finding likely indicated that P-CREB primarily regulated the stimulated expression of CART and other *cis*-regulatory elements present in the CART promoter and/or that other CREB superfamily members were involved in maintaining basal levels of CART gene expression.

In addition, EMSA/SS assays examining the effects of CREB over expression on NAc TF binding to the CART promoter CRE *cis*-regulatory element did not reveal any differences between sham, HSV-LacZ or HSV-CREB injected animals (**Figure 3.12**). As mentioned above, the quantity of P-CREB increase due to viral over expression of CREB alone combined with compensatory mechanisms enacted in the rat brain to bring P-CREB

levels back to homeostatic levels could have been one reason why more binding wasn't observed from HSV-CREB treated samples.

In conclusion, the portion of the dissertation examining *in vivo* effects of CREB over expression on CART gene regulation, demonstrated that over expression of CREB by HSV-1 viral gene transfer increased the quantity of CART mRNA and peptides in the rat NAc, which supported the overall hypothesis that the CART gene was a CREB-regulated gene *in vivo*. Furthermore, since over expression of CREB in the NAc by the same viral vectors was previously shown to decrease animals' sensitivities to cocaine, the findings presented in this part of the dissertation suggested that CART peptides in the NAc functioned, in part, as homeostatic regulators of the reward pathway that were part of a larger, more complex system of CREB-mediated pharmacodynamic tolerance that blunted the behavioral effects of psychostimulants. Thatwas an important finding because, although psychostimulants regulated CREB activity in the NAc, the precise genes up- or down-regulated in response to different types cocaine exposure (such as chronic versus acute, high dose versus low dose, etc.) were not completely known. Identifying CREB-regulated genes in the NAc, such as CART, furthered the basic research regarding the molecular mechanisms of the reinforcing effects of cocaine. That, in turn, may lead to the development of medications to treat addiction.

6.4 General conclusion

After chronic exposure to psychostimulants, GABA-containing, medium spiny striatal output neurons in the NAc up-regulated the cAMP/PKA pathway and increased P-CREB levels and the transcription of CREB target genes (**Figure 2.2** and (Carlezon et al

1998; Cole et al 1995; Hyman et al 1995; Shaw-Lutchman et al 2003; Terwilliger et al

1991)). In mice and rats, CREB over expression in the NAc along with the

pharmacological activation of P-CREB with PKA activators were shown to reduce

cocaine reward in CPP and self-administration studies (Carlezon et al 2000; Carlezon et

al 1998; Choi et al 2006; Dinieri et al 2009; Edwards et al 2007; Sakai et al 2002; Self et

al 1998; Walters et al 2003). CART was found to be co-expressed with GABA in

medium spiny output neurons of the NAc that expressed c-Fos in response to cocaine

administration (Dallvechia-Adams et al 2002; Hubert & Kuhar 2006; 2008; Smith et al

1997), and CART mRNA was also up-regulated by psychostimulants in the NAc

(Douglass et al 1995; Fagergren & Hurd 1999; Hubert & Kuhar 2008; Hunter et al 2005),

though by complex, not completely understood mechanisms. Intra-NAc CART peptide

administration, like increases in CREB activity, also reduced psychostimulant reward in

addition to psychostimulant-induced locomotor activity and sensitization (Jaworski et al

2008; Jaworski et al 2003; Kim et al 2003; Kim et al 2007). That neuroanatomical and

functional relationship between CREB and CART formed the basis for the general

hypothesis of this dissertation that the cAMP/PKA signaling pathway might have been

able to regulate CART gene expression *in vivo*, in the NAc. Furthermore, CART may, in

part, have mediated some of the behavioral effects of CREB over expression.

A hypothesis about the mechanism(s) by which over activity of CREB in the NAc

was able to reduce the rewarding properties of cocaine centered on up- and down-

regulation of neuropeptides that could influence emotional and motivational responses to

stimulation of the reward pathway by drugs of abuse (Nestler 2004b). The NAc and

related regions of the limbic system were known to integrate experiential events to direct

emotional responses to environmental stimuli, such as drug exposure, by enacting

homeostatic, feedback neuroadaptations in the reward pathway which allowed an

organism to adapt to a changing environment (Carlezon et al 2005; Nestler 2004b;

Shirayama & Chaki 2006). Those neuroadaptations involved neuroplastic changes

manifested from alterations in gene expression patterns which ultimately altered

behavioral responses to novel environments.

CREB over activity in the NAc as a result of chronic drug use seemed to be a

homeostatic, negative feedback adaptation in response to chronic over activation of the

reward system (Nestler 2004a). That pharmacodynamic tolerance contributed to a form

of behavioral tolerance associated with chronic drug use; decreases in an animal's

emotional response to repeated drug exposures (Nestler 2004b). The impairment of the

reward system by elevated CREB activity also caused psychological drug dependence

because the emotional response to external cues and stimuli had been toned down so

much that naturally rewarding experiences no longer evinced positive emotional

responses from the limbic system as they should (Nestler 2004a). During drug

abstinence, in that case, human drug addicts experienced emotional numbing and

anhedonia (Nestler 2004b), similar to core symptoms seen in clinical depression

(Shirayama & Chaki 2006).

The complete panel of genes regulated by CREB in the NAc which mediated

pharmacodynamic tolerance and psychological dependence in psychostimulant addiction

were not known, but some CREB target genes that were known to mediate cocaine

reward were prodynorphin (Carlezon et al 1998), which negatively regulated DA

neurotransmission; c-Fos, which activated a wave of AP1 family transcription factors and

CREB itself; and G-protein coupled receptor kinase 3, which was up-regulated and

facilitated opioid receptor internalization (Dinieri et al 2009). The data from this

dissertation showing that the CART gene consensus CRE *cis*-regulatory element was able

to bind to CREB and P-CREB in the chromatin of genomic DNA, and that CREB over

expression in the rat NAc increased CART mRNA and peptide levels, strongly suggested

that the CART gene was a physiologic target of CREB in the rat NAc. Those findings

provided a sound rationale for future studies to begin examining a function for CART

peptides in terms of CREB-mediated pharmacodynamic tolerance and psychological

dependence. That research is vital to the health of millions of people around the world

left without medications to treat addiction, because identifying target genes through

which CREB caused neuroplastic neuroadaptations in response to chronic drug exposure

could, hopefully, lead to the development of pharmacotherapy treatments which may

reverse those neurological changes (Nestler 2004a).

References

Albertson DN, Pruetz B, Schmidt CJ, Kuhn DM, Kapatos G, Bannon MJ. 2004. Gene expression profile of the nucleus accumbens of human cocaine abusers: evidence for dysregulation of myelin. *J Neurochem* 88:1211-9

Asakawa A, Inui A, Yuzuriha H, Nagata T, Kaga T, et al. 2001. Cocaine-amphetamine-regulated transcript influences energy metabolism, anxiety and gastric emptying in mice. *Horm Metab Res* 33:554-8

Barrett P, Davidson J, Morgan P. 2002. CART gene promoter transcription is regulated by a cyclic adenosine monophosphate response element. *Obes Res* 10:1291-8

Barrett P, Morris MA, Moar KM, Mercer JG, Davidson JA, et al. 2001. The differential regulation of CART gene expression in a pituitary cell line and primary cell cultures of ovine pars tuberalis cells. *J Neuroendocrinol* 13:347-52

Beaudry G, Zekki H, Rouillard C, Levesque D. 2004. Clozapine and dopamine D3 receptor antisense reduce cocaine- and amphetamine-regulated transcript expression in the rat nucleus accumbens shell. *Synapse* 51:233-40

Bech P, Winstanley V, Murphy KG, Sam AH, Meeran K, et al. 2008. Elevated cocaine- and amphetamine-regulated transcript immunoreactivity in the circulation of patients with neuroendocrine malignancy. *J Clin Endocrinol Metab* 93:1246-53

Brenz Verca MS, Widmer DA, Wagner GC, Dreyer J. 2001. Cocaine-induced expression of the tetraspanin CD81 and its relation to hypothalamic function. *Mol Cell Neurosci* 17:303-16

Brischoux F, Fellmann D, Risold PY. 2001. Ontogenetic development of the diencephalic MCH neurons: a hypothalamic 'MCH area' hypothesis. *Eur J Neurosci* 13:1733-44

Brischoux F, Griffond B, Fellmann D, Risold PY. 2002. Early and transient ontogenetic expression of the cocaine- and amphetamine-regulated transcript peptide in the rat mesencephalon: correlation with tyrosine hydroxylase expression. *J Neurobiol* 52:221-9

Carlezon WA, Jr., Duman RS, Nestler EJ. 2005. The many faces of CREB. *Trends Neurosci* 28:436-45

Carlezon WA, Jr., Nestler EJ, Neve RL. 2000. Herpes simplex virus-mediated gene transfer as a tool for neuropsychiatric research. *Crit Rev Neurobiol* 14:47-67

Carlezon WA, Jr., Thome J, Olson VG, Lane-Ladd SB, Brodkin ES, et al. 1998. Regulation of cocaine reward by CREB. *Science* 282:2272-5

Choi KH, Whisler K, Graham DL, Self DW. 2006. Antisense-induced reduction in nucleus accumbens cyclic AMP response element binding protein attenuates cocaine reinforcement. *Neuroscience* 137:373-83

Cole RL, Konradi C, Douglass J, Hyman SE. 1995. Neuronal adaptation to amphetamine and dopamine: molecular mechanisms of prodynorphin gene regulation in rat striatum. *Neuron* 14:813-23

Dall Vechia S, Lambert PD, Couceyro PC, Kuhar MJ, Smith Y. 2000. CART peptide immunoreactivity in the hypothalamus and pituitary in monkeys: analysis of ultrastructural features and synaptic connections in the paraventricular nucleus. *J Comp Neurol* 416:291-308

Dallvechia-Adams S, Kuhar MJ, Smith Y. 2002. Cocaine- and amphetamine-regulated transcript peptide projections in the ventral midbrain: colocalization with gamma-aminobutyric acid, melanin-concentrating hormone, dynorphin, and synaptic interactions with dopamine neurons. *J Comp Neurol* 448:360-72

Damaj MI, Hunter RG, Martin BR, Kuhar MJ. 2004. Intrathecal CART (55-102) enhances the spinal analgesic actions of morphine in mice. *Brain Res* 1024:146-9

Damaj MI, Martin BR, Kuhar MJ. 2003. Antinociceptive effects of supraspinal rat cart (55-102) peptide in mice. *Brain Res* 983:233-6

Dandekar MP, Singru PS, Kokare DM, Subhedar NK. 2009. Cocaine- and amphetamine-regulated transcript peptide plays a role in the manifestation of depression: social isolation and olfactory bulbectomy models reveal unifying principles. *Neuropsychopharmacology* 34:1288-300

de Lartigue G, Dimaline R, Varro A, Dockray GJ. 2007. Cocaine- and amphetamine-regulated transcript: stimulation of expression in rat vagal afferent neurons by cholecystokinin and suppression by ghrelin. *J Neurosci* 27:2876-82

del Giudice EM, et al. 2006. Adolescents carrying a missense mutation in the CART gene exhibit increased anxiety and depression. *Depression and Anxiety*:90-2

del Giudice EM, Santoro N, Cirillo G, D'Urso L, Di Toro R, Perrone L. 2001. Mutational screening of the CART gene in obese children: identifying a mutation (Leu34Phe) associated with reduced resting energy expenditure and cosegregating with obesity phenotype in a large family. *Diabetes* 50:2157-60

Dey A, Xhu X, Carroll R, Turck CW, Stein J, Steiner DF. 2003. Biological processing of the cocaine and amphetamine-regulated transcript precursors by prohormone convertases, PC2 and PC1/3. *J Biol Chem* 278:15007-14

Dinieri JA, Nemeth CL, Parsegian A, Carle T, Gurevich VV, et al. 2009. Altered sensitivity to rewarding and aversive drugs in mice with inducible disruption of cAMP response element-binding protein function within the nucleus accumbens. *J Neurosci* 29:1855-9

Dominguez G. 2006. The CART gene: structure and regulation. *Peptides* 27:1913-8

Dominguez G, del Giudice EM, Kuhar MJ. 2004. CART peptide levels are altered by a mutation associated with obesity at codon 34. *Mol Psychiatry* 9:1065-6

Dominguez G, Kuhar MJ. 2004. Transcriptional regulation of the CART promoter in CATH.a cells. *Brain Res Mol Brain Res* 126:22-9

Dominguez G, Lakatos A, Kuhar MJ. 2002. Characterization of the cocaine- and amphetamine-regulated transcript (CART) peptide gene promoter and its activation by a cyclic AMP-dependent signaling pathway in GH3 cells. *J Neurochem* 80:885-93

Douglass J, Daoud S. 1996. Characterization of the human cDNA and genomic DNA encoding CART: a cocaine- and amphetamine-regulated transcript. *Gene* 169:241-5

Douglass J, McKinzie AA, Couceyro P. 1995. PCR differential display identifies a rat brain mRNA that is transcriptionally regulated by cocaine and amphetamine. *J Neurosci* 15:2471-81

Dun NJ, Dun SL, Kwok EH, Yang J, Chang J. 2000a. Cocaine- and amphetamine-regulated transcript-immunoreactivity in the rat sympatho-adrenal axis. *Neurosci Lett* 283:97-100

Dun SL, Brailoiu GC, Yang J, Chang JK, Dun NJ. 2006. Cocaine- and amphetamine-regulated transcript peptide and sympatho-adrenal axis. *Peptides* 27:1949-55

Dun SL, Castellino SJ, Yang J, Chang JK, Dun NJ. 2001. Cocaine- and amphetamine-regulated transcript peptide-immunoreactivity in dorsal motor nucleus of the vagus neurons of immature rats. *Brain Res Dev Brain Res* 131:93-102

Dun SL, Chianca DA, Jr., Dun NJ, Yang J, Chang JK. 2000b. Differential expression of cocaine- and amphetamine-regulated transcript-immunoreactivity in the rat spinal preganglionic nuclei. *Neurosci Lett* 294:143-6

Dylag T, Kotlinska J, Rafalski P, Pachuta A, Silberring J. 2006a. The activity of CART peptide fragments. *Peptides* 27:1926-33

Dylag T, Rafalski P, Kotlinska J, Silberring J. 2006b. CART (85-102)-inhibition of psychostimulant-induced hyperlocomotion: importance of cyclization. *Peptides* 27:3183-92

Edwards S, Graham DL, Bachtell RK, Self DW. 2007. Region-specific tolerance to cocaine-regulated cAMP-dependent protein phosphorylation following chronic self-administration. *Eur J Neurosci* 25:2201-13

Ekblad E. 2006. CART in the enteric nervous system. *Peptides* 27:2024-30

Ekblad E, Kuhar M, Wierup N, Sundler F. 2003. Cocaine- and amphetamine-regulated transcript: distribution and function in rat gastrointestinal tract. *Neurogastroenterol Motil* 15:545-57

Fagergren P, Hurd Y. 2007. CART mRNA expression in rat monkey and human brain: relevance to cocaine abuse. *Physiol Behav* 92:218-25

Fagergren P, Hurd YL. 1999. Mesolimbic gender differences in peptide CART mRNA expression: effects of cocaine. *Neuroreport* 10:3449-52

Faiger H, Ivanchenko M, Cohen I, Haran TE. 2006. TBP flanking sequences: asymmetry of binding, long-range effects and consensus sequences. *Nucleic Acids Res* 34:104-19

Faiger H, Ivanchenko M, Haran TE. 2007. Nearest-neighbor non-additivity versus long-range non-additivity in TATA-box structure and its implications for TBP-binding mechanism. *Nucleic Acids Res* 35:4409-19

Gautvik KM, de Lecea L, Gautvik VT, Danielson PE, Tranque P, et al. 1996. Overview of the most prevalent hypothalamus-specific mRNAs, as identified by directional tag PCR subtraction. *Proc Natl Acad Sci U S A* 93:8733-8

Green TA, Alibhai IN, Hommel JD, DiLeone RJ, Kumar A, et al. 2006. Induction of inducible cAMP early repressor expression in nucleus accumbens by stress or amphetamine increases behavioral responses to emotional stimuli. *J Neurosci* 26:8235-42

Green TA, Alibhai IN, Unterberg S, Neve RL, Ghose S, et al. 2008. Induction of activating transcription factors (ATFs) ATF2, ATF3, and ATF4 in the nucleus accumbens and their regulation of emotional behavior. *J Neurosci* 28:2025-32

Hai T, Curran T. 1991. Cross-family dimerization of transcription factors Fos/Jun and ATF/CREB alters DNA binding specificity. *Proc Natl Acad Sci U S A* 88:3720-4

Hao H, Liu H, Gonye G, Schwaber JS. 2008. A fast carrier chromatin immunoprecipitation method applicable to microdissected tissue samples. *J Neurosci Methods* 172:38-42

Herdegen T, Leah JD. 1998. Inducible and constitutive transcription factors in the mammalian nervous system: control of gene expression by Jun, Fos and Krox, and CREB/ATF proteins. *Brain Res Brain Res Rev* 28:370-490

Herdegen T, Waetzig V. 2001. AP-1 proteins in the adult brain: facts and fiction about effectors of neuroprotection and neurodegeneration. *Oncogene* 20:2424-37

Holmberg M, Leonardsson G, Ny T. 1995. The species-specific differences in the cAMP regulation of the tissue-type plasminogen activator gene between rat, mouse and human is caused by a one-nucleotide substitution in the cAMP-responsive element of the promoters. *Eur J Biochem* 231:466-74

Hope B, Kosofsky B, Hyman SE, Nestler EJ. 1992. Regulation of immediate early gene expression and AP-1 binding in the rat nucleus accumbens by chronic cocaine. *Proc Natl Acad Sci U S A* 89:5764-8

Hope BT, Nye HE, Kelz MB, Self DW, Iadarola MJ, et al. 1994. Induction of a long-lasting AP-1 complex composed of altered Fos-like proteins in brain by chronic cocaine and other chronic treatments. *Neuron* 13:1235-44

Hubert GW, Jones DC, Moffett MC, Rogge G, Kuhar MJ. 2008. CART peptides as modulators of dopamine and psychostimulants and interactions with the mesolimbic dopaminergic system. *Biochem Pharmacol* 75:57-62

Hubert GW, Kuhar MJ. 2005. Colocalization of CART with substance P but not enkephalin in the rat nucleus accumbens. *Brain Res* 1050:8-14

Hubert GW, Kuhar MJ. 2006. Colocalization of CART peptide with prodynorphin and dopamine D1 receptors in the rat nucleus accumbens. *Neuropeptides* 40:409-15

Hubert GW, Kuhar MJ. 2008. Cocaine administration increases the fraction of CART cells in the rat nucleus accumbens that co-immunostain for c-Fos. *Neuropeptides* 42:339-43

Hunter RG, Bellani R, Bloss E, Costa A, Romeo RD, McEwen BS. 2007. Regulation of CART mRNA by stress and corticosteroids in the hippocampus and amygdala. *Brain Res* 1152:234-40

Hunter RG, Jones D, Vicentic A, Hue G, Rye D, Kuhar MJ. 2006. Regulation of CART mRNA in the rat nucleus accumbens via D3 dopamine receptors. *Neuropharmacology* 50:858-64

Hunter RG, Vicentic A, Rogge G, Kuhar MJ. 2005. The effects of cocaine on CART expression in the rat nucleus accumbens: a possible role for corticosterone. *Eur J Pharmacol* 517:45-50

Hurd YL, Fagergren P. 2000. Human cocaine- and amphetamine-regulated transcript (CART) mRNA is highly expressed in limbic- and sensory-related brain regions. *J Comp Neurol* 425:583-98

Hurd YL, Svensson P, Ponten M. 1999. The role of dopamine, dynorphin, and CART systems in the ventral striatum and amygdala in cocaine abuse. *Ann N Y Acad Sci* 877:499-506

Hyman SE, Cole RL, Konradi C, Kosofsky BE. 1995. Dopamine regulation of transcription factor-target interactions in rat striatum. *Chem Senses* 20:257-60

Jaworski JN, Hansen ST, Kuhar MJ, Mark GP. 2008. Injection of CART (cocaine- and amphetamine-regulated transcript) peptide into the nucleus accumbens reduces cocaine self-administration in rats. *Behav Brain Res* 191:266-71

Jaworski JN, Jones DC. 2006. The role of CART in the reward/reinforcing properties of psychostimulants. *Peptides* 27:1993-2004

Jaworski JN, Kozel MA, Philpot KB, Kuhar MJ. 2003. Intra-accumbal injection of CART (cocaine-amphetamine regulated transcript) peptide reduces cocaine-induced locomotor activity. *J Pharmacol Exp Ther* 307:1038-44

Jean A, Conductier G, Manrique C, Bouras C, Berta P, et al. 2007. Anorexia induced by activation of serotonin 5-HT4 receptors is mediated by increases in CART in the nucleus accumbens. *Proc Natl Acad Sci U S A* 104:16335-40

Jones DC, Kuhar MJ. 2006. Cocaine-amphetamine-regulated transcript expression in the rat nucleus accumbens is regulated by adenylyl cyclase and the cyclic adenosine 5'-monophosphate/protein kinase a second messenger system. *J Pharmacol Exp Ther* 317:454-61

Jones DC, Kuhar MJ. 2008. CART receptor binding in primary cell cultures of the rat nucleus accumbens. *Synapse* 62:122-7

Jones DC, Lakatos A, Rogge GA, Kuhar MJ. 2009. Regulation of cocaine- and amphetamine-regulated transcript mRNA expression by calcium-mediated signaling in GH3 cells. *Neuroscience* 160:339-47

Joyce AR, Easterling K, Holtzman SG, Kuhar MJ. 2006. Modeling the onset of drug dependence: a consideration of the requirement for protein synthesis. *J Theor Biol* 240:531-7

Jung SK, Hong MS, Suh GJ, Jin SY, Lee HJ, et al. 2004. Association between polymorphism in intron 1 of cocaine- and amphetamine-regulated transcript gene with alcoholism, but not with bipolar disorder and schizophrenia in Korean population. *Neurosci Lett* 365:54-7

Kalinichev M, Easterling KW, Holtzman SG. 2003. Long-lasting changes in morphine-induced locomotor sensitization and tolerance in Long-Evans mother rats as a result of periodic postpartum separation from the litter: a novel model of increased vulnerability to drug abuse? *Neuropsychopharmacology* 28:317-28

Kappeler L, Gourdji D, Zizzari P, Bluet-Pajot MT, Epelbaum J. 2003. Age-associated changes in hypothalamic and pituitary neuroendocrine gene expression in the rat. *J Neuroendocrinol* 15:592-601

Keller PA, Compan V, Bockaert J, Giacobino JP, Charnay Y, et al. 2006. Characterization and localization of cocaine- and amphetamine-regulated transcript (CART) binding sites. *Peptides* 27:1328-34

Kim JH, Creekmore E, Vezina P. 2003. Microinjection of CART peptide 55-102 into the nucleus accumbens blocks amphetamine-induced locomotion. *Neuropeptides* 37:369-73

Kim S, Yoon HS, Kim JH. 2007. CART peptide 55-102 microinjected into the nucleus accumbens inhibits the expression of behavioral sensitization by amphetamine. *Regul Pept* 144:6-9

Kimmel HL, Gong W, Vechia SD, Hunter RG, Kuhar MJ. 2000. Intra-ventral tegmental area injection of rat cocaine and amphetamine-regulated transcript peptide 55-102 induces locomotor activity and promotes conditioned place preference. *J Pharmacol Exp Ther* 294:784-92

Konradi C, Cole RL, Heckers S, Hyman SE. 1994. Amphetamine regulates gene expression in rat striatum via transcription factor CREB. *J Neurosci* 14:5623-34

Konradi C, Kobierski LA, Nguyen TV, Heckers S, Hyman SE. 1993. The cAMP-response-element-binding protein interacts, but Fos protein does not interact, with the proenkephalin enhancer in rat striatum. *Proc Natl Acad Sci U S A* 90:7005-9

Koob GF. 2009. Neurobiological substrates for the dark side of compulsivity in addiction. *Neuropharmacology* 56 Suppl 1:18-31

Koob GF, Nestler EJ. 1997. The neurobiology of drug addiction. *J Neuropsychiatry Clin Neurosci* 9:482-97

Koob GF, Volkow ND. 2009. Neurocircuitry of Addiction. *Neuropsychopharmacology*

Koylu EO, Couceyro PR, Lambert PD, Kuhar MJ. 1998. Cocaine- and amphetamine-regulated transcript peptide immunohistochemical localization in the rat brain. *J Comp Neurol* 391:115-32

Koylu EO, Couceyro PR, Lambert PD, Ling NC, DeSouza EB, Kuhar MJ. 1997. Immunohistochemical localization of novel CART peptides in rat hypothalamus, pituitary and adrenal gland. *J Neuroendocrinol* 9:823-33

Kreibich AS, Blendy JA. 2004. cAMP response element-binding protein is required for stress but not cocaine-induced reinstatement. *J Neurosci* 24:6686-92

Kristensen P, Judge ME, Thim L, Ribel U, Christjansen KN, et al. 1998. Hypothalamic CART is a new anorectic peptide regulated by leptin. *Nature* 393:72-6

Kuhar MJ. 2009. Measuring levels of proteins by various technologies: Can we learn more by measuring turnover? *Biochem Pharmacol*

Kuhar MJ, Jaworski JN, Hubert GW, Philpot KB, Dominguez G. 2005. Cocaine- and amphetamine-regulated transcript peptides play a role in drug abuse and are potential therapeutic targets. *Aaps J* 7:E259-65

Kuhar MJ, Ritz MC, Sharkey J. 1988. Cocaine receptors on dopamine transporters mediate cocaine-reinforced behavior. *NIDA Res Monogr* 88:14-22

Kuhar MJ, Yoho LL. 1999. CART peptide analysis by Western blotting. *Synapse* 33:163-71

Kuriyama G, Takekoshi S, Tojo K, Nakai Y, Kuhar MJ, Osamura RY. 2004. Cocaine- and amphetamine-regulated transcript peptide in the rat anterior pituitary gland is localized in gonadotrophs and suppresses prolactin secretion. *Endocrinology* 145:2542-50

Lakatos A, Dominguez G, Kuhar MJ. 2002. CART promoter CRE site binds phosphorylated CREB. *Brain Res Mol Brain Res* 104:81-5

Lakatos A, Prinster S, Vicentic A, Hall RA, Kuhar MJ. 2005. Cocaine- and amphetamine-regulated transcript (CART) peptide activates the extracellular signal-regulated kinase (ERK) pathway in AtT20 cells via putative G-protein coupled receptors. *Neurosci Lett* 384:198-202

Lambert PD, Couceyro PR, McGirr KM, Dall Vechia SE, Smith Y, Kuhar MJ. 1998. CART peptides in the central control of feeding and interactions with neuropeptide Y. *Synapse* 29:293-8

Larsen PJ, Seier V, Fink-Jensen A, Holst JJ, Warberg J, Vrang N. 2003. Cocaine- and amphetamine-regulated transcript is present in hypothalamic neuroendocrine neurones and is released to the hypothalamic-pituitary portal circuit. *J Neuroendocrinol* 15:219-26

Lee DK, Bian S, Rahman MA, Shim YB, Shim I, Choe ES. 2008. Repeated cocaine administration increases N-methyl-d-aspartate NR1 subunit, extracellular signal-

regulated kinase and cyclic AMP response element-binding protein phosphorylation and glutamate release in the rat dorsal striatum. *Eur J Pharmacol* 590:157-62

Levy AD, Li QA, Kerr JE, Rittenhouse PA, Milonas G, et al. 1991. Cocaine-induced elevation of plasma adrenocorticotropin hormone and corticosterone is mediated by serotonergic neurons. *J Pharmacol Exp Ther* 259:495-500

Liu JL, Papachristou DN, Patel YC. 1994. Glucocorticoids activate somatostatin gene transcription through co-operative interaction with the cyclic AMP signalling pathway. *Biochem J* 301 (Pt 3):863-9

Livak KJ, Schmittgen TD. 2001. Analysis of relative gene expression data using real-time quantitative PCR and the 2(-Delta Delta C(T)) Method. *Methods* 25:402-8

Lonze BE, Ginty DD. 2002. Function and regulation of CREB family transcription factors in the nervous system. *Neuron* 35:605-23

Ludvigsen S, Thim L, Blom AM, Wulff BS. 2001. Solution structure of the satiety factor, CART, reveals new functionality of a well-known fold. *Biochemistry* 40:9082-8

Maletinska L, Maixnerova J, Matyskova R, Haugvicova R, Sloncova E, et al. 2007. Cocaine- and amphetamine-regulated transcript (CART) peptide specific binding in pheochromocytoma cells PC12. *Eur J Pharmacol* 559:109-14

Marie-Claire C, Laurendeau I, Canestrelli C, Courtin C, Vidaud M, et al. 2003. Fos but not Cart (cocaine and amphetamine regulated transcript) is overexpressed by several drugs of abuse: a comparative study using real-time quantitative polymerase chain reaction in rat brain. *Neurosci Lett* 345:77-80

Matthews RP, Guthrie CR, Wailes LM, Zhao X, Means AR, McKnight GS. 1994. Calcium/calmodulin-dependent protein kinase types II and IV differentially regulate CREB-dependent gene expression. *Mol Cell Biol* 14:6107-16

Mattson BJ, Bossert JM, Simmons DE, Nozaki N, Nagarkar D, et al. 2005. Cocaine-induced CREB phosphorylation in nucleus accumbens of cocaine-sensitized rats is enabled by enhanced activation of extracellular signal-related kinase, but not protein kinase A. *J Neurochem* 95:1481-94

Mayr B, Montminy M. 2001. Transcriptional regulation by the phosphorylation-dependent factor CREB. *Nat Rev Mol Cell Biol* 2:599-609

McClung CA, Nestler EJ. 2003. Regulation of gene expression and cocaine reward by CREB and DeltaFosB. *Nat Neurosci* 6:1208-15

Mello NK, Mendelson JH. 1997. Cocaine's effects on neuroendocrine systems: clinical and preclinical studies. *Pharmacol Biochem Behav* 57:571-99

Motulsky HJ. 2003. Prism 4 Statistics Guide--Statistical Analyses For Laboratory and Clinical Researchers. *Graphpad Software, Inc., San Diego, CA*

Murphy KG, Abbott CR, Mahmoudi M, Hunter R, Gardiner JV, et al. 2000. Quantification and synthesis of cocaine- and amphetamine-regulated transcript peptide (79-102)-like immunoreactivity and mRNA in rat tissues. *J Endocrinol* 166:659-68

Nestler EJ. 2004a. Historical review: Molecular and cellular mechanisms of opiate and cocaine addiction. *Trends Pharmacol Sci* 25:210-8

Nestler EJ. 2004b. Molecular mechanisms of drug addiction. *Neuropharmacology* 47 Suppl 1:24-32

Nestler EJ, Malenka RC. 2004. The addicted brain. *Sci Am* 290:78-85

Neve RL, Neve KA, Nestler EJ, Carlezon WA, Jr. 2005. Use of herpes virus amplicon vectors to study brain disorders. *Biotechniques* 39:381-91

Ogden CA, Rich ME, Schork NJ, Paulus MP, Geyer MA, et al. 2004. Candidate genes, pathways and mechanisms for bipolar (manic-depressive) and related disorders: an expanded convergent functional genomics approach. *Mol Psychiatry* 9:1007-29

Ogryzko VV, Schiltz RL, Russanova V, Howard BH, Nakatani Y. 1996. The transcriptional coactivators p300 and CBP are histone acetyltransferases. *Cell* 87:953-9

Pandey SC, Chartoff EH, Carlezon WA, Jr., Zou J, Zhang H, et al. 2005. CREB gene transcription factors: role in molecular mechanisms of alcohol and drug addiction. *Alcohol Clin Exp Res* 29:176-84

Paxinos G, Watson C. 2002. The Rat Brain in Stereotaxic Coordinates. *Academic Press, New York.*

Philpot K, Smith Y. 2006. CART peptide and the mesolimbic dopamine system. *Peptides* 27:1987-92

Philpot KB, Dallvechia-Adams S, Smith Y, Kuhar MJ. 2005. A cocaine-and-amphetamine-regulated-transcript peptide projection from the lateral hypothalamus to the ventral tegmental area. *Neuroscience* 135:915-25

Ritz MC, Lamb RJ, Goldberg SR, Kuhar MJ. 1987. Cocaine receptors on dopamine transporters are related to self-administration of cocaine. *Science* 237:1219-23

Ritz MC, Lamb RJ, Goldberg SR, Kuhar MJ. 1988. Cocaine self-administration appears to be mediated by dopamine uptake inhibition. *Prog Neuropsychopharmacol Biol Psychiatry* 12:233-9

Rogge G, Jones D, Hubert GW, Lin Y, Kuhar MJ. 2008. CART peptides: regulators of body weight, reward and other functions. *Nat Rev Neurosci* 9:747-58

Rogge GA, Jones DC, Green T, Nestler E, Kuhar MJ. 2009. Regulation of CART peptide expression by CREB in the rat nucleus accumbens in vivo. *Brain Res* 1251:42-52

Sakai N, Thome J, Newton SS, Chen J, Kelz MB, et al. 2002. Inducible and brain region-specific CREB transgenic mice. *Mol Pharmacol* 61:1453-64

Salinas A, Wilde JD, Maldve RE. 2006. Ethanol enhancement of cocaine- and amphetamine-regulated transcript mRNA and peptide expression in the nucleus accumbens. *J Neurochem* 97:408-15

Sarkar S, Wittmann G, Fekete C, Lechan RM. 2004. Central administration of cocaine- and amphetamine-regulated transcript increases phosphorylation of cAMP response element binding protein in corticotropin-releasing hormone-producing neurons but not in prothyrotropin-releasing hormone-producing neurons in the hypothalamic paraventricular nucleus. *Brain Res* 999:181-92

Self DW, Genova LM, Hope BT, Barnhart WJ, Spencer JJ, Nestler EJ. 1998. Involvement of cAMP-dependent protein kinase in the nucleus accumbens in cocaine self-administration and relapse of cocaine-seeking behavior. *J Neurosci* 18:1848-59

Sen A, Bettegowda A, Jimenez-Krassel F, Ireland JJ, Smith GW. 2007. Cocaine- and amphetamine-regulated transcript regulation of follicle-stimulating hormone signal transduction in bovine granulosa cells. *Endocrinology* 148:4400-10

Shaw-Lutchman TZ, Impey S, Storm D, Nestler EJ. 2003. Regulation of CRE-mediated transcription in mouse brain by amphetamine. *Synapse* 48:10-7

Shieh KR. 2003. Effects of the cocaine- and amphetamine-regulated transcript peptide on the turnover of central dopaminergic neurons. *Neuropharmacology* 44:940-8

Shirayama Y, Chaki S. 2006. Neurochemistry of the nucleus accumbens and its relevance to depression and antidepressant action in rodents. *Curr Neuropharmacol* 4:277-91

Smith SM, Vaughan JM, Donaldson CJ, Fernandez RE, Li C, et al. 2006. Cocaine- and amphetamine-regulated transcript is localized in pituitary lactotropes and is regulated during lactation. *Endocrinology* 147:1213-23

Smith SM, Vaughan JM, Donaldson CJ, Rivier J, Li C, et al. 2004. Cocaine- and amphetamine-regulated transcript activates the hypothalamic-pituitary-adrenal axis through a corticotropin-releasing factor receptor-dependent mechanism. *Endocrinology* 145:5202-9

Smith Y, Kieval J, Couceyro PR, Kuhar MJ. 1999. CART peptide-immunoreactive neurones in the nucleus accumbens in monkeys: ultrastructural analysis, colocalization studies, and synaptic interactions with dopaminergic afferents. *J Comp Neurol* 407:491-511

Smith Y, Koylu EO, Couceyro P, Kuhar MJ. 1997. Ultrastructural localization of CART (cocaine- and amphetamine-regulated transcript) peptides in the nucleus accumbens of monkeys. *Synapse* 27:90-4

Spiess J, Villarreal J, Vale W. 1981. Isolation and sequence analysis of a somatostatin-like polypeptide from ovine hypothalamus. *Biochemistry* 20:1982-8

Stanley SA, Murphy KG, Bewick GA, Kong WM, Opacka-Juffry J, et al. 2004. Regulation of rat pituitary cocaine- and amphetamine-regulated transcript (CART) by CRH and glucocorticoids. *Am J Physiol Endocrinol Metab* 287:E583-90

Stein J, Shah R, Steiner DF, Dey A. 2006a. RNAi-mediated silencing of prohormone convertase (PC) 5/6 expression leads to impairment in processing of cocaine- and amphetamine-regulated transcript (CART) precursor. *Biochem J* 400:209-15

Stein J, Steiner DF, Dey A. 2006b. Processing of cocaine- and amphetamine-regulated transcript (CART) precursor proteins by prohormone convertases (PCs) and its implications. *Peptides* 27:1919-25

Tang WX, Fasulo WH, Mash DC, Hemby SE. 2003. Molecular profiling of midbrain dopamine regions in cocaine overdose victims. *J Neurochem* 85:911-24

Terwilliger RZ, Beitner-Johnson D, Sevarino KA, Crain SM, Nestler EJ. 1991. A general role for adaptations in G-proteins and the cyclic AMP system in mediating the chronic actions of morphine and cocaine on neuronal function. *Brain Res* 548:100-10

Thim L, Kristensen P, Nielsen PF, Wulff BS, Clausen JT. 1999. Tissue-specific processing of cocaine- and amphetamine-regulated transcript peptides in the rat. *Proc Natl Acad Sci U S A* 96:2722-7

Thim L, Nielsen PF, Judge ME, Andersen AS, Diers I, et al. 1998. Purification and characterisation of a new hypothalamic satiety peptide, cocaine and amphetamine regulated transcript (CART), produced in yeast. *FEBS Lett* 428:263-8

Tremblay JJ, Lanctot C, Drouin J. 1998. The pan-pituitary activator of transcription, Ptx1 (pituitary homeobox 1), acts in synergy with SF-1 and Pit1 and is an upstream regulator of the Lim-homeodomain gene Lim3/Lhx3. *Mol Endocrinol* 12:428-41

Tropea TF, Kosofsky BE, Rajadhyaksha AM. 2008. Enhanced CREB and DARPP-32 phosphorylation in the nucleus accumbens and CREB, ERK, and GluR1 phosphorylation in the dorsal hippocampus is associated with cocaine-conditioned place preference behavior. *J Neurochem* 106:1780-90

Unterwald EM, Fillmore J, Kreek MJ. 1996. Chronic repeated cocaine administration increases dopamine D1 receptor-mediated signal transduction. *Eur J Pharmacol* 318:31-5

Vicentic A. 2006. CART peptide diurnal variations in blood and brain. *Peptides* 27:1942-8

Vicentic A, Dominguez G, Hunter RG, Philpot K, Wilson M, Kuhar MJ. 2004. Cocaine- and amphetamine-regulated transcript peptide levels in blood exhibit a diurnal rhythm: regulation by glucocorticoids. *Endocrinology* 145:4119-24

Vicentic A, Hunter RG, Kuhar MJ. 2005a. Effect of corticosterone on CART peptide levels in rat blood. *Peptides* 26:531-3

Vicentic A, Lakatos A, Hunter R, Philpot K, Dominguez G, Kuhar MJ. 2005b. CART peptide diurnal rhythm in brain and effect of fasting. *Brain Res* 1032:111-5

Vicentic A, Lakatos A, Kuhar MJ. 2005c. CART (cocaine- and amphetamine-regulated transcript) peptide receptors: specific binding in AtT20 cells. *Eur J Pharmacol* 528:188-9

Vrang N. 2006. Anatomy of hypothalamic CART neurons. *Peptides* 27:1970-80

Vrang N, Larsen PJ, Kristensen P. 2002. Cocaine-amphetamine regulated transcript (CART) expression is not regulated by amphetamine. *Neuroreport* 13:1215-8

Vrang N, Larsen PJ, Tang-Christensen M, Larsen LK, Kristensen P. 2003. Hypothalamic cocaine-amphetamine regulated transcript (CART) is regulated by glucocorticoids. *Brain Res* 965:45-50

Vrang N, Tang-Christensen M, Larsen PJ, Kristensen P. 1999. Recombinant CART peptide induces c-Fos expression in central areas involved in control of feeding behaviour. *Brain Res* 818:499-509

Walters CL, Kuo YC, Blendy JA. 2003. Differential distribution of CREB in the mesolimbic dopamine reward pathway. *J Neurochem* 87:1237-44

Wierup N, Bjorkqvist M, Kuhar MJ, Mulder H, Sundler F. 2006. CART regulates islet hormone secretion and is expressed in the beta-cells of type 2 diabetic rats. *Diabetes* 55:305-11

Wierup N, Kuhar M, Nilsson BO, Mulder H, Ekblad E, Sundler F. 2004. Cocaine- and amphetamine-regulated transcript (CART) is expressed in several islet cell types during rat development. *J Histochem Cytochem* 52:169-77

Wierup N, Richards WG, Bannon AW, Kuhar MJ, Ahren B, Sundler F. 2005. CART knock out mice have impaired insulin secretion and glucose intolerance, altered beta cell morphology and increased body weight. *Regul Pept* 129:203-11

Wise RA, Bauco P, Carlezon WA, Jr., Trojniar W. 1992. Self-stimulation and drug reward mechanisms. *Ann N Y Acad Sci* 654:192-8

Xu W, Cooper GM. 1995. Identification of a candidate c-mos repressor that restricts transcription of germ cell-specific genes. *Mol Cell Biol* 15:5369-75

Yamada K, Yuan X, Otabe S, Koyanagi A, Koyama W, Makita Z. 2002. Sequencing of the putative promoter region of the cocaine- and amphetamine-regulated-transcript gene and identification of polymorphic sites associated with obesity. *Int J Obes Relat Metab Disord* 26:132-6

Yanagisawa S, Schmidt RJ. 1999. Diversity and similarity among recognition sequences of Dof transcription factors. *Plant J* 17:209-14

Yermolaieva O, Chen J, Couceyro PR, Hoshi T. 2001. Cocaine- and amphetamine-regulated transcript peptide modulation of voltage-gated Ca2+ signaling in hippocampal neurons. *J Neurosci* 21:7474-80

Zhou Y, Spangler R, Schlussman SD, Ho A, Kreek MJ. 2003. Alterations in hypothalamic-pituitary-adrenal axis activity and in levels of proopiomelanocortin and corticotropin-releasing hormone-receptor 1 mRNAs in the pituitary and hypothalamus of the rat during chronic 'binge' cocaine and withdrawal. *Brain Res* 964:187-99

Zhou Y, Spangler R, Schlussman SD, Yuferov VP, Sora I, et al. 2002. Effects of acute "binge" cocaine on preprodynorphin, preproenkephalin, proopiomelanocortin, and corticotropin-releasing hormone receptor mRNA levels in the striatum and hypothalamic-pituitary-adrenal axis of mu-opioid receptor knockout mice. *Synapse* 45:220-9

<u>Internet website reference</u>

"Cocaine." *Wikipedia, The Free Encyclopedia*. 31 January 2010. Web. 1 November
    2009.